



Universidade de Aveiro Departamento de Química  
2011

**DIANA LUÍSA  
DUARTE DE LIMA**

**MÉTODOS ANALÍTICOS: DESTINO AMBIENTAL DE  
POLUENTES ORGÂNICOS**

**ANALYTICAL METHODS TO STUDY FATE OF  
ORGANIC POLLUTANTS IN ENVIRONMENT**



DIANA LUÍSA  
DUARTE DE LIMA

## MÉTODOS ANALÍTICOS: DESTINO AMBIENTAL DE POLUENTES ORGÂNICOS

### ANALYTICAL METHODS TO STUDY FATE OF ORGANIC POLLUTANTS IN ENVIRONMENT

Tese apresentada à Universidade de Aveiro para cumprimento dos requisitos necessários à obtenção do grau de Doutor em Química, realizada sob a orientação científica do Doutor Valdemar Inocêncio Esteves, Professor Auxiliar do Departamento de Química da Universidade de Aveiro e do Doutor Rudolf Josef Schneider, Investigador com agregação do BAM Federal Institute for Materials and Testing e *lecturer* da Technical University of Berlin.



UNIÃO EUROPEIA  
Fundo Social Europeu



PROGRAMA OPERACIONAL POTENCIAL HUMANO



QUADRO  
DE REFERÊNCIA  
ESTRATÉGICO  
NACIONAL  
PORTUGAL 2007-2013



Fundação para a Ciência e a Tecnologia  
MINISTÉRIO DA CIÊNCIA, TECNOLOGIA E ENSINO SUPERIOR

Apoio financeiro da FCT e do FSE no âmbito do QREN-POPH. Tipologia 4.1  
Apoio via Bolsa de Doutoramento  
SFRH/BD/36086/2007.

Aos meus pais e ao meu chatinho.

## **o júri**

presidente

**Prof. Doutor Aníbal Manuel de Oliveira Duarte**  
professor catedrático da Universidade de Aveiro

**Prof. Doutor Rudolf Josef Schneider**  
Investigador com agregação do BAM Federal Institute for Materials Research and Testing e  
*lecturer* da Technical University of Berlin, Germany

**Prof. Doutor Joaquim Esteves da Silva**  
professor associado com agregação da Faculdade de Ciências da Universidade do Porto

**Prof. Doutora Marcela Alves Segundo**  
professora auxiliar da Faculdade de Farmácia da Universidade do Porto

**Prof. Doutora Maria Eduarda Bastos Henriques dos Santos**  
professora auxiliar da Universidade de Aveiro

**Prof. Doutor Valdemar Inocêncio Esteves**  
professor auxiliar da Universidade de Aveiro



## agradecimentos

A realização e conclusão deste trabalho não teria sido possível sem a colaboração, presença e apoio de diversas pessoas a quem eu gostaria de deixar expresso o meu reconhecimento e profundo agradecimento.

Ao meu orientador, Doutor Valdemar I. Esteves, por toda a amizade, apoio, paciência e motivação que sempre me transmitiu, quer nos bons momentos, quer nos menos bons, e que me fizeram olhar em frente e nunca desistir!

Ao meu co-orientador, Rudolf J. Schneider, pela sua inteira disponibilidade e apoio durante a realização deste trabalho. À BAM Federal Institute for Materials and Testing por me ter proporcionado as condições necessárias à realização de um estágio sobre ensaios imunológicos nas suas instalações. Ao INRES – Institute of Plant Nutrition, University of Bonn pelas amostras de solos disponibilizadas para a realização deste trabalho.

À Escola Superior de Tecnologia da Saúde de Coimbra, sua Direcção, corpo docente e funcionários, pela compreensão e flexibilidade de horário ao longo destes quatro anos. Um agradecimento especial à Paula Fonseca, pela amizade, apoio e incentivo.

Aos meus colegas de trabalho e amigos, em particular à Pati, à Luci e à DiMoni, por toda a amizade, pelos bons momentos de convívio e, principalmente, pela alegria que trazem à minha vida.

Ao grupo de Química Analítica e Ambiental pelo seu companheirismo, em particular à Patrícia Silva, à Vânia Calisto, ao Guillaume Erny e à Joana Leal pela sua colaboração em algumas partes deste trabalho.

Aos amigos de sempre, Isaura, Micas, Cátia, Paulinha e Carlos, simplesmente por fazerem parte da minha vida.

Aos meus amigos e familiares, em particular, ao meu pai e irmão pela amizade, compreensão e motivação.

À minha mãe, por tudo o que me proporcionou ao longo da vida, pelo exemplo de Mulher de força e coragem que é, e pelo facto de que, sem ela, nunca poderia ser quem sou.

As palavras finais vão para o meu chatinho, por me fazer sorrir sempre que tinha vontade de chorar!

## palavras-chave

Atrazina, 17 $\alpha$ -etinilestradiol, adsorção-dessorção, electroforese capilar, desconvolução espectral, ELISA.

## resumo

O transporte de poluentes no ambiente envolve processos distintos, tais como a volatilização, a lixiviação e escoamento através dos solos atingindo águas superficiais. A adsorção e a dessorção são dos factores que mais influenciam a lixiviação, tendo assim um papel fundamental no destino dos poluentes orgânicos e na sua distribuição no sistema solo/água. O trabalho desenvolvido envolve a optimização de metodologias analíticas para a monitorização da sorção de poluentes orgânicos, 17 $\alpha$ -etinilestradiol (EE2) e atrazina, e do seu destino no ambiente aquático.

Inicialmente, foram desenvolvidas várias metodologias, baseadas na cromatografia micelar electrocinética, na desconvolução de espectros de absorvência e de fluorescência, e, ainda, em ensaios imunoenzimáticos. Neste trabalho, encontram-se também descritas as optimizações dos referidos métodos juntamente com a avaliação do seu desempenho. Avaliou-se ainda a aplicabilidade dos métodos desenvolvidos fazendo estudos de adsorção da atrazina e do EE2, a diferentes amostras de solos. O trabalho desenvolvido facultava assim várias opções, no que diz respeito a metodologias analíticas para monitorizar a adsorção da atrazina a solos, incrementando a liberdade de escolha, a qual será dependente das condições disponíveis no laboratório e das preferências do analista.

Na segunda parte do trabalho faz-se o estudo do comportamento de sorção dos dois poluentes orgânicos em causa a diferentes amostras de solos. A caracterização química da matéria orgânica dos solos serve de base para a interpretação dos mecanismos de interacção responsáveis pelas ligações estabelecidas entre os poluentes e os constituintes do solo. No caso da atrazina, os resultados demonstraram que os grupos aromáticos e carboxílicos da matéria orgânica dos solos são os agentes de ligação mais eficientes. O EE2 liga-se fortemente à matéria orgânica e é essencialmente estabilizado por interacções hidrofóbicas através de associações face-a-face dos núcleos aromáticos do EE2 com os da superfície dos solos e/ou com os das outras moléculas de EE2. A fertilização com estrumes de animais introduz mais estruturas aromáticas e grupos carboxílicos, indicando que a sua utilização poderá minimizar a toxicidade residual do EE2 e da atrazina presente nos solos, através do aumento da sua adsorção e, conseqüentemente, redução da sua lixiviação.

Uma vez que as águas residuais, superficiais e/ou subterrâneas podem ser o destino final dos poluentes orgânicos, foi ainda realizada a quantificação do EE2 e da atrazina em diversas amostras de diferentes ambientes aquáticos.

**keywords**

Atrazine, 17 $\alpha$ -ethinylestradiol, adsorption-desorption, capillary electrophoresis, spectral deconvolution, ELISA.

**abstract**

Environmental transport of pollutants comprises distinct processes such as volatilization, leaching and surface runoff. Sorption is one of the most important phenomena that affects leaching, and thus the fate of hydrophobic organic pollutants in soils and also control their distribution in the soil/water environment. The work developed focuses the optimization of analytical techniques for monitoring the sorption behaviour of organic pollutants, 17 $\alpha$ -ethinylestradiol (EE2) and atrazine, and their fate in aqueous environment. Initially, the development of several analytical techniques, such as micellar electrokinetic chromatography, spectral deconvolution, using UV-Vis and fluorescence spectroscopy, and also enzyme linked immunosorbent assay was performed. Optimization, method performance and recovery tests are described and results discussed. Moreover, in order to evaluate the applicability of the previously optimized method, atrazine and EE2 sorption to soil samples was performed. The work developed provide several options, in terms of methodology to follow sorption of atrazine onto soils, however the choice depends on the laboratory conditions and on the analyst preferences. The advantages and disadvantages of each methodology should be evaluated first.

The second part of this work consisted in the sorption behaviour study of those two different hydrophobic organic pollutants onto different soil samples. Soil organic matter chemical characterization, being essential to understand the binding mechanism responsible for the interactions, was made. The results of atrazine binding to organic matter pointed out that carboxyl units and aromatic-rich organic matter are the most efficient binding agents for atrazine. EE2 adsorbs strongly to soil organic matter and is mainly stabilized by hydrophobic interactions, through aromatic nuclei face to face with surface and/or another EE2 molecule association. Farmyard manure soil contains higher aromatic and carboxyl units, indicating that this type of manure can be effectively used to minimize the residual toxicity of EE2 and atrazine present in soils, increasing the sorption and reducing leaching onto water resources.

Since the final destination of organic pollutants can be ground, surface and/or waste water, atrazine and 17 $\alpha$ -ethinylestradiol were quantified in several water samples.

# CONTENTS

# Contents

---

## **PART I – Introduction**

### **Introduction**

Hydrophobic organic pollutants .....	1
Atrazine .....	1
Description .....	1
Sources of pesticides in water.....	2
17 $\alpha$ -Ethinylestradiol .....	4
Description .....	4
Sources of estrogens in waters .....	5
Fate of HOP in the environment.....	6
References .....	11

## **PART II – Development of analytical procedures to follow sorption behaviour of HOP onto soils**

### **Chapter 1 – Atrazine analysis by capillary electrophoresis**

1.1. Introduction .....	15
1.2. Experimental procedure .....	16
1.2.1. Soil sample .....	16
1.2.2. Instrumentation.....	17
1.2.3. Buffer and standards .....	18
1.2.4. Capillary column conditioning .....	18
1.2.5. Separation conditions.....	19
1.2.6. Suitability of the MEKC method.....	19
1.2.7. Adsorption studies.....	19
1.2.8. Data analysis .....	20
1.3. Results and discussion .....	21
1.3.1. Electrophoretic separation of atrazine .....	21
1.3.2. Performance of the method .....	22
1.3.3. Preliminary studies and kinetic experiments .....	23
1.3.4. Adsorption studies.....	24
1.3.5. MEKC and HPLC methods – comparison .....	26
1.4. Conclusions .....	28
1.5. References .....	29

### **Chapter 2 – Spectral deconvolution to follow sorption behaviour of organic pollutants**

2.1. Introduction.....	31
2.2. Principle of spectral deconvolution.....	32

2.3. UVSD for atrazine .....	34
2.3.1. Experimental procedure .....	34
2.3.1.1. Soil sample.....	34
2.3.1.2. Instrumentation.....	34
2.3.1.3. Adsorption studies.....	34
2.3.1.4. MEKC analysis.....	35
2.3.1.5. UV determination.....	35
2.3.2. Results and discussion .....	36
2.3.2.1. UV Spectral deconvolution method .....	36
2.3.2.2. Analytical curves by UVSD and MEKC.....	37
2.3.2.3. Adsorption experiments – Evaluation of the analytical methods .....	38
2.4. Fluorescence SD for EE2 .....	40
2.4.1. Experimental procedure .....	40
2.4.1.1. Soil sample.....	40
2.4.1.2. Instrumentation.....	40
2.4.1.3. Fluorescence spectra acquisition .....	41
2.4.1.4. Adsorption studies.....	42
2.4.2. Results and discussion .....	43
2.4.2.1. Fluorescence spectral deconvolution method .....	43
2.4.2.2. Evaluation of the deconvolution method.....	45
2.4.2.3. Adsorption experiments.....	46
2.5. Conclusions.....	50
2.6. References.....	51
<b>Chapter 3 – Development of an enzyme linked immunosorbent assay to follow atrazine sorption onto soils</b>	
3.1. Introduction.....	55
3.1.1. Antibodies.....	56
3.1.1.1. Structural and functional properties .....	57
3.1.1.2. Antibody production .....	58
3.1.2. Tracer synthesis .....	60
3.1.3. Immunoassays .....	62
3.1.4. Application in environmental analysis.....	66
3.1.4.1. Using ELISA to follow sorption behaviour .....	67
3.2. Experimental procedure .....	69
3.2.1. Soil sample .....	69
3.2.2. ELISA development .....	69
3.2.2.1. Reagents and materials.....	69
3.2.2.2. Preparation of enzyme conjugates via mixed anhydride route .....	71

3.2.2.3. Preparation of enzyme conjugates via activated ester route .....	73
3.2.2.4. Tracer and antibody binding specificity .....	78
3.2.2.5. ELISA procedure.....	78
3.2.3. Adsorption experiment.....	79
3.3. Results and discussion .....	79
3.3.1. Tracer and antibody binding specificity.....	79
3.3.2. Optimization of antibody and tracer dilutions .....	88
3.3.3. Evaluation of assay performance .....	89
3.3.4. Evaluation of soil matrix effects .....	93
3.3.5 Adsorption experiment.....	95
3.4. Conclusions.....	96
3.5. References.....	97

### **PART III – Fate and persistence of HOP on environment**

#### **Chapter 4 – Characterization of soil samples subjected to different organic long-term amendments**

4.1. Introduction.....	101
4.2. Experimental procedure .....	102
4.2.1. Soil samples description .....	102
4.2.2. Total organic matter, total organic carbon, total nitrogen .....	102
4.2.3. <sup>13</sup> C NMR spectroscopy .....	102
4.2.4. FT-IR spectroscopy.....	103
4.2.5. Capillary zone electrophoresis.....	103
4.3. Results and discussion .....	105
4.3.1. Total organic matter, total organic carbon, total nitrogen .....	105
4.3.2. <sup>13</sup> C NMR spectroscopy .....	106
4.3.3. FT-IR spectroscopy.....	108
4.3.4. Phenolic compounds content .....	111
4.4. Conclusions.....	114
4.5. References.....	116

#### **Chapter 5 – Sorption behaviour of HOP on soils subjected to different organic long-term amendments**

5.1. Introduction.....	119
5.2. Atrazine sorption behaviour.....	122
5.2.1. Experimental procedure .....	122
5.2.1.1. Soil samples .....	122
5.2.1.2. Instrumentation and analysis conditions .....	122
5.2.1.3. Adsorption studies.....	122
5.2.1.4. Desorption studies.....	123

5.2.1.5. Data analysis .....	123
5.2.2. Results and discussion .....	124
5.2.1.1. Adsorption .....	124
5.2.1.2 Desorption .....	127
5.3. EE2 sorption behaviour .....	132
5.3.1. Experimental procedure .....	132
5.3.1.1. Soil samples .....	132
5.3.1.2. Instrumentation and analysis conditions .....	132
5.3.1.3. Adsorption studies.....	132
5.3.1.4. Molecular modelling studies .....	132
5.3.2. Results and discussion .....	134
5.4. Conclusions.....	143
5.5. References.....	145
<b>Chapter 6 – Determination of HOP in water samples using ELISA</b>	
6.1. Introduction.....	149
6.2. Experimental procedure .....	152
6.2.1. Water samples .....	152
6.2.2. Reagents and materials .....	155
6.2.3. ELISA procedure.....	156
6.2.4. Matrix effects.....	157
6.3. Results and discussion .....	157
6.3.1. Atrazine determination.....	157
6.3.1.1. Evaluation of matrix effects.....	157
6.3.1.2. Quantification of atrazine in ground, surface and wastewaters .....	165
6.3.2. EE2 determination .....	166
6.3.2.1. Optimization of antibody and tracer dilutions .....	166
6.3.2.2. Evaluation of assay performance .....	167
6.3.2.3. Cross-reactivity .....	169
6.3.2.4. Evaluation of matrix effects.....	170
6.3.2.5. Quantification of EE2 in ground, surface and wastewaters .....	176
6.4. Conclusions.....	178
6.5. References.....	179
<b>PART IV – Conclusions and Future work</b>	
<b>Conclusions</b> .....	181
<b>Future Work</b> .....	185



# List of Figures

---

<b>Figure I.I.</b> Major pathways for pesticide transport into waters (Gerecke et al., 2002).....	<b>3</b>
<b>Figure I.II.</b> Pathways of pollutants degradation and transport.....	<b>7</b>
<b>Figure 1.1.</b> Chromatogram of an aqueous soil solution from a batch experimental sample (a) matrix peak; (b) atrazine (c) ethylvanillin analysed using buffers with 0, 25 and 50 mmol L <sup>-1</sup> SDS.....	<b>22</b>
<b>Figure 1.2.</b> Influence of contact time on atrazine adsorption on soil. Initial atrazine concentration 5 mg L <sup>-1</sup> in 0.01 mol L <sup>-1</sup> CaCl <sub>2</sub> (n = 3); Q <sub>t</sub> – adsorbed concentration at time t (h) (mg kg <sup>-1</sup> ).....	<b>23</b>
<b>Figure 1.3.</b> Freundlich adsorption isotherms for atrazine in soils subjected to different fertilizations (MIN – mineral fertilizer; COM – compost fertilizer; FYM – farmyard manure; SLU – sewage sludge fertilizer; Error bars represent 95% confidence interval for n = 3).....	<b>25</b>
<b>Figure 2.1.</b> UV spectra from adsorption experiments on soil fertilized with sewage sludge (a) UV Reference spectra of background (0.01 mol L <sup>-1</sup> CaCl <sub>2</sub> ), RSWE and atrazine; (b) Combined spectrum of the three reference spectra; (c) Residual plots.....	<b>37</b>
<b>Figure 2.2.</b> Adsorption isotherms of atrazine onto soil fertilized with sewage sludge obtained by UVSD (■) and by MEKC (x).....	<b>39</b>
<b>Figure 2.3.</b> Change in EE2 adsorption percentage with the soil/solution ratio; Initial EE2 concentration 2 mg L <sup>-1</sup> . Soil sample fertilized with farmyard manure.....	<b>42</b>
<b>Figure 2.4.</b> Residual plots obtained after the deconvolution of a 20 µg L <sup>-1</sup> EE2 standard spiked into a farmyard manure soil extract using emission spectra range between a) 290 and 650 nm; b) 295 and 350 nm. λ <sub>exc</sub> = 280 nm.....	<b>44</b>
<b>Figure 2.5.</b> Influence of contact time on EE2 adsorption onto soil. Initial EE2 concentration of 2 mg L <sup>-1</sup> in 0.01 mol L <sup>-1</sup> CaCl <sub>2</sub> (n=3); Q <sub>t</sub> – adsorbed concentration at time t (h) (mg kg <sup>-1</sup> ).....	<b>47</b>

<b>Figure 2.6.</b> Adsorption isotherms with fitting using Hill Equation; SLU, sewage sludge fertilizer; MIN, mineral fertilizer; FYM, farmyard manure; COM, compost from organic household waste; COM_LOI, composted soil submitted to loss on ignition.....	<b>48</b>
<b>Figure 3.1.</b> Structural diagram representing the IgG (antibody); Fab = fragment of antigen binding region; Fc = constant fragment which binds to various cell receptors and complement proteins.....	<b>57</b>
<b>Figure 3.2.</b> The generation of hybridoma cells for monoclonal antibody production (adapted from Mikkelsen and Cortón, 2004).....	<b>59</b>
<b>Figure 3.3.</b> Coupling of the hapten to HRP using the mixed anhydride method.....	<b>61</b>
<b>Figure 3.4.</b> Coupling of the hapten to HRP using the active ester method.....	<b>62</b>
<b>Figure 3.5.</b> Principle of non-competitive immunoassay – sandwich assay.....	<b>63</b>
<b>Figure 3.6.</b> Principle of direct competitive immunoassay.....	<b>63</b>
<b>Figure 3.7.</b> Principle of indirect competitive immunoassay.....	<b>64</b>
<b>Figure 3.8.</b> Typical 4-parameter logistic function graph for a competitive immunoassay format.....	<b>64</b>
<b>Figure 3.9.</b> Triazine derivatives: a) 2-(tert-butylamino)-4-[(1-carboxypent-5-yl)amino]-6-(ethylamino)-1,3,5-triazine (t-Bu/Et/C6); b) 2-(tert-butylamino)-4-[(1-carboxyeth-2-yl)-thio]-6-(ethylamino)-1,3,5-triazine (t-Bu/Et/SC3); c) 2-[(1-carboxyeth-2-yl)-thio]-4-(ethylamino)-6-(isopropylamino)-1,3,5-triazine (i-Pr/Et/SC3); d) 2-[(1-carboxypent-5-yl)amino]-4-chloro-6-amino-1,3,5-triazine (H/Cl/C6); e) 2-(tert-butylamino)-4-[(1-carboxypent-5-yl)amino]-6-chloro-1,3,5-triazine (t-bu/Cl/C6); f) 2-[(1-carboxypent-5-yl)amino]-4-(ethylamino)-6-(isopropylamino)-1,3,5-triazine (i-Pr/Et/C6); g) 2-[(1-carboxypent-5-yl)amino]-4-chloro-6-(isopropylamino)-1,3,5-triazine (i-Pr/Cl/C6); (for nomenclature and abbreviations, <i>cf.</i> to Weller and Niessner, 1997).....	<b>70</b>
<b>Figure 3.10.</b> Collection of the tracer T1: t-Bu/Et/C6 fractions after separation by means of a Sephadex G-25 PD-10 <sup>®</sup> column using mixed anhydride method.....	<b>72</b>
<b>Figure 3.11.</b> Collection of the tracer T2: t-Bu/Et/SC3 fractions after separation by means of a Sephadex PD-10 <sup>®</sup> column using mixed anhydride method.....	<b>73</b>
<b>Figure 3.12.</b> Collection of the tracer T3: Et/i-Pr/SC3 fractions after separation by means of a Sephadex G-25 PD-10 <sup>®</sup> column using mixed anhydride method.....	<b>73</b>

**Figure 3.13.** Collection of the tracer T1: t-Bu/Et/C6 fractions after separation by means of a Sephadex G-25 PD-10<sup>®</sup> column using the active ester method with DMF as solvent.....**75**

**Figure 3.14.** Collection of the tracer T2: t-Bu/Et/SC3 fractions after separation by means of a Sephadex G-25 PD-10<sup>®</sup> column using the active ester method with DMF as solvent.....**75**

**Figure 3.15.** Collection of the tracer T1: t-Bu/Et/C6 fractions after separation by means of a Sephadex G-25 PD-10<sup>®</sup> column using active ester method with THF as solvent.....**76**

**Figure 3.16.** Collection of the tracer T2: t-Bu/Et/SC3 fractions after separation by means of a Sephadex G-25 PD-10<sup>®</sup> column using active ester method with THF as solvent.....**76**

**Figure 3.17.** Collection of the tracer T4: H/Cl/C6 fractions after separation by means of a Sephadex G-25 PD-10<sup>®</sup> column using active ester method with THF as solvent.....**77**

**Figure 3.18.** Collection of the tracer T5: t-Bu/Cl/C6 fractions after separation by means of a Sephadex G-25 PD-10<sup>®</sup> column using active ester method with THF as solvent.....**77**

**Figure 3.19.** Representation of the OD values obtained for each standard, A – blank (water) and H – atrazine concentration 1000 µg L<sup>-1</sup> obtained using different tracers (synthesized differently) and microtiter plate coated using the polyclonal antibody S84. T1: t-Bu/Et/C6; T2: t-Bu/Et/SC3; T3: Et/i-Pr/SC3; T5: t-Bu/Cl/C6; T6: i-Pr/Et/C6 and T7: i-Pr/Cl/C6.....**80**

**Figure 3.20.** Representation of the OD values obtained for each standard between A – blank (water) and H – atrazine concentration 1000 µg L<sup>-1</sup> obtained using different tracers (synthesized differently) and microtiter plate coated using the polyclonal antibody S84. T2: t-Bu/Et/SC3; T3: Et/i-Pr/SC3; T5: t-Bu/Cl/C6.....**81**

**Figure 3.21.** Representation of the OD values obtained for each standard, A – blank (water) and H – atrazine concentration 1000 µg L<sup>-1</sup> obtained using different tracers (synthesized differently) and microtiter plate coated using the polyclonal antibody Ak15. T1: t-Bu/Et/C6; T2: t-Bu/Et/SC3 and T3: Et/i-Pr/SC3.....**82**

**Figure 3.22.** Representation of the OD values obtained for each standard, A – blank (water) and H – atrazine concentration 1000 µg L<sup>-1</sup> obtained using different tracers (synthesized differently) and microtiterplate coated using the polyclonal antibody Ak19. T1: t-Bu/Et/C6; T2: t-Bu/Et/SC3 and T3: Et/i-Pr/SC3.....**82**

**Figure 3.23.** Representation of the OD values obtained for each standard between A – blank (water) and H – atrazine concentration  $1000 \mu\text{g L}^{-1}$  obtained using different tracers (synthesized differently) and microtiter plate coated using the polyclonal antibody Ak15. T1: t-Bu/Et/C6; T3: Et/i-Pr/SC3.....**83**

**Figure 3.24.** Representation of the OD values obtained for each standard between A – blank (water) and H – atrazine concentration  $1000 \mu\text{g L}^{-1}$  obtained using different tracers (synthesized differently) and microtiter plate coated using the polyclonal antibody Ak19. T1: t-Bu/Et/C6; T3: Et/i-Pr/SC3.....**84**

**Figure 3.25.** Representation of the OD values obtained for each standard, A – blank (water) and H – atrazine concentration  $1000 \mu\text{g L}^{-1}$  obtained using different tracers (synthesized differently) and microtiter plate coated using the polyclonal antibody CWoNr. T1: t-Bu/Et/C6; T2: t-Bu/Et/SC3; T3: Et/i-Pr/SC3; T5: t-Bu/Cl/C6; T6: i-Pr/Et/C6 and T7: i-Pr/Cl/C6.....**85**

**Figure 3.26.** Representation of the OD values obtained for each standard, A – blank (water) and H – atrazine concentration  $1000 \mu\text{g L}^{-1}$  obtained using different tracers (synthesized differently) and microtiter plate coated using the polyclonal antibody C193. T1: tBu/Et/C6; T2 - tBu/Et/SC3; T3: Et/iPr/SC3; T5: tBu/Cl/C6; T6: iPr/Et/C6 and T7: iPr/Cl/C6.....**86**

**Figure 3.27.** Calibration curves obtained for direct ELISA using polyclonal antibody C193 and enzyme tracers produced with the 3 haptens T3: Et/i-Pr/SC3, T5: t-Bu/Cl/C6 and T7: i-Pr/Cl/C6. Y-axis corresponds to normalized OD according to the equation given in Section 3.1.3. Antibody dilution 1:5000; tracers dilution 1:5000.....**87**

**Figure 3.28.** Calibration curves obtained using different antibody and tracer dilutions for direct ELISA using polyclonal antibody C193 and enzyme tracers produced with the hapten T5: t-Bu/Cl/C6.....**88**

**Figure 3.29.** Calibration curve (pink squares) of ELISA ( $A = 0.697$ ;  $B = 0.776$ ;  $C = 0.036$ ;  $D = 0.058$ ;  $r = 0.9968$ ) and precision profile (black squares). The precision profile and the relative error of concentration were calculated in accordance with Ekins (1981).....**90**

**Figure 3.30.** Plot of concentration obtained for each well for  $0.03 \mu\text{g L}^{-1}$  (purple squares) and  $0.08 \mu\text{g L}^{-1}$  (blue squares) atrazine standards and the respective upper and lower limits of the allowed interval.....**91**

<b>Figure 3.31.</b> Plot of concentration obtained for each well for 0.3 $\mu\text{g L}^{-1}$ (purple squares) and 0.5 $\mu\text{g L}^{-1}$ (blue squares) atrazine standards and the respective upper and lower limits of the allowed interval.....	<b>91</b>
<b>Figure 3.32.</b> Influence of soil matrix on atrazine determination by ELISA. Shown are the calibration curves obtained from standard solutions prepared in raw extract matrix of the soil and in subsequent matrix dilution. Calibration curve obtained from calibrators prepared in ultrapure water is also shown for comparison.....	<b>94</b>
<b>Figure 4.1.</b> Solid state $^{13}\text{C}$ CPMAS-NMR spectra from soil samples supplied with different fertilizers (MIN – mineral fertilizer; FYM – farmyard manure; SLU – sewage sludge fertilizer; COM – compost fertilizer).....	<b>106</b>
<b>Figure 4.2.</b> FT-IR spectra of soil samples supplied with different fertilizers (MIN – mineral fertilizer; FYM – farmyard manure; SLU – sewage sludge fertilizer; COM – compost fertilizer).....	<b>109</b>
<b>Figure 4.3.</b> Selected zoomed parts of the spectra presented in Figure 4.2.: a) region 3050 to 2800 $\text{cm}^{-1}$ ; b) region 1900 to 900 $\text{cm}^{-1}$ (MIN – mineral fertilizer; FYM – farmyard manure; SLU – sewage sludge fertilizer; COM – compost fertilizer).....	<b>110</b>
<b>Figure 5.1.</b> Freundlich adsorption isotherms for atrazine in soils subjected to different fertilizations (MIN – mineral fertilizer; COM – compost fertilizer; FYM – farmyard manure; SLU – sewage sludge fertilizer; Error bars represent 95% confidence interval for n = 5)....	<b>124</b>
<b>Figure 5.2.</b> Freundlich sorption isotherms (filled symbol) and sequential desorption steps (open symbols) for atrazine onto soil subjected to compost fertilizations (COM).....	<b>128</b>
<b>Figure 5.3.</b> Freundlich sorption isotherms (filled symbol) and sequential desorption steps (open symbols) for atrazine onto soil subjected to farmyard manure (FYM).....	<b>128</b>
<b>Figure 5.4.</b> Freundlich sorption isotherms (filled symbol) and sequential desorption steps (open symbols) for atrazine onto soil subjected to sewage sludge fertilizer (SLU).....	<b>129</b>
<b>Figure 5.5.</b> Freundlich sorption isotherms (filled symbol) and sequential desorption steps (open symbols) for atrazine onto soil subjected to mineral fertilizer (MIN).....	<b>129</b>

<b>Figure 5.6.</b> Linear relationship between sorbed amount of EE2 and the square root of time (hours) needed to attain sorption equilibrium. Initial EE2 concentration 2 mg L <sup>-1</sup> . Soil sample fertilized with farmyard manure.....	<b>134</b>
<b>Figure 5.7.</b> Adsorption isotherms with fitting using Hill Equation; SLU, sewage sludge fertilizer; MIN, mineral fertilizer; FYM, farmyard manure; COM, compost from organic household waste; COM_LOI, composted soil submitted to loss on ignition.....	<b>135</b>
<b>Figure 5.8.</b> Association between two EE2 molecules: a) lowest energy co-conformation obtained in gas phase simulation; b) and c) co-conformations adopted during 5 ns of simulation in aqueous solution. Carbon, hydrogen and oxygen atoms are shown in grey, light grey and dark grey, respectively.....	<b>138</b>
<b>Figure 6.1.</b> Aerial photograph of North STP (adapted from SimRia, 2011); 1– Pre-treatment building; 2– Primary sedimentation; 3– Biological treatment; 4– Secondary sedimentation 5– Sludge thickening; 6– Primary digestion; 7– Sludge treatment building; 8 – Secondary digestion and gasometer; 9– Sludge silo; 10– Transformation point and workshop; 11– Offices.....	<b>150</b>
<b>Figure 6.2.</b> Photograph of North STP where A) biological treatment and B) secondary sedimentation occurs.....	<b>151</b>
<b>Figure 6.3.</b> Map and the bathymetry of the Ria de Aveiro lagoon. Sampling sites: S1 Barrinha de Mira; S2 Poço da Cruz; S3 Costa Nova; S4 Torreira; S5 Cais do Bico; S6 Cais da Fonte Nova; S7 Rossio Channel; S8 S. Roque Channel; S9 Rio Novo Príncipe; S10 Mataduços; S11 Vouga River; M1 and M2: mines; C1-C4: water collecting wells; RBF: water from riverine bank filtration system in Vouga river; W1: North STP; W2: South STP (Image adapted from Dias and Lopes, 2006b).....	<b>153</b>
<b>Figure 6.4.</b> Pictures of sampling sites. A: RBF - water from riverine bank filtration system on Vouga river; B: mine; C: Rossio Channel; D: Rio Novo Príncipe; E: North STP after primary treatment; F: North STP after secondary treatment.....	<b>154</b>
<b>Figure 6.5.</b> Evaluation of the organic matter effects on the ELISA calibration curves without sample buffer. Calibration curves obtained in the absence of organic matter and in the presence of 1, 10 and 20 mg L <sup>-1</sup> of HA.....	<b>158</b>

<b>Figure 6.6.</b> Evaluation of the organic matter effects on the ELISA calibration curves using sample buffer. Calibration curves obtained in the absence of organic matter and in the presence of 1, 10 and 20 mg L <sup>-1</sup> of HA.....	<b>160</b>
<b>Figure 6.7.</b> Calibration curve (pink squares) of ELISA (A = 0.513; B = 0.835; C = 0.043; D = 0.033; r = 0.998) and precision profile (black squares). The precision profile and determination of the relative error of concentration were calculated in accordance with Ekins (1981).....	<b>161</b>
<b>Figure 6.8.</b> Recovery rates for a 0.03 µg L <sup>-1</sup> atrazine standard with different HA concentrations (between 0.5 and 20 mg L <sup>-1</sup> ) (n=9) with (green bars) and without (pink bars) the use of the sample buffer.....	<b>162</b>
<b>Figure 6.9.</b> Recovery rates for a 0.03 µg L <sup>-1</sup> atrazine standard with different NaCl concentrations (between 10 and 30 g L <sup>-1</sup> ) (n=9) with (green bars) and without (pink bars) the use of the sample buffer.....	<b>163</b>
<b>Figure 6.10.</b> Recovery rates for a 0.3 µg L <sup>-1</sup> atrazine standard with different NaCl concentrations (between 10 and 30 g L <sup>-1</sup> ) (n=9) with (green bars) and without (pink bars) the use of the sample buffer.....	<b>163</b>
<b>Figure 6.11.</b> Calibration curves obtained using different antibody and tracer dilutions for direct ELISA for EE2 measurements.....	<b>166</b>
<b>Figure 6.12.</b> Calibration curve (pink squares) of ELISA (A = 1.360; B = 0.683; C = 0.729; D = 0.030; r = 0.999) and precision profile (black squares). The precision profile and determination of the relative error of concentration were calculated in accordance with Ekins (1981).....	<b>168</b>
<b>Figure 6.13.</b> Plot of concentration obtained for each well for 1 µg L <sup>-1</sup> EE2 standard and respective upper and lower limit for a 25% deviation.....	<b>169</b>
<b>Figure 6.14.</b> Evaluation of the organic matter effect on the ELISA calibration curve.....	<b>170</b>
<b>Figure 6.15.</b> Evaluation of the organic matter effect on the ELISA calibration curve in the presence of sample buffer.....	<b>172</b>

<b>Figure 6.16.</b> Calibration curve (pink squares) of ELISA ( $A = 0.574$ ; $B = 0.776$ ; $C = 1.610$ ; $D = 0.052$ ; $r = 0.998$ ) and precision profile (black squares). The precision profile and determination of the relative error of concentration were calculated in accordance with Ekins (1981).....	<b>173</b>
<b>Figure 6.17.</b> Recovery rates for a $1 \mu\text{g L}^{-1}$ EE2 standard with different HA concentrations (between $0.5$ and $20 \text{ mg L}^{-1}$ ) ( $n=9$ ) with (green bars) and without (pink bars) the use of sample buffer.....	<b>174</b>
<b>Figure 6.18.</b> Recovery rates for a $1 \mu\text{g L}^{-1}$ EE2 standard with different NaCl concentrations (between $10$ and $30 \text{ g L}^{-1}$ ) ( $n=9$ ) with (green bars) and without (pink bars) the use of the sample buffer.....	<b>175</b>
<b>Figure 6.19.</b> Plot of EE2 concentrations determined by ELISA without sample buffer after spiking a STP sample (pink squares) and a surface water sample (green diamonds) with three EE2 concentrations.....	<b>176</b>



# List of Tables

---

<b>Table I.I.</b> Molecular structure and some physicochemical properties of atrazine.....	<b>1</b>
<b>Table I.II.</b> Molecular structure and some physicochemical properties of EE2.....	<b>5</b>
<b>Table 1.1.</b> Summary of characteristics for comparison between MEKC and HPLC.....	<b>26</b>
<b>Table 2.1.</b> Statistical parameter ( $\pm$ standard errors) for typical analytical curves obtained by UV spectral deconvolution and by MEKC.....	<b>38</b>
<b>Table 2.2.</b> Mean ( $\pm$ standard errors) Freundlich $K_F$ and $N$ parameters for adsorption of atrazine onto a soil obtained by UVSD and MEKC.....	<b>40</b>
<b>Table 2.3.</b> Statistical parameter ( $\pm$ standard errors) for the analytical curves obtained by FSD for each soil sample used.....	<b>45</b>
<b>Table 2.4.</b> Recoveries results obtained for EE2 spiked into 0.01 mol L <sup>-1</sup> CaCl <sub>2</sub> and also into soil extract solution.....	<b>46</b>
<b>Table 3.1.</b> Schematic list of the synthesized tracers using different methodologies.....	<b>77</b>
<b>Table 3.2.</b> Parameter values obtained for the four-parametric logistic equation (4PL) using tracer T3: i-Pr/Et/SC3, T5: t-Bu/Cl/C6 and T7: i-Pr/Cl/C6 and polyclonal antibody C193.....	<b>86</b>
<b>Table 3.3.</b> Parameter values obtained for the four-parametric logistic equation (4PL) using different dilutions of polyclonal antibody C193 and tracer T3: i-Pr/Et/SC3.....	<b>89</b>
<b>Table 3.4.</b> Atrazine mean concentration and respective RSD for 4 standards (n = 32) .....	<b>92</b>
<b>Table 3.5.</b> Cross-reactivities (CR [%]) of some selected triazine herbicides and their main metabolites at the center points of their calibration curves.....	<b>93</b>
<b>Table 3.6.</b> Mean ( $\pm$ standard errors) Freundlich $K_F$ and $N$ parameters for adsorption of atrazine onto a luvisol soil amended with sewage sludge. Concentration measurements by ELISA and MEKC, respectively.....	<b>95</b>
<b>Table 4.1.</b> Influence of long-term application of different organic fertilizers and mineral fertilizer, respectively, on chemical soil parameters; (MIN – mineral fertilizer; FYM – farmyard manure; SLU – sewage sludge fertilizer; COM – compost fertilizer).....	<b>105</b>

<b>Table 4.2.</b> Relative area distribution (% of total spectrum area) of solid-state <sup>13</sup> C CPMAS-NMR spectra; (MIN – mineral fertilizer; FYM – farmyard manure; SLU – sewage sludge fertilizer; COM – compost fertilizer).....	<b>107</b>
<b>Table 4.3.</b> Calibration parameters for the eleven quantified phenolic compounds. Values are presented as average ± standard deviation ( <i>n</i> =3).....	<b>112</b>
<b>Table 4.4.</b> Phenolic compound contents of soil samples subjected to the application of different fertilizers. Values are presented as average ± standard deviation ( <i>n</i> =3).....	<b>112</b>
<b>Table 5.1.</b> Parameters of the Freundlich equation describing the adsorption isotherms of atrazine to the four soils samples used.....	<b>125</b>
<b>Table 5.2.</b> Correlation coefficients ( <i>r</i> ) between the parameter <i>K<sub>F</sub></i> or <i>K<sub>FOC</sub></i> and TOC or relative area distribution (% of total spectrum area) of solid-state <sup>13</sup> C CPMAS-NMR spectra.....	<b>126</b>
<b>Table 5.3.</b> Parameters of the Freundlich equation describing the desorption isotherms of atrazine to the four soils samples used (MIN – mineral fertilizer; SLU – sewage sludge fertilizer; FYM – farmyard manure; COM – compost fertilizer).....	<b>130</b>
<b>Table 5.4.</b> Parameters obtained for the adsorption isotherm fitting with Hill equation.....	<b>136</b>
<b>Table 5.5.</b> Correlation coefficients ( <i>r</i> ) between Parameter <i>K<sub>1</sub></i> or <i>K<sub>10c</sub></i> and TOC or Relative Area Distribution (Percent of Total Spectrum Area) of Solid-State <sup>13</sup> C CPMAS-NMR Spectra.....	<b>140</b>
<b>Table 6.1.</b> Parameter values obtained for the four-parametric logistic equation (4PL) using atrazine standards prepared with and without HA.....	<b>159</b>
<b>Table 6.2.</b> Parameters of linear regression for determination of atrazine recovery rates in surface and waste water.....	<b>164</b>
<b>Table 6.3.</b> Atrazine concentrations (± standard deviation).....	<b>165</b>
<b>Table 6.4.</b> Parameter values obtained for the 4PL equation using different dilutions of polyclonal antibody and tracer for EE2.....	<b>167</b>
<b>Table 6.5.</b> Cross-reactivities (CR, %) of some selected hormones at the center points of their calibration curves.....	<b>170</b>
<b>Table 6.6.</b> Parameter values obtained for the 4PL equation using EE2 standards prepared with and without HA.....	<b>171</b>
<b>Table 6.7.</b> EE2 concentrations (± standard deviation) detected in STP.....	<b>177</b>

# Abbreviations

---

4PL – Four-parameter logistic equation

Ab – Antibodies

AHI – Apparent Hysteresis Index

BSA – Bovine Serum Albumin

CE – Capillary Electrophoresis

COM – Soil fertilized with compost from organic household waste

COM\_LOI – soil fertilized with compost from organic household waste and subjected to loss on ignition

CPMAS-NMR – Cross-Polarization Magic-Angle Spinning Nuclear Magnetic Resonance

CR – Cross Reactivity

CV – Coefficient of Variation

CZE – Capillary Zone Electrophoresis

DAD – Diode Array Detector

DCC – *N,N'*-Dicyclohexylcarbodiimide

DMF – Dimethylformamide

DOC – Dissolved Organic Carbon

E1 – Estrone

E2 – 17 $\beta$ -estradiol

E3 – Estriol

EDCs – Endocrine Disrupting Compounds

EE2 – 17 $\alpha$ -ethinylestradiol

ELISA – Enzyme-Linked Immunosorbent Assay

EU – European Union

Fab – Fragment containing the antibody binding site

Fc – Fragment that crystallizes

FSD – Fluorescence Spectral Deconvolution

FT-IR – Fourier Transform Infrared Spectroscopy

FYM – Soil fertilized with farmyard manure

GC – Gas Chromatography

H/Cl/C6 – 2-[(1-carboxypent-5-yl)amino]-4-chloro-6-amino-1,3,5-triazine

HA – Humic Acids

HF – Hydrofluoric acid

HF-LPME – Hollow-Fiber Liquid Phase Microextraction

HOC – Hydrophobic Organic Compounds

HOP – Hydrophobic Organic Pollutants

HPLC – High Performance Liquid Chromatography

HRP – Horseradish Peroxidase

IBCF – Isobutylchloroformiate

Ig – Immunoglobulin

i-Pr/Cl/C6 – 2-[(1-carboxypent-5-yl)amino]-4-chloro-6-(isopropylamino)-1,3,5-triazine

i-Pr/Et/C6 – 2-[(1-carboxypent-5-yl)amino]-4-(ethylamino)-6-(isopropylamino)-1,3,5-triazine

i-Pr/Et/SC3 – 2-[(1-carboxyeth-2-yl)-thio]-4-(ethylamino)-6-(isopropylamino)-1,3,5-triazine

IS – Internal Standard

LC – Liquid Chromatography

Lin – Linearity

LOD – Limit Of Detection

LOI – Loss On Ignition

LOQ – Limit Of Quantification

LSC – Liquid Scintillation Counting

MEKC – Micellar Electrokinetic Chromatography

MIN – Soil fertilized with mineral fertilizer

MIPs – Molecularly Imprinted Polymers

MS – Mass Spectrometer

NHS – N-hydroxysuccinimide

NMR – Nuclear Magnetic Resonance Spectroscopy

OC – Organic Carbon

OD – Optical Density

PBS – Phosphate Buffer Solution

PCBs – Polychlorinated Biphenyls

ppb – part per billion

PPCPs – Pharmaceuticals and Personal Care Products

ppm – part per million

ppt – part per trillion

REF – Reference Spectra

RIA – Radioimmunoassay

RSD – Relative Standard Deviation

RSD<sub>b</sub> – Relative Standard Deviation of the slope

RSWE – Raw soil water extract

RT – Room Temperature

S/V – Syringic-to-Vanillic unities

SDS – Sodium Dodecyl Sulphate

SLU – Soil fertilized with sewage sludge from municipal water treatment facilities

SOM – Soil Organic Matter

SPE – Solid Phase Extraction

STPs – Sewage Treatment Plants

t-Bu/Cl/C6 – 2-(tert-butylamino)-4-[(1-carboxypent-5-yl)amino]-6-chloro-1,3,5-triazine

t-Bu/Et/C6 – 2-(tert-butylamino)-4-[(1-carboxypent-5-yl)amino]-6-(ethylamino)-1,3,5-triazine

t-Bu/Et/SC3 – 2-(tert-butylamino)-4-[(1-carboxyeth-2-yl-)thio]-6-(ethylamino)-1,3,5-triazine

THF – Tetrahydrofuran

TMB – Tetramethylbenzidine

TN – Total Nitrogen

TOC – Total Organic Carbon

TOM – Total Organic Matter

UV-Vis – Ultraviolet-visible

UVSD – Ultraviolet Spectral Deconvolution

# Symbols

---

$a$  – is the intercept of the regression line

$A$  – OD of a zero control

$a_i$  – contribution coefficient of the  $i^{\text{th}}$  REF in the linear combination

$b$  – empirical parameter which varies with the degree of heterogeneity

$B$  – slope at the inflection point

$B/B_0$  – Normalized OD

$C$  – concentration value at the inflection point

$C_e$  – solution-phase concentration ( $\text{mg L}^{-1}$ )

$C_{\text{standard}}$  – parameter of the 4PL giving the antigen concentration at the inflection point

$C_{\text{test}}$  – parameter of the 4PL giving the antigen concentration of the cross-reacting compound at its inflection point

$D$  – OD at a standard excess

$K_1$  – affinity parameter

$K_{1\text{OC}}$  – normalized affinity parameter ( $K_1$ ) to total organic content

$K_d$  – sorption partition coefficient ( $\text{L kg}^{-1}$ )

$K_F$  – Freundlich distribution coefficient ( $\text{mg kg}^{-1})(\text{mg L}^{-1})^{-N}$ )

$K_{F\text{des}}$  – Desorption Freundlich distribution coefficient ( $\text{mg kg}^{-1})(\text{mg L}^{-1})^{-N}$ )

$K_{F\text{OC}}$  – Freundlich distribution coefficient normalized to soil organic carbon ( $\text{mg kg}^{-1})(\text{mg L}^{-1})^{-N}$ )

$K_{F\text{OCdes}}$  – Desorption Freundlich distribution coefficient normalized to soil organic carbon ( $\text{mg kg}^{-1})(\text{mg L}^{-1})^{-N}$ )

$K_{\text{OC}}$  – sorption coefficient normalized to soil organic carbon ( $\text{L Kg}^{-1}$ )

$K_{\text{OW}}$  – octanol-water partition coefficient

$\text{Log } K_{\text{OW}}$  – logarithmic octanol-water partition coefficient

Mol. Wt. – Molecular weight ( $\text{g mol}^{-1}$ )

$N$  – isotherm nonlinearity factor

$N_{\text{des}}$  – Desorption isotherm nonlinearity factor

OD – optical density

$p$  – number of reference spectra

$Q_e$  – total sorbed concentration ( $\text{mg Kg}^{-1}$ )

$Q_{\max}$  – maximum adsorption capacity ( $\text{mg kg}^{-1}$ )

$r$  – error of restitution at each wavelength or correlation coefficient

REF – Reference Spectra

$S_s$  – Sample absorbance

$S_w$  – Solubility in water ( $\text{mg L}^{-1}$ )

$Sy/x$  – statistical parameter which estimates the random errors in the y-axis (signal)

# PART I

## INTRODUCTION



# INTRODUCTION



## INTRODUCTION

---

---

Hydrophobic organic pollutants .....	1
Atrazine .....	1
Description .....	1
Sources of pesticides in waters.....	2
17 $\alpha$ -Ethinylestradiol .....	4
Description .....	4
Sources of estrogens in waters .....	5
Fate of HOP in the environment.....	6
References .....	11

## Hydrophobic organic pollutants

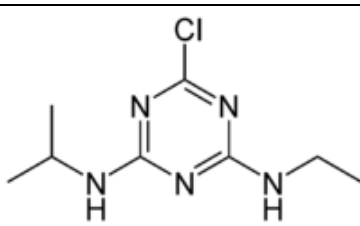
Large amounts of chemicals reach the environment via industrial discharges and/or other anthropogenic activities. Hydrophobic organic compounds (HOC), due to their physicochemical properties and their ability to accumulate in the environment, attract the attention of a large number of researchers. Among the so-called hydrophobic organic pollutants (HOP), herbicides, such as atrazine, have been frequently found in soils and surface waters (Yang et al., 2009). Estrogenic compounds, such as 17 $\alpha$ -ethinylestradiol, with low water solubility, and thus considered non-polar hydrophobic compounds, have also been detected, becoming problematic for the environment (Feng et al., 2010).

### *Atrazine*

#### *Description*

Atrazine (2-chloro-4-ethylamino-6-isopropylamino-s-triazine) is a weak-base selective herbicide with a pKa of 1.7 (Table I.I.) used to control annual grasses and broadleaf weeds in corn and sorghum (Mersie and Seybold, 1996; Smith et al., 2003).

**Table I.I.** Molecular structure and some physicochemical properties of atrazine

	Atrazine
Structure <sup>a</sup>	
Mol. Wt. (g mol <sup>-1</sup> ) <sup>a</sup>	215.7
$S_w$ (mg L <sup>-1</sup> ) <sup>a</sup> at 20 °C	33
Log $K_{ow}$ <sup>a</sup>	2.34
Vapour Pressure (mm Hg) <sup>b</sup> at 20 °C	$2.89 \times 10^{-7}$

<sup>a</sup>Prata et al., 2003

<sup>b</sup>Kovaios et al., 2006

Atrazine is relatively hydrophobic presenting a logarithmic octanol-water partition coefficient ( $\log K_{ow}$ ) of 2.34 and a relatively low solubility ( $33 \text{ mg L}^{-1}$ ). From properties presented in Table I.I., it may also be concluded that atrazine is a compound with low volatility.

When applied in agricultural fields it is adsorbed mainly by the shoots and then by the roots and its mechanism of action is based on the inhibition of photosynthesis by binding to specific sites within the plant's chloroplasts and preventing electron transport process (Kovaios et al., 2006; Nemeth-Konda et al., 2002). Even though this herbicide has been banned in some countries due to its resistance against chemical and biological degradation, and therefore accumulate in the environment (Celano et al., 2008), the application is yet allowed in many countries (more than 80) to control weeds. It is still one of the most widely used herbicides, with a worldwide production of over 70 million kg annually (Ben-Hur et al., 2003; Yang et al., 2009). As a result of its extensive use, atrazine and metabolites have been detected at alarmingly high concentrations in soils, groundwater, rivers and lakes (Celano et al., 2008), being one of the most important pollutants found in groundwater of many countries (Correia et al., 2007). The Directive 98/83/EC has set the maximum concentration of atrazine to  $0.1 \text{ } \mu\text{g L}^{-1}$  and the total concentration for all pesticides to  $0.5 \text{ } \mu\text{g L}^{-1}$  in what concerns to quality of the water for human consumption (Kovaios et al., 2006). Atrazine was banned in the European Union (EU) in 2004 (Directive 2004/248/CE) because of its persistent groundwater contamination (Ackerman, 2007). In the United States, however, atrazine is one of the most widely used herbicides, where nearly 30 million kg is applied each year (Yang et al., 2009). Several effects of atrazine have been reported, such as increase risk of cancer in humans, induce several hormonal disturbances in amphibians and tumors in rats. However, these are still controversial conclusions (Kovaios et al., 2006; Yang et al., 2009).

### *Sources of pesticides in waters*

Pesticides have been found in water samples, and even in ground waters, at high concentrations (Loos et al., 2010). Many of these substances are introduced into the

aquatic system through different pathways. The reduction of water contamination by pesticides is only possible if such pathways are known.

Different possibilities are illustrated on Figure I.I. Pesticides can be used either on agriculture or in urban areas. One of the important pathways for pesticide transport is the spray drift during application, surface runoff and leaching during rain events into aquatic systems (Figure I.I., source 1). If farmers are not careful during critical operations, such as filling of sprayers, washing of measuring utilities, disposal of packing material or unused products and cleaning of spraying equipment, they can cause an immediate input of pesticides into the sewerage, septic tank or surface waters (Figure I.I., source 2). Most of pesticides are not significantly eliminated in sewage treatment plants (STPs) and usually end up on effluents' receiving waters.

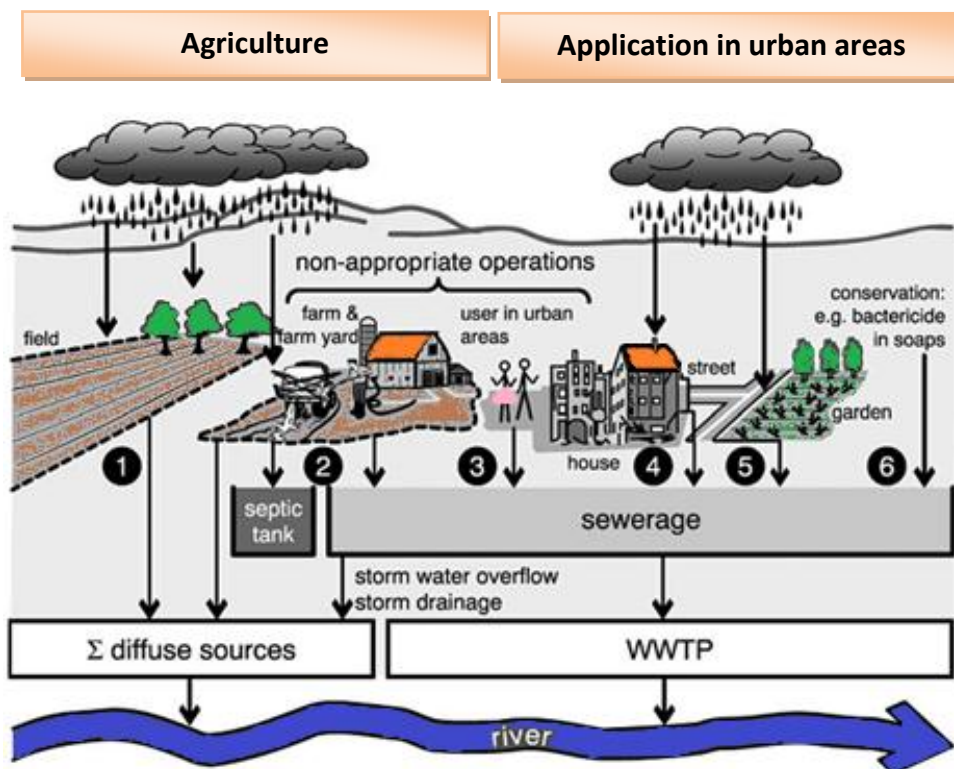


**Figure I.I.** Major pathways for pesticide transport into waters (Gerecke et al., 2002)

Contamination caused by application on urban areas has almost the same causes as the ones described above. Inappropriate operations performed, for example, by gardeners (Figure I.I., source 3), or pesticides present in building materials to prevent

biological deterioration (Figure I.I., source 4) can be leached during rain events and end up on sewage treatment plants or surface waters. Pesticides applied on lawns, streets, places or roads that are prone to be flushed into sewerage during rain events, are also pathways for pesticide contamination (Figure I.I., source 5). Another source of contamination can occur by products for protection of materials, like bactericide used in soaps that end-up in STPs (Figure I.I., source 6).

### *17 $\alpha$ -Ethinylestradiol*

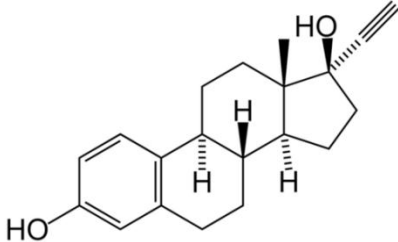
#### *Description*

Recently, has been a growing concern about the harmful effects of endocrine disrupting chemicals (EDCs) on the reproduction and development of animals and humans, becoming important the study of their persistence in the environment (Hildebrand et al., 2006). EDCs have been defined as “exogenous agents that interfere with the production, release, transport, metabolism, binding action or elimination of the natural hormones in the body (of a human and/or wildlife species) responsible for the maintenance of homeostasis and the regulation of development process” (Lee et al., 2003). Natural estrogens, such as 17 $\beta$ -estradiol (E2), estrone (E1) and estriol (E3), are predominantly female hormones, biologically active steroid hormones, mainly excreted by humans, but also by livestock (*e.g.* animal manure) and wildlife (Fan et al., 2007; Feng et al., 2010; Ying et al., 2002; Yu et al., 2004). 17 $\alpha$ -ethinylestradiol (EE2), presented in Table I.II., is a manufactured pharmaceutical chemical used for birth control and medical treatments of cancer, hormonal imbalance, osteoporosis, and other ailments (Yu et al., 2004).

Physicochemical properties, such as low water solubility, high log  $K_{OW}$  values and low vapour pressure demonstrate the hydrophobic nature, high sorption potential and low volatility, respectively, of this compound. When present in soils, the behaviour and fate of such compounds is determined by their physicochemical properties. High log  $K_{OW}$  values (greater than 4.0) promote high sorption potential of the compound, log  $K_{OW}$  > 2.5 and <

4.0 yields medium sorption potential, and  $\log K_{ow} < 2.5$  yields low sorption potential (Jones-Lepp and Stevens, 2007).

**Table I.II.** Molecular structure and some physicochemical properties of EE2<sup>c</sup>

	<b>17<math>\alpha</math>-ethinylestradiol</b>
<b>Structure</b>	
<b>Mol. Wt. (g mol<sup>-1</sup>)</b>	296.4
<b>S<sub>w</sub> (mg L<sup>-1</sup>)</b>	4.8
<b>Log K<sub>ow</sub></b>	4.15
<b>Vapour Pressure (mm Hg) at 20 °C</b>	4.15 x 10 <sup>-11</sup>

<sup>c</sup>Adapted from Ying et al., 2002

### *Sources of estrogens in waters*

Estrogens are compounds of great concern since they can bioaccumulate mainly in the bile and in ovaries of aquatic organisms exposed to contaminated water (Hintemann et al., 2006). These natural and synthetic compounds have gained attention due to their occurrence not only in municipal wastewater, but also in surface and groundwater (Ying et al., 2002).

All humans and animals can excrete hormone steroids from their bodies that will end up in the environment through sewage discharge and animal waste disposal (Ying et al., 2002). Usually they are released in urine as conjugated glucuronides or sulphate complexes (Feng et al., 2010) which are rapidly cleaved and metabolized during transport and treatment of domestic waste, releasing the fully potent hormones with sewage sludge (Emmerik et al., 2003). Women typically excrete 0.5 to 5  $\mu\text{g day}^{-1}$  (up to 400  $\mu\text{g}$

day<sup>-1</sup> for pregnant women), but hormone steroids are also excreted by men. The excretion rate of E1, an important pregnancy estrogen and E2 metabolite, is between 3 and 20 µg day<sup>-1</sup>, while for E3 is up to 64 µg day<sup>-1</sup> (Racz and Goel, 2010). The daily excretion of EE2 was estimated as being 35 µg day<sup>-1</sup> (Ying et al., 2002). STPs are not designed to remove estrogens or other micropollutants, thus estrogens that are not degraded during wastewater treatment processes are released into the environment in the effluent (Racz and Goel, 2010). From STPs two products are obtained: one is the liquid effluent and the other is the sludge. The liquid effluent is usually discharged into surface waters or, in some cases, used for irrigation. Sludge, on the other hand, can be disposed in the form of soil amendment or fertilizer. Such disposal can result in leaching of residues present in the sludge into the ground water. Studies have shown that the disposal of animal manures, waste water and sewage sludge to agricultural land can lead to the contamination, by E2 and EE2, of surface and groundwaters (Stumpe and Marschner, 2009). Although the concentrations observed were extremely low (ng L<sup>-1</sup>) when compared to other anthropogenic organic contaminants, these compounds are extremely potent (Sarmah et al., 2008), particularly EE2 with an estrogenic potency about ten times that of natural hormones. EE2 has been detected in effluents of different STPs (up to 94 ng L<sup>-1</sup>) (Feng et al., 2010; Stumpe and Marschner, 2009; Yu et al., 2004) and in surface waters (up to 7 ng L<sup>-1</sup>) (Sarmah et al., 2008).

## Fate of HOP in the environment

---

Aquatic environment is particularly sensitive to pollution, thus drinking water and aquatic organisms also pose a direct threat to human health. The prediction of the aquatic fate of HOP and their distribution in the environment is, therefore, of great importance. Most of these compounds have very low solubility in water (Shim et al., 2007). The water phase is energetically unfavorable for hydrophobic pollutants, thus these tend to associate with organic phases, such as sediments and biological tissues, or to escape from the aqueous phase to the atmosphere.



Once the organic pollutants reach the soil they can undergo different pathways: volatilize, leach and degrade, among others (Haygarth and Jarvis, 2002), which are represented on Figure I.II.

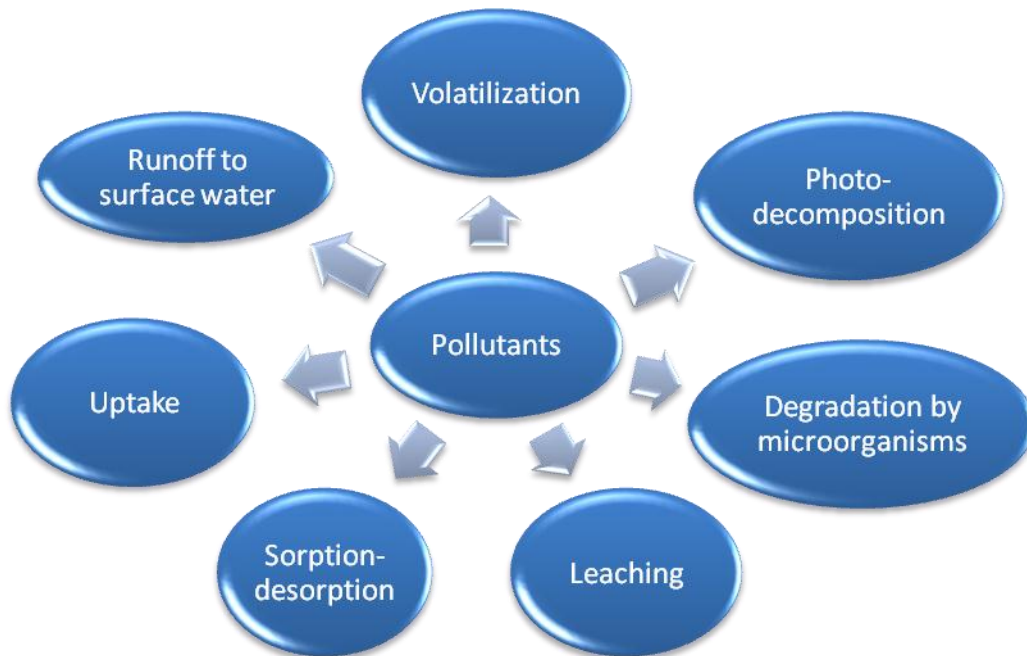


**Figure I.II.** Pathways of pollutants degradation and transport.

Pollutants that enter the soil environment are subjected to a diversity of degradative and transport processes. Environmental transport of pollutants comprises distinct processes, such as volatilization, leaching and surface runoff. Pesticides are immediately subjected to volatilization during the application to agricultural soils. Pollutants, when present in soils, can volatilize at higher rates if they are not adsorbed to soil (Haygarth and Jarvis, 2002).

Another fundamental soil process, related to environmental transport of pollutants, is the leaching, where pollutants, dissolved or suspended in soil solution phase, are lost from the soil profile by the action of percolating liquid water. This process has been identified as the major cause of groundwater contamination. Surface runoff has also impact on surface and groundwater quality and has been a major concern for the last three decades (Haygarth and Jarvis, 2002). Pesticide runoff includes dissolved, suspended

particulate and sediment-adsorbed pesticide that is transported by water from a polluted surface (Haygarth and Jarvis, 2002).

Pollutants degradation is one of the main loss processes of pollutants in the soil. These losses may be due to biological degradation, where microorganisms mediate the transformation process of the pollutant. However, abiotic degradation is often seen as the prevailing process for pollutants degradation and includes hydrolysis, oxidation-reduction and photolysis. Hydrolytic degradation occurs in soil pore water or on surface of clay minerals, while photolysis is due to their exposure to radiation. Although photolysis was not considered, initially, as an important degradation pathway for pollutants in soils, recently, evidence suggests that photoinduced transformations can, in some cases, be significant (Haygarth and Jarvis, 2002).

Retention phenomena comprise several mechanisms, such as sorption-desorption, sequestration and bound residue formation. Sorption and sequestration can be considered as one process, initially fast and then gradually becoming slower. Sorption comprises the physical-chemical processes throughout the pollutant molecule present in soil solution binds to the soil particles. This binding can vary from complete reversibility to total irreversibility and interaction may be physical (van der Waals forces) and/or chemical (electrostatic interactions). One or more of these mechanisms can occur simultaneously. Chemical reactions often lead to the formation of stable chemical linkages, increasing the persistence of the residue in soil. On the other hand, this linkage cause the loss of the chemical identity and, from a toxicological point of view, will lead to: a decrease of its availability to interact with biota; a reduction in the toxicity of the compound; and an immobilization of the compound, thereby reducing its leaching and transport. The extent of sorption depends on several factors, such as properties of soil and pollutant, which include size, shape, configuration, molecular structure, chemical functions, solubility and polarity, among others (Correia et al., 2007; Haygarth and Jarvis, 2002).

Sorption of a pollutant can be divided into fast and slow phase. The fast sorption phase includes surface processes, while slow phase refers to diffusion into and out of humic substances. A very slow diffusion also leads to a very slow release of the pesticide,

since desorption from the interior of the humic matrix back into solution is more difficult. When desorption is too slow, the pollutant can be considered to be irreversibly adsorbed and named “bound residue” fraction. Bound residues formation plays an important role in the dissipation of hydrophobic pollutants in soil (Prata et al., 2003). Sorption isotherms are mathematical equations widely used to describe retention of chemicals by soils components (Hinz, 2001). A difference between sorption-desorption isotherms is a phenomenon frequently observed and denominated hysteresis. Sorption-desorption hysteresis is usually explained by irreversible chemical binding, sequestration of a solute into specific components of the soil organic matter, or entrapment of the solute into microporous structures or into the soil organic matter (SOM) matrix (Chefetz et al., 2004).

Pollutant sorption to soil is often described using a distribution constant of the pollutant between the soil and the solution at the equilibrium,  $K_d$  (Spark and Swift, 2002). The partition coefficient describes an apparent sorption constant that is time, soil, and pesticide dependent (Smith et al., 2003). High values of  $K_d$  indicate a strong adsorption of the pollutant by the soil, and also resistant to microbial degradation (Wauchope et al., 2002). Generally, there is a high correlation between organic matter content of the soils and the distribution constant. Thus, such observation leads to a theory that soil organic matter is the main sorbent in soils, attracting pollutants because they are normally non-polar organic molecules. Therefore, the soil organic carbon sorption coefficient ( $K_{OC}$ ) of a pesticide is calculated by dividing a measured  $K_d$  in a specific soil, by the organic carbon fraction of the same soil.  $K_{OC}$  values are universally measures of the relative potential mobility of pesticides in soils (Wauchope et al., 2002). Nonionic organic compounds isotherms are usually considered to be linear. However, when sorption is evaluated over a large range of concentrations, the partitioning coefficient of most pollutants is not linear. In order to describe more accurately the isotherms of most organic compounds curvilinear equations should be used (Smith et al., 2003). Simple equations, such as Freundlich or Langmuir isotherms are commonly used to describe the sorption data. Every time such equations are not accurate describing the data, more complex expressions are available. Although Freundlich equation is the most commonly used, it is

crucial to choose an equation that is suitable for the data obtained experimentally (Hinz, 2001).

As mentioned before, even though there are several factors affecting mobility and fate of organic pollutants in the environment, sorption and desorption are considered the most important ones. A fundamental understanding of adsorption-desorption mechanisms is therefore critical for accurate predictions of the environmental load of released HOP and the effective implementation of remedial strategies. In this work, analytical techniques able to follow adsorption-desorption mechanisms of organic pollutants to soil organic matter were developed and optimized. Such techniques were then applied to follow the phenomena in different soil samples (previously characterized) and correlations between content and type of organic matter and its sorption capacity were evaluated.

## References

---

- Ackerman, F., **2007**. The economics of atrazine. *Int. J. Occup. Environ. Health* 13, 441-449.
- Ben-Hur, M., Letey, J., Farmer, W.J., Williams, C.F., Nelson, S.D., **2003**. Soluble and solid organic matter effects in atrazine adsorption in cultivated soils. *Soil Sci. Soc. Am. J.* 67, 1140-1146.
- Celano, G., Šmejkalová, D., Spaccini, R., Piccolo, A., **2008**. Interactions of three s-triazines with humic acids of different structure. *J. Agr. Food Chem.* 57, 7360-7366.
- Chefetz, B., Bilkis, Y.I., Polubesova, T., **2004**. Sorption-desorption behaviour of atrazine and phenylurea herbicides in Kishon river sediments. *Water Res.* 38, 4383-4394.
- Correia, F.V., Macrae, A., Guilherme, L.R.G., Langenbach, T., **2007**. Atrazine sorption and fate in a Ultisol from humid tropical Brazil. *Chemosphere* 67, 847-854.
- Emmerik, T.V., Angove, M.J., Johnson, B.B., Wells, J.D., Fernandes, M.B., **2003**. Sorption of 17 $\beta$ -estradiol onto selected soil minerals. *J. Colloid Interf. Sci.* 266, 33-39.
- Fan, Z., Casey, F.X.M., Hakk, H., Larsen, G., **2007**. Persistence and fate of 17 $\beta$ -estradiol and testosterone in agricultural soils. *Chemosphere* 67, 886-895.
- Feng, Y., Zhang, Z., Gao, P., Su, H., Yu, Y., Ren, N., **2010**. Adsorption behaviour of EE2 (17 $\alpha$ -ethinylestradiol) onto the inactivated sewage sludge: Kinetics, thermodynamics and influence factors. *J. Hazard. Mater.* 175, 970-976.
- Gerecke, A.C., Schärer, M., Singer, H.P., Müller, S.R., Schwarzenbach, R.P., Sägesser, M., Ochsenein, U., Popow, G., **2002**. Sources of pesticides in surface waters in Switzerland: pesticide load through waste water treatment plants – current situation and reduction potential. *Chemosphere* 48, 307-315.
- Haygarth, P.M., Jarvis, S.C., **2002**. Agriculture, hydrology and water quality. *CABI Publishing*, First Edition, Wallingford, UK.
- Hildebrand, C., Londry, K.L., Farenhorst, A., **2006**. Sorption and desorption of three endocrine disruptors in soils. *J. Environ. Sci. Heal. B* 41, 907-921.
- Hintemann, T., Schneider, C., Schöler, H.F., Schneider, R.J., **2006**. Field study using two immunoassays for the determination of estradiol and ethinylestradiol in the aquatic environment. *Water Res.* 40, 2287-2294.
- Hinz, C., **2001**. Description of sorption data with isotherm equations. *Geoderma* 99, 225-243.
- Jones-Lepp, T.L., Stevens, R., **2007**. Pharmaceuticals and personal care products in biosolids/sewage sludge: interface between analytical chemistry and regulation. *Anal. Bioanal. Chem.* 387, 1173-1183.

- Kovaios, I.D., Parakeva, C.A., Koutsoukos, P.G., Payatakes, A.C., **2006**. Adsorption of atrazine on soils: Model study. *J. Colloid Interf. Sci.* 299, 88-94.
- Lee, L.S., Strock, T.J., Sarmah, A.K., Rao, P.S.C., **2003**. Sorption and dissipation of testosterone, estrogens, and their primary transformation products in soils and sediment. *Environ. Sci. Technol.* 37, 4098-4105.
- Loos, R., Locoro, G., Comero, S., Contini, S., Schwesig, D., Werres, F., Balsaa, P., Gans, O., Weiss, S., Blaha, L., Bolchi, M., Gawlik, B.M., **2010**. Pan-European survey on the occurrence of selected polar organic persistent pollutants in ground water. *Water Res.* 44, 4115-4126.
- Mersie, W., Seybold, C., **1996**. Adsorption and desorption of atrazine, deethylatrazine, deisopropylatrazine, and hydroxyatrazine on levy wetland soil. *J. Agr. Food Chem.* 44, 1925-1929.
- Nemeth-Konda, L., Füleky, G., Morovjan, G., Csokan, P., **2002**. Sorption behaviour of acetochlor, atrazine, carbendazim, diazinon, imidacloprid and isoproturon on Hungarian agricultural soil. *Chemosphere* 48, 545-552.
- Prata, F., Lavorenti, A., Vanderborght, J., Burauel, P., Vereecken, H., **2003**. Miscible displacement, sorption and desorption of atrazine in a Brazilian oxisol. *Vadose Zone J.* 2, 728-738.
- Racz, L., Goel, R.K., **2010**. Fate and removal of estrogens in municipal wastewater. *J. Environ. Monit.* 12, 58-70.
- Sarmah, A.K., Northcott, G.L., Scherr, F.F., **2008**. Retention of estrogenic steroid hormones by selected New Zealand soils. *Environ. Int.* 34, 749-755.
- Shim, J.-K., Park, I.-S., Kim, J.-Y., **2007**. Use of amphiphilic polymer nanoparticles as a nano-absorbent for enhancing efficiency of micelle-enhanced ultrafiltration process. *J. Ind. Eng. Chem.* 13, 917-925.
- Smith, M.C., Shaw, D.R., Massey, J.H., Boyette, M., Kingery, W., **2003**. Using nonequilibrium thin-disc and batch equilibrium techniques to evaluate herbicide sorption. *J. Environ. Qual.* 32, 1393-1404.
- Spark, K.M., Swift, R.S., **2002**. Effect of soil composition and dissolved organic matter on pesticide sorption. *Sci. Total Environ.* 298, 147-161
- Stumpe, B., Marschner, B., **2009**. Factors controlling the biodegradation of 17 $\alpha$ -estradiol, estrone and 17 $\alpha$ -ethinylestradiol in different natural soils. *Chemosphere* 74, 556-562.
- Wauchope, R.D., Yeh, S., Linders, J.B.H.J., Kloskowski, R., Tanaka, K., Rubin, B., Katayama, A., Kordel, W., Gerstl, Z., Lane, M., Unsworth, J.B., **2002**. Pesticide soil sorption parameters: theory, measurement, uses, limitations and reliability. *Pest. Manag. Sci.* 58, 419-445.

- Yang, W., Zhang, J., Zhang, C., Zhu, L., Chen, W., **2009**. Sorption and resistant desorption of atrazine in typical Chinese soils. *J. Environ. Qual.* 38, 171-179.
- Ying, G.-G., Kookana, R.S., Ru, Y.-J., **2002**. Occurance and fate of hormone steroids in the environment. *Environ. Int.* 28, 545-551.
- Yu, Z., Xiao, B., Huang, W., Peng, P., **2004**. Sorption of steroid estrogens to soils and sediments. *Environ. Toxicol. Chem.* 23, 531-539.

# PART II

DEVELOPMENT OF ANALYTICAL PROCEDURES TO  
FOLLOW SORPTION BEHAVIOUR OF HOP ONTO SOILS



# CHAPTER 1

**ATRAZINE ANALYSIS BY CAPILLARY ELECTROPHORESIS**



## CHAPTER 1

### ATRAZINE ANALYSIS BY CAPILLARY ELECTROPHORESIS\*

1.1.	Introduction.....	15
1.2.	Experimental procedure.....	16
1.2.1.	Soil sample .....	16
1.2.2.	Instrumentation .....	17
1.2.3.	Buffer and standards.....	18
1.2.4.	Capillary column conditioning.....	18
1.2.5.	Separation conditions .....	19
1.2.6.	Suitability of the MEKC method .....	19
1.2.7.	Adsorption studies .....	19
1.2.8.	Data analysis.....	20
1.3.	Results and discussion.....	21
1.3.1.	Electrophoretic separation of atrazine .....	21
1.3.2.	Performance of the method.....	22
1.3.3.	Preliminary studies and kinetics experiments .....	23
1.3.4.	Adsorption studies .....	24
1.3.5.	MEKC and HPLC methods – comparison .....	26
1.4.	Conclusions.....	28
1.5.	References.....	29

\* Diana L.D. Lima, Guillaume L. Erny, Valdemar I. Esteves, 2009. Application of MEKC to the monitoring of atrazine sorption behaviour on soils. *Journal of Separation Science* 32, 1-6.

## 1.1. Introduction

---

The most common method for direct measurement of the adsorption coefficient of an organic molecule, such as atrazine and EE2, in soils is batch experiments. The main advantage of this method is the possibility of separate soil and solution, obtaining a large volume of solution for analysis. Also, the method can be easily used for routine laboratory following the OECD Guideline TG 106 (2000). Several studies have been made to follow the sorption-desorption phenomena using different analysis techniques such as liquid scintillation (LSC) (Ben-Hur et al., 2003; Mbuya et al., 2001; Prata et al., 2003; Smith et al., 2003), or high performance liquid chromatography (HPLC) (Chefetz et al., 2004; Drori et al., 2005; Park et al., 2004; Socías-Vicianá et al., 1999). However, LSC is a very expensive technique, not available in every laboratory and HPLC presents several drawbacks in what concerns to dissolved organic matter. Filipe et al. (2007) refer that, for studying the adsorption of a fungicide either on soils or on humic substances, a clean-up procedure is required before analysis by an HPLC-UV to remove interferences such as organic matter from solution. Organic matter present in samples can compete for the binding sites of the stationary phase and also be co-eluted with atrazine. Another consequence of the organic matter presence is the possibility of a decrease in the signal-noise ratio, due to the noise increase. Some components of organic matter can attach strongly to the stationary phase, in a way that is necessary to increase the analysis time to remove them from the column, with the possibility of damaging the column. The calcium chloride present in the adsorption studies, used to simulate soil conditions, can also suffer a decrease in solubility, when in contact with the eluent, and precipitate, damaging the column. The need of a clean-up procedure before HPLC analysis becomes clear in the work of Gao et al. (1998) and Nemeth-Konda et al. (2002) that used solid phase extraction (SPE) before the analysis by HPLC.

Capillary electrophoresis (CE) is a family of techniques that use buffer-filled capillary tube, typically 10 to 100  $\mu\text{m}$  of internal diameter and 40 to 100 cm in length. Electrophoresis is a separation technique based on the differential rate of migration of charged molecules in a buffer solution, when submitted to an electrical field. In capillary zone electrophoresis (CZE) the buffer composition is maintained constant throughout the

region of the separation and the applied potential causes the different ionic components of the mixture to migrate, according to each own mobility, and to separate into zones. CZE is suitable to separate charged molecules. However, when a surfactant, such as sodium dodecyl sulphate (SDS), is added to the buffer at a concentration level at which micelles are formed, separation of uncharged molecules becomes also possible. Micelles constitute a stable second phase, capable of absorbing nonpolar compounds into the hydrocarbon interior of the micelles. Thus, when a sample is introduced into this system, the components distribute themselves between the aqueous phase and the hydrocarbon phase in the interior of the micelles, migrating at different rates. Capillary electrophoresis carried out in the presence of micelles is termed micellar electrokinetic chromatography (MEKC) (Skoog et al., 1998). MEKC is now an accepted analytical separation technique that is routinely used in numerous fields (Silva, 2009; Terabe, 2009). The presented method has been applied by several authors in order to determine triazines in water samples (Martínez et al., 1996; Turiel et al., 2000), but there are possible new applications, as the one presented in this chapter. MEKC exhibit high efficiency, short analysis time, and a very low solvent consumption. However, one of the particular advantages of this technique, that seems particularly relevant here, is the possibility to inject complex matrixes (saliva, urine, plasma...) without (or with minimal) sample treatment (Lloyd, 2008). This is due to the absence of packing materials that are more prone to clogging or deterioration via permanent sorption. The aim of this work was to use this advantage to follow the adsorption phenomena of atrazine on soils without any clean-up procedures allowing (1) a higher throughput and (2) a higher accuracy by avoiding potential losses during the sample clean-up.

## 1.2. Experimental procedure

---

### *1.2.1. Soil sample*

Soil samples (0 - 30 cm) were collected 30 month after the last application of the organic fertilizers – from a long-term field experiment which was established in 1962 at

the experimental farm of INRES - Institute of Plant Nutrition, University of Bonn, on a luvisol derived from loess (17.8% clay, 76.3% silt, 5.9% sand) – following a cereal-root crop sequence. The treatments selected for the present investigations were: sewage sludge from municipal water treatment facilities ( $14.88 \text{ t ha}^{-1}$ ) (SLU), farmyard manure ( $9 \text{ t ha}^{-1}$ ) (FYM), compost from organic household waste ( $58 \text{ t ha}^{-1}$ ) (COM) and mineral fertilizer (MIN). These amounts (given on a dry weight basis) were applied every second year until 1997, then the amounts were changed to  $10 \text{ t ha}^{-1}$  sewage sludge and  $90 \text{ t ha}^{-1}$  compost once in 3 years. The organic fertilizers were incorporated into the whole ploughing depth of 30 cm. The application rates of FYM and MIN fertilizer were kept on the same level. The following mean amounts of mineral fertilizers were applied:  $120 \text{ kg/ha/year}$  N as ammoniumnitrate plus  $\text{CaCO}_3$ ,  $30 \text{ kg/ha/year}$  P as Superphosphate and  $150 \text{ kg/ha/year}$  K as KCl. From 1997, the crop sequence is cereal-cereal-root crop. The soil possesses over a high microbial activity so that the decomposition of the applied organic fertilizers is assumed to be no longer than 9 month. That means that soil samples were free of organic particles, which could be derived from the applied organic fertilizers. The particle size of applied compost was  $< 20 \text{ mm}$ , of sewage sludge  $< 10 \text{ mm}$  and of farmyard manure (straw component)  $< 40 \text{ mm}$ . Because of the fast decomposition of the organic fertilizers, caused by the high microbial activity, no organic substrates could be detected in the soil samples. Soil samples were air-dried and passed through a sieve, mesh size 2 mm.

### *1.2.2. Instrumentation*

All experiments were performed using a Beckman P/ACE MDQ capillary electrophoresis system equipped with a diode array detector. Separation was carried out on an uncoated fused silica capillary 60 cm total length (50 cm effective length to the detector),  $75 \mu\text{m}$  internal diameter and  $375 \mu\text{m}$  of external diameter.

### 1.2.3. Buffer and standards

The run buffer used, after a previous optimization step, was prepared weekly with 10 mmol L<sup>-1</sup> of NaH<sub>2</sub>PO<sub>4</sub>·2H<sub>2</sub>O (99% m/m, Fluka) and 50 mmol L<sup>-1</sup> SDS (99% m/m, Panreac) in ultra-pure water, obtained from a Milli-Q Millipore (Millipore Q plus 185) system; pH was adjusted to 8.50 ± 0.02 with 1 mol L<sup>-1</sup> NaOH. A stock of internal standard (IS) solution, ethylvanillin (99% m/m, Aldrich) was prepared dissolving in a small quantity of acetonitrile and completing with ultra-pure water. A stock standard solution of atrazine (97.4% m/m, Riedel-de Haën) was prepared in methanol and standard solutions were prepared, from stock solution, in order to obtain a final concentration ranging from 0.3 mg L<sup>-1</sup> and 10 mg L<sup>-1</sup>. All the dilutions were made using a CaCl<sub>2</sub> solution in order to have the same concentration of CaCl<sub>2</sub> present in the samples. The internal standard was added to sample and standards in order to obtain a final concentration of 1.67 mg L<sup>-1</sup>. Buffer, standards and samples were filtered through a 0.22 µm filter (Millex-GV from Millipore) before analysis.

### 1.2.4. Capillary column conditioning

New capillaries were conditioned with 1 mol L<sup>-1</sup> NaOH for 7 min, followed by 60 min, with 0.1 mol L<sup>-1</sup> NaOH, 5 min with ultra-pure water and finally 5 min with run buffer. The capillary was conditioned every day with 1 mol L<sup>-1</sup> NaOH, 0.1 mol L<sup>-1</sup> NaOH, ultra-pure water and run buffer for 5 min each, in order to obtain a stable baseline and to improve the repeatability of the retention time. Before each injection the capillary was flushed with 0.1 mol L<sup>-1</sup> NaOH for 3 min, ultra-pure water for 2 min and run buffer for 3 min. All flushing was performed using 137.9 KPa pressure.

### *1.2.5. Separation conditions*

Standards and samples were injected using 3447 Pa pressure during 3 s. Electrophoretic separations were carried out at positive power supply of 20 kV for 7 min, maintaining the capillary temperature at 25 °C, resulting in a current of ~60 µA.

Atrazine and ethylvanillin were monitored by detection at 214 nm or in the range 190-600 nm for multi-wavelength detecting. The run buffer vials were used for six consecutive injections before the replacement with new vials.

### *1.2.6. Suitability of the MEKC method*

In order to test the suitability of the method, an appropriate volume of 0.01 mol L<sup>-1</sup> CaCl<sub>2</sub> was agitated with a soil sample for 4 h. The mixture was centrifuged and the aqueous phase filtered. A certain volume of the atrazine stock solution was added and the solution analysed by MEKC. One blank, without the test substance, was included in order to check for artefacts in the analytical method and also for matrix effects. The recovery rates were calculated and, according to the OECD guideline 106 (2000), an analytical method was considered suitable if the obtained recoveries were between 90 and 110%. All experiments were made in triplicate.

### *1.2.7. Adsorption studies*

The key parameters that can influence the accuracy of sorption measurements include: a) the adsorption on the surface of the test vessel and stability of the test substance; b) the capacity to attain the sorption equilibrium.

Some information on the adsorption of atrazine on the surface vessels, as well as its stability, can be obtained analysing the control samples when subjected to the same process of the samples. Control samples containing 2 mg L<sup>-1</sup> of atrazine were agitated in a head-over-head shaker for 24 h, using polypropylene and glass tubes, then centrifuged at 4000 rpm for 20 min and analysed, using ethylvanillin as IS. An atrazine solution of 2 mg L<sup>-1</sup>

<sup>1</sup> was kept at 4 °C in the dark and used as a reference standard. Recovery rates were obtained for both polypropylene and glass centrifuge tubes.

Kinetics experiments were made in order to evaluate the sorption contact time between the solution and the soil using batch experiments. Tubes with soil solution ratio 1:2 were agitated in a head-over-head shaker during a variable period of time between 0 and 48 h, centrifuged and analysed, as described previously. All experiments were made in triplicate.

Adsorption isotherms of atrazine were made using the batch equilibration technique (OECD, 2000). Five atrazine concentrations ranging from 2 to 10 mg L<sup>-1</sup>, were prepared in 0.01 mol L<sup>-1</sup> calcium chloride solution. A 4 mL aliquot of each concentration of atrazine solution was added to each soil in order to obtain a final 1:2 soil/solution ratio. Five replicates were made for each concentration. The tubes were agitated 24 h at 20±1 °C, centrifuged and analysed, as described previously.

### *1.2.8. Data analysis*

The Freundlich parameters ( $K_F$  and  $N$ ) were calculated from the fitting, of non-linear regression of the equation  $Q_e = K_F \times C_e^N$ , to the experimental data, where  $Q_e$  is the total sorbed concentration (mg kg<sup>-1</sup>),  $C_e$  is the solution-phase concentration (mg L<sup>-1</sup>),  $K_F$  (mg kg<sup>-1</sup>)(mg L<sup>-1</sup>)<sup>-N</sup> is the Freundlich distribution coefficient, and  $N$  is the isotherm nonlinearity factor. Isotherms were plotted ( $Q_e$  vs.  $C_e$ ), and  $K_F$  and  $N$  were obtained after performing the non-linear regression. The  $K_F$  values were normalized to the organic carbon (OC) content of the soil to obtain  $K_{FOC}$ . The sorption partition coefficient ( $K_D$ ) was calculated ( $Q_e = K_D \times C_e$ ) for the linear portion of the isotherms (up to a sorbed atrazine concentration of 4 mg kg<sup>-1</sup> soil). The  $K_D$  values were normalized to the OC level of the soil to obtain  $K_{OC}$ .



## 1.3. Results and discussion

---

### *1.3.1. Electrophoretic separation of atrazine*

Optimization of the separation between atrazine and matrix components, such as calcium chloride and dissolved organic matter, was evaluated using buffer with SDS concentrations between 0 and 50 mmol L<sup>-1</sup>.

Several authors used surfactants to improve separation efficiency (Khrolenko et al., 2002; Martínez et al., 1996; Santos et al., 2007; Turiel et al., 2000). The MEKC allows better separations for both charged and neutral small molecules. However, the major drawback in MEKC is the low system loadability. Accordingly, in some cases the technique must be coupled with a pre-concentration step in order to decrease the limit of detection (LOD). As mentioned before, MEKC separation is based on the different distribution of the analytes between the buffer and the micelles (Turiel et al., 2000).

Figure 1.1. shows different chromatograms from aqueous soil samples obtained from a 0.01 mol L<sup>-1</sup> CaCl<sub>2</sub> solution agitated with a soil sample during 24h, centrifuged, filtered and spiked with atrazine. It is possible to observe that retention time of atrazine increases with the increase of SDS concentration. This effect is not so evident in the retention of ethylvanillin, used as internal standard. The increase in SDS concentration until 50 mmol L<sup>-1</sup> leads to an improvement of separation between atrazine and some peaks attributed to dissolve organic matter. Without SDS, atrazine and dissolved organic matter are the first to arrive at the detector, forming only one narrow peak. As can be seen in the chromatogram, under optimized conditions, a stable base line and a good resolution between peaks can be achieved with 50 mmol L<sup>-1</sup> of SDS in buffer solution.

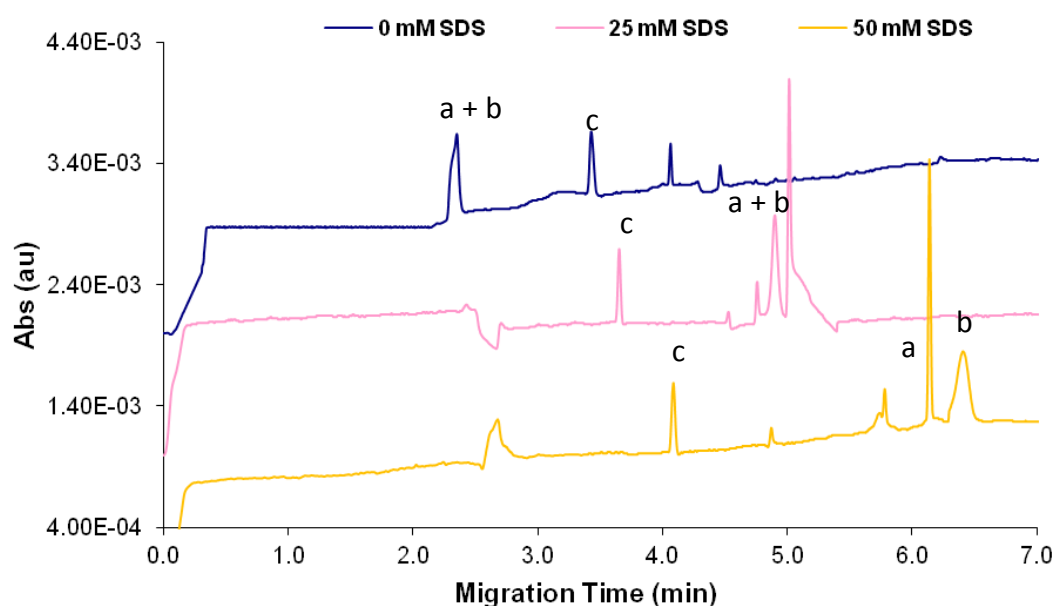


**Figure 1.1.** Chromatogram of an aqueous soil solution from a batch experimental sample (a) matrix peak; (b) atrazine (c) ethylvanillin analysed using buffers with 0, 25 and 50 mmol L<sup>-1</sup> SDS.

### 1.3.2. Performance of the method

Linearity, limit of detection and repeatability were calculated from the data obtained using six standards, with the concentrations ranging between 0.3 and 10 mg L<sup>-1</sup>. Each experiment was done in triplicate. The repeatability of retention time and related areas were measured via the relative standard deviation (RSD). The low RSD values obtained for both retention time (below 1%) and peak area (below 2.8%) prove the good repeatability of the method.

The linearity (Lin) response was calculated by the equation:

$$\text{Lin (\%)} = 100 - \text{RSD}_b$$

where RSD<sub>b</sub> is the relative standard deviation of the slope. Correlation coefficient and linearity obtained were 1.000 and 99.963%, respectively, suggesting that the method used is linear for the range of concentration tested. The limit of detection was 0.26 mg L<sup>-1</sup>

<sup>1</sup>. The suitability of the method was also tested by the results obtained when samples were spiked with known volumes of an atrazine stock solution. Recovery rates were calculated by dividing the obtained concentration by the expected one. All recoveries obtained were between 95 and 100%, and as mentioned earlier recoveries between 90 and 110% can be considered suitable (OECD, 2000).

### 1.3.3. Preliminary studies and kinetics experiments

Preliminary studies on the adsorption of atrazine to the test vessel showed that, results obtained when using glass or polypropylene tubes, were not statistically different (data not shown) and also showed no apparently adsorption of the test substance to both of the test vessels. Based on these results it was decided to use polypropylene tubes. In what concerns to the stability of the atrazine, results showed that no degradation during the period of the experimental procedure was observed.

Also preliminary experiments were conducted to find the time needed to attain equilibrium. The rate of the adsorption process is very high and adsorbed atrazine on soil reaches 70% of its final amount almost instantly. A plateau value was attained in about 8 h as may be seen in Figure 1.2.

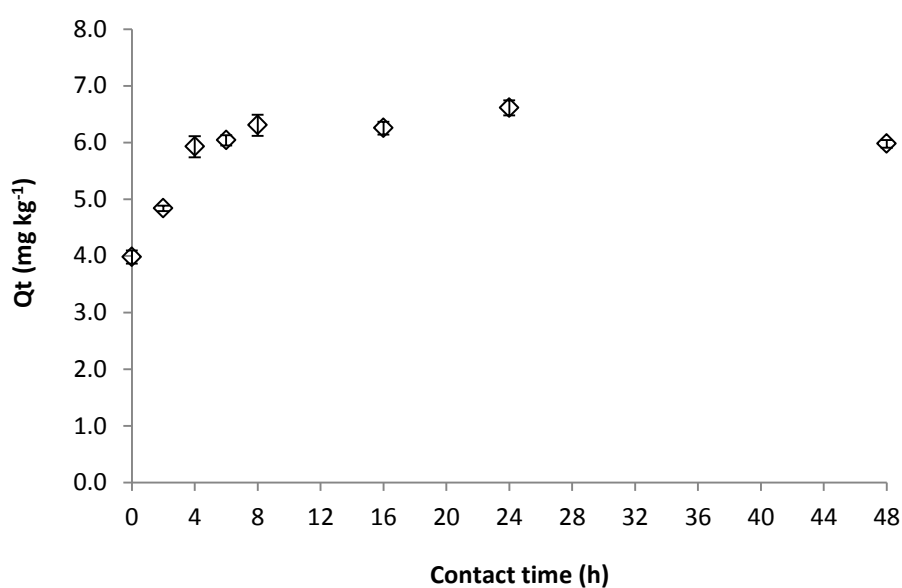


**Figure 1.2.** Influence of contact time on atrazine adsorption on soil. Initial atrazine concentration 5 mg L<sup>-1</sup> in 0.01 mol L<sup>-1</sup> CaCl<sub>2</sub> (n = 3); Qt – adsorbed concentration at time t (h) (mg kg<sup>-1</sup>).

Observing the figure is possible to see a typical adsorption experimental result, in which pesticide, initially in the solution phase, undergoes initial rapid adsorption followed by a slow approach to equilibrium.

#### *1.3.4. Adsorption studies*

Adsorption isotherms, obtained by plotting the amount of atrazine adsorbed per unit weight of soil at equilibrium ( $Q_e$ , mg Kg<sup>-1</sup>) versus the amount of chemical per volume of solution at equilibrium ( $C_e$ , mg L<sup>-1</sup>) for each soil, is shown in Figure 1.3.

The Freundlich equation has reasonably described the adsorption of atrazine on the soil samples used with correlation coefficients ranging from 0.966 to 0.995. Freundlich adsorption coefficient is an empirical constant of the Freundlich model, expressing soil sorbent capacity (sorption isotherm slope) for a given range of atrazine concentration where greater the value, stronger is the adsorption. The low  $K_F$  value between 0.81 and 2.20 mg kg<sup>-1</sup> (mg L<sup>-1</sup>)<sup>-N</sup> obtained reflects low adsorption capacity and is commonly associated with greater permeability and higher leaching (Correia et al., 2007). The values were similar to the ones mentioned for atrazine by Nemeth-Konda et al. (2002) (0.91), by Correia et al. (2007) (0.99) and also by Boivin et al. (2005) with values ranging from 1.3 and 6.3, depending on soil characteristics.

Sorption isotherm was non-linear, exhibiting N value from 0.57 and 0.79. Values lower than 1 indicated that the percentage of atrazine adsorbed to the soil decreased as the initial concentration increased. Similar results were obtained by Nemeth-Konda et al. (2002) (0.49). The  $K_F$  values normalized to the organic carbon (OC) level of the soil,  $K_{FOC}$ , obtained were from 65.5 and 117.3 and relates de  $K_F$  value with the organic carbon content present in the soil sample used on the sorption study.

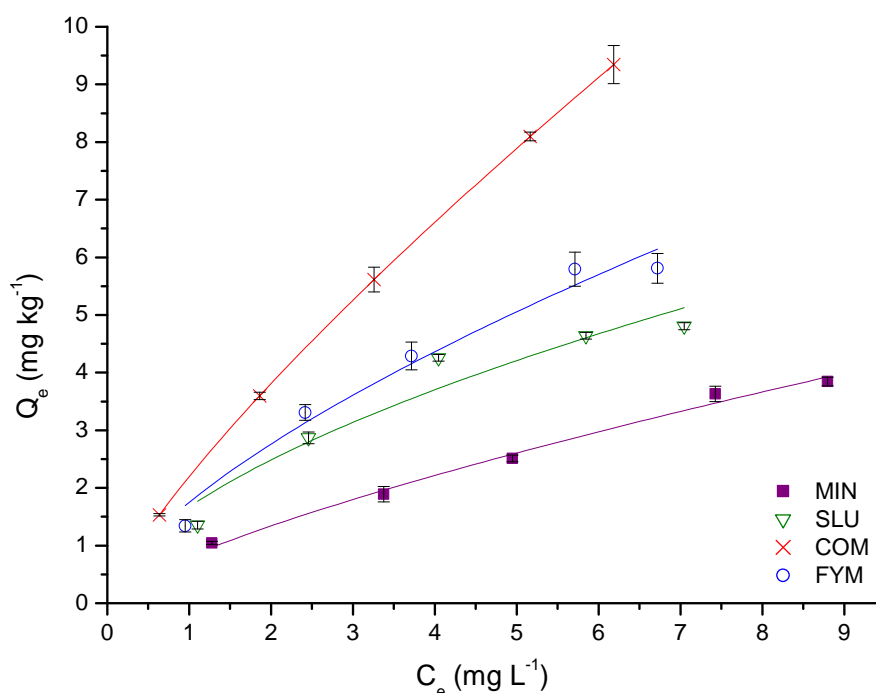


**Figure 1.3.** Freundlich adsorption isotherms for atrazine in soils subjected to different fertilizations (MIN – mineral fertilizer; COM – compost fertilizer; FYM – farmyard manure; SLU – sewage sludge fertilizer; Error bars represent 95% confidence interval for  $n = 3$ ).

The sorption partition coefficient ( $K_D$ ) was calculated for the linear portion of the isotherms (up to a sorbed atrazine concentration of  $4 \text{ mg kg}^{-1}$  soil) obtaining values between 0.54 and 1.73 and the  $K_D$  values normalized to the OC level of the soil,  $K_{OC}$ , between 43.6 and 83.5. The organic carbon normalized adsorption coefficient  $K_{OC}$  represents a single value which characterises the partitioning mainly of non-polar organic chemicals between organic carbon in the soil or sediment and water. The adsorption of these chemicals is correlated with the organic content of the soil; thus  $K_{OC}$  values depend on the specific characteristics of the humic fractions which differ considerably in sorption capacity, due to differences in origin, genesis, etc (OECD, 2000). For both  $K_{OC}$  and  $K_{FOC}$  our results confirm the expected interactions previously described by Chefetz et al. (2004) and also by Drori et al. (2005) presenting similar values.

### 1.3.5. MEKC and HPLC methods – comparison

On Table 1.1. is presented a summary comparing both methods in discussion.

Considering the sample preparation and the time of analysis, each sample replicate analysed by HPLC is higher than 30 min, which include a previous step of solid phase extraction (SPE) (for aqueous soil solutions). Additionally, the HPLC method requires near 30 min of column conditioning before starting up the analysis (Santos et al., 2005). Using MEKC the time for each sample replicate analysis, including capillary conditioning, is about 15 min.

**Table 1.1.** Summary of characteristics for comparison between MEKC and HPLC

	Estimated time of analysis	Cost/sample replicate	Environmental problem	LOD	Linearity	RSD (%)	Recovery
CE	15 min	Low	n.a.	0.26 mg L <sup>-1</sup>	Up to 10 mg L <sup>-1</sup>	< 3%	93.4 to 100.2%
HPLC <sup>a</sup>	30 min	High	Use of organic solvents	0.2 μg L <sup>-1</sup>	Up to 5 mg L <sup>-1</sup>	< 5%	92.9 to 101.7%

<sup>a</sup> Data obtained from Nemeth-Konda et al., 2002

To calculate the cost/sample replicate for HPLC we must consider the price of the SPE cartridge, the price of the solvents and the price for the development of the SPE method, which will be surely higher than 5€/sample replicate. For MEKC analysis the reagents used are usually cheaper than solvents for HPLC and much smaller volumes are used. Another important factor to consider, when comparing these two methodologies, is the environmental impact of each one. The need to use a lot of organic solvents associated to the HPLC application (Santos et al., 2005) is a major disadvantage, when comparing to MEKC that makes no use of this type of solvents.

The disposal of organic solvents is a global environmental problem in terms of risk to humans and environmental impact. Reducing or, if possible, eliminating the use of organic solvents is, therefore, an important goal in terms of environmental conservation, human health and the economy. The overall sample preparation time and analysis, as well as the consumption of toxic organic solvents and the cost/sample replicate is minimized using MEKC. On the other hand, in what concerns to method performance, although repeatability and recoveries were similar, the HPLC method is more sensitive, having detection limit of  $0.2 \mu\text{g L}^{-1}$ , probably due to SPE application.

## 1.4. Conclusions

---

The proposed micellar electrokinetic chromatography method has proven to be useful and a valid alternative, to the more common SPE-HPLC procedure, for the routine determination of the atrazine in complex matrix samples, containing  $0.01 \text{ mol L}^{-1} \text{ CaCl}_2$  and dissolved organic matter, without the need to clean up the sample using a solid phase extraction method or other cleaning methods. Other advantages of the proposed MEKC method respect to the more established HPLC methodologies for the same application can be obtained in terms of equipment simplicity and operation price, less time-consuming (no need to clean the sample and time of analysis inferior to 15 min), less sample manipulation and less waste generation.

The Freundlich parameters ( $K_F$  and  $N$ ) obtained for the adsorption isotherms, using MEKC, were similar to the ones presented by other authors using different methodologies, such as HPLC and LSC. This work demonstrates that MEKC can be used to monitor atrazine sorption behaviour on soils through its adsorption isotherms, in order to evaluate the persistence and transport of these pesticides through soils.



## 1.5. References

---

- Ben-Hur, M., Letey, J., Farmer, W.J., Williams, C.F., Nelson, S.D., **2003**. Soluble and solid organic matter effects in atrazine adsorption in cultivated soils. *Soil Sci. Soc. Am. J.* 67, 1140-1146.
- Boivin, A., Cherrier, R., Schiavon, M., **2005**. A comparison of five pesticides adsorption and desorption processes in thirteen contrasting field soils. *Chemosphere* 61, 668-676.
- Chefetz, B., Bilkis, Y.I., Polubesova, T., **2004**. Sorption-desorption behaviour of atrazine and phenylurea herbicides in Kishon river sediments. *Water Res.* 38, 4383-4394.
- Correia, F.V., Macrae, A., Guilherme, L.R.G., Langenbach, T., **2007**. Atrazine sorption and fate in a Ultisol from humid tropical Brazil. *Chemosphere* 67, 847-854.
- Drori, Y., Aizenshtat, Z., Chefetz, B., **2005**. Sorption-Desorption behaviour of Atrazine in soils irrigated with reclaimed wastewater. *Soil Sci. Soc. Am. J.* 69, 1703-1710.
- Filipe, O.M.S., Vidal, M.M., Duarte, A.C., Santos, E.B.H., **2007**. A solid-phase extraction procedure for the clean up of thiram from aqueous solutions containing high concentrations of humic substances. *Talanta* 72, 1235-1238.
- Gao, J.P., Maguhn, J., Spitzauer, P., Kettrup, A., **1998**. Sorption of pesticides in the sediment of the Teufelsweiher pond (southern Germany) I: Equilibrium assessments, effect of organic carbon content and pH. *Water Res.* 32, 1662-1672.
- Khrolenko, M., Dzygiel, P., Wieczorek, P., **2002**. Combination of supported liquid membrane and solid-phase extraction for sample pretreatment of triazine herbicides in juice prior to capillary electrophoresis determination. *J. Chromatogr. A* 975, 219-227.
- Lloyd, D.K., **2008**. Capillary electrophoresis analysis of biofluids with a focus on less commonly analyzed matrices. *J. Chromatogr. B* 866, 154-166.
- Martínez, R.C., Gonzalo, E.R., Domínguez, A.I.M., Alvarez, J.D., Méndez, J.H., **1996**. Determination of triazine herbicides in water by micellar electrokinetic capillary chromatography. *J. Chromatogr. A* 733, 349-360.
- Mbuya, O.S., Nkedi-Kizza, P., Boote, K.J., **2001**. Fate of atrazine in sandy soil cropped with sorghum. *J. Environ. Qual.* 30, 71-77.
- Nemeth-Konda, L., Füleky, Gy., Morovjan, Gy., Csokan, P., **2002**. Sorption behaviour of acetochlor, atrazine, carbendazim, diazinon, imidacloprid and isoproturon on Hungarian agricultural soil. *Chemosphere* 48, 545-552.

- OECD, **2000**. Guideline TG 106. OECD Guideline for the Testing of Chemicals. Adsorption – Desorption using a Batch Equilibrium Method. *Organization for Economic Co-operation and Development* (OECD), Paris.
- Park, J.-H., Feng, Y., Cho, S.Y., Voice, T.C., Boyd, S.A., **2004**. Sorbed atrazine shifts into non-desorbable sites of soil organic matter during aging. *Water Res.* 38, 3881-3892.
- Prata, F., Lavorenti, A., Vanderborght, J., Burauel, P., Vereecken, H., **2003**. Miscible displacement, sorption and desorption of atrazine in a Brazilian oxisol. *Vadose Zone J.* 2, 728-738.
- Santos, L.B.O., Abate, G., Masini, J.C., **2005**. Application of sequential injection–square wave voltammetry (SI–SWV) to study the adsorption of atrazine onto a tropical soil sample. *Talanta* 68, 165-170.
- Santos, S.M., Duarte, A.C., Esteves, V.I., **2007**. Development and application of a capillary electrophoresis based method for the assessment of monosaccharide in soil using acid hydrolysis. *Talanta* 72, 165-171.
- Scherer, H.W., Goldbach, H.E., Clemens, J., **2003**. Potassium dynamics in the soil and yield formation in a long-term field experiment. *Plant Soil Environ.* 49, 531-535.
- Silva, M., **2009**. Micellar electrokinetic chromatography: Methodological and instrumental advances focused on practical aspects. *Electrophoresis* 30, 50-64.
- Skoog, D.A., Holler, F.J., Nieman, T.A., **1998**. Principles of instrumental analysis. *Saunders College Publishing*, 5<sup>th</sup> Edition, Florida, USA.
- Smith, M.C., Shaw, D.R., Massey, J.H., Boyette, M., Kingery, W., **2003**. Using nonequilibrium thin-disc and batch equilibrium techniques to evaluate herbicide sorption. *J. Environ. Qual.* 32, 1393-1404.
- Socias-Viciano, M.M., Fernández-Pérez, M., Villafranca-Sánchez, M., González-Pradas, E., Flores-Céspedes, F., **1999**. Sorption and leaching of atrazine and MCPA in natural and peat-amended calcareous soils from Spain. *J. Agric. Food Chem.* 47, 1236-1241.
- Terabe, S., **2009**. Capillary separation: Micellar electrokinetic chromatography. *Annu. Rev. Anal. Chem.* 2, 99-120.
- Turiel, E., Fernández, P., Pérez-Conde, C., Cámara, C., **2000**. Trace-level determination of triazines and several degradation products in environmental waters by disk solid-phase extraction and micellar electrokinetic chromatography. *J. Chromatogr. A* 872, 299-307.

# CHAPTER 2

**SPECTRAL DECONVOLUTION TO FOLLOW SORPTION  
BEHAVIOUR OF ORGANIC POLLUTANTS**



## CHAPTER 2

### Spectral deconvolution to follow sorption behaviour of organic pollutants\*

2.1.	Introduction.....	31
2.2.	Principle of spectral deconvolution.....	32
2.3.	UVSD for atrazine .....	34
2.3.1.	Experimental procedure.....	34
2.3.1.1	Soil sample .....	34
2.3.1.2	Instrumentation .....	34
2.3.1.3	Adsorption studies .....	34
2.3.1.4	MEKC analysis .....	35
2.3.1.5	UV determination .....	35
2.3.2.	Results and discussion.....	36
2.3.2.1	UV Spectral deconvolution method.....	36
2.3.2.2	Analytical curves by UVSD and MEKC.....	37
2.3.2.3	Adsorption experiments – Evaluation of the analytical methods .....	38
2.4.	Fluorescence SD for EE2 .....	40
2.4.1.	Experimental procedure.....	40
2.4.1.1	Soil sample .....	40
2.4.1.2	Instrumentation .....	40
2.4.1.3	Fluorescence spectra acquisition.....	41
2.4.1.4	Adsorption studies .....	42
2.4.2.	Results and discussion.....	43
2.4.2.1	Fluorescence spectral deconvolution method .....	43
2.4.2.2	Evaluation of the deconvolution method .....	45
2.4.2.3	Adsorption experiments .....	46
2.5.	Conclusions.....	50
2.6.	References.....	51

\*Diana L.D. Lima, Carla Patrícia Silva, Guillaume L. Erny, Valdemar I. Esteves, 2010. Comparison between MEKC and UV spectral deconvolution to follow sorption experiment in soil. *Talanta* 81, 1489-1493.

\*Diana L.D. Lima, Vânia Calisto, Valdemar I. Esteves, 2011. Adsorption behaviour of 17 $\alpha$ -ethynylestradiol onto soils followed by fluorescence spectral deconvolution. *Chemosphere* 84, 1072-1078.

## 2.1. Introduction

---

HPLC is an official method for monitoring sorption-desorption phenomena of several hydrophobic organic pollutants onto soils (Chefetz et al., 2004; Drori et al., 2005; Emmerik et al., 2003; Feng et al., 2010; Lee et al., 2003; Park et al., 2004; Robinson and Hellou, 2009; Sarmah et al., 2008; Socias-Viciano et al., 1999; Sun et al., 2007; Yu et al., 2004). As referred in chapter 1, this method requires a long sample preparation due to clean-up procedure needed before analysis by an HPLC-UV to remove interferences, such as the ones derived from the presence of organic matter in solutions. Several other techniques have been used to follow the sorption-desorption phenomena such as liquid scintillation (Ben-Hur et al., 2003; Caron et al., 2010; Fan et al., 2007; Mbuya et al., 2001; Prata et al., 2003; Smith et al., 2003; Stumpe and Marschner, 2007, 2009, 2010). However, LSC requires an appropriate apparatus to read radioactivity as well as radiolabeled chemicals that are rather expensive. Others, such as MEKC, developed in the previous chapter (Lima et al., 2009), and voltammetry (Santos et al., 2005) can still be costly and/or time consuming. The need of a faster, easier and less expensive technique, to follow sorption phenomena, seems to be a necessity.

UV spectral deconvolution (UVSD) is a multiwavelength deterministic or semi-deterministic procedure with UV spectrum exploitation based on the fact that the UV spectrum of a sample is a linear combination of pre-selected representative absorption spectra, called reference spectra (REF), and that the combination of the pre-defined reference spectra allows the restitution of the shape of the UV spectrum of any unknown sample (Coulomb et al., 2006; Hassouna et al., 2007; Nam et al., 2008). This approach was first developed by Thomas et al. (1993) for estimation of several wastewater parameters. Coulomb et al. (2006) and Escalas et al. (2003) used UVSD to determine total and dissolved organic carbon (TOC, DOC) in water samples. Moreover, Hassouna et al. (2007) used this approach for quantification of water extractable organic carbon and nitrate concentrations in soil water extracts. Nam et al. (2008) also used this method to quantify nitrate but this time in vegetables. Because of the growing concern about water pollution and the need of a fast, easy and low cost determination procedure, recently UVSD was applied to monitor and detect EDCs in natural water (Kibbey et al., 2009).

Atrazine absorbs in the UV region, which make UV spectrophotometry an attractive method for quantification. However, the fact that atrazine is present in a complex matrix which also absorb in the same region, creates the need to use the UVSD. On the other hand, EE2 presents a low UV light absorbance, but a high fluorescence capacity. Thus, seems reasonable to apply the same UVSD principle, but using EE2 fluorescence emission spectra.

The aim of this work was to (1) apply the UVSD to monitor the adsorption of atrazine to a soil sample and compare the results with the ones obtained with the MEKC method already optimized and (2) develop a fluorescence spectral deconvolution (FSD) to follow adsorption of EE2 onto soil samples.

## 2.2. Principle of spectral deconvolution

---

The principle of application of the UVSD approach, subject of some publications (Coulomb et al., 2006; Hassouna et al., 2007; Nam et al., 2008; Thomas et al., 1993, 1996; Escalas et al., 2003; Kibbey et al., 2009), relies on the assumption that any unknown UV spectrum can be substituted by a linear combination of a small number of well defined and representative spectra, the REF.

UVSD is a multiwavelength approach based on a procedure of matrix algebra where each spectrum corresponds to a linear combination of a small number  $p$  of reference spectra. In the model, the coefficients  $a_i$  of the linear combination are calculated by the resolution of a system based on the following relation established for each wavelength:

$$S_s = \sum_{i=1}^p a_i REF_i(\lambda) \pm r$$

where,  $S_s$  is the sample absorbance,  $REF_i(\lambda)$  is the absorbance of the  $i^{\text{th}}$  REF at each wavelength  $\lambda$ ,  $a_i$  is the contribution coefficient of the  $i^{\text{th}}$  REF in the linear combination,  $p$  is the number of reference spectra and  $r$  is the error of restitution at each  $\lambda$  (Coulomb et al., 2006; Hassouna et al., 2007; Nam et al., 2008).

When applied to determine HOP concentration present in solution, after the sorption equilibrium is reached, the UV spectrum of such sample is a linear combination of three reference spectra:

$$S_s = a_1 REF_1(\lambda) + a_2 REF_2(\lambda) + a_3 REF_3(\lambda) \pm r$$

where  $S_s$  is the sample absorbance,  $REF_1(\lambda)$  is the absorbance of the 1<sup>st</sup> REF (raw soil water extract, RSWE) at each wavelength  $\lambda$ ,  $a_1$  is the contribution coefficient of the 1<sup>st</sup> REF in the linear combination,  $REF_2(\lambda)$  is the absorbance of the 2<sup>nd</sup> REF (0.01 M calcium chloride solution) at each wavelength  $\lambda$ ,  $a_2$  is the contribution coefficient of the 2<sup>nd</sup> REF in the linear combination,  $REF_3(\lambda)$  is the absorbance of the 3<sup>rd</sup> REF (atrazine solution in 0.01M calcium chloride solution) at each wavelength  $\lambda$ ,  $a_3$  the contribution coefficient of the 3<sup>rd</sup> REF in the linear combination and  $r$  is the error of restitution at each  $\lambda$  (Coulomb et al., 2006; Hassouna et al., 2007; Nam et al., 2008).

Our primary goal is to determine the best set of parameters  $a_i$  such that the model predicts experimental values (sample absorbance for each wavelength) as accurately as possible. The associated contribution coefficients ( $a_i$ ) of each reference spectra in the linear combination are calculated using several complex programs. The regression output using the Microsoft Excel is very easy and fast, allowing anyone, with less knowledge about complex statistical programs, to perform the UV spectral deconvolution and to obtain the associated contribution coefficients ( $a_i$ ) of each reference spectra and also the deconvolution residuals.

The calibration of the method consists in a linear regression between HOP concentration and the coefficient  $a_3$  of the linear combination obtained for each standard prepared in soil water extract. Since spectrum depends of soil water extract, a calibration curve is needed every time a new soil sample is used. The coefficient  $a_3$  of the reference spectra in the unknown samples is calculated by spectral deconvolution and the corresponding concentration obtained using the calibration curve previously obtained.

The deconvolution residual (or error, or deviation) is the difference between the observed value (sample absorbance for each wavelength) and the corresponding value given by the regression function. If there is an obvious correlation between the residuals

and the independent variable  $x$  (wavelength), for example, residuals systematically increase with increasing  $x$ , it means that the chosen model is not adequate to fit the experiment. A plot of residuals is very helpful in detecting such a correlation.

## 2.3. UVSD for atrazine

---

### *2.3.1. Experimental procedure*

#### *2.3.1.1 Soil sample*

The soil samples used to test UVSD, as an analytical technique to follow sorption behaviour of atrazine, were the ones described on section 1.2.1.

#### *2.3.1.2. Instrumentation*

MEKC analyses were performed using a Beckman P/ACE MDQ capillary electrophoresis system equipped with a diode array detector. Separation was carried out on an uncoated fused silica capillary 60 cm total length (50 cm effective length to the detector), 75  $\mu\text{m}$  internal diameter and 375  $\mu\text{m}$  of external diameter. The UV measurements were performed using UV-Vis Shimadzu spectrophotometer.

#### *2.3.1.3. Adsorption studies*

Adsorption isotherm of atrazine was made using the batch equilibration technique (OECD, 2000). Five pesticide concentrations (2 to 10  $\text{mg L}^{-1}$ ) were prepared in 0.01  $\text{mol L}^{-1}$  calcium chloride. A 4 mL aliquot of each concentration of atrazine solution was added to 2 g of soil. Five adsorption experiments were made for each concentration. The tubes containing the mixtures were agitated, in a head over head shaker at 100 rpm for 24 h at  $20 \pm 1$   $^{\circ}\text{C}$ , centrifuged and the supernatant filtered and analysed. The equilibrium concentration after the sorption experiment was determined using MEKC and UVSD and the Freundlich parameters ( $K_F$  and  $N$ ) were calculated from the fitting.



#### 2.3.1.4. MEKC analysis

All reagents used were of analytical grade and all working solutions were prepared in ultra-pure water, obtained from a Milli-Q Millipore (Millipore Q plus 185) system. A stock standard solution of atrazine (97.4%, Riedel-de Haën) was prepared in methanol and standard solutions were prepared by diluting this stock solution with  $0.01 \text{ mol L}^{-1} \text{ CaCl}_2$ . A stock of IS solution, ethylvanillin (99%, Aldrich) was prepared, dissolving in a small quantity of acetonitrile and completing with ultra-pure water. Run buffer was prepared weekly with  $10 \text{ mmol L}^{-1}$  of  $\text{NaH}_2\text{PO}_4 \cdot 2\text{H}_2\text{O}$  (99%, Fluka) and  $50 \text{ mmol L}^{-1}$  SDS (99%, Panreac) in ultra-pure water. Buffer pH was adjusted to  $8.50 \pm 0.02$  with  $1 \text{ mol L}^{-1}$  NaOH. Buffer, standards and samples were filtered through a  $0.22 \mu\text{m}$  filter (Millex-GV from Millipore) before analysis.

After adsorption experiment, samples were filtered through a  $0.22 \mu\text{m}$  filter (Millex-GV from Millipore), IS was added and analysed directly by MECK as described previously (Chapter 1). Standards, with concentrations ranging from  $0.3$  to  $10 \text{ mg L}^{-1}$ , and samples were injected using  $3447 \text{ Pa}$  pressure during  $3 \text{ s}$ . Electrophoretic separations were carried out at positive power supply of  $20 \text{ kV}$  for  $7 \text{ min}$ , maintaining the capillary temperature at  $25 \text{ }^\circ\text{C}$ , resulting in a current of  $\sim 60 \mu\text{A}$ . Atrazine and ethylvanillin were monitored by detection at  $214 \text{ nm}$  or in the range  $190\text{-}600 \text{ nm}$  for multi-wavelength detection. The run buffer vials were used for six consecutive injections before the replacement with new vials.

#### 2.3.1.5. UV determination

Standards, with concentrations ranging from  $0.1$  to  $10 \text{ mg L}^{-1}$ , for UV determination were prepared in the raw soil water extract containing  $0.01 \text{ mol L}^{-1} \text{ CaCl}_2$ . UV absorbance reference spectra ( $\text{REF}_1$ ,  $\text{REF}_2$ ,  $\text{REF}_3$ ) were registered for the RSWE, for the  $0.01 \text{ mol L}^{-1} \text{ CaCl}_2$  and for an atrazine solution in  $0.01 \text{ mol L}^{-1} \text{ CaCl}_2$ , respectively. Ammonium hydroxide was added to standards, samples and reference solutions in order to obtain  $0.1 \text{ mol L}^{-1}$  as final concentration and all of them were diluted 5 times prior to analysis, resulting in a calibration curve from  $0.1$  to  $2 \text{ mg L}^{-1}$ . Ammonium hydroxide was used to

buffer the solution and improve the repeatability and to avoid the formation of aggregates of organic matter. However, as a consequence of increasing the pH of the solutions, a calcium hydroxide precipitate was observed and removed by centrifugation and filtration of the samples and standards.

The UV absorbance was performed using 1 cm light-path UV micro cuvettes Plastibrand from Brand and was registered at 1 nm bandwidth between 220 and 300 nm.

## *2.3.2. Results and discussion*

### *2.3.2.1. UV Spectral deconvolution method*

All samples were subjected to centrifugation and filtration prior to the analysis. Preliminary studies showed the importance of these two steps in reproducibility of the obtained spectra, since the precipitate formed, due to the addition of the ammonium hydroxide as buffer solution, interfere in the UV spectra of samples. An example of the three reference spectra, background, dissolved organic matter and atrazine spectra obtained for soil fertilized with sewage sludge, composing the deconvolution basis are represented in Figure 2.1.a). The combined spectrum of the three reference spectra is represented in Figure 2.1.b). The residuals plot is showed in Figure 2.1.c) and represents the difference between the observed value and the corresponding value given by the regression linear function at each wavelength. As mentioned before the plot of the residuals is very helpful to detect an existence of an obvious correlation between the residuals and the independent variable  $x$ , and to evaluate if the chosen model is adequate or not to fit the experiment. The fact that the residuals look random (Figure 2.1.c) is an indication that there is no obvious correlation with the variable  $x$ .

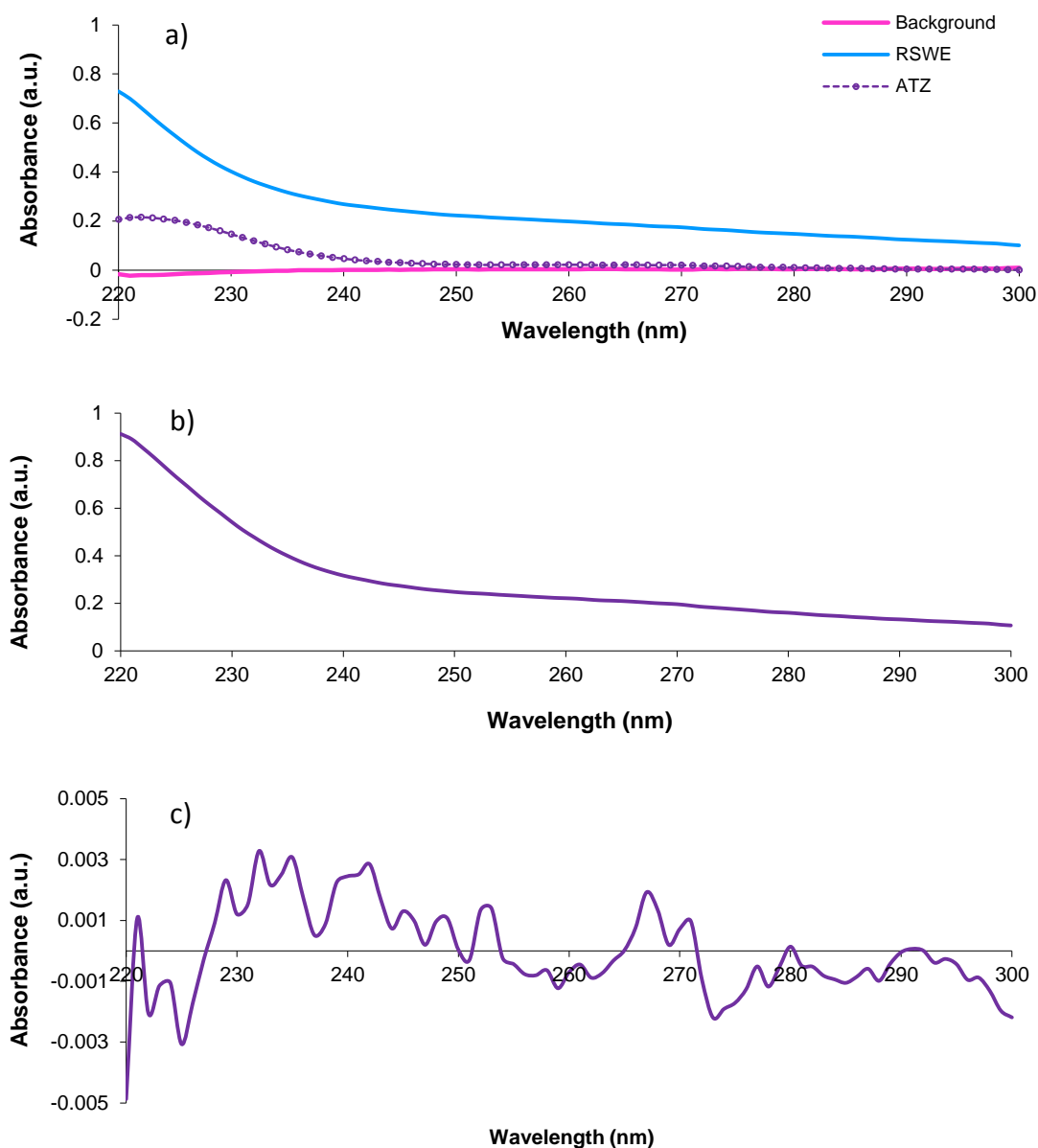


**Figure 2.1.** UV spectra from adsorption experiments on soil fertilized with sewage sludge (a) UV Reference spectra of background ( $0.01 \text{ mol L}^{-1} \text{ CaCl}_2$ ), RSWE and atrazine; (b) Combined spectrum of the three reference spectra; (c) Residual plots.

### 2.3.2.2. Analytical curves by UVSD and MEKC

The UVSD method was performed using standards prepared spiking atrazine into the same RSWE as the one presented in the adsorption experiments. The calibration curve was obtained plotting the coefficient  $a_3$  of the linear combination, obtained for each

atrazine standard using the linear regression, in function of the atrazine concentration. Since spectrum depends on soil matrix composition, a calibration curve is needed for each soil sample.

Table 2.1. shows statistical parameters of the analytical curves obtained either by UVSD and MEKC (obtained in chapter 1) for the determination of atrazine concentration present in solution after the adsorption experiment.

**Table 2.1.** Statistical parameter ( $\pm$  standard errors) for typical analytical curves obtained by UV spectral deconvolution and by MEKC.

	Slope	Intercept	$r$	LOD (mg L <sup>-1</sup> )	Linearity
UVSD (SLU) <sup>a</sup>	0.83 $\pm$ 0.01	-0.014 $\pm$ 0.007	0.998	0.066	99.986
UVSD (MIN) <sup>a</sup>	0.85 $\pm$ 0.02	0.005 $\pm$ 0.008	0.998	0.074	99.984
UVSD (FYM) <sup>a</sup>	0.91 $\pm$ 0.01	-0.05 $\pm$ 0.02	0.999	0.12	99.986
MEKC <sup>b</sup>	2.75 $\pm$ 0.02	-0.03 $\pm$ 0.02	1.000	0.26	99.963

<sup>a</sup> Statistical parameters valid for the concentration range between 0.1 and 2 mg L<sup>-1</sup>

<sup>b</sup> Statistical parameters valid for the concentration range between 0.3 and 10 mg L<sup>-1</sup>

Comparing the results, we can observe that both methods present a good correlation coefficient ( $r$ ), very close to 1. The limit of detection was calculated as  $a + 3S_y/x$ , where  $a$  is the intercept of the regression line and  $S_y/x$  the statistical parameter which estimates the random errors in the  $y$ -axis (signal). UVSD presents a much lower value for LOD, between 0.066 and 0.12 mg L<sup>-1</sup>, than the one obtained using MEKC, 0.26 mg L<sup>-1</sup>. In what concerns the linearity, the values are very similar to each other.

### 2.3.2.3. Adsorption experiments – Evaluation of the analytical methods

Adsorption isotherms were obtained by plotting the amount of atrazine adsorbed per weight unit of soil at equilibrium ( $Q_e$ , mg Kg<sup>-1</sup>), versus the amount of chemical per volume of solution at equilibrium ( $C_e$ , mg L<sup>-1</sup>). The adsorption isotherms of atrazine onto soil

fertilized with sewage sludge obtained by the proposed UVSD method in comparison to the curve obtained by MEKC are presented in Figure 2.2.

The Freundlich equation has reasonably described the adsorption of atrazine on soils used ( $r > 0.963$ ). Freundlich adsorption coefficient is an empirical constant of the Freundlich model expressing soil sorbent capacity (sorption isotherm slope), for a given range of atrazine concentration, and greater the value, stronger is the adsorption.

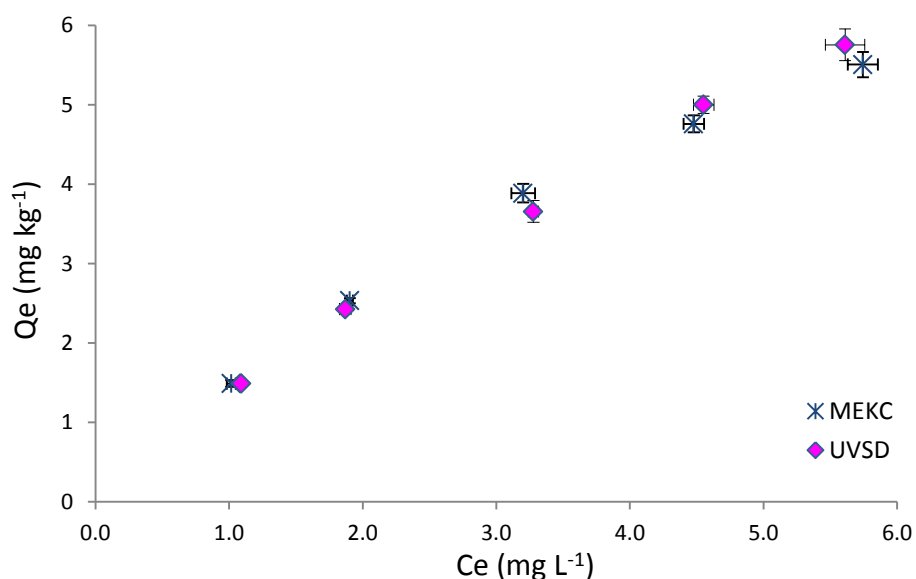


**Figure 2.2.** Adsorption isotherms of atrazine onto soil fertilized with sewage sludge obtained by UVSD (◆) and by MEKC (x).

The low  $K_F$  value obtained for mineral soil (Table 2.2.), using both methods, reflects low adsorption capacity and is commonly associated with greater permeability and high leaching (Correia et al., 2007). Sorption isotherm was non-linear, exhibiting  $N$  values smaller than 1, indicating that the percentage of atrazine adsorbed to the soil decreased as the initial concentration increased.

The  $t$ -test was applied to compare the results obtained by both methods for each soil sample used. Since the  $t$  calculated presented lower values, for both  $K_F$  and  $N$ , in all soil samples tested than the critical  $t$  value, for 4 degrees of freedom at 95% confidence level, it is possible to confirm that there are no significant differences between the results obtained by UVSD and MEKC.

**Table 2.2.** Mean ( $\pm$  standard errors) Freundlich  $K_F$  and  $N$  parameters for adsorption of atrazine onto a soil obtained by UVSD and MEKC.

Soil Sample		$K_F$ ( $\text{mg kg}^{-1} (\text{mg L}^{-1})^{-N}$ )	$N$	$r$
SLU	UVSD	$1.45 \pm 0.07^b$	$0.8 \pm 0.3$	0.993
	MEKC	$1.54 \pm 0.06$	$0.76 \pm 0.03$	0.994
	$t$ student <sup>a</sup>	1.72	0.201	
MIN	UVSD	$0.68 \pm 0.1^b$	$0.85 \pm 0.09$	0.963
	MEKC	$0.81 \pm 0.08$	$0.72 \pm 0.05$	0.995
	$t$ student <sup>a</sup>	1.77	2.21	
FYM	UVSD	$1.9 \pm 0.1^b$	$0.61 \pm 0.04$	0.996
	MEKC	$1.7 \pm 0.2$	$0.67 \pm 0.08$	0.987
	$t$ student <sup>a</sup>	1.39	1.23	

<sup>a</sup> Critical  $t$  value for 4 degrees of freedom, at 95% confidence level, is 2.78.

<sup>b</sup> Results are an average of triplicate adsorption experiments.

## 2.4. Fluorescence SD for EE2

### 2.4.1. Experimental procedure

#### 2.4.1.1. Soil sample

Soil samples used were described in section 1.2.1. Soil treated with compost from organic household waste was subjected to a loss on ignition (LOI) at 550°C in a furnace for 5 h. This soil (denominated COM\_LOI), without any organic matter, was also used to perform sorption studies.

#### 2.4.1.2. Instrumentation

The fluorescence spectra were obtained using the Spectrofluorometer Fluoromax-4 (Horiba Jobin Yvon). The fluorescence spectra were obtained using an excitation wavelength of 280 nm and emission spectra were recorded between 295 and 350 nm. Excitation and emission slits were maintained at 5 nm.

DOC was determined using the Total Organic Carbon Analyser TOC-V<sub>CPH</sub> from SHIMADZU.

### 2.4.1.3. Fluorescence spectra acquisition

All reagents were of analytical grade and all working solutions were prepared in ultra-pure water, obtained from a Milli-Q Millipore (Millipore Q plus 185) system. A stock standard solution of EE2 (98%, Sigma) was prepared in methanol and standard solutions were prepared by diluting this stock solution with  $0.01 \text{ mol L}^{-1} \text{ CaCl}_2$ .

The RSWE containing  $0.01 \text{ mol L}^{-1} \text{ CaCl}_2$  was prepared by adding 12.5 mL of  $0.01 \text{ mol L}^{-1} \text{ CaCl}_2$  solution to 250 mg of soil and shaking them in a head over head shaker at 100 rpm for 15 h at  $22 \pm 1 \text{ }^\circ\text{C}$ . The mixture was then centrifuged at 4000 rpm for 5 min and the supernatant filtered with a  $0.22 \text{ }\mu\text{m}$  pore resulting in the RSWE referred.

For fluorescence intensities measurements, standard solutions with concentrations ranging from  $0.4$  to  $4 \text{ mg L}^{-1}$ , were prepared in the RSWE containing  $0.01 \text{ mol L}^{-1} \text{ CaCl}_2$ . Fluorescence reference emission spectra ( $\text{REF}_1$ ,  $\text{REF}_2$ ,  $\text{REF}_3$ ) were registered for the RSWE, for the  $0.01 \text{ mol L}^{-1} \text{ CaCl}_2$  and for an EE2 solution in  $0.01 \text{ mol L}^{-1} \text{ CaCl}_2$ . DOC values of soil extracts (soil/solution ratio 1:50) were  $6.4 \pm 0.1 \text{ mg L}^{-1}$  for mineral fertilized soil,  $10.82 \pm 0.04 \text{ mg L}^{-1}$  for soil fertilized with compost from organic household waste,  $6.71 \pm 0.02 \text{ mg L}^{-1}$  for soil fertilized with sewage sludge from municipal wastewater treatment facilities and  $6.79 \pm 0.04 \text{ mg L}^{-1}$  for soil fertilized with farmyard manure.

Ammonium hydroxide was added to standards, samples and reference solutions in order to obtain  $0.1 \text{ mol L}^{-1}$  as final concentration and all of them were diluted 100 times prior to analysis, resulting in a calibration curve from  $4$  to  $40 \text{ }\mu\text{g L}^{-1}$ . Ammonium hydroxide was used to buffer the solution, as molecular fluorescence is pH dependent, improving the repeatability, and to avoid the formation of aggregates of organic matter.

In order to evaluate the accuracy and precision of the deconvolution method, recovery tests with concentrations ranging from  $4$  to  $40 \text{ }\mu\text{g L}^{-1}$  were made using solutions prepared by spiking EE2 in  $0.01 \text{ mol L}^{-1} \text{ CaCl}_2$  and in RSWE. All experiments were made in triplicate.

#### 2.4.1.4. Adsorption studies

Selection of appropriate soil to solution ratios for adsorption studies depends on the distribution coefficient  $K_d$  and the relative degree of adsorption desired. Therefore, as a general practice, it is useful to settle on a fixed ratio, for which the percentage adsorbed is above 20%, and preferably >50% (OECD, 2000). In this study several ratios were tested, 1:50, 1:25, 1:10, 1:5 and 1:2 (w/v), in order to choose the most adequate (Figure 2.3.).

The concentration of EE2 was  $2 \text{ mg L}^{-1}$ . Tubes with tested soil solution ratios were shaken in a head-over-head shaker at 100 rpm during 6 hours at  $22 \pm 1 \text{ }^\circ\text{C}$ , centrifuged at 4000 rpm for 5 min and the fluorescence was read, as described previously. All experiments were made in triplicate. As it was expected, the adsorption percentage increases with the increase of the soil amount in the tube since more sorption sites, for the same EE2 quantity, are available for binding (Figure 2.3.). The ratio 1:50 (w/v) was chosen since almost 40% of EE2 is adsorbed.

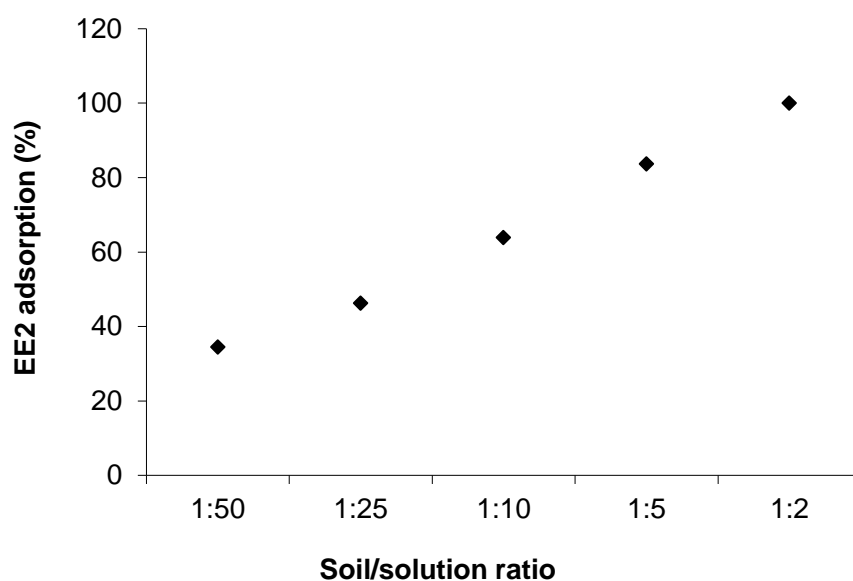


**Figure 2.3.** Change in EE2 adsorption percentage with the soil/solution ratio; initial EE2 concentration  $2 \text{ mg L}^{-1}$ . Soil sample fertilized with farmyard manure.

Kinetics experiments were also made in order to evaluate the adsorption contact time between the solution and the soil, using batch experiments. Tubes with a soil



solution ratio 1:50 (w/v) were shaken in a head-over-head shaker during a variable period of time between 0 and 24 h, centrifuged at 4000 rpm for 5 min and analysed, as described previously. All experiments were made in triplicate. Adsorption of EE2 onto glassware and filters, as well as EE2 degradation during experimental procedure was controlled using control samples (EE2 standards subjected to the same procedure).

Adsorption isotherm of EE2 was performed using the batch equilibration technique (OECD, 2000). Six hormone concentrations (0.4 to 4 mg L<sup>-1</sup>) were prepared in 0.01 mol L<sup>-1</sup> CaCl<sub>2</sub>. A 12.5 mL aliquot of each concentration was added to 250 mg of soil. Three replicates were made for each concentration. The tubes containing the mixtures were shaken head-over-head at 100 rpm for 15 h at 22±1 °C, centrifuged at 4000 rpm for 5 min and the supernatant filtered with a 0.22 µm pore. The equilibrium concentration was then determined.

## *2.4.2. Results and discussion*

### *2.4.2.1. Fluorescence spectral deconvolution method*

Initially, UVSD was tested for EE2; however, the obtained residual plots and the recovery tests performed (based on the work reported on section 2.3.2.1.) were not satisfactory. These first findings are probably explained by the low UV light absorbance that characterizes these compounds. Due to the high fluorescence capacity of these compounds it was decided to test the same spectral deconvolution principle, but using EE2 fluorescence emission spectra. The principle of FSD approach is similar to the UVSD, but in this case instead of using the absorbance spectrum it was used the emission fluorescence spectrum of the sample.

As mentioned before, the plot of the residuals is very helpful to detect the existence of an obvious correlation between the residuals and the independent variable  $x$ , and to evaluate if the chosen model is adequate or not to fit the experiment.

In order to select the adequate range of emission wavelength, several spectral deconvolution procedures were made using different wavelength ranges (Figure 2.4.).

The first attempt was made using an excitation wavelength of 280 nm to obtain an emission spectra between 290 and 650 nm and, as it can be seen in Figure 2.4.a (example for farmyard manure soil), there is a significantly trend in the residual results and the obtained residuals can reach high values. The residuals obtained using emission spectra between 290 and 350 or 295 and 350 nm (Figure 2.4.b) were much lower than the previous case and similar to each other, being indifferent to use one or another. The range chosen was from 295 to 350 nm. The randomness of the residuals is an indication that there is no obvious correlation with the variable x.

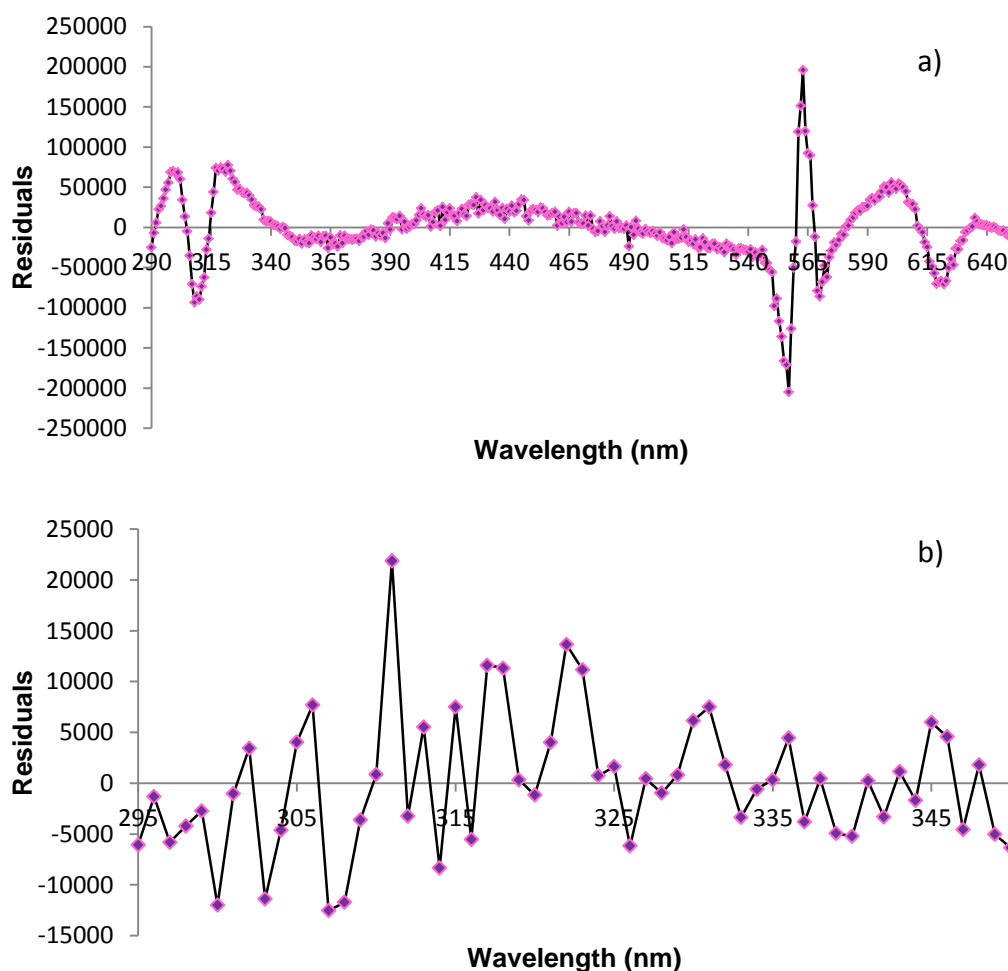


**Figure 2.4.** Residual plots obtained after the deconvolution of a  $20 \mu\text{g L}^{-1}$  EE2 standard spiked into a farmyard manure soil extract, using emission spectra range between a) 290 and 650 nm; b) 295 and 350 nm.  $\lambda_{\text{exc}} = 280 \text{ nm}$ .

### 2.4.2.2. Evaluation of the deconvolution method

The FSD method was performed using standards prepared through spiking EE2 into the same RSWE and conditions as those used in the adsorption experiments. The calibration curve was obtained plotting the coefficient  $a_3$  of the linear combination, obtained for each EE2 standard using the linear regression, as a function of the EE2 concentration. Since spectrum depends on RSWE composition, a calibration curve is needed for each soil sample. Table 2.3. shows statistical parameters of the analytical curves obtained for each soil sample and used for the determination of the concentration of EE2 present in solution after the adsorption experiment.

**Table 2.3.** Statistical parameter ( $\pm$  standard errors) for the analytical curves obtained by FSD for each soil sample used.

Soil	Slope	Intercept	$r$	LOD ( $\mu\text{g L}^{-1}$ )	Linearity
SLU <sup>a</sup>	$0.0423 \pm 0.0006$	$-0.03 \pm 0.03$	0.999	2.79	99.999
MIN <sup>a</sup>	$0.0438 \pm 0.0008$	$-0.05 \pm 0.02$	0.999	1.58	99.999
FYM <sup>a</sup>	$0.040 \pm 0.002$	$0.01 \pm 0.04$	0.996	4.15	99.998
COM <sup>a</sup>	$0.0493 \pm 0.0008$	$0.02 \pm 0.02$	0.999	1.73	99.999
COM_LOI <sup>a</sup>	$0.0357 \pm 0.0003$	$0.06 \pm 0.01$	1.000	2.79	100.000

<sup>a</sup> Statistical parameters valid for the concentration range between 4 and 40  $\mu\text{g L}^{-1}$

FSD presents a low limit of detection, between 1.58 and 4.15  $\mu\text{g L}^{-1}$ , which corresponds to the concentration prior to dilution of 0.158 and 0.415  $\text{mg L}^{-1}$ . Correlation coefficients obtained ranged between 0.996 and 1.000 and linearity was higher than 99.998%.

The suitability of the method was tested performing recovery tests using 0.01  $\text{mol L}^{-1}$   $\text{CaCl}_2$  and RSWE from soil fertilized with farmyard manure spiked with a known concentration of EE2, ranging from 4 to 40  $\mu\text{g L}^{-1}$ . The obtained recoveries (Table 2.4.) ranged between 87.4% and 112.2%, in a 0.01  $\text{mol L}^{-1}$   $\text{CaCl}_2$  solution and 91.6 and 113.8%, in a RSWE.

**Table 2.4.** Recovery results obtained for EE2 spiked into 0.01 mol L<sup>-1</sup> CaCl<sub>2</sub> and also into soil extract solution

Concentration level (µg L <sup>-1</sup> )	Results in CaCl <sub>2</sub>		Results in soil extract	
	Recovery (%)	RSD (%) (n=3)	Recovery (%)	RSD (%) (n=3)
4	99.1	9.8	101.7	10.7
12	87.4	5.8	91.6	11.2
16	101.5	1.4	104.8	9.1
24	107.2	1.7	113.8	4.4
32	112.2	0.7	103.3	3.6
40	105.8	4.7	108.0	0.8

RSD – Relative Standard Deviation

These recoveries can be considered suitable and the method seems to present high accuracy. Also, there appears to be no problem attributed to the presence of soil organic extract in recoveries obtained by spectral deconvolution method, since the results obtained with or without organic matter are rather similar. In what concerns the precision of the method, RSD values are all below 11.2%, indicating that the method is highly precise in the range of concentrations of 4 to 40 µg L<sup>-1</sup>.

#### 2.4.2.3. Adsorption experiments

Preliminary studies were performed to find the time needed to attain the equilibrium. After two hours 70% of the total adsorption amount was achieved. A plateau was attained after 6 hours (Figure 2.5.).

Kinetic results demonstrated a typical experimental result, in which the pollutant, initially in the solution phase, undergoes initial rapid adsorption followed by a slow approach to equilibrium. Although the equilibrium is reached after 6 hours, the time chosen for equilibration was 15 h since it was left agitating during the night.

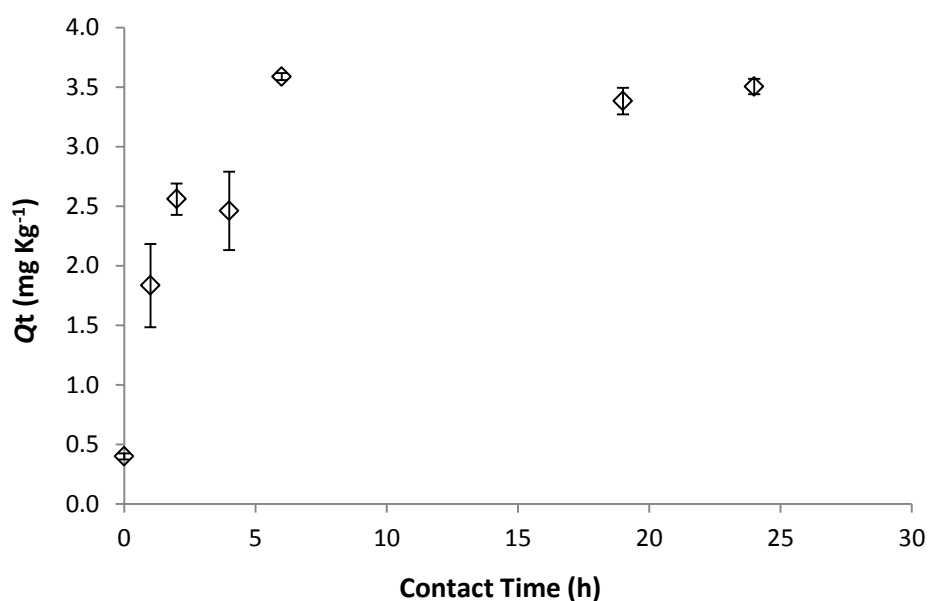


**Figure 2.5.** Influence of contact time on EE2 adsorption onto soil. Initial EE2 concentration of  $2 \text{ mg L}^{-1}$  in  $0.01 \text{ mol L}^{-1} \text{ CaCl}_2$  ( $n=3$ );  $Q_t$  – adsorbed concentration at time  $t$  (h) ( $\text{mg kg}^{-1}$ ).

Transport models for assessing the mobility of chemicals require isotherm equations and determination of its parameters. Giles et al. (1974) classified sorption isotherms based on their initial slopes and curvatures and distinguished between high affinity (H), Langmuir (L), constant partition (C) and sigmoidal-shaped (S) isotherm classes. Langmuir, Freundlich and Langmuir-Freundlich models are the most frequently applied to describe the behaviour of the adsorption isotherms experimental data (Calace et al., 2002). As it can be seen in Figure 2.6., results present a sigmoidal-shaped (S) isotherm. Generally, S isotherms have a concave shape at low concentrations. The best fitting results were obtained using the Langmuir-Freundlich and Hill equations. Langmuir-Freundlich model assumes that surface is homogeneous but also that a cooperative process due to sorbate-sorbate interactions is present. For positive interactions  $b > 1$ , the equation is known as Hill equation (Calace et al., 2002):

$$Q_e = Q_{max}(K_1 C_e)^b / (1 + (K_1 C_e)^b) \quad \text{Hill equation } (b > 1)$$

where,  $Q_e$  is the amount adsorbed at equilibrium ( $\text{mg kg}^{-1}$ ),  $C_e$  is the equilibrium concentration of the sorbate ( $\text{mg L}^{-1}$ ) and  $Q_{max}$  ( $\text{mg kg}^{-1}$ ) is the maximum adsorption capacity,  $K_1$  is an affinity parameter and  $b$  is an empirical parameter which varies with the degree of heterogeneity (Calace et al., 2002). Since the obtained  $b$  value was higher than 1, the Hill equation was chosen.

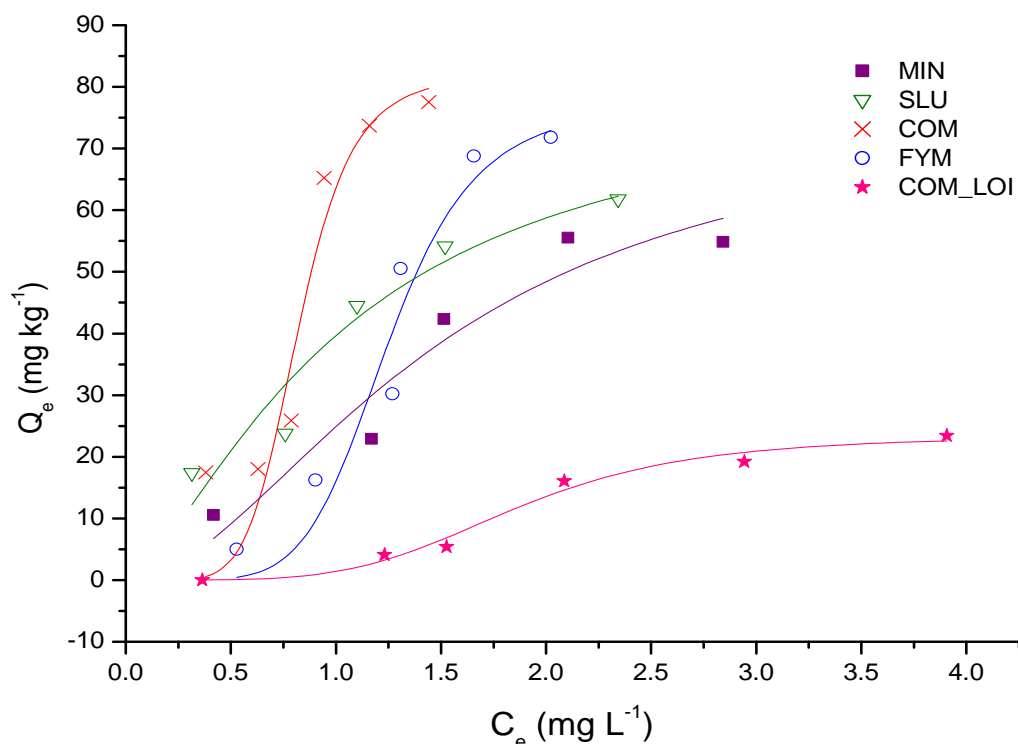


**Figure 2.6.** Adsorption isotherms with fitting using Hill Equation; SLU, sewage sludge fertilizer; MIN, mineral fertilizer; FYM, farmyard manure; COM, compost from organic household waste; COM\_LOI, composted soil submitted to loss on ignition.

As referred by Sarmah et al. (2008), although there have been a great number of studies that follow sorption of steroids hormones, such as EE2, on soils employing batch equilibration techniques, the experimental protocols in those studies differ considerably. This fact becomes a problem when the comparison of the obtained data with results already published is needed. Also the most common equation used to describe sorption behaviour is Freundlich, where  $K_f$  (Freundlich coefficient) is obtained. Thus, in order to

compare the results with the ones presented by Hildebrand et al. (2006) for EE2, distribution coefficient  $K_D$  (ratio between the content of the substance in the soil phase and the mass concentration of the substance in the aqueous solution when adsorption equilibrium is reached) was calculated, as well as  $K_{OC}$  (organic carbon normalized adsorption coefficient). Results for  $K_{OC}$  ranged between 1714 and 2715 L kg<sup>-1</sup> and are similar to the ones reported by Hildebrand et al. (2006), suggesting that the method developed is suitable to follow adsorption of EE2 onto soil organic matter.

## 2.5. Conclusions

---

In the present work, we demonstrate that HOP concentration can be correctly determined in a complex soil water matrix using mathematical spectral deconvolution, either using UV or fluorescence emission spectra. This is particularly interesting to study interactions of HOP with soil organic matter, a field of growing importance. In batch experiments, the measurements of equilibrium concentration are often the bottle-neck of the approach. When using HPLC or CE, each measurement, including pre-treatment, column equilibration, and separation, will take between 15 and 60 min in average, depending on the compound. Here, a recording takes less than 1 min. It is important to emphasize that this approach is reliable only if the spectra of the matrix and the compound used as reference are invariant. UVSD was developed to follow adsorption of atrazine onto different soil samples. The Freundlich parameters ( $K_F$  and  $N$ ) were obtained for the adsorption isotherm, using both UVSD and MEKC techniques. UVSD has proven to be an accurate methodology, since the results obtained did not present statistical significant differences at 95% confidence level. Moreover, the LOD obtained using UVSD (between 0.066 and 0.12 mg L<sup>-1</sup>) presented a much lower value than the one obtained using MEKC (0.26 mg L<sup>-1</sup>). Also, a fluorescence spectral deconvolution method was developed, but to follow adsorption behaviour of EE2 onto soils. Preliminary FSD studies showed that: residuals obtained using emission spectra between 290 and 350 nm looked random, indicating that there was no obvious correlation with the variable  $x$ ; calibration curve (plotting the coefficient  $\alpha_i$  of the linear combination in function of EE2 concentration) presented a low limit of detection, up to 1.58  $\mu\text{g L}^{-1}$  and good correlation coefficient ( $>0.996$ ); recovery tests ranged between 87.4 and 112.2%. Also the obtained results for  $K_{OC}$  were similar to the ones reported previously by other authors, suggesting that the developed method is suitable to follow adsorption of EE2 onto soil organic matter. This approach could be applied to study the adsorption of several other compounds to different soil samples, as long as the compound is stable enough for its UV or fluorescence emission spectra to be considered invariant, for a relatively short period of time. The cost of this approach is also particularly low as its only requirements are a UV-Vis or a fluorescence spectrometer and a spreadsheet with statistical tool (i.e. Excel).



## 2.6. References

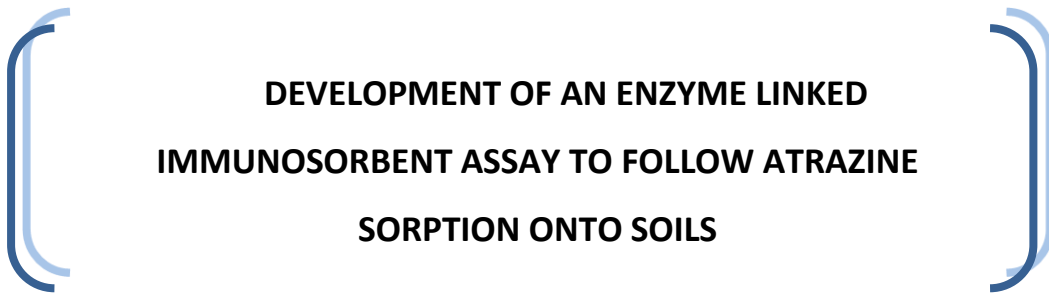
---

- Ben-Hur, M., Letey, J., Farmer, W.J., Williams, C.F., Nelson, S.D., **2003**. Soluble and solid organic matter effects in atrazine adsorption in cultivated soils. *Soil Sci. Soc. Am. J.* 67, 1140-1146.
- Calace, N., Nardi, E., Petronio, B.M., Pietroletti, M., **2002**. Adsorption of phenols by papermill sludges. *Environ. Pollut.* 118, 315-319.
- Caron, A., Farenhorst, A., Zvomuya, F., Gaultier, J., Rank, N., Goddard, T., Sheedy, C., **2010**. Sorption of four estrogens by surface soils from 41 cultivated fields in Alberta, Canada. *Geoderma* 155, 19-30.
- Chefetz, B., Bilkis, Y.I., Polubesova, T., **2004**. Sorption-desorption behaviour of atrazine and phenylurea herbicides in Kishon river sediments. *Water Res.* 38, 4383-4394.
- Correia, F.V., Macrae, A., Guilherme, L.R.G., Langenbach, T., **2007**. Atrazine sorption and fate in a Ultisol from humid tropical Brazil. *Chemosphere* 67, 847-854.
- Coulomb, B., Richarson, Y., Brach-Papa, C., Boudenne, J.-L., Theraulaz, F., **2006**. Rapid estimation of TOC in a marine urban sewage area by UV spectral deconvolution. *Inter. J. Environ. An. Ch.* 86, 1079-1093.
- Drori, Y., Aizenshtat, Z., Chefetz, B., **2005**. Sorption-desorption behaviour of Atrazine in soils irrigated with reclaimed wastewater. *Soil Sci. Soc. Am. J.* 69, 1703-1710.
- Emmerik, T.V., Angove, M.J., Johnson, B.B., Wells, J.D., Fernandes, M.B., **2003**. Sorption of 17 $\beta$ -estradiol onto selected soil minerals. *J. Colloid Interf. Sci.* 266, 33-39.
- Escalas, A., Droguet, M., Guadayol, J.M., Caixach, J., **2003**. Estimating DOC regime in a wastewater treatment plant by UV deconvolution. *Water Res.* 37, 2627-2635.
- Fan, Z., Casey, F.X.M., Hakk, H., Larsen, G., **2007**. Persistence and fate of 17 $\beta$ -estradiol and testosterone in agricultural soils. *Chemosphere* 67, 886-895.
- Feng, Y., Zhang, Z., Gao, P., Su, H., Yu, Y., Ren, N., **2010**. Adsorption behaviour of EE2 (17 $\alpha$ -ethinylestradiol) onto the inactivated sewage sludge: Kinetics, thermodynamics and influence factors. *J. Hazard. Mater.* 175, 970-976.
- Giles, C.H., Smith, D., Huitson, A., **1974**. A general treatment and classification of the solute adsorption isotherm. I: Theoretical. *J. Colloid Interf. Sci.* 47, 755-765.
- Hassouna, M., Theraulaz, F., Massiani, C., **2007**. Direct estimation of nitrate, total and fractionated water extractable organic carbon (WEOC) in an agricultural soil using direct UV absorbance deconvolution. *Talanta* 71, 861-867.

- Hildebrand, C., Londry, K.L., Farenhorst, A., **2006**. Sorption and desorption of three endocrine disrupters in soils. *J. Environ. Sci. Heal. B* 41, 907-921.
- Kibbey, T.C.G., Chen, L., Singhaputtangkul, N., Sabatini, D.A., **2009**. A UV-transparent passive concentrator/spectrum deconvolution method for simultaneous detection of endocrine disrupting chemicals (EDCs) and related contaminants in natural waters. *Chemosphere* 76, 1249-1257.
- Lee, L.S., Strock, T.J., Sarmah, A.K., Rao, P.S.C., **2003**. Sorption and dissipation of testosterone, estrogens, and their primary transformation products in soils and sediment. *Environ. Sci. Technol.* 37, 4098-4105.
- Lima, D.L.D., Erny, G.L., Esteves, V.I., **2009**. Application of MEKC to the monitoring of atrazine sorption behaviour on soils. *J. Sep. Sci.* 32, 4241-4246.
- Lima, D.L.D., Silva, C.P., Erny, G.L., Esteves, V.I., **2010**. Comparison between MEKC and UV spectral deconvolution to follow sorption experiment in soil. *Talanta* 81, 1489-1493.
- Mbuya, O.S., Nkedi-Kizza, P., Boote, K.J., **2001**. Fate of atrazine in sandy soil cropped with sorghum. *J. Environ. Qual.* 30, 71-77.
- Nam, P.H., Alejandra, B., Frédéric, H., Didier, B., **2008**. A new quantitative and low-cost determination method of nitrate in vegetables, based on deconvolution of UV spectra. *Talanta* 76, 936-940.
- OECD, Guideline TG 106, **2000**. OECD Guideline for the Testing of Chemicals. Adsorption – Desorption using a Batch Equilibrium Method. *Organization for Economic Co-operation and Development (OECD)*, Paris.
- Park, J.H., Feng, Y., Cho, S.Y., Voice, T.C., Boyd, S.A., **2004**. Sorbed atrazine shifts into non-desorbable sites of soil organic matter during aging. *Water Res.* 38, 3881-3892.
- Prata, F., Lavorenti, A., Vanderborght, J., Burauel, P., Vereecken, H., **2003**. Miscible displacement, sorption and desorption of atrazine in a Brazilian oxisol. *Vadose Zone J.* 2, 728-738.
- Robinson, B.J., Hellou, J., **2009**. Biodegradation of endocrine disrupting compounds in harbour seawater and sediments. *Sci. Total Environ.* 407, 5713-5718.
- Santos, L.B.O., Abate, G., Masini, J.C., **2005**. Application of sequential injection–square wave voltammetry (SI–SWV) to study the adsorption of atrazine onto a tropical soil sample. *Talanta* 68, 165-170.
- Sarmah, A.K., Northcott, G.L., Scherr, F.F., **2008**. Retention of estrogenic steroid hormones by selected New Zealand soils. *Environ. Int.* 34, 749-755.

- Smith, M.C., Shaw, D.R., Massey, J.H., Boyette, M., Kingery, W., **2003**. Using nonequilibrium thin-disc and batch equilibrium techniques to evaluate herbicide sorption. *J. Environ. Qual.* 32, 1393-1404.
- Socías-Viciano, M.M., Fernández-Pérez, M., Villafranca-Sánchez, M., González-Pradas, E., Flores-Céspedes, F., **1999**. Sorption and leaching of atrazine and MCPA in natural and peat-amended calcareous soils from Spain. *J. Agr. Food Chem.* 47, 1236-1241.
- Stumpe, B., Marschner, B., **2007**. Long-term sewage sludge application and wastewater irrigation on the mineralization and sorption of 17 $\beta$ -estradiol and testosterone in soils. *Sci. Total Environ.* 374, 282-291.
- Stumpe, B., Marschner, B., **2009**. Factors controlling the biodegradation of 17 $\beta$ -estradiol, estrone and 17 $\alpha$ -ethinylestradiol in different natural soils. *Chemosphere* 74, 556-562.
- Stumpe, B., Marschner, B., **2010**. Dissolved organic carbon from sewage sludge and manure can affect estrogen sorption and mineralization in soils. *Environ. Pollut.* 158, 148-154.
- Sun, W. L., Ni, J. R., Xu, N., Sun, L. Y., **2007**. Fluorescence of sediment humic substance and its effect on the sorption of selected endocrine disruptors. *Chemosphere* 66, 700-707.
- Thomas, O., Theraulaz, F., Agnel, C., Suryani, S., **1996**. Advanced UV examination of wastewater. *Environ. Technol.* 17, 251-261.
- Thomas, O., Theraulaz, F., Domeizel, M., Massiani, C., **1993**. UV spectral deconvolution: A valuable tool for waste water quality determination. *Environ. Technol.* 14, 1187-1192.
- Yu, Z., Xiao, B., Huang, W., Peng, P., **2004**. Sorption of steroid estrogens to soils and sediments. *Environ. Toxicol. Chem.* 23, 531-539.

# CHAPTER 3



**DEVELOPMENT OF AN ENZYME LINKED  
IMMUNOSORBENT ASSAY TO FOLLOW ATRAZINE  
SORPTION ONTO SOILS**



## CHAPTER 3

### DEVELOPMENT OF AN ENZYME LINKED IMMUNOSORBENT ASSAY TO FOLLOW ATRAZINE SORPTION ONTO SOILS\*

3.1. Introduction .....	55
3.1.1. Antibodies .....	56
3.1.1.1. Structural and functional properties .....	57
3.1.1.2. Antibody production .....	58
3.1.2. Tracer synthesis.....	60
3.1.3. Immunoassays.....	62
3.1.4. Application in environmental analysis .....	66
3.1.4.1. Using ELISA to follow sorption behaviour.....	67
3.2. Experimental procedure .....	69
3.2.1. Soil sample .....	69
3.2.2. ELISA development.....	69
3.2.2.1. Reagents and materials.....	69
3.2.2.2. Preparation of enzyme conjugates via mixed anhydride route.....	71
3.2.2.3. Preparation of enzyme conjugates via activated ester route.....	73
3.2.2.4. Tracer and antibody binding specificity.....	78
3.2.2.5. ELISA procedure .....	78
3.2.3. Adsorption experiment .....	79
3.3. Results and discussion .....	79
3.3.1. Tracer and antibody binding specificity .....	79
3.3.2. Optimization of antibody and tracer dilutions.....	88
3.3.3. Evaluation of assay performance .....	89
3.3.4. Evaluation of soil matrix effects.....	93
3.3.5. Adsorption experiment .....	95
3.4. Conclusion .....	96
3.5. References .....	97

\* **Diana L.D. Lima**, Carla P. Silva, Rudolf J. Schneider, Valdemar I. Esteves, 2011. Development of an ELISA procedure to study sorption of atrazine onto a sewage sludge-amended luvisol soil. *Talanta* 85, 1494-1499.

## 3.1. Introduction

---

Immunochemical methods have been used for decades in clinical chemistry, since they are simple and reliable tools of control analysis (Franek and Hruska, 2005). Yalow and Berson (1959) won the Nobel Prize in 1977 *“for creating the Yalow-Berson method to measure minute amounts of peptide hormones using antibodies”*. They developed the, later famous and widely used, radioimmunoassay (RIA) technique. Since then, immunochemical assays have been widely spread to veterinary medicine, agriculture and other areas, such as environmental and food analysis (Franek and Hruska, 2005). Around 1970 the first assay for pesticides, aldrin and dieldrin, was developed by Langone and Vanvunakis (Langone and Vanvunakis, 1975). Before the development of the Enzyme-Linked Immunosorbent Assay (ELISA), the only option for conducting an immunoassay was RIA, a technique using radioactively labeled antigens or antibodies. In RIA, the radioactivity provides the signal, which indicates whether a specific antigen or antibody is present in the sample. However, radioisotopes are costly, hazardous and require inconvenient monitoring and disposal procedures (Mikkelsen and Cortón, 2004). A suitable alternative to radioimmunoassay would be substituting the radioactively-labeled antigens or antibodies for non-radioactively labeled ones. Enzymes, such as peroxidase, react with appropriate substrates (such as 3,3',5,5'-tetramethylbenzidine) and a change of colour is observed. Engvall and Perlmann (1971) published their first paper on ELISA in 1971 and demonstrated quantitative measurement of immunoglobulin G in rabbit serum, with alkaline phosphatase as the reporter label. In the early eighties a discussion started about the application of these assays in environmental as well as food samples for pollutant detection (Nunes, 2004). Examples of contaminants, which can be rapidly and efficiently determined by these methods, are chemical pesticides, polychlorinated biphenyls (PCBs) and antibiotics. The growing interest on antibody-based methods becomes clear observing the publications number trend in recent decades (Franek and Hruska, 2005).

Immunochemical methods present several advantages, like being highly sensitive assays, with very low limits of detection; highly specific, being able to determine accurately one compound, even in the presence of another with similar structure;

extremely simple to execute and with the possibility of simultaneously analyse several samples. Concluding, the main qualities of these methodologies are sensitivity, specificity, simplicity and time and cost-efficiency (Franek and Hruska, 2005; Hennion and Barceló, 1998).

### *3.1.1. Antibodies*

Immunochemical methods rely on the use of antibodies (Ab) and are characterized by specific recognition sites in their structures, which enable highly specific interactions with the antigens (Hennion and Barceló, 1998). Antibodies are produced as an immune response to an immunogen, compound with high molecular mass ( $> 1$  kDa), defined as an agent capable of eliciting an immune response. On the other hand, antigens are species that are able to bind selectively to antibodies, but not necessarily capable of generating an immune response. All immunogens are also antigens, but not all antigens are immunogens (Mikkelsen and Cortón, 2004). The difficulty of generating antibodies for small molecules, such as pesticides, arises from the fact that they are not able to produce the necessary immune response (Hennion and Barceló, 1998). This problem is the major reason for the latter application of immunochemical methods in environmental analysis. Haptens are low molecular weight compounds that when chemically bound to high molecular weight compounds, such as a carrier protein, can produce an immune response. The way the chemical binding of the hapten to a protein is achieved strongly affects antibody specificity. The conjugation of haptens, such as pesticides, to a carrier protein and immunisation of animals with the synthesized immunogens will generate antibodies specific to the hapten used in the immunization. Having the problems around the development of antibodies for small molecules solved, partially explain the strong application of these methods in environmental analysis in the last decade (Hennion and Barceló, 1998).

### 3.1.1.1. Structural and functional properties

Antibodies are large, Y-shaped macromolecules that belong to a glycoprotein family, the so-called immunoglobulins (Ig). There are different types of immunoglobulins present in blood serum, IgG, IgA, IgM, IgD and IgE, differing from each other in size, charge, amino acid composition, carbohydrate content and thus biological properties. However, they all share the same principle of binding specifically to a given antigen (Gault and McClenaghan, 2009).

To understand the interaction between antibodies and their antigens it is important to have some knowledge about the antibody structure. Structurally, antibodies present one or more copies of a characteristic unit with a Y shape (Figure 3.1.); for example, they can be monomeric (with one Ig unit; *e.g.* IgG), dimeric (two Ig units; *e.g.* IgA) or pentameric (five Ig units; *e.g.* IgM). IgG molecules contain four polypeptides – two identical copies of a polypeptide known as the heavy chain (55000 Da) and two identical copies of a polypeptide called the light chain (25000 Da) (Harlow and Lane, 1999).

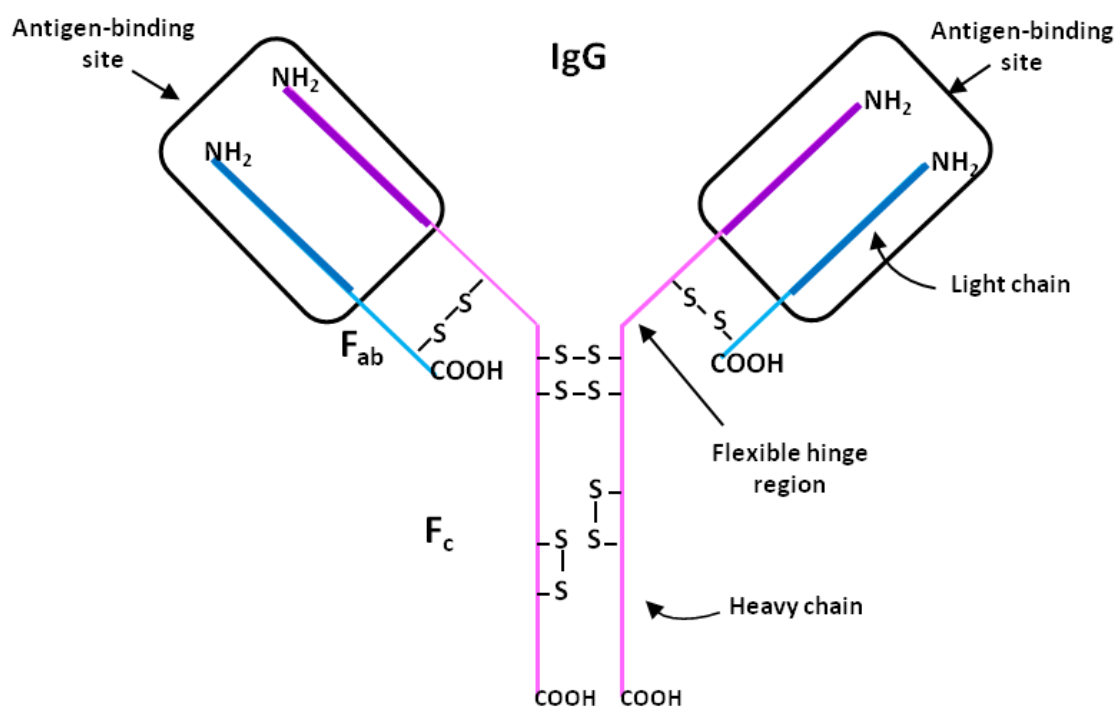


**Figure 3.1.** Structural diagram representing the IgG (antibody); Fab = fragment of antigen binding region; Fc = constant fragment which binds to various cell receptors and complement proteins.



The heavy chains are held together by covalent disulfide bridges (-S-S-) and each of the heavy chains is held to a light chain by another covalent disulfide bridge (-S-S-) and non-covalent bonds. One light chain associates with the amino-terminal region of one heavy chain to form the antigen-binding domain and are called Fab fragments (named for the fragment containing the antigen binding site). The carboxy-terminal regions of the two heavy chains fold together to make the Fc fragment (fragment that crystallizes). The Fc fragment is involved in immune regulation and determines the antibody class. The connector between the antigen-binding region and the Fc region is called the hinge, a short peptide sequence that links the Fab and Fc regions and provides a flexible linker between the major functional regions of the antibody (Harlow and Lane, 1999; Mikkelsen and Cortón, 2004).

The selectivity of antigen-antibody interactions is analogous to the selectivity of substrate-enzyme interactions, known as “lock-and-key” interaction. The antigen-binding site of the antibody has a structure that allows a complementary fit with structural elements and functional groups of the antigen. This specific part of the antigen that interacts with the antigen-binding site of the antibody is called the epitope. Binding interactions between antibody and antigen may involve electrostatic, hydrophobic, and van der Waals interactions, as well as hydrogen bonding (Mikkelsen and Cortón, 2004).

### *3.1.1.2. Antibody production*

Antibodies are useful reagents that can bind with high affinity to chosen antigens. Specific antibodies can be used: to determine the subcellular location of an antigen, to isolate an individual antigen from a complex mixture of competing molecules; to find other macromolecules that interact with the antigen; to determine the exact concentration of an antigen (Harlow and Lane, 1999). These applications make antibodies very important and thus their production is crucial.

Antibodies can be divided into polyclonal and monoclonal, depending on the preparation procedure. Polyclonal antibodies are the most commonly used reagents for immunochemical techniques and are directly isolated from blood serum. The immunogen

used to generate polyclonal antibodies may consist of a small molecule (a hapten) covalently bound to a carrier protein and it is administered by an injection in the animal. After a period of time, blood samples are taken and allowed to clot; the liquid phase (blood serum), from which antibodies are prepared and purified, is then removed. The serum is a good source of polyclonal antibodies that will contain a mixture of antibodies that bind to different epitopes of the hapten carrier conjugate, as well as antibodies generated in response to other immunogens present in the animal organism. Monoclonal antibodies are a homogeneous population of identical antibody molecules having affinity for a single antigenic epitope. In 1975 Köhler and Milstein described the first version of a monoclonal production method (presented in Figure 3.2.), for which they were awarded the Nobel Prize (Harlow and Lane, 1999; Mikkelsen and Cortón, 2004).

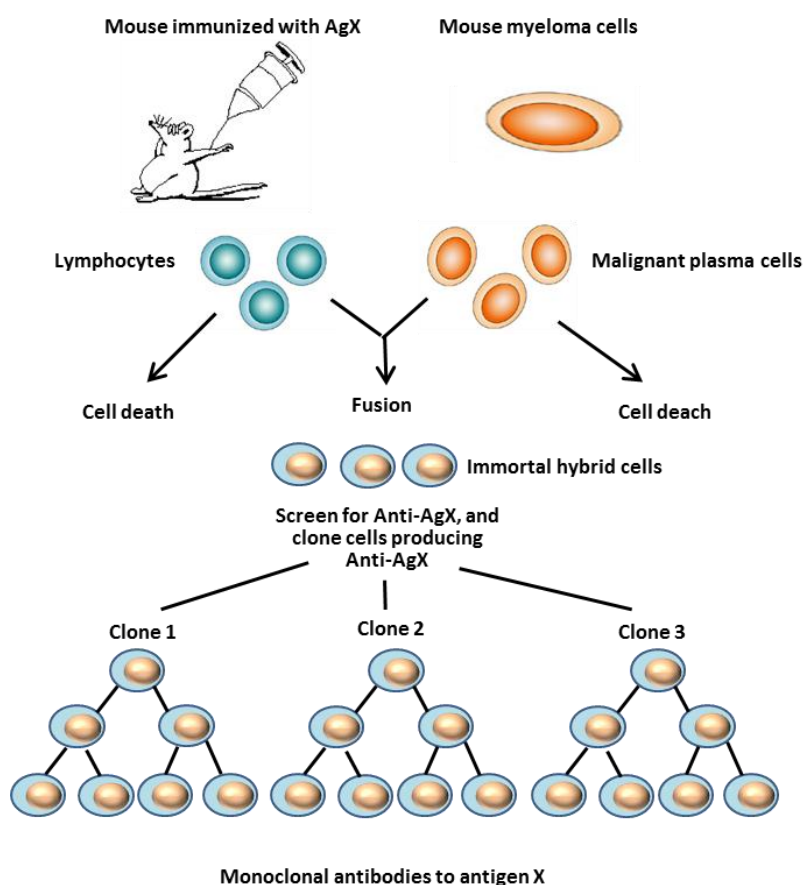


**Figure 3.2.** The generation of hybridoma cells for monoclonal antibody production (adapted from Mikkelsen and Cortón, 2004).

The production method begins with the synthesis of the immunogen, by the conjugation of a protein, such as bovine serum albumin (BSA), to the hapten, followed by the immunization of the animal with the immunogen. Lymphocytes (antibody producers) are isolated from the spleen of the immunized animal 8-12 weeks later. These cells are short-lived and can exist in cell culture only for a few days. Lymphocytes, which produce one specific antibody, are therefore fused with malignant plasma cells (myelomas), resulting in hybridoma cells. Hybridomas are then cloned from the single cells and cultured. From each lymphocyte fused a different hybridoma cell is obtained, thus a different clone. Each clone will produce antibodies of single epitope specificity. Hybrid cells retain the antibody producing characteristics of the spleen cells and the immortality of the malignant plasma cells.

Polyclonal antibodies are easy to obtain, while monoclonal antibodies production requires a very high initial investment. That can explain the fact that polyclonal antibodies are the most widely used reagents in immunochemical analysis so far (Franek and Hruska, 2005). A certain drawback of this method is the impossibility of producing identical antibody specificity even when using animals of the same species. Monoclonal antibodies present single epitope selectivity but still cannot avoid the cross-reactions due to structural similarities of antigens. So, the primary advantage of this antibody production method is the immortality of the hybridoma cell line, enabling the continuing antibody production with the same affinity and specificity (Mikkelsen and Cortón, 2004).

### *3.1.2. Tracer synthesis*

Immunoassay methods rely on the specific interaction between antibody and antigen. Such interaction is only quantifiable due to the use of a labelled antigen or antibody, denominated as tracer. Different label types can be used, depending on the immunoassay: radioisotopes, fluorophores, chemiluminophores and enzymes, among others (Mikkelsen and Cortón, 2004). The more common enzyme markers are horseradish peroxidase (HRP) and alkaline phosphatase (Hennion and Barceló, 1998).

The hapten, a modified analyte derivative, can be used for the synthesis of the immunogenic conjugate (using BSA) or for the enzyme tracer (using HRP) (Maqbool et al., 2002). The hapten should contain a “handle”, terminated with a functional group capable of binding covalently to a carrier protein. Common functional groups are  $-\text{COOH}$ ,  $-\text{OH}$ ,  $-\text{NH}_2$  or  $-\text{SH}$  (Hennion and Barceló, 1998). The first step is the production of the antigen derivative with the introduction of a carboxylic acid group. The location of this “linker” should be chosen carefully and attached as far as possible from important recognition sites. Small molecules need a spacer arm in the linker to favour the recognition by the immune system. Spacer lengths between three to six carbon atoms have proven to be most favourable (Hennion and Barceló, 1998). Once the hapten has been synthesized, it should be coupled to the appropriate protein. The coupling of the hapten to the HRP can be performed using several methods, like the mixed anhydride method described by Munro et al. (1984) or the active ester method described by Schneider and Hammock (1992).

One version of the mixed anhydride method uses isobutylchloroformate (IBCF) to generate a mixed anhydride (Figure 3.3.). This mixed anhydride reaction product is reactive towards primary amine groups of the HRP protein (Mikkelsen and Cortón, 2004).

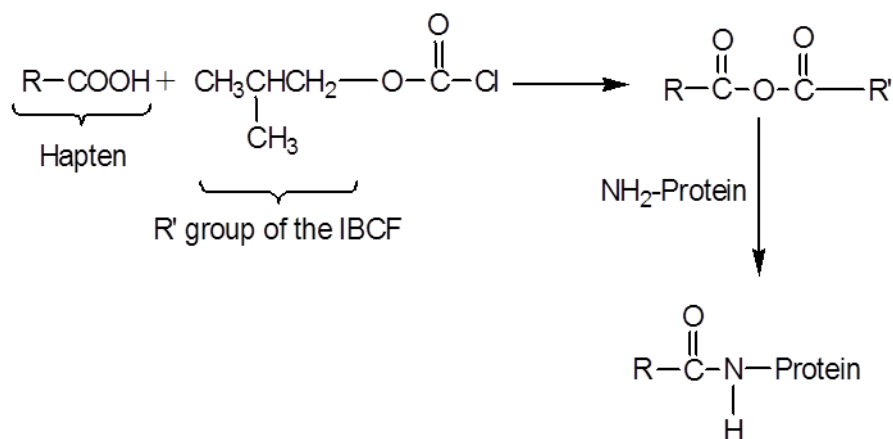


**Figure 3.3.** Coupling of the hapten to HRP using the mixed anhydride method.

Carboxylic acids may also be activated using the active ester method described by Schneider and Hammock (1992). The hapten first reacts with *N,N'*-Dicyclohexylcarbodiimide (DCC) producing an unstable reactive ester (Figure 3.4.). Then,

this unstable ester (1) reacts with N-hydroxysuccinimide (NHS) resulting in a semi-stable NHS ester (2) that can react with the enzyme, originating the hapten-enzyme conjugate (tracer) (Kaur et al., 2008). These two labeling reactions were used in this work and results are presented further on.

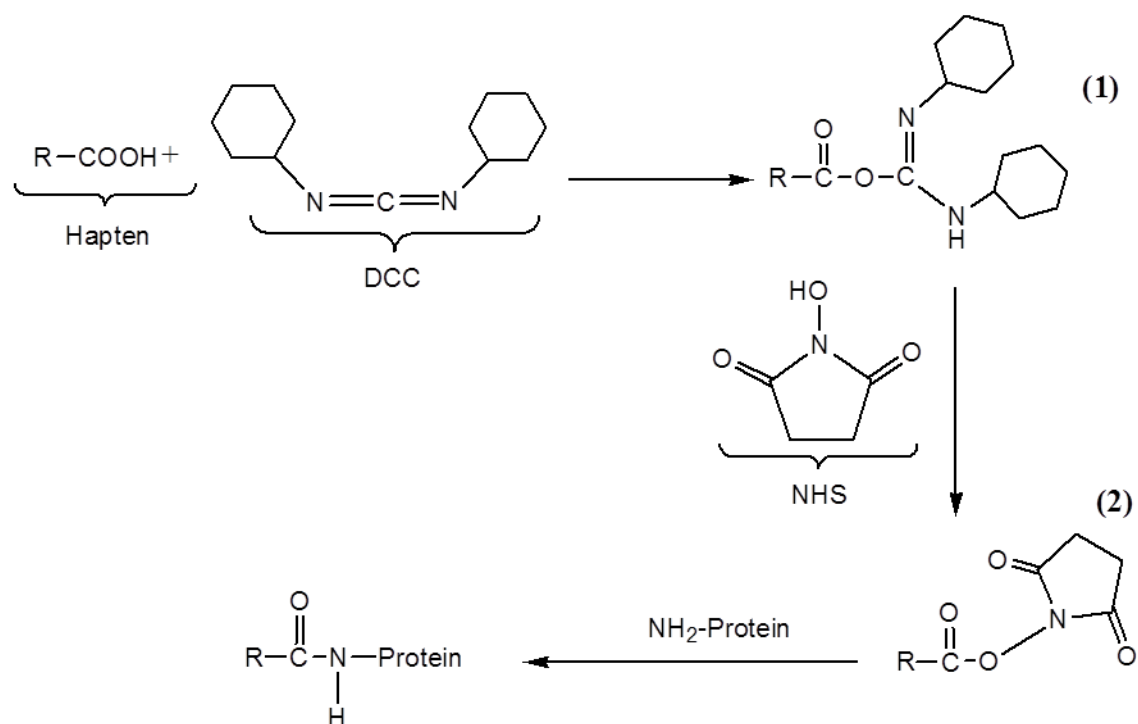


**Figure 3.4.** Coupling of the hapten to HRP using the active ester method.

### 3.1.3. Immunoassays

Many immunoassays require a separation step prior to quantification, in order to separate the bound and free fractions of the labelled species. This type of assay is considered a heterogeneous immunoassay. The classification of the assay is made according to a number of criteria, the most important one being whether occupied or unoccupied binding sites are measured (Hennion and Barceló, 1998). Based on this criterion they may be competitive or non-competitive.

Non-competitive ELISA methods are based on sandwich assays (Figure 3.5.) and rely on the measurement of the occupied binding sites by using an excess concentration of antibodies. First the antigen binds to the previous immobilized antibody; then, an excess

of labelled antibody is added and will bind to the immobilized antigen. Non-competitive ELISAs yield calibration curves in which enzyme activity increases with increasing antigen concentration (Mikkelsen and Cortón, 2004). This method can only be applied when the analyte of interest possesses at least two binding sites. Thus, it is not appropriate for pesticides which are small molecules (Hennion and Barceló, 1998).

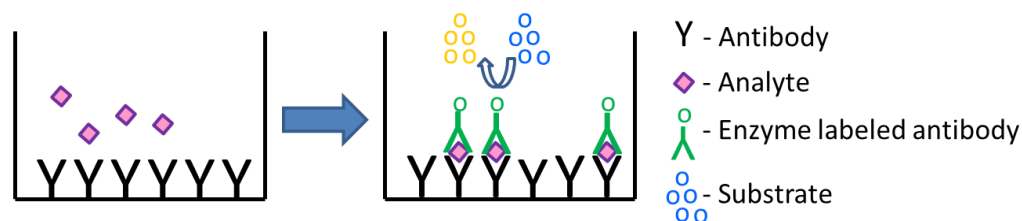


**Figure 3.5.** Principle of non-competitive immunoassay – sandwich assay.

In a competitive ELISA there is a measurement of unoccupied sites when using a limiting antibody concentration. The competitive ELISA can be direct or indirect.

In direct competitive ELISA, sample analyte and labelled analyte compete for antibody binding sites on the support (Figure 3.6.).

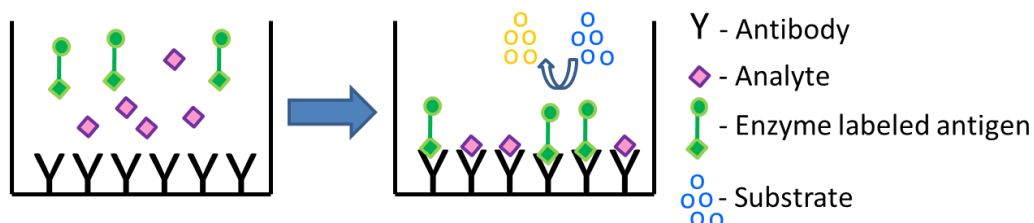


**Figure 3.6.** Principle of direct competitive immunoassay.

After a separation method, which allows the removal of free analyte and free labelled analyte, the concentration of the bound labelled antigen is measured as the signal generated by the tracer. This procedure is suitable for analyte of all sizes, but requires the synthesis of the enzyme labelled antigen, the tracer.

In indirect competitive ELISA, antigens are immobilized on the solid support and antibodies are added to the medium together with the analytes to be determined (Figure

3.7.). The immobilized analyte will compete for the antibody binding sites with the sample analyte. The amount linked to the immobilized analytes is determined by the addition of the labelled “secondary” antibodies which can specifically bind to the “primary” antibodies.

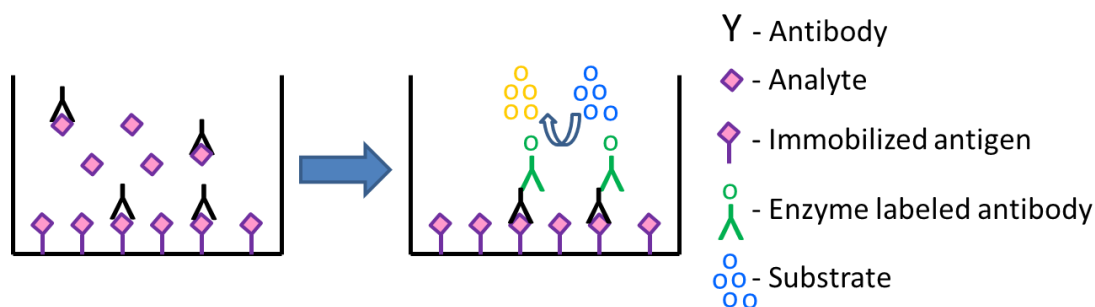


**Figure 3.7.** Principle of indirect competitive immunoassay.

Competitive ELISAs (indirect and direct) yield calibration curves in which enzyme activity decreases with increasing antigen concentration (Mikkelsen and Cortón, 2004).

In a competitive ELISA format the photometric determination of the enzyme label bound by measuring absorbance is related to the analyte concentration via a dose-response curve (Figure 3.8.).

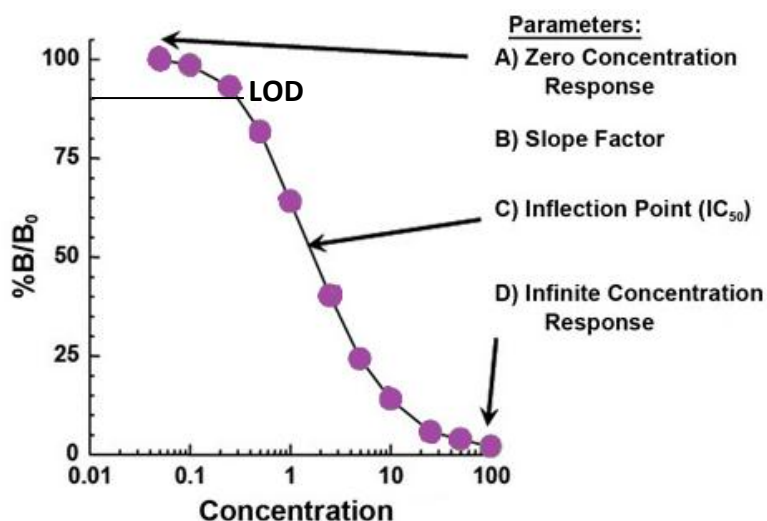


**Figure 3.8.** Typical 4-parameter logistic function graph for a competitive immunoassay format.

The calibration curves are obtained using different concentrations of antigen (analyte) standards. The experimental values are usually fitted to a four-parametric logistic equation (4PL) (Dudley et al., 1985):

$$y = [(A - D) / [1 + (x/C)^B]] + D$$

where,  $y$  is the optical density (OD);  $x$ , the antigen concentration;  $A$ , the OD of a zero control;  $B$ , the slope at the inflection point;  $C$ , the concentration value at the inflection point;  $D$ , the OD at a standard excess.

However, in order to compare several standard curves, the OD data should be normalized between 100 % (OD of a zero standard) and 0% (OD of a standard excess), according to the equation:

$$\% B/B_0 = \frac{OD - D}{A - D}$$

where,  $\%B/B_0$  is the normalized OD, OD is the optical density,  $A$  and  $D$  are parameters of the 4PL (Schneider et al., 2005).

Sensitivity can be expressed by the LOD, generally considered as the lower concentration that produces a signal significantly different from the blank signal. Although there is no standardized way to define LOD, there is a general consensus for selecting the dose which inhibits 10% of the enzyme tracer binding to the antibody, thus 90%  $B/B_0$ . The limit of quantification (LOQ) is considered the value above which quantitative results can be obtained with a stated relative precision, or a specific degree of confidence. Sometimes LOD is not in the linear range of the curve, and the selected LOQ is defined by the upper and lower limits of the linear range of the dose-response curve (Hennion and Barceló, 1998).

The precision profile is, quite clearly, one of the fundamental indicators of the assay performance. It undoubtedly represents the performance characteristics of the assay/operator combination with regard to random errors and is thus one of the fundamental indices of assay quality (Ekins, 1981). The relative error of the analyte concentration is calculated and plotted against the concentration to obtain the precision profile of the assay as described by Ekins (1981). Allowing a maximum value for the



coefficient of variation, CV (%), it is possible to define the working range of the assay (the maximum and minimum concentration quantifiable with a reasonable precision).

The cross-reactivity (CR) profile is an indicator of the assay specificity and has critical importance for immunoassay methods, in which a particular analyte is determined in the presence of very similar species (Mikkelsen and Cortón, 2004). CR is calculated as the ratio of molar concentrations at the inflection points (midpoints, C parameter in the 4PL) of the corresponding calibration curves and expressed in percentage relative to the midpoint for the antigen (Schneider et al., 2005).

$$CR = \frac{C_{Standard}}{C_{test}} \times 100$$

where, CR describes the cross-reactivity (%),  $C_{standard}$  is a parameter of the 4PL, giving the antigen concentration at the inflection point and  $C_{test}$  refers to the concentration of the cross-reacting compound at its inflection point (Schneider et al., 2005).

Cross-reactivity depends on the selectivity of an antibody for a particular epitope, and can be slightly controlled in the design of the immunogen used to produce antibodies. The site of attachment and the nature of the hapten linkage, to the carrier protein, are critical for the selectivity of the assay (Mikkelsen and Cortón, 2004). However, cross-reactivity is expected to occur, in monoclonal as well as in polyclonal immunoassays, due to the existence of several analogues and metabolites of the target compound. This makes it important to measure and understand the major cross-reactivities possible (Hennion and Barceló, 1998).

#### *3.1.4. Application in environmental analysis*

Due to the increasing research interest in food and environmental analysis, the development of analytical methods that are highly sensitive while being simple becomes more and more important. Since the 1980s, the application of immunochemical methods, such as ELISA, for pesticide detection in water samples has been growing, as this technique is specific, cost effective and fast (Kaur et al., 2008).

Due to the selectivity and sensitivity, as well as simplicity, a wide range of ELISA applications, for organic pollutants, have been reported in literature. A direct competitive ELISA for the determination of polychlorinated biphenyls in soil samples was developed by Deng and co-workers (2002). Phenoxyacetic acid herbicides have also been determined by ELISA in water samples (Kaur et al., 2008). Farré et al. (2007) reviewed a number of papers about ELISA application to environmental analysis: herbicides in water and soil samples; insecticides in water, soil and food samples; fungicides in water and food samples; hormones ( $17\beta$ -estradiol, estrone,  $17\alpha$ -ethinylestradiol) in water samples; pharmaceutical compounds in water, milk, and honey; phenols in water and urine samples; and also surfactants in water samples.

In what concerns the application of ELISA on atrazine determination, Kramer et al. (2001) developed an ELISA for screening atrazine residues in soil samples, while Maqbool et al. (2002) dedicated their work to the determination of atrazine residues in water samples. ELISA was also used by Toscano et al. (1998) to follow adsorption of atrazine onto humic substances.

Although many pesticides can be analysed using conventional (sometimes highly sophisticated) analytical techniques, there are many more that cannot be analysed or can only be analysed with insufficient sensitivity. Conventional procedures for sample preparation prior to chromatographic analysis are expensive and time-consuming and usually involve derivatization of target compounds. Immunotechniques present low detection limits, parts per billion (ppb) to parts per trillion (ppt) for water analysis and parts per million (ppm) to ppb for other types of samples (Nunes et al., 1998).

#### *3.1.4.1. Using ELISA to follow sorption behaviour*

Sample preparation for traditional analytical detection techniques, can involve considerable time in extracting and concentrating pesticide residues before analysis (Amistadi et al., 1997). HPLC is the most commonly used method for monitoring sorption of atrazine onto soils (Chefetz et al., 2004; Drori et al., 2005; Park et al., 2004; Socías-Viciano et al., 1999). Other possible techniques are LSC (Ben-Hur et al., 2003; Mbuya et

al., 2001; Prata et al., 2003; Smith et al., 2003), MEKC (Lima et al., 2009a) and voltammetry (Santos et al., 2005). These methods can be costly and time-consuming; conversely, ELISA offers a way to quantitatively determine residual pesticide concentrations in water and soil samples with much less effort, higher sensitivity, simplicity, quicker sample turnover time and often no need for sample clean-up or pre-concentration steps (Amistadi et al., 1997; Stearman and Wells, 1993). Accordingly, ELISA has been favourably compared with gas chromatography (GC) analysis when used for the evaluation of pesticide levels in surface and groundwater samples (Bushway et al., 1988; Gruessner et al., 1995; Thurman et al., 1990).

However, like in all analytical procedures, when using enzyme immunoassays on soil extracts some problems may arise due to co-extraction of cross-reacting compounds or matrix effects. Matrix effects derived from the interference of synthetic or natural substances, including structurally similar compounds, halogens and DOC that interact with the antibody or the enzyme tracer impairing binding or activity of the tracer. Such interference leads to a lower signal generated by the tracer and may yield an overestimation of the obtained results, resulting in false-positive quantifications (Amistadi et al., 1997; Gascón et al., 1995). The effect of DOC in an immunoassay has been assessed before and matrix effects were attributed to interference in the attachment of atrazine to the antibody (Amistadi et al., 1997). However, diluting the soil extract in water, the possible matrix effects were reduced (Lawruk et al., 1993).

The aim of this study was to develop an ELISA technique that could be used in the determination of atrazine in soil samples from batch equilibrium experiments, in order to follow the sorption behaviour of this pesticide onto soil samples. The optimized ELISA was applied to a soil sample and the obtained results were compared with the ones obtained in the experiments described in chapter 1.

## 3.2. Experimental procedure

---

### 3.2.1. Soil sample

The soil sample used is the same as the one described in section 1.2.1.

### 3.2.2. ELISA development

#### 3.2.2.1. Reagents and materials

All reagents were of analytical or biochemical grade and were used as received. HRP (EIA grade) was obtained from Roche, Guardian™ (an enzyme stabilizer) was from Perbio. Tetramethylbenzidine (TMB) and Tween™ 20 were purchased from Serva, sodium azide was from VWR. Ultrapure water was obtained by running demineralized water through a Milli-Q water purification system from Millipore. Atrazine and all buffer salts were supplied by Sigma-Aldrich. Sephadex columns were from Amersham Biosciences. For the immunoassay the following buffers were used: washing buffer concentrate (60x) ( $43\text{ mmol L}^{-1} \text{ KH}_2\text{PO}_4$ ,  $375\text{ mmol L}^{-1} \text{ K}_2\text{HPO}_4$ ,  $1.33\text{ mmol L}^{-1}$  sorbic acid potassium salt and 3% Tween™ 20, pH 7.6), phosphate buffer solution (PBS) ( $10\text{ mmol L}^{-1} \text{ NaH}_2\text{PO}_4 \cdot 2\text{H}_2\text{O}$ ,  $70\text{ mmol L}^{-1} \text{ Na}_2\text{HPO}_4 \cdot 2\text{H}_2\text{O}$ ,  $145\text{ mmol L}^{-1} \text{ NaCl}$ , pH 7.6), coating buffer ( $15\text{ mmol L}^{-1} \text{ Na}_2\text{CO}_3$ ,  $35\text{ mmol L}^{-1} \text{ NaHCO}_3$ ,  $3\text{ mmol L}^{-1} \text{ NaN}_3$ , pH 9.6) and substrate buffer ( $200\text{ mmol L}^{-1}$  citric acid monopotassium salt buffer containing  $3\text{ mmol L}^{-1} \text{ H}_2\text{O}_2$  and 0.01% sorbic acid potassium salt, pH 3.8). A stabilized TMB solution ( $41\text{ mmol L}^{-1}$  TMB,  $8\text{ mmol L}^{-1}$  tetrabutylammoniumborohydride in dimethylacetamide) was prepared according to Frey et al. (2000). The final substrate solution consists of  $540\text{ }\mu\text{L}$  TMB solution in  $21.5\text{ mL}$  substrate buffer and was freshly prepared for each run. Microtiter plates of high protein-binding capacity polystyrene used were transparent with 96 flat-bottom wells (MaxiSorp™, Nunc). Washing steps were carried out using an automatic plate washer (Atlantis, Asys Hitech). The incubation of the plates was performed using a plate shaker (Titramax 100, Heidolph). Absorbance was measured at  $450\text{ nm}$  and referenced to  $620\text{ nm}$  with a plate reader (UVM 340, Asys Hitech).

Six triazine derivatives were selected for tracer synthesis (Figure 3.9).

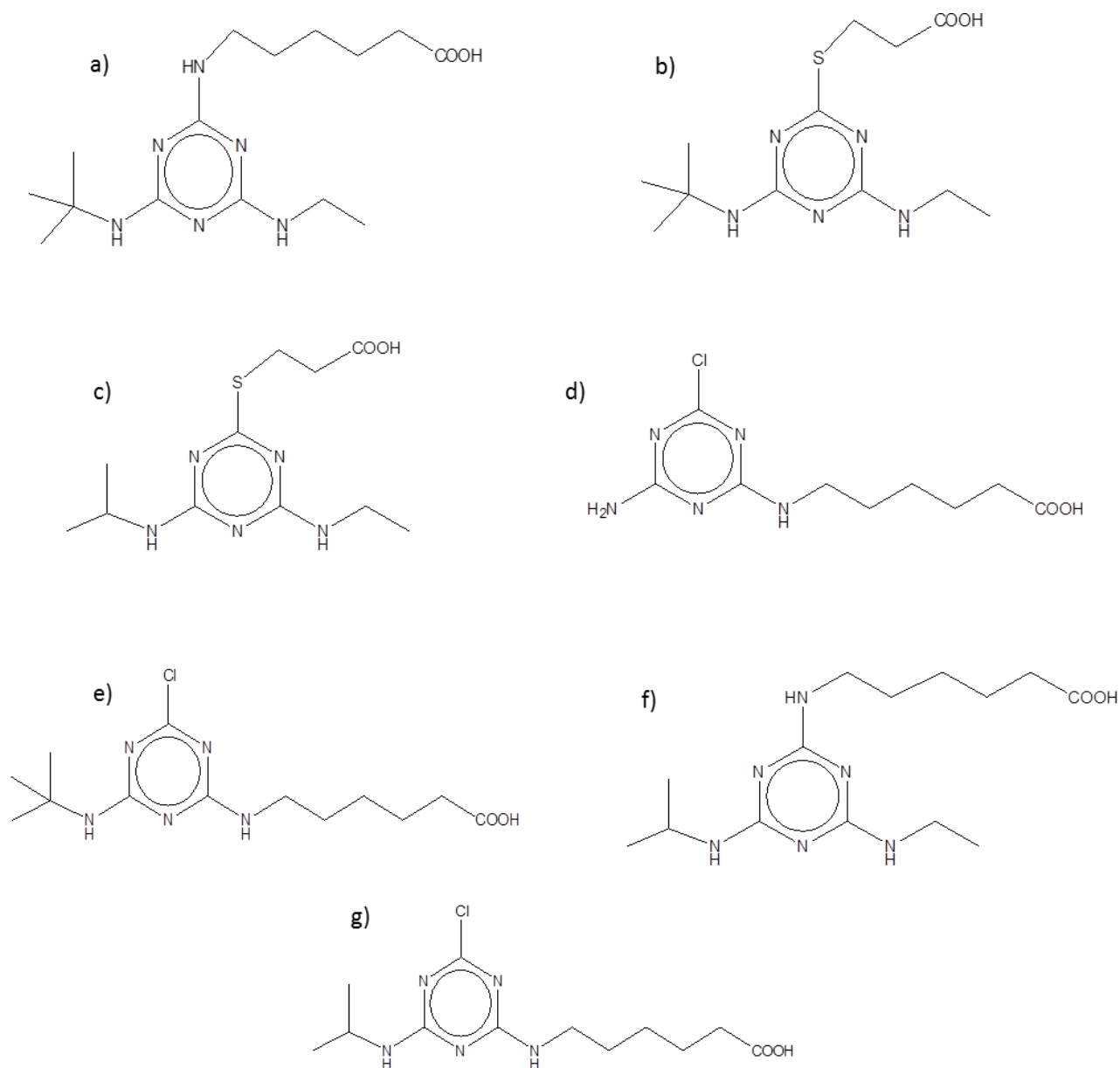


**Figure 3.9.** Triazine derivatives:

- a) 2-(tert-butylamino)-4-[(1-carboxypent-5-yl)amino]-6-(ethylamino)-1,3,5-triazine (t-Bu/Et/C6);  
 b) 2-(tert-butylamino)-4-[(1-carboxyeth-2-yl)thio]-6-(ethylamino)-1,3,5-triazine (t-Bu/Et/SC3);  
 c) 2-[(1-carboxyeth-2-yl)thio]-4-(ethylamino)-6-(isopropylamino)-1,3,5-triazine (i-Pr/Et/SC3);  
 d) 2-[(1-carboxypent-5-yl)amino]-4-chloro-6-amino-1,3,5-triazine (H/Cl/C6);  
 e) 2-(tert-butylamino)-4-[(1-carboxypent-5-yl)amino]-6-chloro-1,3,5-triazine (t-bu/Cl/C6);  
 f) 2-[(1-carboxypent-5-yl)amino]-4-(ethylamino)-6-(isopropylamino)-1,3,5-triazine (i-Pr/Et/C6);  
 g) 2-[(1-carboxypent-5-yl)amino]-4-chloro-6-(isopropylamino)-1,3,5-triazine (i-Pr/Cl/C6);  
 (for nomenclature and abbreviations, cf. to Weller and Niessner, 1997).

Synthesis and naming of derivatives were carried out by Weller (Weller et al., 1992; Weller and Niessner, 1997), as well as the initial comparison of their binding properties (Ulrich et al., 1991; Weller and Niessner, 1997).

#### *3.2.2.2. Preparation of enzyme conjugates via mixed anhydride route*

In order to produce enzyme tracers of different structure the selected triazine derivatives were coupled to HRP using modifications of the method described by Munro et al. (1984) for synthesis of progesterone conjugates. This type of conjugation is usually addressed in literature as “mixed anhydride” method.

##### **Step 1: Production of the mixed anhydride**

- a) The hapten (3.0  $\mu\text{mol}$ ; T1: t-Bu/Et/C6,  $m = 0.970$  mg; T2: t-Bu/Et/SC3,  $m = 0.894$  mg; T3: Et/i-Pr/SC3,  $m = 1.000$  mg) was maintained overnight in a vacuum environment.
- b) To 240  $\mu\text{L}$  of anhydrous dimethylformamide (DMF) were added 1.92  $\mu\text{L}$  of *N*-Methylmorpholine (colourless/clear) at  $-21^\circ\text{C}$  under protective gas (Argon, 0.5 bar).
- c) 60.5  $\mu\text{L}$  of the solution prepared in b) were added to each 3.0  $\mu\text{mol}$  of hapten with continuous agitation at  $-21^\circ\text{C}$  under protective gas (Argon, 0.5 bar).
- d) 0.48  $\mu\text{L}$  IBCF were added at  $-21^\circ\text{C}$  under protective gas (Argon, 0.5 bar)
- e) The mixture was agitated during 30 min at  $-21^\circ\text{C}$ .

##### **Step 2: Coupling of the mixed anhydride to HRP**

- a) To 200  $\mu\text{L}$  of water, 120  $\mu\text{L}$  of DMF were added.
- b) To 10 mg of HRP, 70  $\mu\text{L}$  of the solution prepared in a) were added.
- c) From the HRP solution prepared, 48  $\mu\text{L}$  were transferred to a 2 mL tube and cooled to  $-21^\circ\text{C}$  together with a stir bar.

- d) Each hapten solution prepared in Step 1 was added to the 48  $\mu\text{L}$  of HRP. This procedure needed to be done very slowly and with continuous agitation and refrigeration.
- e) The solution was stirred at  $-21^{\circ}\text{C}$  for 1h and then another 2h at  $0^{\circ}\text{C}$ , after which the solution was directly poured on a Sephadex™ G-25 PD-10® gel chromatography column.

### Step 3: Purification of the conjugate

- a) To purify the conjugate, PBS (pH 8.90, 1  $\text{mmol L}^{-1}$   $\text{NaH}_2\text{PO}_4 \cdot 2\text{H}_2\text{O}$ , 7  $\text{mmol L}^{-1}$   $\text{Na}_2\text{HPO}_4 \cdot 2\text{H}_2\text{O}$ , 14.5  $\text{mmol L}^{-1}$   $\text{NaCl}$ ) was used for the conditioning and elution of the enzyme conjugate from a Sephadex™ G-25 PD-10®.
- b) After conditioning the column, the conjugate was added to the top of the column and after entering the column, more PBS was added.
- c) Fractions of the eluted solution were collected in a microtiter plate, 2 or 3 drops in each well. After the elution, the OD of each well was measured at 405 nm (Figures 3.10., 3.11. and 3.12.).
- d) Fractions from the two wells (F1) presenting highest OD values were pooled, mixed with an equal amount of Guardian™ peroxidase stabilizer (Pierce) and stored at  $4^{\circ}\text{C}$ .

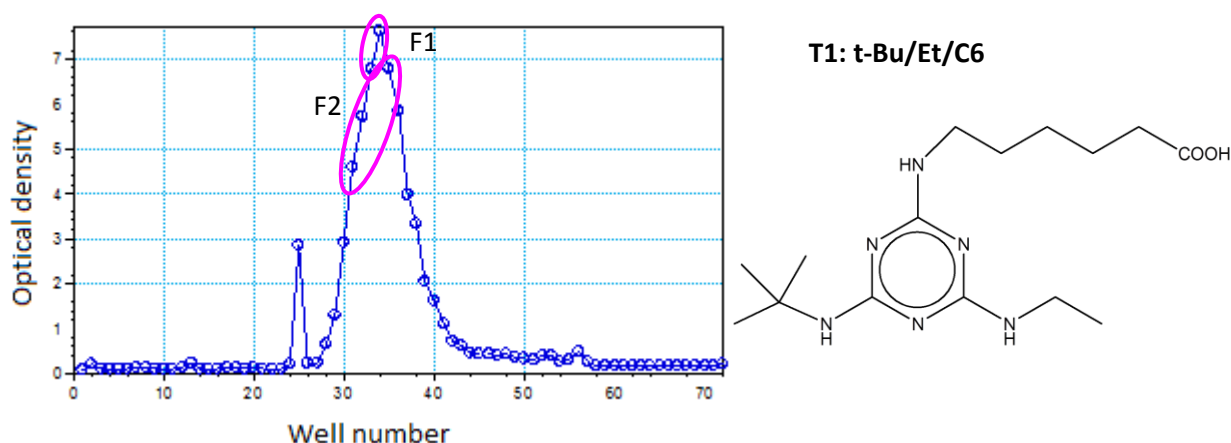


**Figure 3.10.** Collection of the tracer T1: t-Bu/Et/C6 fractions after separation by means of a Sephadex G-25 PD-10® column using mixed anhydride method.

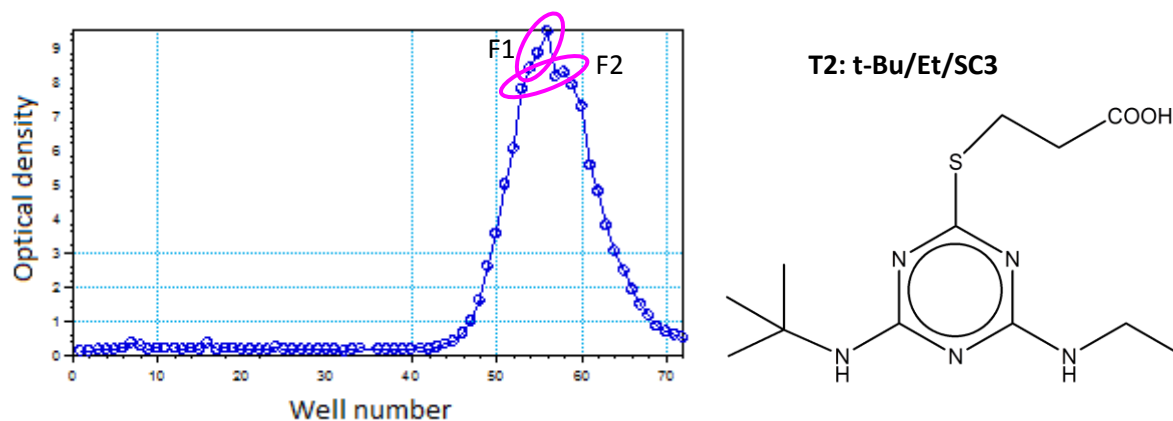


**Figure 3.11.** Collection of the tracer T2: t-Bu/Et/SC3 fractions after separation by means of a Sephadex PD-10<sup>®</sup> column using mixed anhydride method.

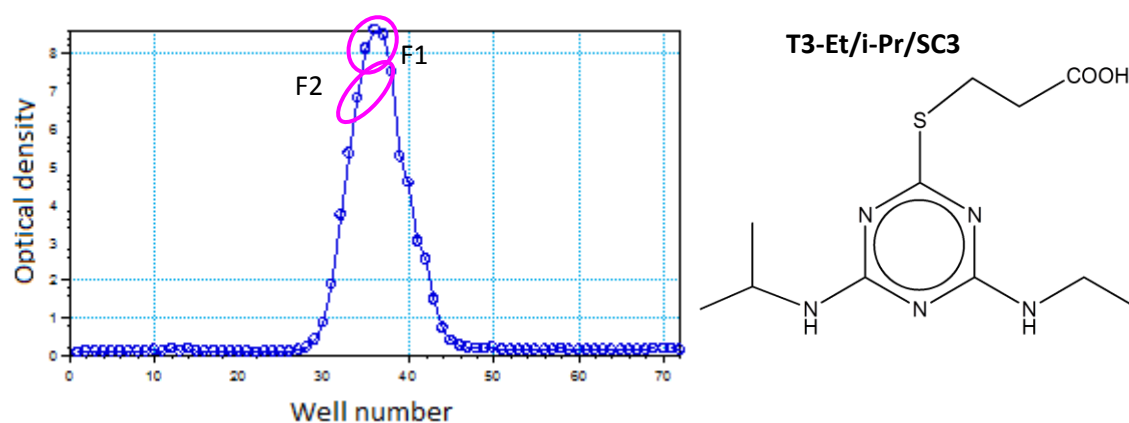


**Figure 3.12.** Collection of the tracer T3: Et/i-Pr/SC3 fractions after separation by means of a Sephadex G-25 PD-10<sup>®</sup> column using mixed anhydride method.

- e) Another fraction (F2), with lower OD values than the first fraction, was stored at 4°C (no Guardian™ was used, and normally this fraction was saved for characterization purposes).

### 3.2.2.3. Preparation of enzyme conjugates via activated ester route

Also the conjugation between hapten and HRP was made using modifications of the active ester method described by Schneider and Hammock (1992). This method was used either using DMF or tetrahydrofuran (THF) as solvent.



**Step 1: Production of the activated ester**

A 1 mL dischargeable tube with planar bottom was placed in a stirrer and a small stirring magnet was put inside the tube. Reactants were added with continuous stirring. (No water around; work took place under nitrogen atmosphere).

- a) 10  $\mu\text{mol}$  of the hapten (T1: t-Bu/Et/C6,  $m = 3.23$  mg; T2: t-Bu/Et/SC3,  $m = 2.98$  mg) were dissolved in 40  $\mu\text{L}$  of anhydrous DMF under nitrogen atmosphere and stirred for a few minutes.
- b) 23.0 mg (200  $\mu\text{mol}$ ) of NHS were dissolved in 400  $\mu\text{L}$  of DMF.
- c) 20.1 mg (100  $\mu\text{mol}$ ) of DCC were dissolved in 400  $\mu\text{L}$  of DMF.
- d) 40  $\mu\text{L}$  of the NHS solution (20  $\mu\text{mol}$ ) were added to the hapten solution and stirred again.
- e) 40  $\mu\text{L}$  of the DCC solution (10  $\mu\text{mol}$ ) were added to the previous solution.
- f) Tube was protected from the light with aluminium foil and let stir over night (18 hours) at room temperature (RT).
- g) The tube was centrifuged at 15°C, 1750  $g$ , during 10 minutes.
- h) If some suspended particles were still visible in the solution, centrifugation was prolonged for 5 more minutes.

**Step 2: Conjugation between the activated ester and HRP**

- a) A 0.13 mol L<sup>-1</sup> solution of sodium bicarbonate was prepared by dissolving 1.092 g of NaHCO<sub>3</sub> in 100 mL of Milli-Q water.
- b) 2.21 mg of HRP (0.05  $\mu\text{mol}$ ) were dissolved in 1 mL sodium bicarbonate (NaHCO<sub>3</sub>) 0.13 mol L<sup>-1</sup>.
- c) 200  $\mu\text{L}$  of the aforementioned solution were pipetted to a 1 mL dischargeable tube with planar bottom and put on the stirrer (with a stir bar inside).
- d) 12  $\mu\text{L}$  of the activated ester solution supernatant prepared on Step 1 was added dropwise to 212  $\mu\text{L}$  of the peroxidase solution.
- e) Solution was stirred for 5 hours at room temperature and protected from the light (using aluminium foil).

**Step 3: Purification of the conjugate**

- To purify the conjugate, PBS (pH 8.90, 1 mmol L<sup>-1</sup> NaH<sub>2</sub>PO<sub>4</sub>·2H<sub>2</sub>O, 7 mmol L<sup>-1</sup> Na<sub>2</sub>HPO<sub>4</sub>·2H<sub>2</sub>O, 14.5 mmol L<sup>-1</sup> NaCl) was used for the conditioning and elution of the enzyme conjugate on a Sephadex™ G-25 PD-10® gel chromatography column (Amersham Biosciences).
- After conditioning, the conjugate was added to the top of the column and after having entered the column, more PBS was added.
- Fractions of the eluted solution were collected in a microtiter plate, 2 or 3 drops in each well. After the elution, the OD of each well was measured at 405 nm (Figures 3.13. and 3.14.).

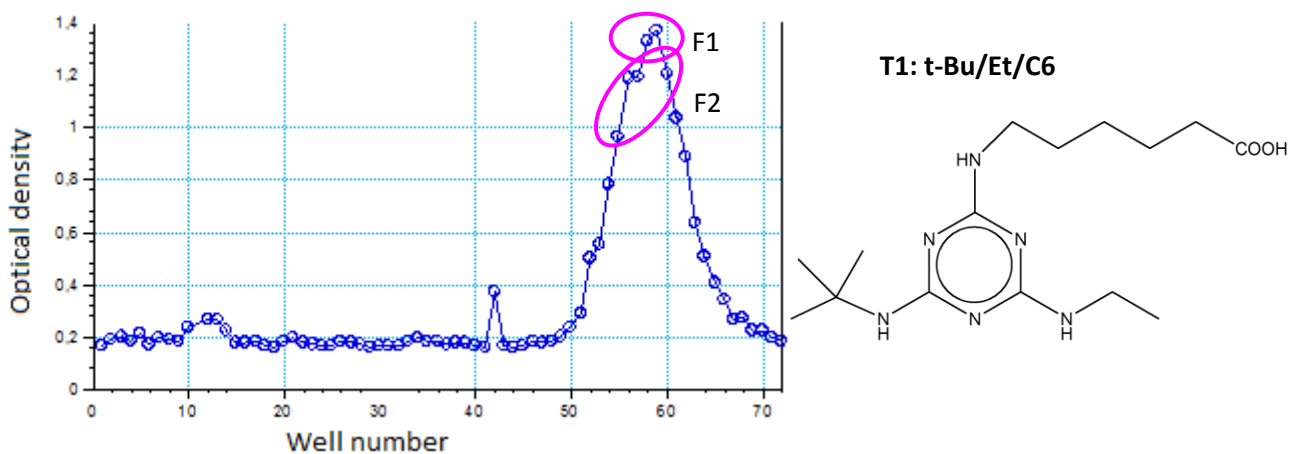


**Figure 3.13.** Collection of the tracer T1: t-Bu/Et/C6 fractions after separation by means of a Sephadex G-25 PD-10® column using the active ester method with DMF as solvent.

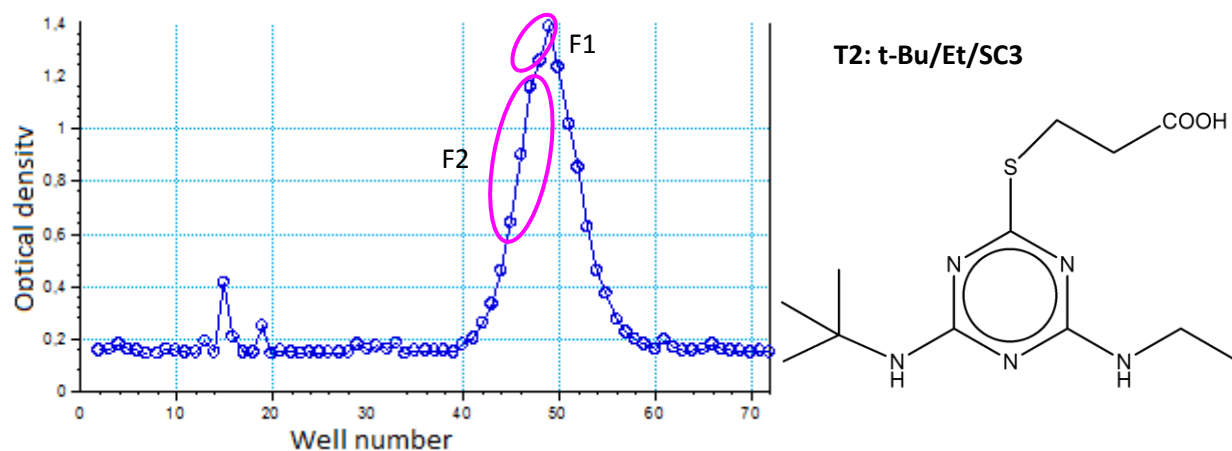


**Figure 3.14.** Collection of the tracer T2: t-Bu/Et/SC3 fractions after separation by means of a Sephadex G-25 PD-10® column using the active ester method with DMF as solvent.

- d) Those fractions from the two wells (F1) presenting highest OD values were pooled, mixed with an equal amount of Guardian™ peroxidase stabilizer (Pierce) and stored at 4°C.
- e) Another fraction (F2), with lower OD values than the first fraction was stored at 4°C (no Guardian™ was used, and normally this fraction was saved for characterization purposes).

The same procedure was applied to hapten T1: t-Bu/Et/C6 ( $m = 3.23\text{mg}$ ), T2: t-Bu/Et/SC3 ( $m = 2.98\text{ mg}$ ), T4: H/Cl/C6 ( $m = 2.45\text{ mg}$ ) and T5: t-Bu/Cl/C6 ( $m = 3.16\text{ mg}$ ) using THF as solvent instead of DMF and the OD values measured for each microtiter plate of each coupled hapten are presented on Figures 3.15. to 3.18.

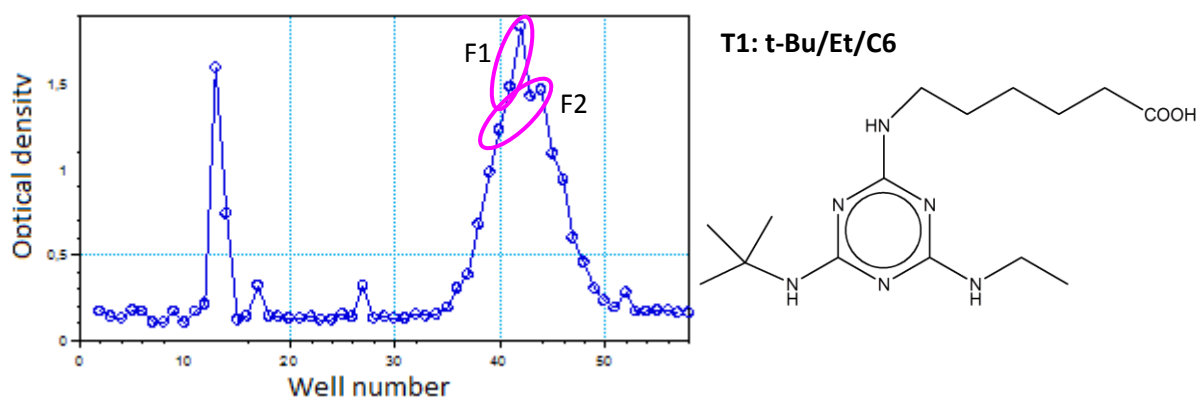


**Figure 3.15.** Collection of the tracer T1: t-Bu/Et/C6 fractions after separation by means of a Sephadex G-25 PD-10® column using active ester method with THF as solvent.

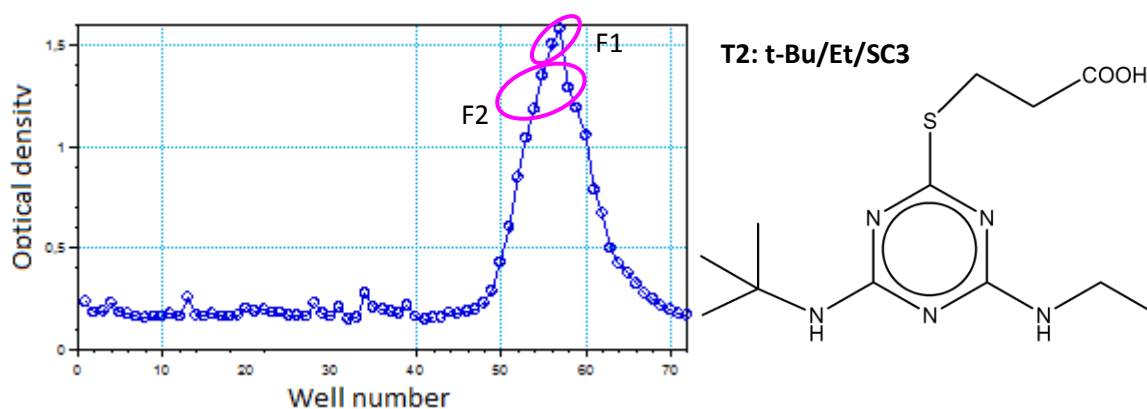


**Figure 3.16.** Collection of the tracer T2: t-Bu/Et/SC3 fractions after separation by means of a Sephadex G-25 PD-10® column using active ester method with THF as solvent.

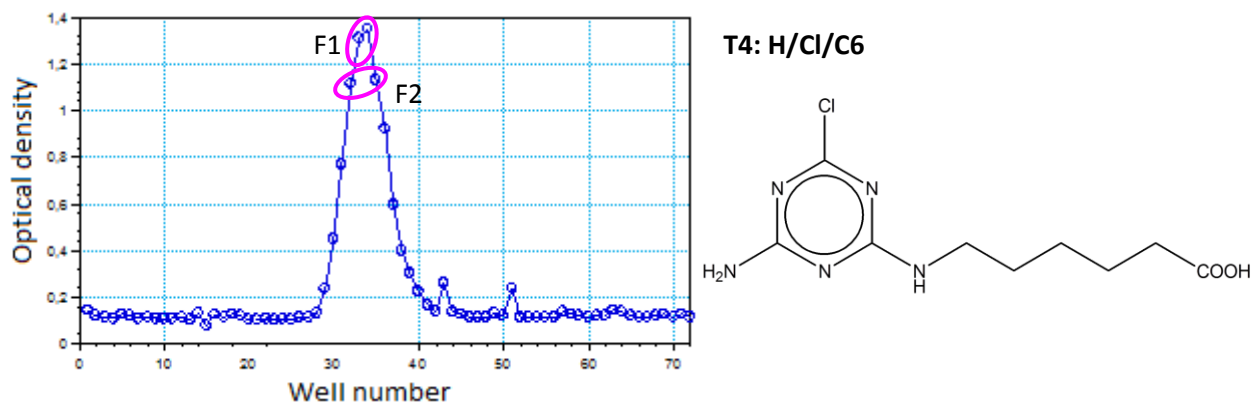


**Figure 3.17.** Collection of the tracer T4: H/Cl/C6 fractions after separation by means of a Sephadex G-25 PD-10<sup>®</sup> column using active ester method with THF as solvent.

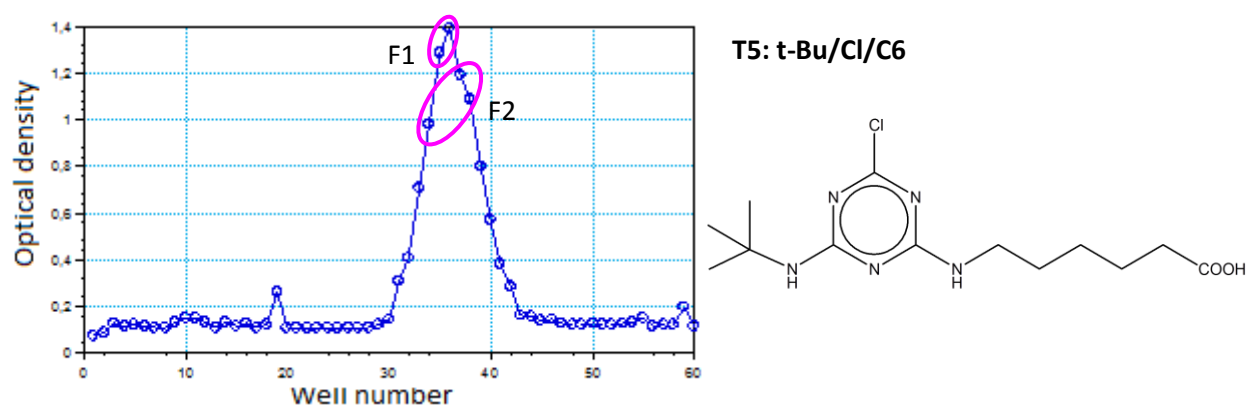


**Figure 3.18.** Collection of the tracer T5: t-Bu/Cl/C6 fractions after separation by means of a Sephadex G-25 PD-10<sup>®</sup> column using active ester method with THF as solvent.

In Table 3.1. a list of the several tracers synthesized using different experimental methodologies is presented.

**Table 3.1.** Schematic list of the synthesized tracers using different methodologies

Tracer \ Method	Tracer 1 t-Bu/Et/C6	Tracer 2 t-Bu/Et/SC3	Tracer 3 Et/i-Pr/SC3	Tracer 4 H/Cl/C6	Tracer 5 t-Bu/Cl/C6
Activated ester using DMF	✓	✓			
Activated ester using THF	✓	✓		✓	✓
Mixed anhydride using THF	✓	✓	✓		

Also two other tracers T6: i-Pr/Et/C6 and T7: i-Pr/Cl/C6 (Figure 3.9.) were available for testing, synthesized previously by Weller (1992).

#### 3.2.2.4. *Tracer and antibody binding specificity*

Several triazines antibodies were available and in order to choose the most appropriate combination of tracer and antibody for atrazine, the OD for two standards of atrazine (blank and 1000  $\mu\text{g L}^{-1}$ ) was determined using different antibody and tracer combinations. All determinations were made in triplicate. The evaluation was made by comparison of the OD obtained for each standard in order to assess tracer binding (high blank signal), important for signal generation, against analyte competition (lowering OD) which determines sensitivity of the assay.

The polyclonal antibodies available and adequate for triazines quantification were S84, Ak15, Ak19, C10, CWoNr and C193 (for nomenclature, *cf.* Weller, 1992). Antiserum production for the polyclonal antibody C193 was described by Wittmann and Hock (1989) and for C10 was described by Wittmann and Hock (1991). All freeze-dried antibodies were dissolved in PBS (0.1%  $\text{NaN}_3$ ) at a concentration of 1 mg  $\text{mL}^{-1}$ . Combinations were chosen according to previous information about the production of those antibodies and also accordingly to tracer binding patterns obtained using different antibodies, presented by Weller and Niessner (1997).

#### 3.2.2.5. *ELISA procedure*

Direct competitive ELISA was adapted for the analysis of atrazine. Microtiter plates were coated with polyclonal antibody serum diluted 1:10000 in coating buffer, using 200  $\mu\text{L}$  per well. Plates were covered with Parafilm™ to prevent evaporation. After overnight incubation at 20°C on the plate shaker at 750 rpm, the plates were washed, three times, with wash buffer concentrate, diluted 60 times. After the three washing cycles standards/samples were added to the plate (100  $\mu\text{L}$  per well) and the plate shaken at room temperature for 30 min. This was followed by addition of the respective enzyme

conjugate in PBS (diluted 1:10000, 100  $\mu\text{L}$  per well); the plate was shaken at room temperature for 30 min, followed by a second three-cycle washing step. Finally, the substrate solution was added (200  $\mu\text{L}$  per well) and incubated for 30 min. The enzyme reaction was stopped by addition of 1 mol  $\text{L}^{-1}$  sulphuric acid (100  $\mu\text{L}$  per well).

For construction of calibration curves, an atrazine stock solution was prepared in methanol and then further diluted with ultra-pure water to obtain standard solutions with concentrations ranging from 0.0001 to 1000  $\mu\text{g L}^{-1}$ .

Absorbance was read at 450 nm and referenced to 620 nm. All determinations were at least made in triplicate. The mean values were fitted to a 4PL equation, previously described (Dudley et al., 1985).

### *3.2.3. Adsorption experiment*

Adsorption isotherms of atrazine were established using the batch equilibration technique (OECD, 2000) in a miniaturized approach analogously to Fruhstorfer et al. (1993). Five pesticide concentrations (2 to 10  $\text{mg L}^{-1}$ ) were prepared in 0.01 mol  $\text{L}^{-1}$  calcium chloride solution. A 4 mL aliquot of each concentration of atrazine solution was added to 2 g of soil. Three adsorption trials were performed for each concentration. The tubes containing the mixtures were shaken, head over head at 100 rpm for 24 h at  $20\pm 1^\circ\text{C}$ , centrifuged and the supernatant filtered and analysed. The equilibrium concentration, after the sorption experiment, was determined using MEKC and ELISA. For ELISA determination, sample solutions were diluted approximately 10000 times. Results were compared with the ones obtained in chapter 1.

## 3.3. Results and discussion

---

### *3.3.1. Tracer and antibody binding specificity*

Several antibodies suitable for triazine determination were available.

From all antibodies reported previously, C10 was the only one that was not suitable for atrazine but appropriate instead for desethylatrazine. For this reason, tracer 4 (H/Cl/C6) was synthesized, since previous information reported that this tracer was specific for this antibody. However, when this combination was tested no colour was observed. This fact is not due to the lack of specificity, but maybe to the antibody degradation.

In order to choose the most appropriate combination of tracer and antibody for atrazine determination, several combinations of tracers and antibodies available were tested. In Figure 3.19. the OD values obtained for each standard in a microtiter plate coated with polyclonal S84 antibody and using different synthesized tracers are presented.

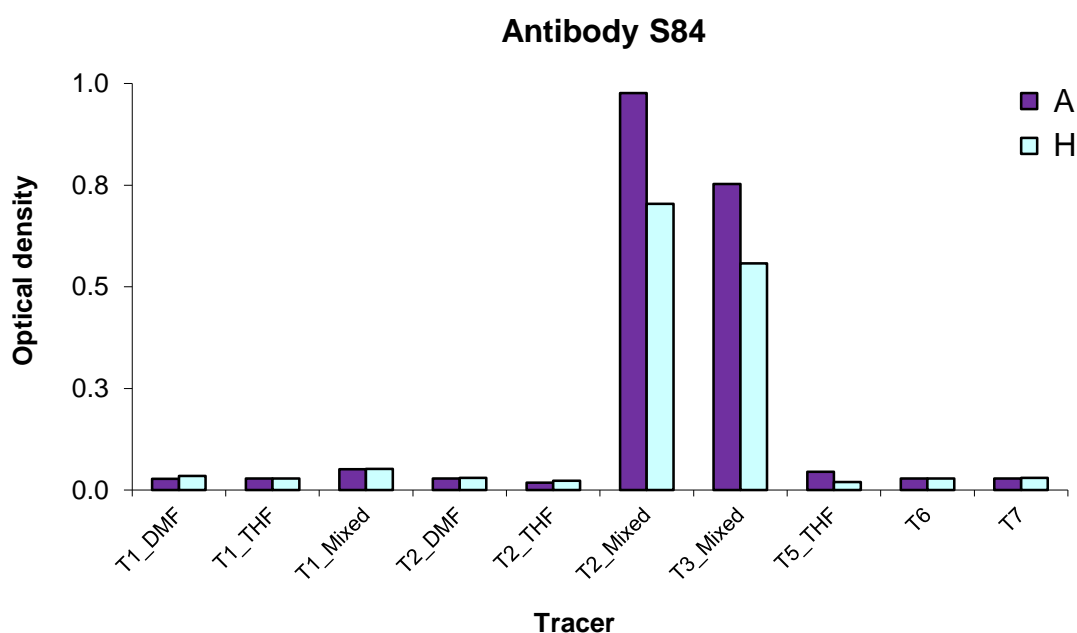


**Figure 3.19.** Representation of the OD values obtained for each standard, A – blank (water) and H – atrazine concentration 1000 µg L<sup>-1</sup> obtained using different tracers (synthesized differently) and microtiter plate coated using the polyclonal antibody S84. T1: t-Bu/Et/C6; T2: t-Bu/Et/SC3; T3: Et/i-Pr/SC3; T5: t-Bu/Cl/C6; T6: i-Pr/Et/C6 and T7: i-Pr/Cl/C6.

The results obtained with the tracers produced by the mixed anhydride method presented colour signal (T2 and T3), although it appears to be an unspecific binding to the

microtiter plate, since low differences in OD between blank and standard  $1000 \mu\text{g L}^{-1}$  are observed. Tracer T5 does not show unspecific binding (low OD for standard  $1000 \mu\text{g L}^{-1}$ ) but the maximum value of absorption for the blank was 0.04, a value too low decreasing sensitivity. To evaluate the possibility of using antibody S84 and T2 (synthesized via mixed anhydride method), T3 or T5 to determine atrazine, the OD using standards from  $0.0001$  to  $1000 \mu\text{g L}^{-1}$  was measured (Figure 3.20.).

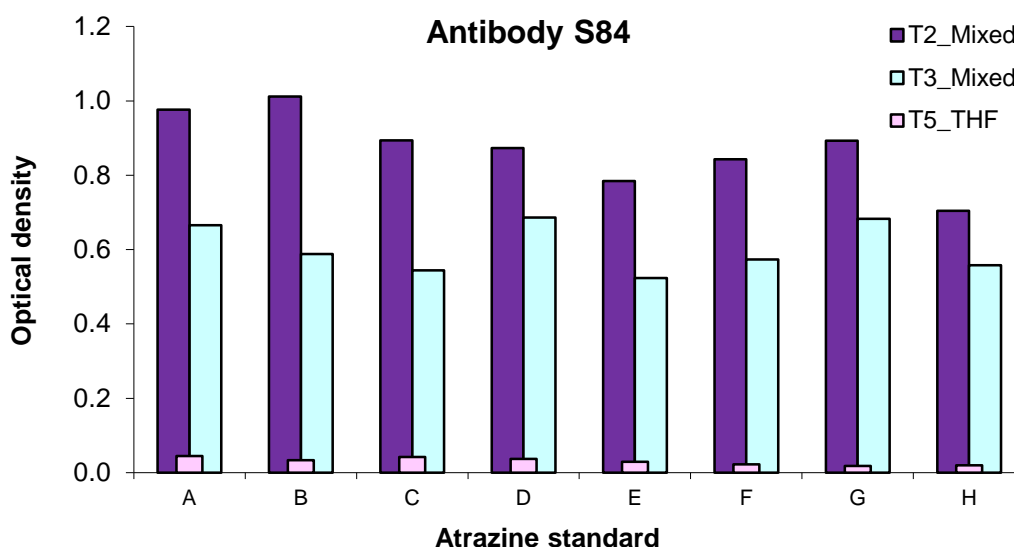
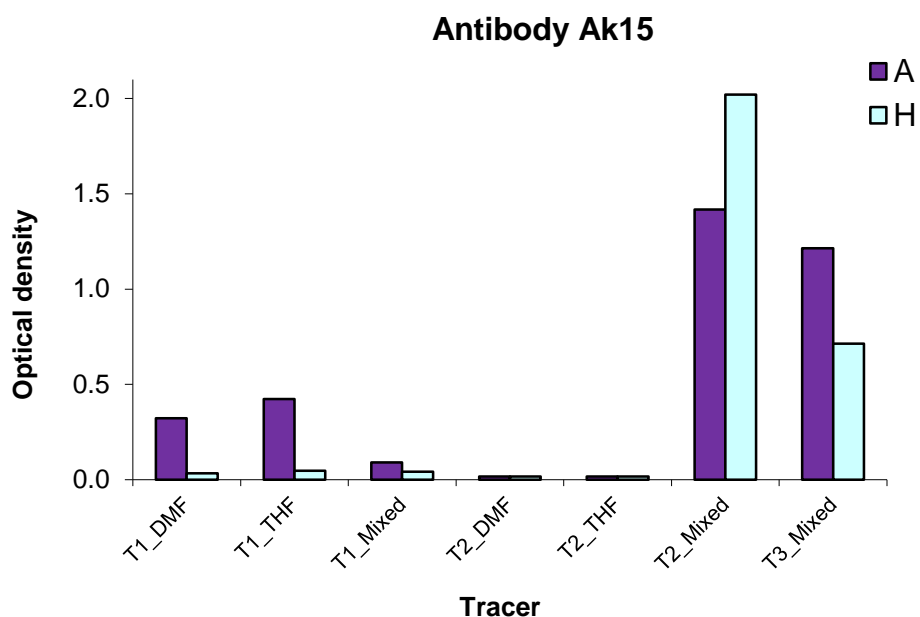


**Figure 3.20.** Representation of the OD values obtained for each standard between A – blank (water) and H – atrazine concentration  $1000 \mu\text{g L}^{-1}$  obtained using different tracers (synthesized differently) and microtiter plate coated using the polyclonal antibody S84. T2: t-Bu/Et/SC3; T3: Et/i-Pr/SC3; T5: t-Bu/Cl/C6.

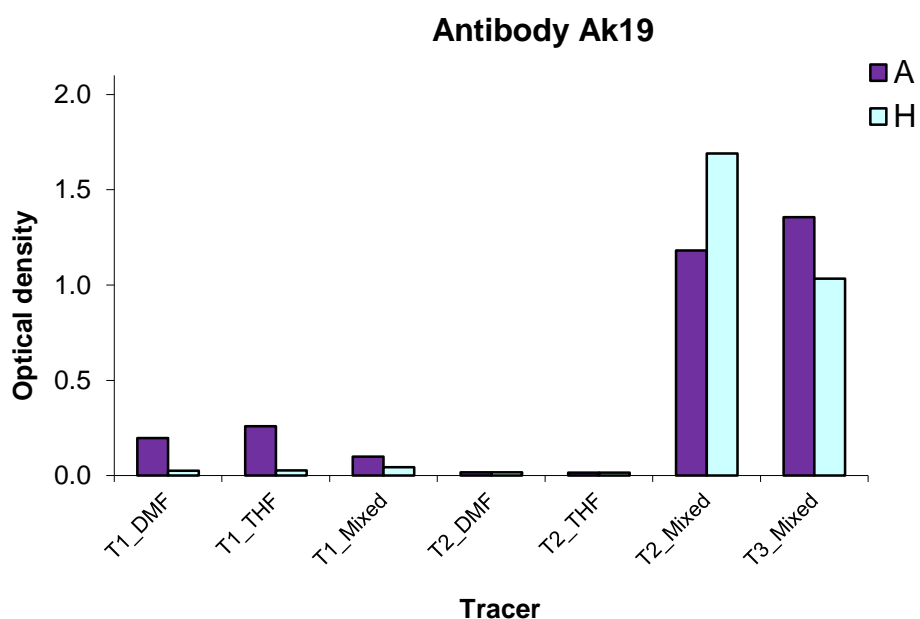
Since no differences are verified between OD for standards with different concentrations, and such signal maintains high and almost constant, it is possible to conclude that none of these tracers present specific binding to polyclonal antibody S84.

According to previous information (Weller, 1992), microtiter plates coated with the antibodies Ak15 and Ak19 were used to test three tracers - T1: t-Bu/Et/C6, T2: t-Bu/Et/SC3 and T3: Et/i-Pr/SC3 - for atrazine determination. Optical densities obtained for each concentration tested with the different antibodies are presented on Figure 3.21. and 3.22.



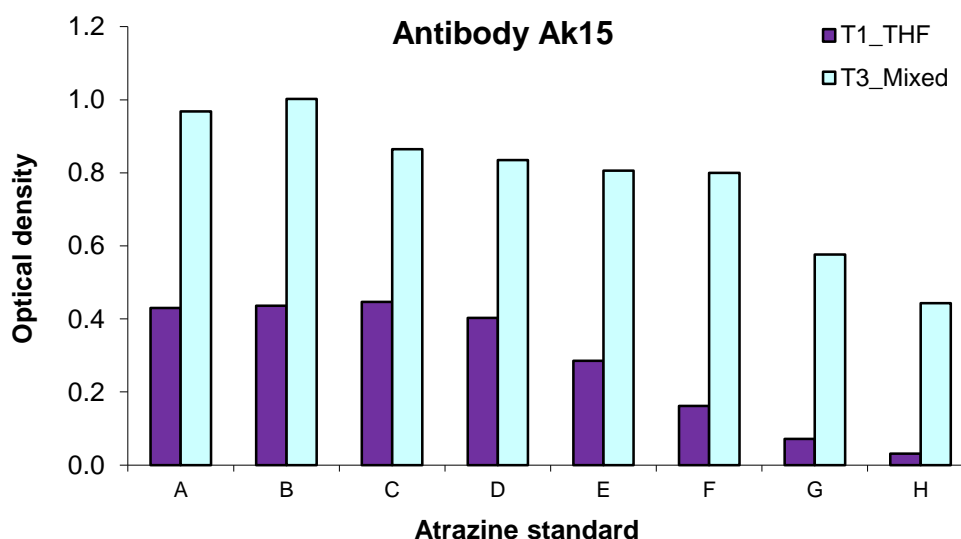


**Figure 3.21.** Representation of the OD values obtained for each standard, A – blank (water) and H – atrazine concentration 1000  $\mu\text{g L}^{-1}$  obtained using different tracers (synthesized differently) and microtiter plate coated using the polyclonal antibody Ak15. T1: t-Bu/Et/C6; T2: t-Bu/Et/SC3 and T3: Et/i-Pr/SC3.



**Figure 3.22.** Representation of the OD values obtained for each standard, A – blank (water) and H – atrazine concentration 1000  $\mu\text{g L}^{-1}$  obtained using different tracers (synthesized differently) and microtiterplate coated using the polyclonal antibody Ak19. T1: t-Bu/Et/C6; T2: t-Bu/Et/SC3 and T3: Et/i-Pr/SC3.

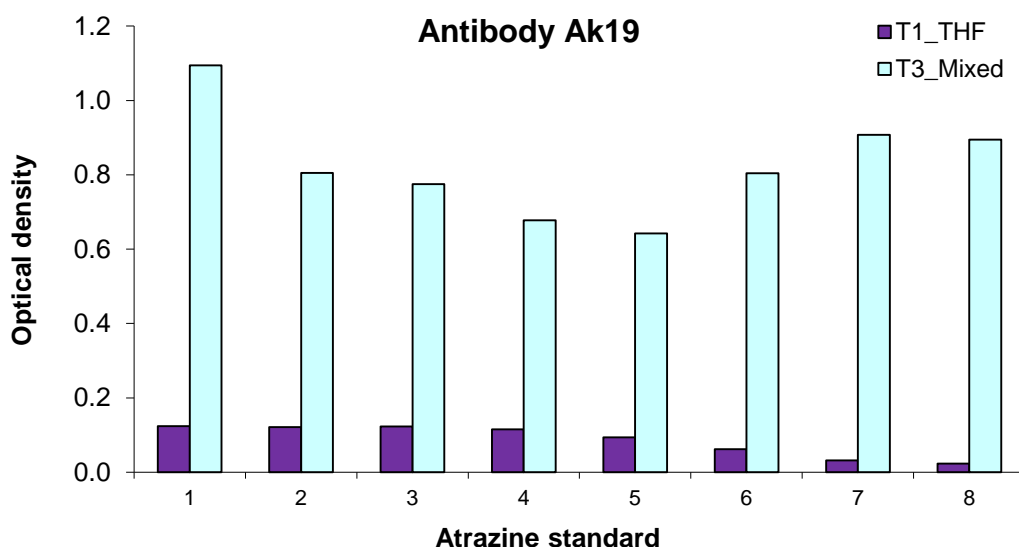
Both antibodies present similar behaviour. From the results (Figures 3.21. and 3.22.) it is deduced that tracer 1 and tracer 3 bind to both antibodies (Ak15 and Ak19). Tracer 2 (produced both in DMF and THF) does not give any colour when tested in microtiter plates coated with these two antibodies. The same tracer, but synthesized using the mixed anhydride method, presents lower OD for blank either using Ak15 or Ak19, which is explained by the existence of non-specific binding. Tracer 1 and 3 presents different OD for the concentrations tested. To evaluate the possibility of using antibody Ak15 and Ak19 with tracer 1 (synthesized via activated ester with THF as solvent) or T3 for atrazine determination, the OD using standards from 0.0001 to 1000  $\mu\text{g L}^{-1}$  was measured (Figures 3.23. and 3.24.).



**Figure 3.23.** Representation of the OD values obtained for each standard between A – blank (water) and H – atrazine concentration 1000  $\mu\text{g L}^{-1}$  obtained using different tracers (synthesized differently) and microtiter plate coated using the polyclonal antibody Ak15. T1: t-Bu/Et/C6; T3: Et/i-Pr/SC3.

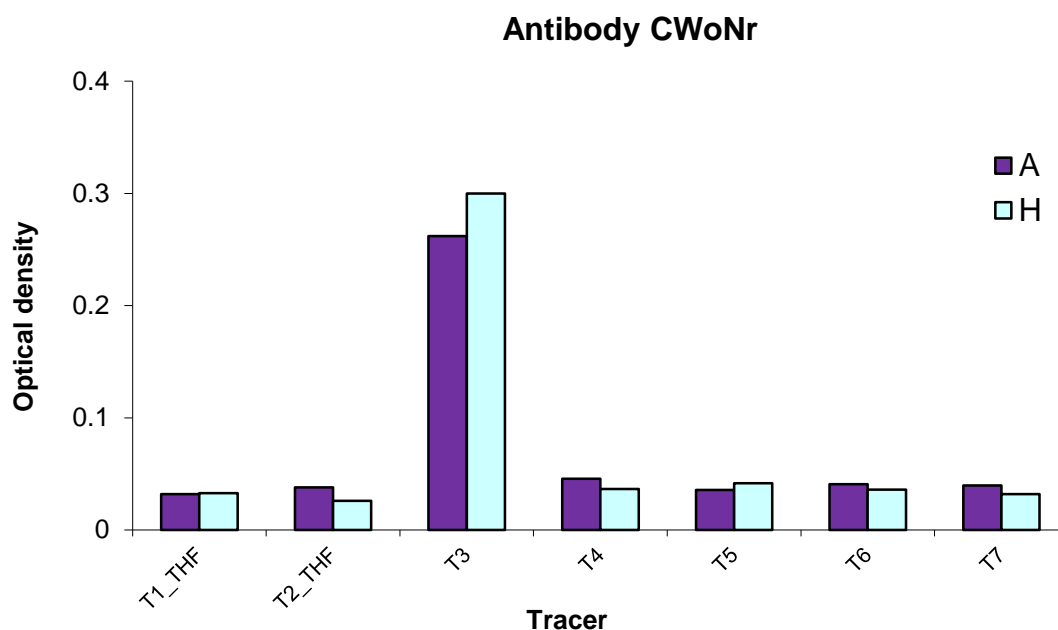
From Figure 3.23. it is possible to conclude that T1 presents a more specific binding to antibody Ak15 than T3. Although in both cases the sensitivity is low; for example, with tracer 1, the OD is almost the same from standard A to D (0.1  $\mu\text{g L}^{-1}$ ), thus it is not possible to distinguish standards with concentration lower than 0.1  $\mu\text{g L}^{-1}$ .

Figure 3.24. demonstrates that T3 presents an unspecific binding to the AK19 antibody, since OD does not decrease with the concentration increase. Thus, this tracer is not suitable for antibody Ak19. On the other hand, T1 seems to present a specific binding, since the optical density decreases with the increase of the atrazine concentration of the standard. However, a higher OD difference between blank and 1000  $\mu\text{g L}^{-1}$  standard would be desirable in order to increase sensitivity.



**Figure 3.24.** Representation of the OD values obtained for each standard between A – blank (water) and H – atrazine concentration 1000  $\mu\text{g L}^{-1}$  obtained using different tracers (synthesized differently) and microtiter plate coated using the polyclonal antibody Ak19. T1: t-Bu/Et/C6; T3: Et/i-Pr/SC3.

Another polyclonal antibody that was available for triazines was CWoNr. All possible combinations were made in order to determine which tracer and antibody pair is more suitable for atrazine. In Figure 3.25. the OD values obtained for each standard in a microtiter plate coated with polyclonal CWoNr antibody and using different synthesized tracers are presented.



**Figure 3.25.** Representation of the OD values obtained for each standard, A – blank (water) and H – atrazine concentration 1000 µg L<sup>-1</sup> obtained using different tracers (synthesized differently) and microtiter plate coated using the polyclonal antibody CWoNr. T1: t-Bu/Et/C6; T2: t-Bu/Et/SC3; T3: Et/i-Pr/SC3; T5: t-Bu/Cl/C6; T6: i-Pr/Et/C6 and T7: i-Pr/Cl/C6.

Results (Figure 3.25.) show similar or higher OD values for the higher standard (1000 µg L<sup>-1</sup>) than the ones obtained for the blank. Thus, it is possible to conclude the existence of unspecific binding for all combinations tested. Such results demonstrate that none of the tracers synthesized are suitable for the antibody CWoNr.

The same evaluation was made for another polyclonal antibody, C193. In Figure 3.26., the optical densities obtained for the blank (A) and for the higher standard (H), generally used in calibration curve, are depicted. The results show that using tracer T2 and T4 the OD obtained for the high atrazine standard is similar to the one obtained for the blank, denoting an unspecific binding that allowed the conclusion that these tracers are not suitable for the determination of atrazine using C193 polyclonal antibody. Using T1 or T6 it is possible to observe a difference between OD obtained for blank and for standard H. However, this difference is not enough to obtain a suitable and sensitive method to quantify atrazine.

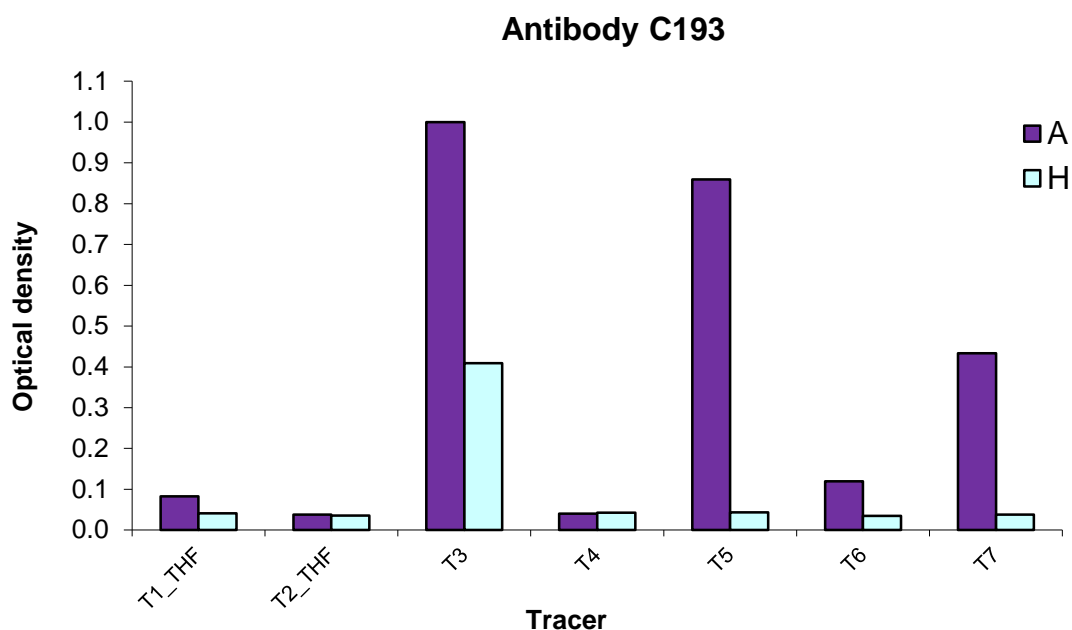


**Figure 3.26.** Representation of the OD values obtained for each standard, A – blank (water) and H – atrazine concentration 1000 µg L<sup>-1</sup> obtained using different tracers (synthesized differently) and microtiter plate coated using the polyclonal antibody C193. T1: tBu/Et/C6; T2 - tBu/Et/SC3; T3: Et/iPr/SC3; T5: tBu/Cl/C6; T6: iPr/Et/C6 and T7: iPr/Cl/C6.

Looking at the results, using T3, T5 and T7, the OD obtained for the blank is always considerably higher than the one obtained for the 1000 µg L<sup>-1</sup> atrazine standard. From all the combinations tested so far, these three were the most promising ones. For this reason, and in order to evaluate the most appropriate tracer, the complete calibration curves (Figure 3.27.) and the correspondent parameters of the 4PL equation were determined for each of the three mentioned tracers (Table 3.2).

**Table 3.2.** Parameter values obtained for the four-parametric logistic equation (4PL) using tracer T3: i-Pr/Et/SC3, T5: t-Bu/Cl/C6 and T7: i-Pr/Cl/C6 and polyclonal antibody C193

Tracer	A	B	C	D
T3	0.792	0.486	0.520	0.464
T5	0.798	0.869	0.117	0.041
T7	0.359	1.028	8.127	0.027

A = signal at zero dose, D = signal at excess dose, C = x-coordinate (concentration) of the turning point of the sigmoidal curve and B = slope parameter.

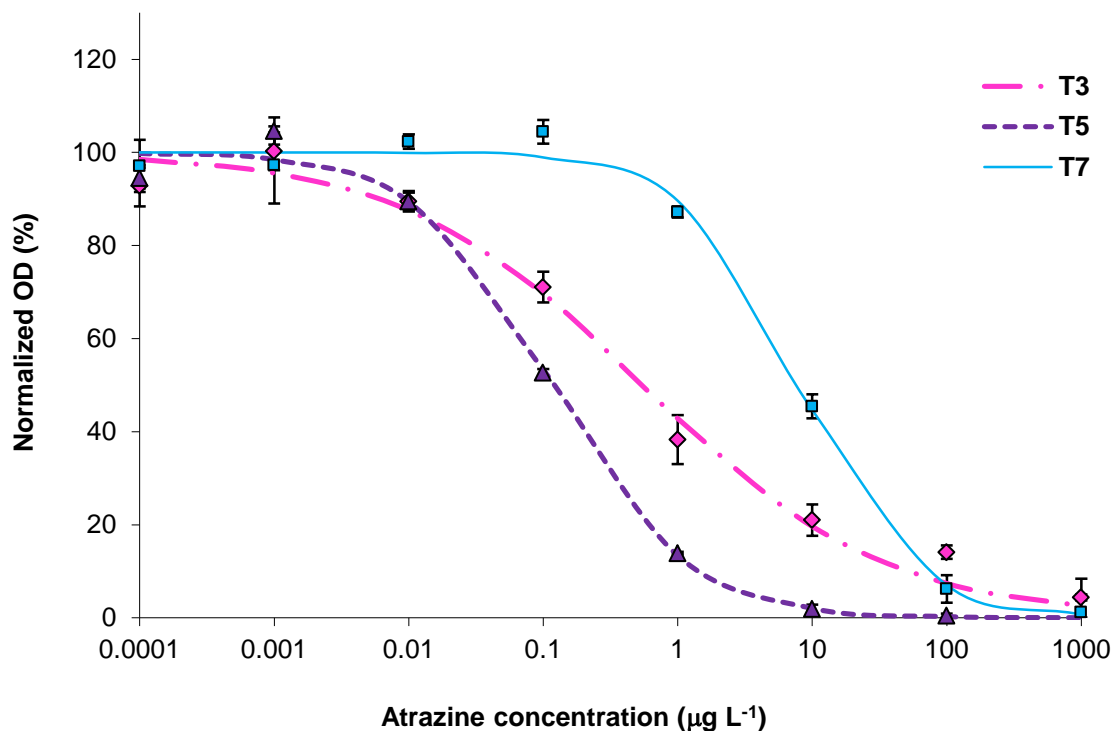


**Figure 3.27.** Calibration curves obtained for direct ELISA using polyclonal antibody C193 and enzyme tracers produced with the 3 haptens T3: Et/i-Pr/SC3, T5: t-Bu/Cl/C6 and T7: i-Pr/Cl/C6. Y-axis corresponds to normalized OD according to the equation given in Section 3.1.3. Antibody dilution 1:5000; tracers dilution 1:5000.

From these three tracers the T5: t-Bu/Cl/C6 is the most suitable since it presents the lowest turning point value (C), indicating the possibility to achieve a lower detection limit. Also, this tracer produces a higher difference between the signal at zero dose (A) and the signal at excess dose (D).

From all the combinations of antibodies and tracers tested, it was decided to choose C193 polyclonal antibody and tracer 5 synthesized using the hapten t-Bu/Cl/C6 via the activated ester route, using THF as solvent, to quantify atrazine in aqueous samples.

### 3.3.2. Optimization of antibody and tracer dilutions

After choosing the suitable tracer for the atrazine quantification it was necessary to optimize the Ab and tracer dilution. Four combinations were tested: Ab diluted 1:10000 and 1:20000 and tracer diluted 1:10000 and 1:20000 (Figure 3.28.).

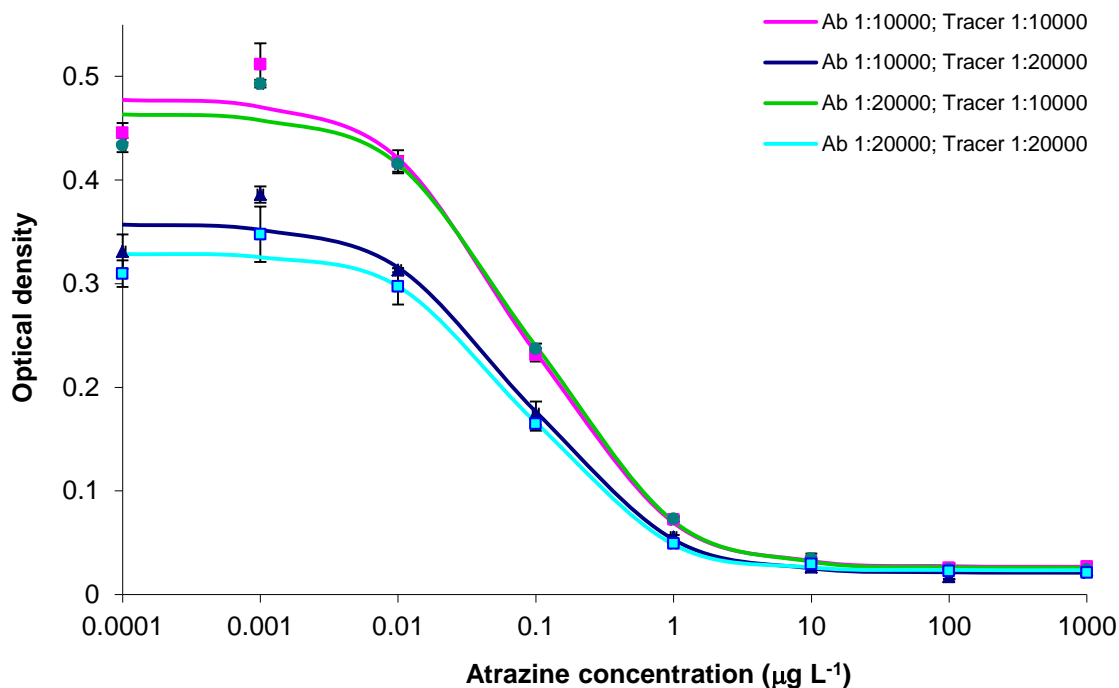


**Figure 3.28.** Calibration curves obtained using different antibody and tracer dilutions for direct ELISA using polyclonal antibody C193 and enzyme tracers produced with the hapten T5: t-Bu/Cl/C6.

The parameters obtained for the 4PL curve fitting using different combinations of antibody and tracer dilution are presented in Table 3.3. These values obtained for each combination tested do not differ considerably. However, the combination that presents the lowest turning point (0.083) is the one with the antibody and tracer dilution of 1:10000. Also, the pair with higher difference between A parameter (signal at zero concentration) and D (signal at excess dose) should be chosen. For these reasons, the ideal combination of antibody and tracer dilution is 1:10000.

**Table 3.3.** Parameter values obtained for the four-parametric logistic equation (4PL) using different dilutions of polyclonal antibody C193 and tracer T3: i-Pr/Et/SC3

Dilutions	A	B	C	D
Ab 1:20000; Tracer 1:20000	0.329	0.996	0.087	0.024
Ab 1:20000; Tracer 1:10000	0.464	0.922	0.095	0.026
Ab 1:10000; Tracer 1:20000	0.358	0.911	0.084	0.021
Ab 1:10000; Tracer 1:10000	0.478	0.910	0.083	0.027

A = signal at zero dose, D = signal at excess dose, C = x-coordinate (concentration) of the turning point of the sigmoidal curve and B = slope parameter.

### 3.3.3. Evaluation of assay performance

After performing the optimization of the ELISA conditions, the assay must be evaluated in terms of precision profile, accuracy and precision. Also, the concentrations encompassing the working range have to be defined.

An ELISA calibration curve and the respective precision profile, determined as described by Ekins (1981), are presented in Figure 3.29. In order to determine the quantification range of the previous optimized assay, 16 standards with concentrations ranging from 0.0001 to 10  $\mu\text{g L}^{-1}$  (six replicates per standard) were used.

Assessing the quantification range via the precision profile allows knowing the highest and lowest concentration which can be quantified, with an acceptable degree of precision. It was calculated using the respective precision profile with a maximum relative standard deviation (RSD) of the concentration result of 30% (Bahlmann et al., 2009).



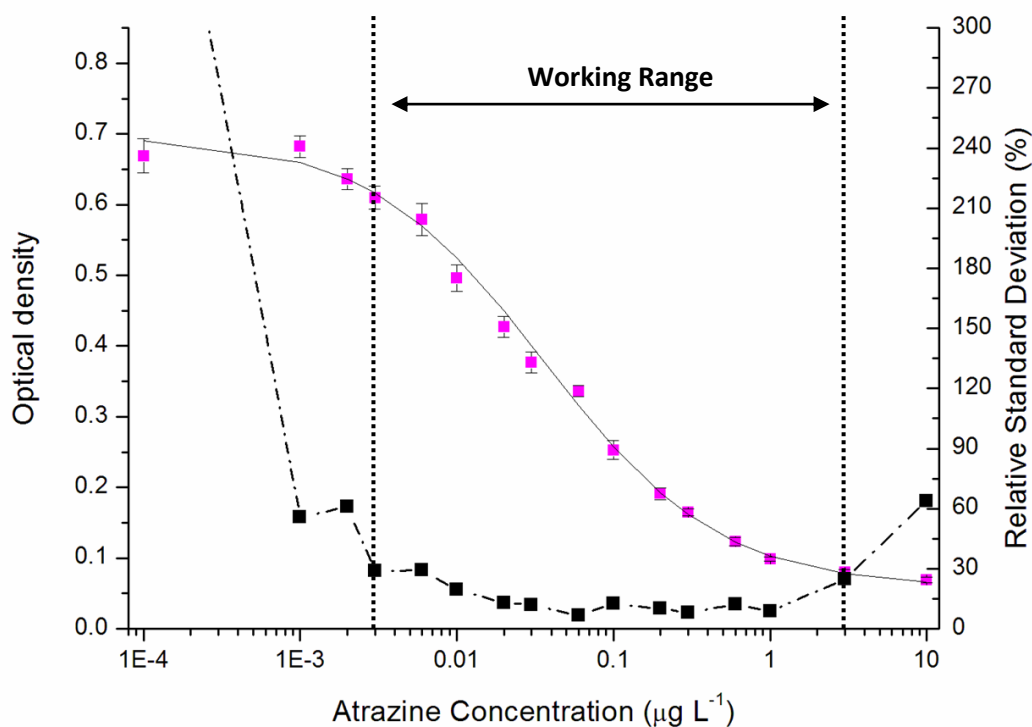


**Figure 3.29.** Calibration curve (pink squares) of ELISA ( $A = 0.697$ ;  $B = 0.776$ ;  $C = 0.036$ ;  $D = 0.058$ ;  $r = 0.9968$ ) and precision profile (black squares). The precision profile and the relative error of concentration were calculated in accordance with Ekins (1981).

Considering this RSD as the maximum value allowed, the analytical working range for atrazine quantification obtained was between 0.003 and 3.0  $\mu\text{g L}^{-1}$ . This means that this assay is usable over three orders of magnitude of analyte concentration.

In order to evaluate the accuracy of the optimized method, four different standards (from 0.03 to 0.5  $\mu\text{g L}^{-1}$ ) were determined (32 replicates for each concentration). A plot of the concentrations obtained for each replicate and the – at this concentration – upper and lower limit allowed, considering a deviation of 25% from the standard real concentration, is presented in Figures 3.30. and 3.31.

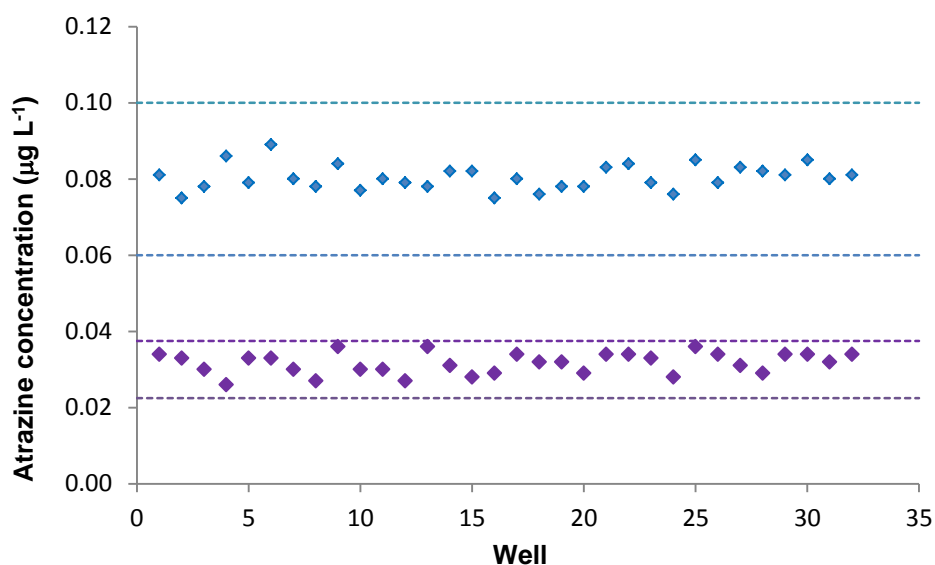


**Figure 3.30.** Plot of concentration obtained for each well for  $0.03 \mu\text{g L}^{-1}$  (purple squares) and  $0.08 \mu\text{g L}^{-1}$  (blue squares) atrazine standards and the respective upper and lower limits of the allowed interval.

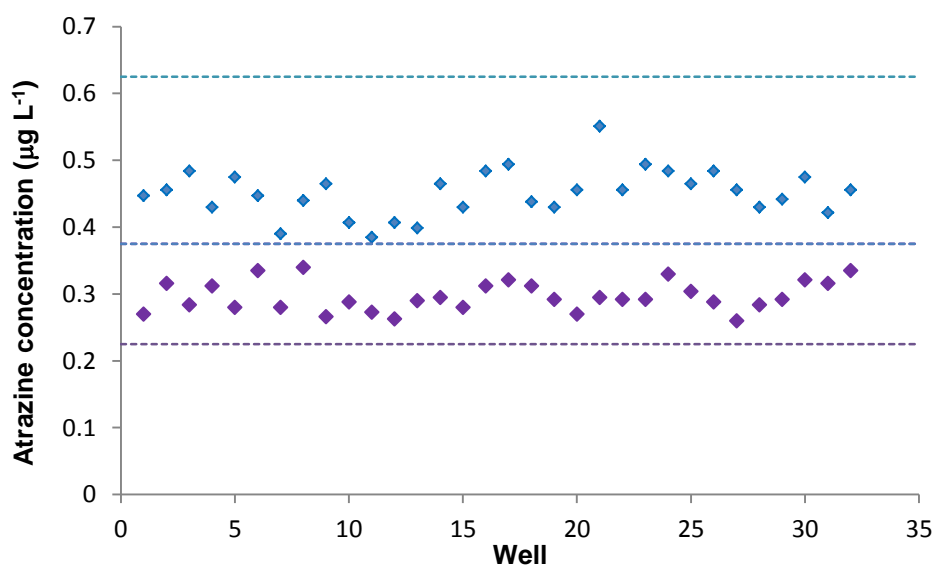


**Figure 3.31.** Plot of concentration obtained for each well for  $0.3 \mu\text{g L}^{-1}$  (purple squares) and  $0.5 \mu\text{g L}^{-1}$  (blue squares) atrazine standards and the respective upper and lower limits of the allowed interval.

The results obtained show that all concentrations, obtained for each well, are between the lower and upper limit allowed, considering the 25% of deviation. Thus, the

optimized method can be considered as an accurate methodology for atrazine determination in the working range determined previously.

Using the values obtained for each concentration in each well the mean and the relative standard error were calculated (Table 3.4.)

**Table 3.4.** Atrazine mean concentration and respective RSD for 4 standards (n = 32).

Atrazine Standard ( $\mu\text{g L}^{-1}$ )	Mean	RSD (%)
0.03	0.032	8.8
0.08	0.080	4.1
0.3	0.30	7.5
0.5	0.45	7.7

Results presented in Table 3.4. show that, besides of being accurate, the method is also precise, since the relative standard deviation using 32 replicates is below 8.8%, for all concentrations evaluated.

Another important aspect that should be taken into consideration is the relative sensitivity of the assay towards triazine herbicides and their main metabolites. Such sensitivity is evaluated by the determination of the CR obtained by division of molar concentrations at the inflection points (C-values) of the corresponding calibration curves and expressed in percentage relative to atrazine. The specificity of the polyclonal antibody, considering five potential cross-reactants, has been studied before (Schneider et al., 1992). Cross-reactivities of the antibody C193 towards selected triazine herbicides and their main metabolites are presented in Table 3.5.

**Table 3.5.** Cross-reactivities (CR [%]) of some selected triazine herbicides and their main metabolites at the center points of their calibration curves.

Triazine herbicide	CR* (%)
Atrazine	100
Terbuthylazine	4
Desethylatrazine	0.4
Desethylterbuthylazine	<0.1
Deisopropylatrazine	0.1
Hydroxyatrazine	0.1

\*Data from Schneider et al. (1992)

Molar cross-reactivity obtained for deisopropylatrazine and hydroxyatrazine was 0.1%. Desethylterbuthylazine presented a molar cross-reactivity lower than 0.1% and desethylatrazine lower than 0.4%. Only terbuthylazine, with a molar cross-reactivity of 4%, can potentially affect the quantification of atrazine in environmental samples. However, since the developed method will be applied to follow sorption behaviour of atrazine onto soil samples, it is not expected to have terbuthylazine present in soil raw aqueous extracts.

### 3.3.4. Evaluation of soil matrix effects

Soil matrix effects on the ELISA were evaluated using calibration curves obtained with standards prepared in water, in soil aqueous extract and in several dilutions of this aqueous extract.

According to Figure 3.32., with increasing concentration of matrix in the standards, the sigmoidal shape of the calibration curve is steadily lost and leads to a flattening of the calibration curves, causing an overestimation of atrazine concentration. Since organic matter present in soil solution is a complex mixture of aromatic and aliphatic hydrocarbon structures linked by and bearing many functional groups (Lima et al., 2009b), the intrinsic mechanisms of interference are unknown. We suppose that it may

be a combination of different effects, as stated already by other researchers (Deng et al., 2003).

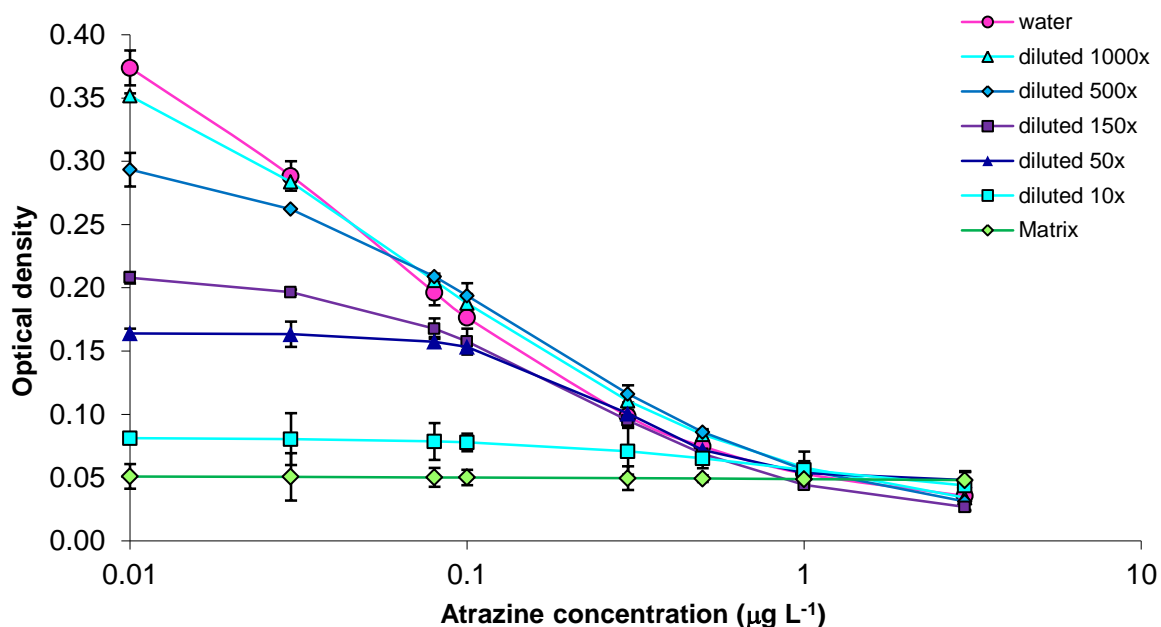


**Figure 3.32.** Influence of soil matrix on atrazine determination by ELISA. Shown are the calibration curves obtained from standard solutions prepared in raw extract matrix of the soil and in subsequent matrix dilution. Calibration curve obtained from calibrators prepared in ultrapure water is also shown for comparison.

Our goal in this study was to develop an assay to follow sorption behavior of atrazine onto soil samples. Therefore, it is important to note from these findings that application of ELISA to samples from the sorption experiments should be possible after dilution of a factor of at least 1000 times. Since sorption experiments were performed using atrazine standard solutions between 2 and 10 mg L<sup>-1</sup>, a dilution of 10000 times will result in samples with concentrations between 0.2 and 1 µg L<sup>-1</sup>. This concentration range is proper for the working range determined for the assay and the dilution of 10000 will overcome any possible matrix effects.

### 3.3.5. Adsorption experiment

The Freundlich parameters ( $K_F$  and  $N$ ) were calculated from the fitting of a non-linear regression, according to the equation  $Q_e = K_F \times C_e^N$ , to the experimental data, where  $Q_e$  is the total sorbed mass concentration ( $\text{mg Kg}^{-1}$ ),  $C_e$  is the solution-phase concentration ( $\text{mg L}^{-1}$ ),  $K_F$  ( $\text{mg Kg}^{-1}(\text{mg L}^{-1})^{-N}$ ) is the Freundlich distribution coefficient, and  $N$  is the isotherm nonlinearity factor.

The Freundlich equation obtained, using ELISA, is able to reasonably describe the adsorption of atrazine on the soil studied ( $r > 0.988$ ). The results obtained for Freundlich equation parameters, using ELISA and also obtained on chapter 1, are presented in Table 3.6.

**Table 3.6.** Mean ( $\pm$  standard errors) Freundlich  $K_F$  and  $N$  parameters for adsorption of atrazine onto a luvisol soil amended with sewage sludge. Concentration measurements by ELISA and MEKC, respectively.

	$K_F$ ( $\text{mg Kg}^{-1} (\text{mg L}^{-1})^{-N}$ )	$N$	$r$
ELISA	$1.6 \pm 0.2^b$	$0.70 \pm 0.09$	0.988
MEKC	$1.6 \pm 0.1$	$0.72 \pm 0.04$	0.996
$t$ student <sup>a</sup>	0.30	0.32	

<sup>a</sup> Critical  $t$  value for 4 degrees of freedom, at 95% confidence level is 2.78

<sup>b</sup> Results are an average of triplicate runs of adsorption experiments

A student  $t$ -test was applied to compare the results obtained by both methods. Since the  $t$  calculated presented lower values for both  $K_F$  and  $N$  than the critical  $t$  value for 4 degrees of freedom, at 95% confidence level, it can be stated that there are no significant differences between the results obtained by ELISA and MEKC. Results obtained demonstrate that ELISA can be used to follow sorption of atrazine onto soil samples.

## 3.4. Conclusion

---

It has been shown that ELISA can be a valid alternative in assaying concentrations from sorption experiments of organic pollutants onto soils. Atrazine was determined by an immunoassay, using a polyclonal antibody, after selection of an appropriate structure for synthesis of a tracer that produces the signal of the assay. Several tracers and antibodies were tested in order to find the proper ones to determine atrazine with higher sensitivity. Also, the precision profile and working range of the assay were determined, as well as its precision and accuracy. Cross-reactivity results were presented, although selectivity against other structurally similar compounds is not an issue in laboratory model experiments. Also sensitivity is not crucial in sorption experiments (starting concentrations can be widely adapted to the measurement range of the analytical method), thus the focus was on matrix effects of co-extracted soil compounds of a high organic carbon soil, and it was found that dilution by a factor of 1000 usually overcomes matrix interferences in the used ELISA.

The student  $t$ -test was applied to compare the results obtained for Freundlich parameters ( $K_F$  and  $N$ ), using both ELISA and MEKC, to quantify atrazine aqueous concentrations. Since the  $t$  calculated presented lower values, for both  $K_F$  and  $N$ , than the critical  $t$  value, for 4 degrees of freedom at 95% confidence level, it can be stated that there are no significant differences between the results obtained by ELISA and MEKC.

## 3.5. References

---

- Amistadi, M.K., Hall, J.K., Bogus, E.R., Mumma, R.O., **1997**. Comparison of gas chromatography and immunoassay methods for the detection of atrazine in water and soil. *J. Environ. Sci. Health B* 32, 845-860.
- Bahlmann, A., Weller, M.G., Panne, U., Schneider, R.J., **2009**. Monitoring carbamazepine in surface and wastewaters by an immunoassay based on a monoclonal antibody. *Anal. Bioanal. Chem.* 395, 1809-1820.
- Ben-Hur, M., Letey, J., Farmer, W.J., Williams, C.F., Nelson, S.D., **2003**. Soluble and solid organic matter effects in atrazine adsorption in cultivated soils. *Soil Sci. Soc. Am. J.* 67, 1140-1146.
- Bushway, R.J., Perkins, B., Savage, S.A., Lekousi, S.J., Ferguson B.S., **1988**. Determination of atrazine residues in water and soil by enzyme immunoassay. *Bull. Environ. Contam. Toxicol.* 40, 647-654.
- Chefetz, B., Bilkis, Y.I., Polubesova, T., **2004**. Sorption-desorption behaviour of atrazine and phenylurea herbicides in Kishon river sediments. *Water Res.* 38, 4383-4394.
- Deng, A., Himmelsbach, M., Zhu, Q.-Z., Sengl, M., Buchberger, W., Niessner, R., Knopp, D., **2003**. Residue analysis of the pharmaceutical diclofenac in different water types using ELISA and GC-MS. *Environ. Sci. Technol.* 37, 3422-3429.
- Deng, A.P., Kolar, V., Ulrich, R., Franek, M., **2002**. Direct competitive ELISA for the determination of polychlorinated biphenyls in soil samples. *Anal. Bioanal. Chem.* 373, 685-690.
- Drori, Y., Aizenshtat, Z., Chefetz, B., **2005**. Sorption-desorption behaviour of atrazine in soils irrigated with reclaimed wastewater. *Soil Sci. Soc. Am. J.* 69, 1703-1710.
- Dudley, R.A., Edwards, P., Ekins, R.P., Finney, D.J., McKenzie, I.G., Raab, G.M., Rodbard, D., Rodgers, R.P., **1985**. Guidelines for immunoassay data processing. *Clin. Chem.* 31, 1264-1271.
- Ekins, R.P., **1981**. The "Precision Profile": Its use in RIA assessment and design. *The Ligand Quarterly* 4, 33-44.
- Engvall, E., Perlmann, P., **1971**. Enzyme-linked immunosorbent assay (ELISA). Quantitative assay of immunoglobulin G. *Immunochemistry* 8, 871-874.
- Farré, M., Kantiani, L., Barceló, D., **2007**. Advances in immunochemical Technologies for analysis of organic pollutants in the environment. *Trends Anal. Chem.* 26, 1100-1112.
- Franek, M., Hruska, K., **2005**. Antibody based methods for environmental and food analysis: a review. *Vet. Med. – Czech* 50, 1-10.



- Frey, A., Meckelein, B., Externest, D., Schmidt, M.A., **2000**. A stable and highly sensitive 3,3',5,5'-tetramethylbenzidine-based substrate reagent for enzyme-linked immunosorbent assays. *J. Immunol. Meth.* 233, 47-56.
- Fruhstorfer, P., Schneider, R., Weil, L., Niessner, R., **1993**. Factors influencing the adsorption of atrazine on montmorillonitic and kaolinitic clays. *Sci. Total Environ.* 138, 317-328.
- Gascón, J., Durand, G., Barceló, D., **1995**. Pilot survey for atrazine and total chlorotriazines in estuarine waters using magnetic particle-based immunoassay and gas chromatography-nitrogen/phosphorus detection. *Environ. Sci. Technol.* 29, 1551-1556.
- Gault, V.A., McClenaghan, H.N., **2009**. Understanding bioanalytical chemistry, principles and applications. *Wiley-Blackwell*, 1<sup>st</sup> ed., West Sussex.
- Gruessner, B., Shambaugh, N.C., Watzin, M.C., **1995**. Comparison of an enzyme immunoassay and gas chromatography/mass spectrometry for the detection of atrazine in surface waters. *Environ. Sci. Technol.* 29, 251-254.
- Harlow, E., Lane, D., **1999**. Using antibodies: A laboratory manual. *Cold Spring Harbor Laboratory Press*.
- Hennion, M.-C., Barceló, D., **1998**. Strengths and limitations of immunoassays for effective and efficient use for pesticide analysis in water samples: A review. *Anal. Chim. Acta* 362, 3-34.
- Kaur, J., Boro, R.C., Wangoo, N., Singh, K.R., Suri, C.R., **2008**. Direct hapten coated immunoassay format for the detection of atrazine and 2,4-dichlorophenoxyacetic acid herbicides. *Anal. Chim. Acta* 607, 92-99.
- Kramer, K., Lepschy, J., Hock, B., **2001**. Long-term monitoring of atrazine contamination in soil by ELISA. *J. AOAC Int.* 84, 150-155.
- Langone, J.J., Vanvunakis, H., **1975**. Radioimmunoassay for dieldrin and aldrin. *Res. Comm. Chem. Path. Pharm.* 10, 163-171.
- Lawruk, T.S., Lachman, C.E., Jourdan, S.W., Fleeker, J.R., Herzog, D.P., Rubio, F.M., **1993**. Quantification of cyanazine in water and soil by a magnetic particle-based ELISA. *J. Agric. Food Chem.* 41, 747-752.
- Lima, D.L.D., Erny, G.L., Esteves, V.I., **2009a**. Application of MEKC to the monitoring of atrazine sorption behaviour on soils. *J. Sep. Sci.* 32, 4241-4246.
- Lima, D.L.D., Santos, S.M., Scherer, H.W., Schneider, R.J., Duarte, A.C., Santos, E.B.H., Esteves, V.I., **2009b**. Effects of organic and inorganic amendments on soil organic matter properties. *Geoderma* 150, 38-45.

- Maqbool, U., Anwar-ul-Haq, Qureshi, M.J., Iqbal, M.Z., Hock, B., Kramer, K., **2002**. Development of ELISA technique for the analysis of atrazine residues in water. *J. Environ. Sci. Health B* 37, 307-322.
- Mbuya, O.S., Nkedi-Kizza, P., Boote, K.J., **2001**. Fate of atrazine in sandy soil cropped with sorghum. *J. Environ. Qual.* 30, 71-77.
- Mikkelsen, S.R., Cortón, E., **2004**. Bioanalytical Chemistry. *John Wiley & Sons, Inc.*, 1<sup>st</sup> ed., New Jersey.
- Munro, C., Stabenfeldt, G., **1984**. Development of a microtitre plate enzyme immunoassay for the determination of progesterone. *J. Endocrinol.* 101, 41-49.
- Nunes, G.S., **2004**. Métodos imunoquímicos para análise de resíduos de pesticidas: uma revisão. *Analytica* 10, 50-59.
- Nunes, G.S., Toscano, I.A., Barceló, D., **1998**. Analysis of pesticides in food and environmental samples by enzyme-linked immunosorbent assays. *Trends Anal. Chem.* 17, 79-87.
- OECD, Guideline TG 106, **2000**. OECD Guideline for the testing of chemicals. Adsorption-desorption using a batch equilibrium method. *Organization for Economic Co-operation and Development (OECD)*, Paris.
- Park, J.H., Feng, Y., Cho, S.Y., Voice, T.C., Boyd, S.A., **2004**. Sorbed atrazine shifts into non-desorbable sites of soil organic matter during aging. *Water Res.* 38, 3881-3892.
- Prata, F., Lavorenti, A., Vanderborght, J., Burauel, P., Vereecken, H., **2003**. Miscible displacement, sorption and desorption of atrazine in a Brazilian oxisol. *Vadose Zone J.* 2, 728-738.
- Santos, L.B.O., Abate, G., Masini, J.C., **2005**. Application of sequential injection–square wave voltammetry (SI–SWV) to study the adsorption of atrazine onto a tropical soil sample. *Talanta* 68, 165-170.
- Schneider, C., Schöler, H.F., Schneider, R.J., **2005**. Direct sub-ppt detection of the endocrine disruptor ethinylestradiol in water with a chemiluminescence enzyme-linked immunosorbent assay. *Anal. Chim. Acta* 551, 92-97.
- Schneider, P., Hammock, B.D., **1992**. Influence of the ELISA format and the hapten-enzyme conjugate on the sensitivity of an immunoassay for s-triazine herbicides using monoclonal antibodies. *J. Agr. Food Chem.* 40, 525-530.
- Schneider, R.J., Weil, L., Niessner, R., **1992**. Identification of two triazines herbicides in top soil layers using immunoassays of different selectivity. *Fresenius J. Anal. Chem.* 343, 145-146.

- Smith, M.C., Shaw, D.R., Massey, J.H., Boyette, M., Kingery, W., **2003**. Using nonequilibrium thin-disc and batch equilibrium techniques to evaluate herbicide sorption. *J. Environ. Qual.* 32, 1393-1404.
- Socías-Viciano, M.M., Fernández-Pérez, M., Villafranca-Sánchez, M., González-Pradas, E., Flores-Céspedes, F., **1999**. Sorption and leaching of atrazine and MCPA in natural and peat-amended calcareous soils from Spain. *J. Agr. Food Chem.* 47, 1236-1241.
- Stearman, G.K., Wells, M.J.M., **1993**. Enzyme immunoassay microtitre plate response to atrazine and metolachor in potentially interfering matrices. *Bull. Environ. Contam. Toxicol.* 51, 588-595.
- Thurman, E.M., Meyer, M., Pomes, M., Perry, C.A., Schwab, A.P., **1990**. Enzyme-linked immunosorbent assay compared with gas chromatography/mass spectrometry for the determination of triazine herbicides in water. *Anal. Chem.* 62, 2043-2048.
- Toscano, I., Gascón, J., Marco, M.-P., Rocha, J.C., Barceló, D., **1998**. Atrazine interaction with tropical humic substances by enzyme linked immunosorbent assay. *Analisis* 26, 130-134.
- Ulrich, P., Weller, M., Weil, L., Niessner, R., **1991**. Optimierung der immunologischen bestimmung von triazin-herbiziden im wasser mit hilfe unterschiedlicher enzymtracer. *Vom Wasser* 76, 251-266.
- Weller, M.G., **1992**. Strukturelle und kinetische untersuchungen zur entwicklung und optimierung von haptent-enzymimmunoassays (ELISAs) am beispiel der bestimmung von triazinherbiziden. *PhD dissertation by Technischen Universität München, Fakultät Chemie, Biologie und Geowissenschaften*.
- Weller, M.G., Niessner, R., **1997**. Affinity patterns of enzyme tracers for triazine immunoassays. *SPIE Proc. Ser.* 3105, 341-352.
- Wittmann, C., Hock, B., **1989**. Improved enzyme immunoassay for the analysis of a-triazines in water samples. *Food Agric. Immunol.* 1, 211-224.
- Wittmann, C., Hock, B., **1991**. Development of an ELISA for the analysis of atrazine metabolites deethylatrazine and deisopropylatrazine. *J. Agric. Food Chem.* 39, 1194-1200.
- Yalow, R.S., Berson, S.A., **1959**. Assay of plasma insulin in human subjects by immunological methods. *Nature* 184, 1648-1649.

# PART III

## FATE AND PERSISTENCE OF HOP ON ENVIRONMENT

# CHAPTER 4

**CHARACTERIZATION OF SOIL SAMPLES SUBJECTED TO  
DIFFERENT ORGANIC LONG-TERM AMENDMENTS**



## CHAPTER 4

### Characterization of soil samples subjected to different organic long-term amendments\*

4.1. Introduction .....	101
4.2. Experimental procedure .....	102
4.2.1. Soil samples description .....	102
4.2.2. Total organic matter, total organic carbon, total nitrogen .....	102
4.2.3. <sup>13</sup> C NMR spectroscopy .....	102
4.2.4. FT-IR spectroscopy.....	103
4.2.5. Capillary zone electrophoresis .....	103
4.3. Results and discussion .....	105
4.3.1. Total organic matter, total organic carbon, total nitrogen .....	105
4.3.2. <sup>13</sup> C NMR spectroscopy .....	106
4.3.3. FT-IR spectroscopy.....	108
4.3.4. Phenolic compounds content.....	111
4.4. Conclusions .....	114
4.5. References .....	116

\* Diana L.D. Lima, Sérgio M. Santos, Heinrich W. Scherer, Rudolf J. Schneider, Armando C. Duarte, Eduarda B.H. Santos, Valdemar I. Esteves, 2009. Effects of organic and inorganic amendments on soil organic matter. *Geoderma* 150, 38-45.

## 4.1. Introduction

---

Organic wastes should be recycled not only from an ecological point of view but also for economical reasons. Therefore the ongoing evolution of waste management strategies, namely efficient waste recycling, is one of the most challenging aims both for soil scientists and environmental engineers. The use of municipal wastes sewage sludge, compost and farmyard manures as fertilizers on agricultural soils has been encouraged as a sustainable alternative to stockpiling and incineration by scientists and governmental regulations. In fact, the use of both farmyard manures and composts has been of common practice for years in traditional agriculture (Werner et al., 1987; Parat et al., 2005). However, the opinions on the benefit of organic amendments on the levels and availability of nutrients, humus status and other chemical and biochemical soil properties, as well as on its contribution on the accumulation of heavy metals, organic pollutants and phytotoxic compounds, are contradictory (Saviozzi et al., 1999). While, according to Kick (1981), organic fertilizers are rich in organic matter and nutrients, and therefore enhance the fertility of soils, the application of sewage sludge may result in an accumulation of different organic non-biogenic (such as chlorine derived compounds, phthalates, oil derived hydrocarbons, etc...) and inorganic substances (such as toxic metals) (Adani and Tambone, 2005); therefore they may cause hazardous effects and effects which are either not yet known or well understood. Therefore, the characterization of the soils supplied with different organic fertilizers over a long period of time is imperative, in order to conveniently establish/unestablish ways for recycling of those residues as fertilizers, as an economically and environmentally-friendly alternative to stockpiling and incineration.

The most usual soil organic matter characterization techniques predominantly employ humic substances isolation and characterization (Sierra et al., 2005) by Fourier Transform Infrared Spectroscopy (FT-IR), Nuclear Magnetic Resonance Spectroscopy (NMR), UV-Vis or fluorescence spectroscopies and exchange/partition chromatography (Janos, 2005). Several other approaches have been used, such as isolation and quantification of polysaccharides (Santos et al., 2007) and phenolic compounds (Lima et al., 2007), as well as semi-direct FT-IR and solid-state NMR (Lorenz et al., 2006) analysis of the soils. The former indirect pathway, however, is time consuming due to long isolation procedures

(Santos et al., 2007; Lima et al., 2007), whereas the latter semi-direct ones are much quicker. Among others, one of the most important advantage on the use of semi-direct FT-IR and NMR as soil organic matter characterization techniques is their non-destructive nature, though need minor sample preparation which leads them to be classified as semi-direct techniques. The preparation commonly involves use of diluted hydrofluoric acid (HF) solutions, for the removal of the majority of paramagnetic materials (for NMR analysis) (Schilling et al., 2004)) and for the increase of organic matter concentration due to demineralization (for both NMR and FT-IR analysis) (Gonçalves et al., 2003).

The objective of this study was to ascertain the influence of repeated applications of compost, sewage sludge and farmyard manure, respectively, when compared to mineral fertilizer over many years on the status of soil organic matter. The work involves the quantification of total organic matter content, semi-direct FT-IR and  $^{13}\text{C}$  NMR analysis of the soils, and quantification of polysaccharides and phenolic compounds.

## 4.2. Experimental procedure

---

### 4.2.1. Soil samples description

Soil samples used are described on section 1.2.1.

### 4.2.2. Total organic matter, total organic carbon, total nitrogen

TOC and total nitrogen (TN) content were determined by dry combustion using a Carlo-Erba NA 1500 carbon/nitrogen/sulphur analyzer. The total organic matter (TOM) content was assessed by LOI of aliquots of soil (ca.20 g) in a furnace at 550 °C for 4 h.

### 4.2.3. $^{13}\text{C}$ NMR spectroscopy

Prior to NMR and FT-IR spectroscopies, samples were de-ashed using successive treatments with 2% aqueous HF solution. For each sample the successive treatment involved shaking of 5 g of soil in 40 mL of 2% HF solution for periods of 1 h (five times), 16



h (three times) and 64 h (once). Between treatments, samples were centrifuged for 10 min at 4000 rpm the supernatant discarded and replaced with fresh 2% aqueous HF solution. After the final treatment, the residue was rinsed two times with deionised water and then freeze-dried (Smernik et al., 2005).

Solid state  $^{13}\text{C}$  Cross-Polarization Magic-Angle Spinning Nuclear Magnetic Resonance (CPMAS-NMR) spectra were obtained using a Bruker Avance 500 spectrometer operating at 125.8 MHz. Spectra were obtained at 7 kHz in a 4 mm diameter rotor, using cross-polarization to transfer magnetization from protons to carbons. A conventional cross-polarization pulse sequence was used, with a 1 ms contact time, along with a recycling delay of 5 s and a 4  $\mu\text{s}$  proton  $90^\circ$  pulse. Chemical shifts are referred to the tetramethylsilane scale.

#### 4.2.4. FT-IR spectroscopy

FT-IR spectra of soil samples were collected with a Nicolet-Magna 550 spectrophotometer, in the 400 to 4000  $\text{cm}^{-1}$  range with a 4  $\text{cm}^{-1}$  resolution. Pellets were prepared by pressing a mixture of 0.8 mg of sample and 80 mg of spectroscopy grade KBr.

#### 4.2.5. Capillary zone electrophoresis

Analyses were carried out with a Beckman P/ACE MDQ Capillary Electrophoresis unit, coupled to a UV/Vis photodiode array detection system, using a 50 cm long (42 cm from sample inlet to detector) uncoated fused-silica capillary with an internal diameter of 75  $\mu\text{m}$ .

For the determination of phenolic compounds a variable duration 0.5 psi hydrostatic injections (7 s for samples and less concentrated standard, 5 s for the medium standards and 3 s for the most concentrated standards) and an applied voltage of 25 kV at a controlled temperature of 25  $^\circ\text{C}$  was used. The separation electrolyte consisted of a daily prepared  $4.3 \times 10^{-2} \text{ mol L}^{-1} \text{ Na}_2\text{B}_4\text{O}_7$  and  $2.7 \times 10^{-2} \text{ mol L}^{-1} \text{ KH}_2\text{PO}_4$  solution with 8.5% acetonitrile (organic modifier), resulting in a final pH of 9.15 (Lima et al., 2007). All electrolyte solutions were prepared in ultra-pure water.

The following 11 phenols: acetosyringone (97%, Aldrich), acetovanillone (98%, Aldrich), syringaldehyde (99%, Aldrich), p-hydroxyacetophenone (99%, Aldrich), vanillin (99%, Merck), syringic acid (98%, Sigma), ferulic acid (99%, Aldrich), p-hydroxybenzaldehyde (99%, BHD), p-coumaric acid (98%, Sigma), vanillic acid (97%, Aldrich) and p-hydroxybenzoic acid (99%, Aldrich) were analysed. Succinctly, the procedure consisted of a CZE analysis of soil sample extracts previously subjected to alkaline CuO oxidation.

The lignin derived phenols were obtained according to the method of Hedges and Ertel (1982), which involves CuO oxidation of 5 g of soil. Samples were placed in an air tight Teflon vial, protected by a steel bomb fitted with a screw cap, along with 200 mg of  $[\text{Fe}(\text{NH}_4)_2(\text{SO}_4)_2 \cdot 6\text{H}_2\text{O}]$ , 2 g of CuO and 7 mL 2 mol L<sup>-1</sup> NaOH purged with N<sub>2</sub>. After preserving the Teflon vials and steel bomb for one night under a N<sub>2</sub> atmosphere in a glove box, they were sealed under N<sub>2</sub> atmosphere.

The oxidation was carried out by heating the bombs at 170 °C for 3 hours in an oven. After cooling under running tap water and adding 10 µL of 0.01 mol L<sup>-1</sup> ethylvanillin (IS), the supernatant of the Teflon vial was collected and the sediment washed with four 5 mL portions of 1 mol L<sup>-1</sup> NaOH purged with N<sub>2</sub>. The supernatants and 1 mol L<sup>-1</sup> NaOH washing solutions were collected, acidified with 6 mol L<sup>-1</sup> HCl to pH 1, transferred to a 50 mL centrifuge tube and centrifuged at 4000 rpm for 10 min. The obtained precipitate was washed with acidified water (pH = 1) and the centrifugation repeated.

The phenolic compounds within the combined supernatants were extracted using SPE. 500 mg C<sub>18</sub> Strata-X cartridges (Phenomenex) were conditioned with 2 mL of acetonitrile, followed by 2 mL of methanol and 2 mL of ultra-pure water. Cartridges were then left to dry before adding the samples. Phenolic compounds were eluted with 5 mL of methanol followed by 2.5 mL of acetonitrile. Finally, the methanol eluate was dried, the residue dissolved in the 2.5 mL acetonitrile eluate, and then diluted with the separation electrolyte to a final volume of 10 mL (Lima et al, 2007).

For the calibration of the CZE method, mixed standard calibration solutions were prepared with concentrations ranging from  $2.50 \times 10^{-6}$  to  $2.00 \times 10^{-4}$  mol L<sup>-1</sup>. The IS, ethylvanillin, was added to the calibration standards in order to obtain a final

concentration of  $1.0 \times 10^{-4}$  mol L<sup>-1</sup>. The ratios between peak areas of analytes and of IS were plotted against the corresponding concentration ratios. Each point of the calibration curve corresponded to the mean value obtained from three independent replicates. Buffer, standards and samples were all filtered through a 0.22  $\mu$ m membrane filter before analysis.

## 4.3. Results and discussion

---

### 4.3.1. Total organic matter, total organic carbon, total nitrogen

As compared with the control treatment (MIN), long-term application of sewage sludge (SLU) increased TOC by 57% and compost application (COM) by 124%, while the increase in the treatment with farmyard manure (FYM) was not significant (Table 4.1.).

**Table 4.1.** Influence of long-term application of different organic fertilizers and mineral fertilizer, respectively, on chemical soil parameters; (MIN – mineral fertilizer; FYM – farmyard manure; SLU – sewage sludge fertilizer; COM – compost fertilizer).

Treatment	pH	TN (%)	TOC (%)
SLU	6.5	0.151	1.983
FYM	6.2	0.131	1.473
COM	7.1	0.227	2.775
MIN	6.1	0.109	1.238

Data obtained by Scherer H.W. in INRES – Department of Plant Nutrition, INRES-Institute of Crop Science and Resource Conservation, University of Bonn

These differences in the TOC content, as well in TN, are the result of the different amounts of C and N applied with the organic materials. TOM content results and their standard deviation (n=3) were the following: COM (9.4±1.0%), SLU (6.2±0.3%), FYM (5.5±0.5%) and MIN (5.3±0.3%).

### 4.3.2. $^{13}\text{C}$ NMR spectroscopy

The influence of the different fertilizers on the solid state  $^{13}\text{C}$  CPMAS-NMR spectra is shown in Figure 4.1. Seven chemical shift regions were assigned to these spectra: R1 = 0–45 ppm (aliphatic region) (Smernik, 2005), R2a = 45–60 ppm (methoxyl groups in lignins and polysaccharides/hemicelluloses, *N*-alkyl C), R2b = 60–90 ppm (*O*-alkyl C in higher alcohols, *C*-2 to *C*-5 of hexoses), R2c = 90–110 ppm (di-*O*-alkyl C, anomeric *C*-1 in polysaccharides, *C*-2 and *C*-6 in syringyl units, *C*-2 in guaiacyl units), R3a = 110–140 ppm (aromatic *C*-*C* and *C*-*H*, olefinic carbons) R3b = 140–160 ppm (aromatic *C*-*O* and *C*-*N* groups) R4 = 160–190 ppm (carboxyl, amide and ester-*C* in lipids and proteins) (Dignac et al., 2002).

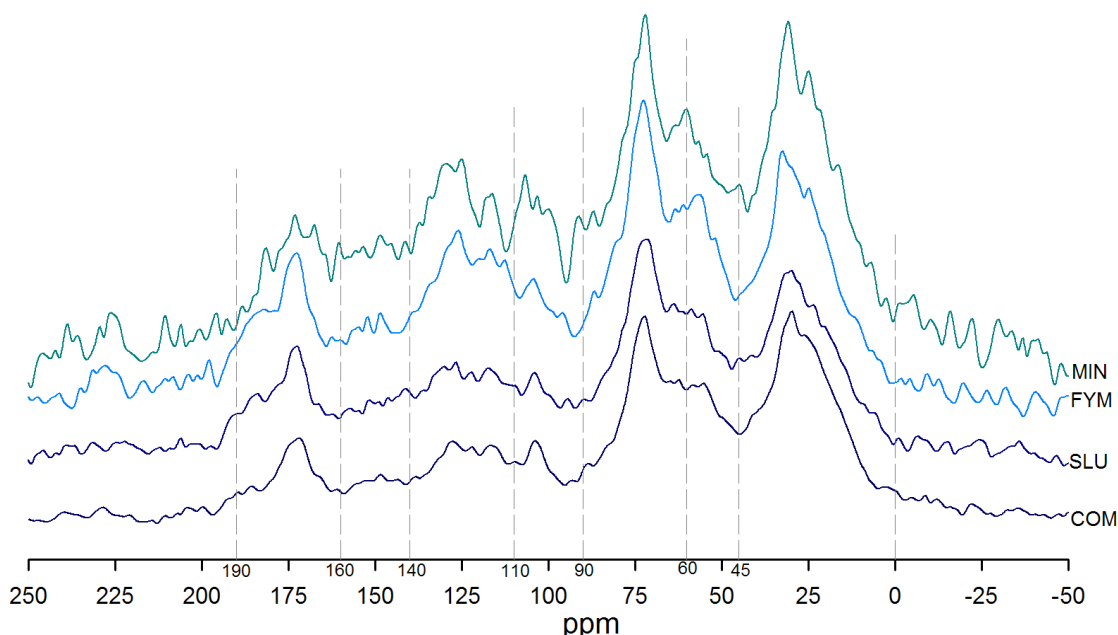


**Figure 4.1.** Solid state  $^{13}\text{C}$  CPMAS-NMR spectra from soil samples supplied with different fertilizers (MIN – mineral fertilizer; FYM – farmyard manure; SLU – sewage sludge fertilizer; COM – compost fertilizer).

Qualitative differences (Figure 4.1.) were found between samples in the considered chemical shift intervals. The aliphatic R1 region (0 – 45 ppm) is dominated by the peaks at 16, 25 and 31 ppm which arise from non-substituted alkyl carbons. The soil sample from the mineral fertilizer treatment has well defined methyl carbon peaks, centered at 16 ppm and at 25 ppm. This higher content of methyl carbons suggests more branched

chains than in other soils samples. On the other hand, the soil supplied with compost presents a higher relative area in the alkyl-C region (R1) (Table 4.2.), suggesting a relatively higher amount of aliphatic components. The fact that the most prominent peak is centred at 31 ppm suggests the presence of methylene ( $-\text{CH}_2$ ) groups in long aliphatic chains, with a possible contribution from lipids and proteins (Dignac et al., 2002).

**Table 4.2.** Relative area distribution (% of total spectrum area) of solid-state  $^{13}\text{C}$  CPMAS-NMR spectra; (MIN – mineral fertilizer; FYM – farmyard manure; SLU – sewage sludge fertilizer; COM – compost fertilizer).

Soil	Chemical shift region / ppm								
	Alkyl	O, N-alkyl				Aromatic			Carboxyl
	<b>R1</b> 0-45	<b>R2</b> 45-110	<b>R2a</b> 45-60	<b>R2b</b> 60-90	<b>R2c</b> 90-110	<b>R3</b> 110-160	<b>R3a</b> 110-140	<b>R3b</b> 140-160	<b>R4</b> 160-190
SLU	29.9	44.2	11.6	26.6	6.0	16.7	12.5	4.2	9.3
FYM	26.2	41.5	10.8	23.6	7.1	21.5	16.5	5.0	10.8
COM	37.4	44.4	13.0	26.3	5.2	12.6	10.4	2.2	5.6
MIN	30.4	43.7	10.8	24.7	8.1	20.2	15.1	5.1	5.7

In the region R2a (45-60 ppm) a sharp signal centered at 55 ppm is usually assigned to methoxy groups associated to lignin and lignin-like products (Sierra et al., 2005). This signal is more intense in the soil sample supplied with FYM, probably due to lignin and lignin-like products derived from the straw applied with this organic fertilizer. However, this region (45-60 ppm) is also characteristic for *N*-substituted alkyl carbon in compounds like lipids and peptides. The fact of soil with compost presenting a higher relative area in this region, suggests a higher presence of proteins or protein-like compounds in this soil. These compounds were enriched in this soil sample and may therefore be derived from compost or formed during its mineralization. The two well defined peaks at 72 ppm in the region R2b (60-90 ppm), and at 104 ppm, in the region R2c (90-110 ppm), are thought to correspond to resonances of carbons in polysaccharide rings, and to anomeric carbons in polysaccharides (Sierra et al., 2005). The soils fertilized with compost and sewage sludge present a higher relative area value in the region between 60 and 90 ppm, suggesting a higher content in polysaccharides. A better defined peak at 104 ppm in those two soil

samples also indicates higher polysaccharide contents. The higher relative area value in region R2c (90-110 ppm) of the mineral fertilizer and farmyard manure treatment soils is probably due to the higher lignin content of these soils and suggests the presence of syringyl units (C-2 and C-6) (Dignac et al., 2002). This assumption is confirmed by the high relative area of region R3 (110-160 ppm), the aromatic region and by the fact that these samples are those with the lowest area in the region R2b, where most of the polysaccharide signals appear. Region R3a (110-140 ppm) is attributed to aromatic C–C and C–H, having well defined peaks at 113, 116 and 129 ppm in the sample of soil fertilized with farmyard manure. The peak at 129 ppm is usually attributed to unsaturated carbons and protonated aryl-C, while the peak at 116 ppm usually indicates the presence of guaiacyl units (Ussiri and Johnson, 2003). Region R3b (140-160 ppm) is attributed to aromatic C–O and C–N carbons and usually presents defined peaks at about 148, 152 and 155 ppm. The sharper peaks at 126 and 148 ppm in the soil fertilized with farmyard manure once again suggest a higher content of lignin and lignin-like products (Ussiri and Johnson, 2003). The same is also suggested by the better defined peak at 152 ppm, characteristic of carbons bonded to phenolic OH (Sierra et al., 2005).

The last considered region of the spectra, between 160 and 190 ppm, is normally attributed to carboxyl, amide and ester functionalities and it shows a well defined peak at 172 ppm. In this region, the farmyard manure based soil sample presents a slightly higher relative area and also a sharper peak at 172 ppm, suggesting a higher content in this type of organic functional groups (Dignac et al., 2002).

### 4.3.3. FT-IR spectroscopy

In FT-IR spectra, functional groups such as phenolic and alcoholic hydroxyls, aromatic and aliphatic carboxyls, carbonyls, aliphatic C–H groups and amides produce bands in characteristic frequencies.

FT-IR spectra of soil samples present a broad band around  $3400\text{ cm}^{-1}$  which corresponds to O–H stretching of hydroxyl groups from phenol, alcohol and/or carboxylic groups (Figure 4.2.).

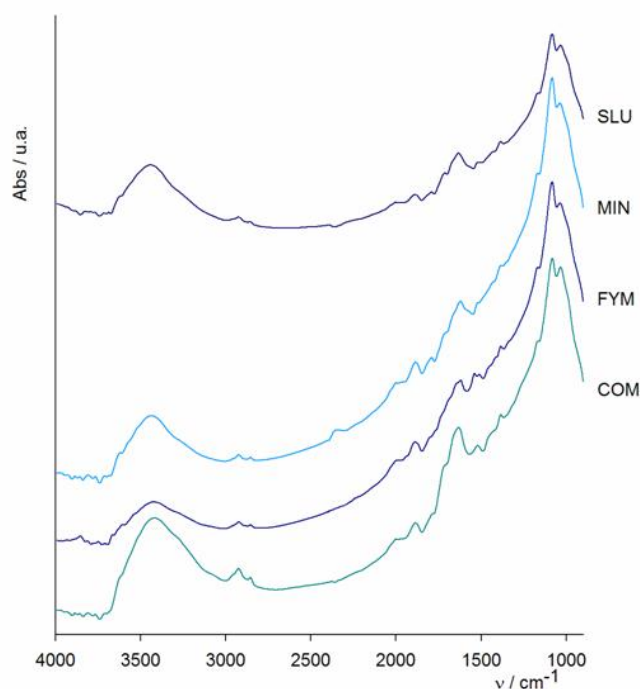


**Figure 4.2.** FT-IR spectra of soil samples supplied with different fertilizers (MIN – mineral fertilizer; FYM – farmyard manure; SLU – sewage sludge fertilizer; COM – compost fertilizer).

However, this band can also be assigned to amide and amine  $N-H$  stretching (Calace et al., 2006). Other bands around  $2900\text{ cm}^{-1}$  can be assigned to symmetric and asymmetric stretching vibrations of aliphatic  $C-H$  bands in  $-CH_3$  and  $-CH_2$  groups. Within the  $3050$  to  $2800\text{ cm}^{-1}$  wavenumber range (Figure 4.3.a) some differences can be detected. In this range, two peaks at  $2962$  and  $2873\text{ cm}^{-1}$  are attributed to the asymmetrical and symmetrical stretching of methyl ( $-CH_3$ ) groups, respectively; and two peaks at  $2920$  and  $2853\text{ cm}^{-1}$  are attributed to the asymmetrical and symmetrical stretching of methylene ( $-CH_2$ ) groups, respectively. The higher intensity of the bands at  $2920$  and  $2853\text{ cm}^{-1}$  relatively to the bands at  $2962$  and  $2873\text{ cm}^{-1}$  suggest a higher content of methylene groups than of methyl groups. The spectrum from the compost amended soil presents higher intensity bands in this aliphatic region, suggesting a higher saturation degree relatively to the other soil samples. These observations are in conformity with the solid state  $^{13}\text{C}$  CPMAS-NMR data.

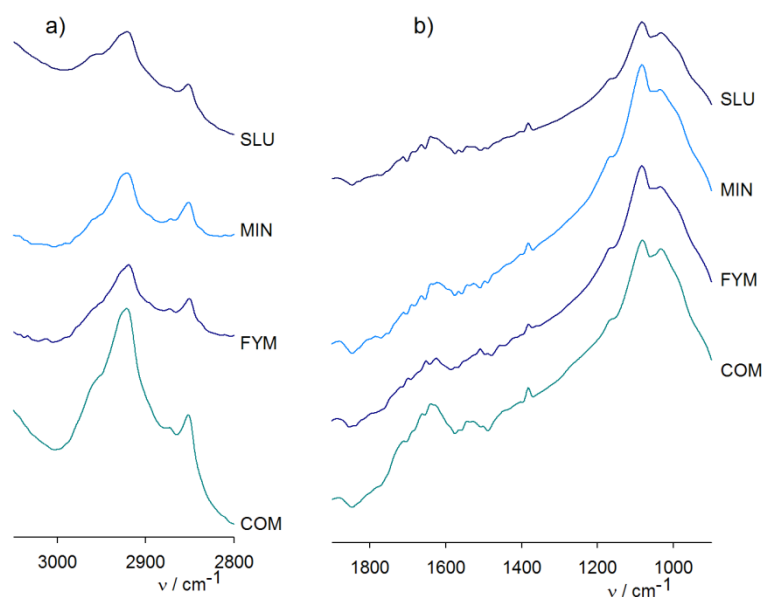


**Figure 4.3.** Selected zoomed parts of the spectra presented in Figure 4.2.: a) region 3050 to 2800  $\text{cm}^{-1}$ ; b) region 1900 to 900  $\text{cm}^{-1}$  (MIN – mineral fertilizer; FYM – farmyard manure; SLU – sewage sludge fertilizer; COM – compost fertilizer).

In the range between 1900 and 900  $\text{cm}^{-1}$  (Figure 4.3.b), distinct peaks are observed, one of which at 1080  $\text{cm}^{-1}$  which is characteristic of C–O stretching of polysaccharides (Sierra et al., 2005). The shoulder observed at 1040  $\text{cm}^{-1}$  has been attributed to aromatic esters and polysaccharides, as well as to Si–O–Si in silicates derived from quartz (Rumpel et al., 2006). At 1170  $\text{cm}^{-1}$  appears a small shoulder, suggesting the presence of alcoholic group vibrations (Calace et al., 2006). Within this wavenumber range some differences between the soil spectra can be identified. The soil sample supplied with compost presents a clearer defined peak at 1040  $\text{cm}^{-1}$ , also characteristic of polysaccharides, as well as of Si–O–Si. Since the soil samples were extensively treated with 2% HF (which is intended to remove inorganic compounds), this peak is probably due to the presence of polysaccharides. Thus, such results suggest a higher polysaccharide content within the compost based soil sample which is also in conformity with the solid state  $^{13}\text{C}$  CPMAS-NMR data.



Further, two other bands were identified: one at  $1540\text{ cm}^{-1}$  and another between  $1600$  and  $1660\text{ cm}^{-1}$  with a shoulder at  $1720\text{ cm}^{-1}$ . The band at  $1540\text{ cm}^{-1}$  is usually attributed to  $C-N$  stretching and  $N-H$  bending vibrations of amide groups (Calace et al., 2006). However, it also can be assigned to aromatic  $C=C$  stretching (Shirshova et al., 2006). The band between  $1600$  and  $1660\text{ cm}^{-1}$ , with a maximum at  $1650\text{ cm}^{-1}$ , is considered to be caused by  $C=O$  stretching of amide groups in proteins (Calace et al., 2006), but is also attributed to aromatic  $C=C$  stretching, amide  $C=O$  stretching and amide  $N-H$  bending (Sierra et al., 2005). The peak at  $1540\text{ cm}^{-1}$  is best defined in the spectra of the sample of the compost treatment (Figure 4.3.). Since this peak can be attributed to different vibrations, a look at the information obtained by  $^{13}\text{C}$  CPMAS-NMR suggests an assignment to  $C-N$  stretching and  $N-H$  bending. This assumption is also supported by the better defined peak at  $1650\text{ cm}^{-1}$  in that soil, which is generally attributed to  $C=O$  stretching of amide groups of proteins or protein-like compounds.

#### 4.3.4. Phenolic compounds content

Linear calibration curves and respective parameters were obtained for all phenols. Regression equation parameters ( $y=a+bx$ ) and regression coefficients ( $r$ ) for each compound along with the LOD are presented in Table 4.3.

The *p*-hydroxyacetophenone was found to be the phenol with lowest detection limit ( $2.64 \times 10^{-6}\text{ mol L}^{-1}$ ), while syringic acid had the highest ( $1.25 \times 10^{-5}\text{ mol L}^{-1}$ ). Correlation coefficients ( $r$ ) for all phenolic compounds were above 0.9960.

**Table 4.3.** Calibration parameters for the eleven quantified phenolic compounds. Values are presented as average  $\pm$  standard deviation ( $n=3$ ).

Compound	LOD (mol L <sup>-1</sup> )	Linear Regression ( $y = (a \pm \sigma_a) + (b \pm \sigma_b)x$ )		Correlation Coef. ( $r$ )
		Equation parameters ( $a \pm \sigma_a$ )	Equation parameters ( $b \pm \sigma_b$ )	
Acetosyringone	$6.74 \times 10^{-6}$	$-0.02_9 \pm 0.01_3$	$1.03_7 \pm 0.01_4$	0.9996
Acetovanillone	$2.94 \times 10^{-6}$	$-0.008_5 \pm 0.005_2$	$0.953_3 \pm 0.005_5$	0.9999
Syringaldehyde	$6.50 \times 10^{-6}$	$-0.03_1 \pm 0.01_5$	$1.19_2 \pm 0.01_5$	0.9997
<i>p</i> -Hydroxyacetophenone	$2.64 \times 10^{-6}$	$0.013_1 \pm 0.003_4$	$0.606_8 \pm 0.006_6$	0.9998
Vanillin	$5.29 \times 10^{-6}$	$-0.02_3 \pm 0.01_2$	$1.19_3 \pm 0.01_2$	0.9998
Syringic Acid	$1.25 \times 10^{-5}$	$-0.07_2 \pm 0.05_0$	$1.89_2 \pm 0.09_8$	0.9960
Ferulic Acid	$4.81 \times 10^{-6}$	$-0.007 \pm 0.01_9$	$1.82_4 \pm 0.03_6$	0.9994
<i>p</i> -Hydroxybenzaldehyde	$7.28 \times 10^{-6}$	$0.02_6 \pm 0.01_1$	$0.82_8 \pm 0.01_2$	0.9998
<i>p</i> -Coumaric Acid	$8.02 \times 10^{-6}$	$-0.03_8 \pm 0.03_9$	$2.29_7 \pm 0.07_6$	0.9983
Vanillic Acid	$7.92 \times 10^{-6}$	$-0.05_1 \pm 0.04_2$	$2.50_2 \pm 0.08_2$	0.9984
<i>p</i> -Hydroxybenzoic Acid	$4.91 \times 10^{-6}$	$0.01_6 \pm 0.02_0$	$2.21_3 \pm 0.02_1$	0.9998

All calibration curves were found to be linear over the concentration range. Phenolic contents in soil samples tested, expressed as  $\mu\text{g}$  of phenolic compounds per g of TOM, are presented in Table 4.4.

**Table 4.4.** Phenolic compound contents of soil samples subjected to the application of different fertilizers. Values are presented as average  $\pm$  standard deviation ( $n=3$ ).

	Content ( $\mu\text{g}_{\text{phenolic compound}} / \text{g}_{\text{TOM}}$ )			
	COM	SLU	FYM	MIN
Acetosyringone	$367 \pm 91a^b$	$273 \pm 32a$	$977 \pm 48b$	$286 \pm 98a$
Acetovanillone	$450 \pm 76b$	$267 \pm 22a$	$423 \pm 37b$	$204 \pm 87a$
Syringaldehyde	$211 \pm 81a$	$137 \pm 16a$	$458 \pm 59b$	$166 \pm 58a$
<i>p</i> -Hydroxyacetophenone	$114 \pm 18a$	$82 \pm 7a$	$82 \pm 9a$	$93 \pm 35a$
Vanillin	$531 \pm 84a$	$431 \pm 38a$	$626 \pm 100a$	$358 \pm 169a$
Syringic Acid	$78 \pm 24a$	$44 \pm 11a$	$143 \pm 29b$	n.d.
Ferulic acid	$87 \pm 17a$	$35 \pm 9b$	n.d.	n.d.
<i>p</i> -Hydroxybenzaldehyde	$140 \pm 41a$	$156 \pm 25a$	$190 \pm 41a$	$124 \pm 46a$
<i>p</i> -Coumaric acid	$82 \pm 10a$	$58 \pm 24a$	$102 \pm 39a$	$97 \pm 48a$
Vanillic Acid	$309 \pm 63a$	$168 \pm 42a$	$279 \pm 49a$	$162 \pm 158a$
<i>p</i> -hydroxybenzoic Acid	$80 \pm 41a$	n.d.	$131 \pm 47a$	$72 \pm 55a$
S/V <sup>a</sup>	$0.42 \pm 0.05a$	$0.43 \pm 0.03a$	$0.99 \pm 0.08b$	$0.6 \pm 0.1c$

<sup>a</sup>Molar ratio of syringic-to-vanillic units (Dittmar and Lara, 2001).

<sup>b</sup>In the same row, values followed by the same letter are not significantly different at  $p < 0.05$  level of probability.

While soil samples from SLU, COM and MIN present vanillin as the most abundant compound, the soil sample from FYM contains higher amounts of acetosyringone. The syringic-to-vanillic unities ratio (S/V) can be used to distinguish the sources of organic matter. Low S/V (approximately zero) values indicate a contribution from gymnospermic plants; on the other hand, higher S/V values indicate an angiospermic source (Javor et al., 2000). The higher S/V value obtained for the FYM sample indicates a predominant contribution of angiospermic plants. This fact, allied to the higher amount of phenolic compounds in this sample can be explained by the incorporation of cereal straw, supplied with FYM. The higher quantity of phenols in the soil with FYM application is in clear agreement with the data obtained from solid state  $^{13}\text{C}$  NMR spectroscopy, in which FYM amended samples were suspected to have higher amounts of phenol levels derived from lignin.

## 4.4. Conclusions

---

All over the world land application of organics produced by the urban population and farmers (compost, sewage sludge and farmyard manure) is a widespread practice that allows the reuse of the increasing amounts of biosolids. However, there are several opinions on the benefits of these different complex organic amendments in what concerns the long-term effect on humus status and humus composition (Saviozzi et al., 1999). Soil organic matter content changes very slowly, and therefore, many years are required to measure significant changes (Pascual et al., 1999). Therefore, effects of management practices on soil fertility criteria are best evaluated using long-term field experiments. Furthermore, the total content of soil organic matter cannot be used as a simple criterion for soil quality (Sparling, 1992). As a result, a multi approach study on long-term effects of different organic amendments on structural characteristics of soil organic matter has been performed. Comparing the three organic amendments, the most significant differences were observed after long-term application of farmyard manure and compost. Application of farmyard manure showed an increase in lignin and lignin-like products in the soil organic matter. Lignin, a highly aromatic polymer, when released in soils by decomposition of plant tissues is highly resistant to microbial decomposition. In soils, lignin is an important source for the formation of soil humus or humic matter, an essential soil component that is known to have beneficial effects on soil physical, chemical and biological properties (Tan, 1994). It may affect plant growth directly and indirectly. Directly, is capable of improving seed germination, root initiation, and elongation, respiration, uptake of plant nutrients, and development of green mass. Indirectly, can modify the properties of the medium in which plants grow, like enhancing soil structure formation, increase soil water holding capacity and cation exchange capacity. It can also reduce micronutrient toxicity in acid soils (Tan, 1994).

According to the obtained results, compost manure appears to contribute to an increase of protein and protein-like, as well as carbohydrates content on soil organic matter. The biowaste nature of the compost fertilizer is probably the basis for the richer polysaccharide content on compost soil samples, as a consequence of the higher levels of carbohydrates encountered in vegetable and bacterial cells, which end up being

transformed (during compost preparation) and added to the soil. Carbohydrate content present in the soil influence the soil physical conditions, cation exchange and metal complexing reactions, anion retention, synthesis of humic substances and biological activity in general. Adsorption of mono and polysaccharides on clay minerals will enhance the aggregation and structural stability of soil particles. Also, polysaccharides are generally strongly hydrophilic and, as such, will enhance water holding capacity of soils. Carbohydrates represent a very active soil organic component (Bowman et al., 1990) and a readily available energy source for microorganisms (Cheshire, 1977). Even eight years after compost application Pascual et al. (1999) found an improved microbial activity. On the other hand, aminoacids and proteins are important sources of nitrogen, which are mainly converted into ammonia. Generally, both carbohydrates and proteins highly contribute to the improvement of soil fertility.

Succinctly, long-term application of organic amendments appears to induce different structural properties, depending on the type of organic fertilizer, which can improve soil aggregation quality and structural stability, as well as fertility.

## 4.5. References

---

- Adani, F., Tambone, F., **2005**. Long-term effect of sewage sludge application on soil humic acids. *Chemosphere* 60, 1214-1221.
- Belitz, H.-D., Grosch, W., Schieberle, P., **2004**. Food Chemistry. *Springer*, 3<sup>rd</sup> Edition, Berlin, p. 245-339.
- Calace, N., Cardellicchio, N., Petronio, B.M., Pietrantonio, M., Pietroletti, M., **2006**. Sedimentary humic substances in the northern Adriatic sea (Mediterranean sea). *Mar. Environ. Res.* 61, 40-58.
- Dahlman, O., Jacobs, A., Liljenberg, A., Olsson, A.I., **2000**. Analysis of carbohydrates in wood and pulps employing enzymatic hydrolysis and subsequent capillary zone electrophoresis. *J. Chromatogr. A* 891, 157-174.
- Dignac, M.F., Knicker, H., Kögel-Knabner, I., **2002**. Effect of N content and soil texture on the decomposition of organic matter in forest soils as revealed by solid-state CPMAS NMR spectroscopy. *Org. Geochem.* 33, 1715-1726.
- Dittmar, T., Lara, J.R., **2001**. Molecular evidence for lignin degradation in sulphate-reduction mangrove sediments (Amazônia, Brazil). *Geochim. Cosmochim. Ac.* 65, 1417-1428.
- Gonçalves, C.N., Dalmolin, R.S.D., Dick, D.P, Knicker, H., Klamt, E., Kögel-Knabner, I., **2003**. The effect of 10% HF treatment on the resolution of CPMAS <sup>13</sup>C NMR spectra and on the quality of organic matter in Ferralsols. *Geoderma* 116, 373-392.
- Hedges, J.I., Ertel, J.R., **1982**. Characterization of lignin by gas capillary chromatography of cupric oxide oxidation products. *Anal. Chem.* 54, 174-178.
- Janos, P., **2003**. Separation methods in the chemistry of humic substances. *J. Chromatogr. A* 983, 1-18.
- Jansen, S.A., Kolla, S., Sein, L.T., J., Paciolla, M.D., Radwan, A., Davies, G., Varnum, J.M., Drozd, J., Donet, S.S., Senini, N., Weber, J. (Eds.), **1997**. The role of humic substances in the ecosystems and in environmental protection. *IHSS*, Grunwaldzka, Wroclaw, Poland.
- Javor, T., Buchberger, W., Tanzcos, I., **2000**. Determination of low-molecular-mass phenolic and non-phenolic lignin degradation compounds in wood digestion solutions by capillary electrophoresis. *Mikrochim. Acta* 135, 45-53.
- Kick, H., **1981**. Phosphorus balance after the application of sewage sludge. In: Hucker, T.W.G. and Catroux, G. (Eds.). Phosphorus in sewage sludge and animal waste slurries. *D. Reidel Publ.*, Dordrecht, The Netherlands.

- Kögel-Knabner, I., **2002**. The macromolecular organic composition of plant and microbial residues as inputs to soil organic matter. *Soil Biol. Biochem.* 34, 139-162.
- Lima, D.L.D., Duarte, A.C., Esteves, V.I., **2007**. Optimization of phenolic compounds analysis by capillary electrophoresis. *Talanta* 72, 1404-1409.
- Lima, D.L.D., Duarte, A.C., Esteves, V.I., **2007**. Solid phase extraction and capillary electrophoresis determination of phenols from soil after alkaline CuO oxidation. *Chemosphere* 69, 561-568.
- Lorenz, K., Preston, C.M., Kandeler, E., **2006**. Soil organic matter in urban soils: Estimation of elemental carbon by thermal oxidation and characterization of organic matter by solid-state  $^{13}\text{C}$  nuclear magnetic resonance (NMR) spectroscopy. *Geoderma* 130, 312-323.
- Miller, J.N., Miller, J.C., **2000**. Statistics and chemometrics for analytical chemistry. *Prentice Hall*, 4<sup>th</sup> Edition, Dorset, England.
- Parat, C., Chaussod, R., Lévêque, J., Andreux, F., **2005**. Long-term effects of metal-containing farmyard and sewage sludge on soil organic matter in fluvisol. *Soil Biol. Biochem.* 37, 673-679.
- Pascual, J.A., García, C., Hernandez, T., **1999**. Lasting microbiological and biochemical effects of the addition of municipal solid waste to an arid soil. *Biol. Fert. Soils* 30, 1-6.
- Polak, J., Sulkowski, W.W., Bartoszek, M., Papież, W., **2005**. Spectroscopic studies of the progress of humification processes in humic acid extracted from sewage sludge. *J. Mol. Struct.* 744-747, 983-989.
- Rumpel, C., Rabia, N., Derenne, S., Quenea, K., Eusterhues, K., Kögel-Knabner, I., Mariotti, A., **2006**. Alteration of soil organic matter following treatment with hydrofluoric acid (HF). *Org. Geochem.* 37, 1437-1451.
- Rydlund, A., Dahlman, O., **1996**. Efficient capillary zone electrophoresis separation of wood-derived neutral and acidic mono and oligosaccharides. *J. Chromatogr. A* 738, 129-140.
- Santos, S.M., Duarte, A.C., Esteves, V.I., **2007**. Development and application of a capillary electrophoresis based method for the assessment of monosaccharide in soil using acid hydrolysis. *Talanta* 72, 165-171.
- Saviozzi, A., Biasci, A., Riffaldi, R., Levi-Minzi, R., **1999**. Long-term-effects of farmyard manure and sewage sludge on some soil biochemical characteristics. *Biol. Fert. Soils* 30, 100-106.
- Schilling, M., Cooper, W.T., **2004**. Effects of chemical treatments on the quality and quantitative reliability of solid-state  $^{13}\text{C}$  NMR spectroscopy of mineral soils. *Anal. Chim. Acta* 508, 207-216.

- Shirshova, L.T., Ghabbour, E.A., Davies, G., **2006**. Spectroscopic characterization of humic acid fractions isolated from soil using different extraction procedures. *Geoderma* 133, 204-216.
- Sierra, M.M.D., Giovanela, M., Parlanti, E., Esteves, V.I., Duarte, A.C., Fransozo, A., Soriano-Sierra, E.J., **2005**. Structural description of humic substances from subtropical coastal environments using elemental analysis, FT-IR and  $^{13}\text{C}$ -solid state NMR data. *J. Coastal Res.* 42, 370-382.
- Smernik, R.J., **2005**. Solid-state  $^{13}\text{C}$  NMR spectroscopic studies of soil organic matter at two magnetic field strengths. *Geoderma* 125, 249-271.
- Sparks, D.L., **1998**. Soil Physical Chemistry. *CRC Press LCC*, United States of America.
- Sparling, G.P., **1992**. Ratio of microbial biomass carbon to soil organic carbon as a sensitive indicator of changes of soil organic matter. *Aust. J. Soil Res.* 30, 195-207.
- Tan, K.H., **1994**. Environmental Soil Science. *Marcel Dekker, Inc.*, United States of America.
- Ussiri, D.A.N., Johnson, C.E., **2003**. Characterization of organic matter in a northern hardwood forest soil by  $^{13}\text{C}$  NMR spectroscopy and chemical methods. *Geoderma* 111, 123-149.
- Werner, W., Olf, H.-W., Scherer, H.W., Warnusz, J., **1987**. Effect of long-term application of sewage sludge and garbage compost on chemical and microbiological soil characteristics. *Proc. 4<sup>th</sup> International CIEC Symposium: Agricultural Waste Management and Environmental Protection* (Welte, E. and Szabolcs, I., eds.), Braunschweig, Germany, pp 189-199.
- Werner, W., Scherer, H.W., Olf, H.-W., **1988**. Influence of long-term application of sewage sludge and compost from garbage with sewage sludge on soil fertility criteria. *J. Agron. Crop Sci.* 160, 173-179.



# CHAPTER 5

**SORPTION BEHAVIOUR OF HOP ON SOILS SUBJECTED TO  
DIFFERENT ORGANIC LONG-TERM AMENDMENTS**



## CHAPTER 5

### SORPTION BEHAVIOUR OF HOP ON SOILS SUBJECTED TO DIFFERENT ORGANIC LONG-TERM AMENDMENTS\*

5.1. Introduction .....	119
5.2. Atrazine sorption behaviour .....	122
5.2.1. Experimental procedure.....	122
5.2.1.1. Soil samples.....	122
5.2.1.2. Instrumentation and analysis conditions.....	122
5.2.1.3. Adsorption studies .....	122
5.2.1.4. Desorption studies .....	123
5.2.1.5. Data analysis .....	123
5.2.2. Results and discussion.....	124
5.2.2.1. Adsorption .....	124
5.2.2.2. Desorption .....	127
5.3. EE2 sorption behaviour.....	132
5.3.1. Experimental procedure.....	132
5.3.1.1. Soil samples.....	132
5.3.1.2. Instrumentation and analysis conditions.....	132
5.3.1.3. Adsorption studies .....	132
5.3.1.4. Molecular modelling studies.....	132
5.3.2. Results and discussion.....	134
5.4. Conclusion.....	143
5.5. References .....	145

\* Diana L.D. Lima, Rudolf J. Schneider, Heinrich W. Scherer, Armando C. Duarte, Eduarda B.H. Santos, Valdemar I. Esteves, 2010. Sorption-desorption behavior of atrazine on soils subjected to different organic long-term amendments. *Journal of Agricultural and Food Chemistry* 58, 3101-3106.

## 5.1. Introduction

---

Hydrophobic organic pollutants comprise a large number of compounds. Among them, atrazine, an herbicide forbidden in European Union, but still one of the most used worldwide, and EE2, an endocrine disrupting compound used as an oral contraceptive and with an estrogenic potency ten times higher than natural hormones, are of great concern. As mentioned before, the transport and fate of hydrophobic organic pollutants in the environment involve complex phenomena which are influenced by many processes (Gao et al., 1998; Lesan and Bhandari, 2003). However, adsorption is one of the most important processes that affects fate of HOP in soils and control their distribution in the soil/water environment (Kah and Brown, 2007).

Due to their hydrophobic properties, estrogens are strongly sorbed in soils (Stumpe and Marschner, 2010), potentially limiting the mobility and transport of estrogens from soils to aquatic ecosystems where they seem to cause more damage (Hildebrand et al., 2006). Several authors related the sorption affinity of estrogens with total organic carbon content (Caron et al., 2010; Emmerik et al., 2003; Ying et al., 2002). Hydrophobic interaction was considered the dominant mechanism of interaction (Lee et al., 2003; Sarmah et al., 2008; Yu et al., 2004). Yu et al. (2004) consider the possibility of specific sorbent-sorbate interactions via hydrogen bonding or covalent bonding probably due to the phenolic function at C-3 and the hydroxyl function at C-17 of EE2 molecule that may tend to react with carboxylic functional groups of humic materials associated with soils and sediments. A correlation between aromatic properties of organic colloids and E2 sorption is also suggested (Stumpe and Marschner, 2007). Other studies provide evidence for incomplete sorption in soils, since traces of hormones are detected at great depths and in groundwater (Stumpe and Marschner, 2009). Although several studies have been performed regarding sorption of steroid hormones onto soils, using batch equilibrium technique, the experimental protocols are considerably different and, as a result, it is often difficult to establish a mechanistic interpretation between different results (Sarmah et al., 2008).

The sorption interactions of pesticides may involve either mineral or organic soil components, or even both (Spark and Swift, 2002). It is widely accepted that organic

matter plays the major role in the sorption phenomena of organic chemicals on soils, mainly for relatively non-polar substances, such as atrazine (Kovaios et al., 2006; Lesan and Bhandari, 2003). However, the contribution of the inorganic soil components, particularly the clay fraction, is also significant, especially in soils containing low organic matter contents (Spark and Swift, 2002). While Sparks and Swift (2002) assume that the total organic matter content is more important for sorption processes than the composition of the organic matter, Kulikova and Perminova (2002) reported that the extent of atrazine sorption to humic substances was strongly correlated to the aromaticity of the organic matter. Desorption of chemicals is also critical as it determines the availability of the species, their release rate into run-off and the risk for groundwater pollution (Boivin et al., 2005; Nemeth-Konda et al., 2002). The degree of reversibility in adsorption-desorption reactions is important for the evaluation of the mobility of pesticides. Several studies have indicated the occurrence of hysteresis (Boivin et al., 2005; Gao et al., 1998), although the exact mechanism of hysteretic adsorption/desorption remains still largely unknown. It is suggested that sorption of pesticides occurs with a limited degree of reversibility depending on the physical-chemical properties of the molecules and soils involved (Boivin et al., 2005). It is usually explained by irreversible chemical binding, sequestration of a solute into specific components of the solid organic matter, or entrapment of the solute into microporous structures or into the solid organic matter matrix (Chefetz et al., 2004). A large number of studies dealt with the interaction between atrazine and soil organic matter; however, the binding mechanism is still a subject of controversial discussions. Between the different mechanisms proposed, only some are generally accepted. According to Spark and Swift (2002) atrazine has functional groups capable of engaging H-bonding, van der Waals-bonding and ligand exchange. The carboxylic and phenolic functional groups of organic matter are considered by Chefetz et al. (2004) to play an important role in the sorption interaction by H-bonding. They suggest that the sorption mechanism of atrazine comprises both non-specific (hydrophobic interactions with aromatic and/or aliphatic domains) and specific (H-bonding to carboxylic and phenolic groups) interactions. Celano et al. (2008) are in favour of a charge-transfer mechanism, at pH lower than 4.5, however such conditions are not environmentally

relevant and also refer to the existence of a predominant role of weak dispersive forces. Kulikova and Perminova (2002) considered the hydrophobic binding as the key interaction underlying the binding of atrazine to humic substances. Boivin et al. (2005) also refers to hydrophobic interactions on weak energetic sites to explain the binding mechanism.

During the past years, numerous investigations were made in order to understand the sorption phenomena of atrazine to soils. In the majority of these works different soil and sediment samples, with different organic and mineral characteristics, were used (Boivin et al., 2005; Chefetz et al., 2004; Loganathan et al., 2009; Nemeth-Konda et al., 2002). Although herbicide sorption on soils has been extensively studied through the world, in this work a soil sample subjected to a mineral and to three different organic fertilizations for more than 45 years are compared. Moreover, the structural characterization of soil organic matter, used to perform the adsorption/desorption experiments, was previously reported on chapter 4.

The aim of this study was to evaluate the effects of SOM with different structural characteristics in the atrazine and EE2 sorption behaviour, using batch equilibrium experiment. We expect that the results can increase our understanding of the mechanism of the sorption phenomena, by revealing the types of interactions present. It is important to understand the sorption behaviour of such compounds in order to assess their potential impact on soils, surface water and groundwater resources. Such information can be useful for defining land management practices for manure disposal and for agri-environmental policies.

## 5.2. Atrazine sorption behaviour

---

### 5.2.1. *Experimental procedure*

#### 5.2.1.1. *Soil samples*

The soil samples used to evaluate atrazine sorption behaviour were described previously in section 1.2.1.

#### 5.2.1.2. *Instrumentation and analysis conditions*

All measurements were performed using a Beckman P/ACE MDQ capillary electrophoresis system equipped with a diode array detector (DAD). Separation was carried out on an uncoated fused silica capillary of 60 cm total length (50 cm effective length to the detector), 75  $\mu\text{m}$  internal and 375  $\mu\text{m}$  of external diameter. The analysis experimental conditions are the same as the ones described previously on chapter 1.

#### 5.2.1.3. *Adsorption studies*

Adsorption isotherms of atrazine were obtained using the batch equilibration technique (OECD, 2000). Five pesticide concentrations were prepared in 0.01 mol L<sup>-1</sup> calcium chloride ranging between 2 and 10 mg L<sup>-1</sup>. An aliquot of each concentration of atrazine solution was added to soil in order to obtain a final 1:2 soil/solution ratio. Five adsorption experiments were made for each concentration. The tubes were agitated in a head-over-head shaker for 24 h at 20 $\pm$ 1°C. According to previous kinetic studies, equilibrium was assumed to be reached within the 8 h equilibration period (data presented in section 1.3.3.). Samples were then centrifuged at 4000 rpm for 20 min and aliquots of 3 mL of the supernatants were filtered and analyzed by capillary electrophoresis, using ethylvanillin as the IS. Previous studies have indicated that degradation and adsorption of atrazine to the test tubes can be ignored during the period of our study (Chapter 1).

The amount of pesticide adsorbed by the soil was calculated from the difference between the initial and the equilibrium pesticide concentrations in solution. The initial concentration was considered to be the amount of atrazine present in the controls (without soil). Sorption isotherms were obtained plotting the amount of atrazine sorbed per weight unit of soil at equilibrium ( $Q_e$ ,  $\text{mg kg}^{-1}$ ) versus the amount of chemical per volume of solution at equilibrium ( $C_e$ ,  $\text{mg L}^{-1}$ ).

#### *5.2.1.4. Desorption studies*

These experiments were conducted immediately after the sorption experiments and the supernatant was removed in order to leave only 25% of the original volume of solution in the vessel. The solution in the vessel was then made up to the original volume with  $\text{CaCl}_2$   $0.01 \text{ mol L}^{-1}$ , after which the tubes were shaken at  $20 \pm 1 \text{ }^\circ\text{C}$  for 24 h, centrifuged at 4000 rpm for 20 min and the supernatant was again analyzed. This procedure was repeated while the concentration of atrazine in solution was above the detection limit of the analytical method. The lower adsorption concentration was not used for the desorption study due to the expected lower concentration, below the analytical method limit of detection.

#### *5.2.1.5. Data analysis*

Data analysis was performed as described in section 1.2.8. Desorption isotherms were obtained and  $K_{F_{des}}$  and  $N_{des}$  calculated. The  $K_{F_{des}}$  values were normalized to the organic carbon content of the soil to obtain  $K_{FOC_{des}}$ . The ratios of the Freundlich exponents for desorption and sorption ( $N_{des}/N$ ) were calculated and used as desorption apparent hysteresis index (AHI). Lower index values indicate increased difficulty of the sorbed analyte to be desorbed from the matrix (Chefetz et al., 2004; Drori et al., 2005).

## 5.2.2. Results and discussion

### 5.2.2.1. Adsorption

Adsorption isotherms, obtained by plotting the amount of atrazine sorbed per weight unit of soil at equilibrium ( $Q_e$ ,  $\text{mg kg}^{-1}$ ) versus the amount of chemical per volume of solution at equilibrium ( $C_e$ ,  $\text{mg L}^{-1}$ ), are shown in Figure 5.1.

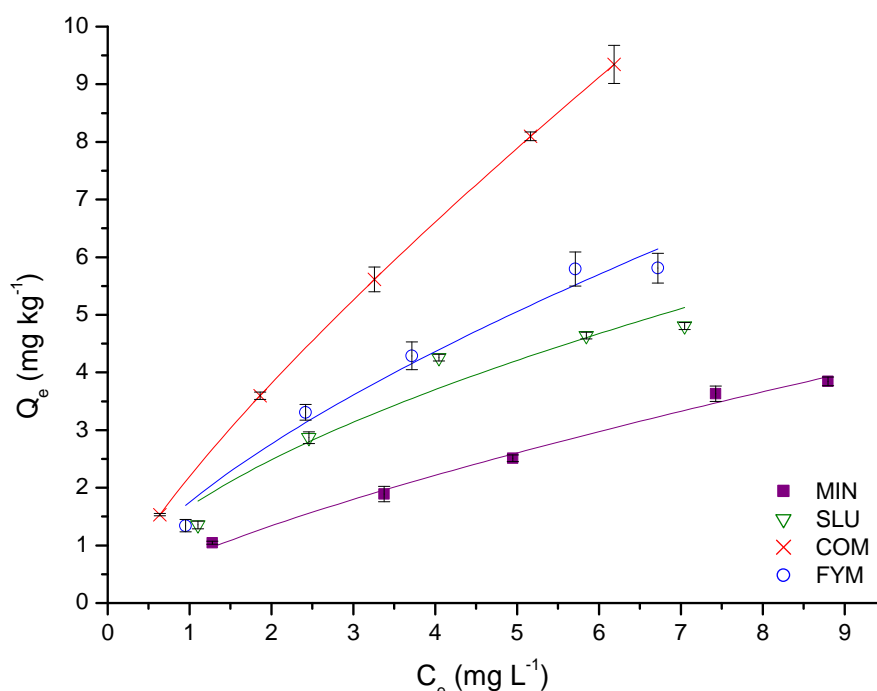


**Figure 5.1.** Freundlich adsorption isotherms for atrazine in soils subjected to different fertilizations (MIN – mineral fertilizer; COM – compost fertilizer; FYM – farmyard manure; SLU – sewage sludge fertilizer; Error bars represent 95% confidence interval for  $n = 5$ ).

The Freundlich equation has reasonably described the adsorption of atrazine on the soil samples used, with correlation coefficients ranging from 0.966, for soil fertilized with sewage sludge, to 0.995, for mineral soil (Table 5.1.). The Freundlich adsorption coefficient is an empirical constant of the Freundlich model expressing soil sorbent capacity (sorption isotherm slope) for a given range of atrazine concentration (Boivin et al., 2005).



**Table 5.1.** Parameters of the Freundlich equation describing the adsorption isotherms of atrazine to the four soil samples used.

Soil sample <sup>a</sup>	$K_F$ <sup>b</sup>	N <sup>b</sup>	$K_{FOC}$ <sup>b</sup>	$r$
MIN	0.81 (0.08)	0.72 (0.05)	65.5 (6.5)	0.995
SLU	1.67 (0.31)	0.57 (0.11)	84.2 (15.6)	0.966
FYM	1.73 (0.23)	0.67 (0.08)	117.3 (15.7)	0.987
COM	2.20 (0.22)	0.79 (0.06)	79.17 (7.9)	0.995

<sup>a</sup> MIN – mineral fertilizer; SLU – sewage sludge fertilizer; FYM – farmyard manure; COM – compost fertilizer.

<sup>b</sup> Standard deviation of the evaluated value is on parenthesis (n=5).

A high  $K_F$  value reflects high adsorption capacity and is commonly associated with lower permeability of soils and thus lower leaching potential (Correia et al., 2007). The highest  $K_F$  value 2.20 (mg kg<sup>-1</sup>) (mg L<sup>-1</sup>)<sup>-N</sup>, among the four soils samples used in this study, was observed for the adsorption of atrazine on soil fertilized with compost, which presented simultaneously the highest organic carbon (2.775%) and nitrogen (0.151%) content. In contrast, the lowest  $K_F$  value (0.81 (mg kg<sup>-1</sup>) (mg L<sup>-1</sup>)<sup>-N</sup>) was found in soil fertilized with mineral salts only, having resulted – over the long-term application period – in a low organic carbon (1.238%) and nitrogen (0.109%) contents. The correlation coefficient between  $K_F$  values and total organic carbon was calculated (Table 5.2.) and based on the results it is possible to verify a positive correlation between organic carbon content and soil sorption capacity. However, since FYM soil, with 1.473% of organic carbon content, presented a slightly higher  $K_F$  value than SLU soil, with 1.983% organic carbon, we presume that the Freundlich adsorption constant can, not only be correlated with the soils organic carbon content but also with their different functional groups. Singh et al. (2010) evaluated the correlation between  $K_F$  and relative structural carbon percentage of SOM fractions. However, Singh et al. (2010) used other pollutants and the SOM was constituted only by humic acids, humin and lignin. In this study, complete soil samples were used and no correlation was found between  $K_F$  and different relative area distribution (% of total spectrum area) of solid-state <sup>13</sup>C CPMAS-NMR spectra. Since we observed a strong correlation between TOC and  $K_F$  that could disguise the real influence of organic matter characteristics, it is important to use  $K_F$  value normalized to the carbon level of soil,  $K_{FOC}$  in the correlation with the different functional groups content. This

normalized constant depends only on the specific characteristics of the soil organic matter which differ considerably in the sorption capacity, due to differences in origin and genesis (OECD, 2000). Thus, alkyl, *O,N*-alkyl, aromatic and carboxyl content was correlated with  $K_{\text{FOC}}$  (Table 5.2.).

**Table 5.2.** Correlation coefficients ( $r$ ) between the parameter  $K_{\text{F}}$  or  $K_{\text{FOC}}$  and TOC or relative area distribution (% of total spectrum area) of solid-state  $^{13}\text{C}$  CPMAS-NMR spectra.

	TOC	Alkyl	<i>O,N</i> -alkyl	Aromatic	Carboxyl
Correlation coefficient ( $r$ )	0.936 <sup>a</sup>	-0.583 <sup>b</sup>	-0.842 <sup>b</sup>	0.397 <sup>b</sup>	0.869 <sup>b</sup>

<sup>a</sup>Correlation using  $K_{\text{F}}$ ; <sup>b</sup> Correlation using  $K_{\text{FOC}}$

A strong positive correlation can be observed between carboxyl units and  $K_{\text{FOC}}$  values.  $^{13}\text{C}$  NMR spectroscopy of soil supplied with farmyard manure presented a higher relative area in the region usually attributed to carboxyl, amide and ester functionalities, followed by soil fertilized with sewage sludge (results presented on section 4.3.2.). The presence of a larger number of carboxyl units that can be responsible for the hydrogen bonding between atrazine and organic matter could be the explanation of the higher  $K_{\text{FOC}}$  values obtained for these soils.

A positive correlation can also be observed for aromatic groups, although this correlation is not very high. It is important to highlight the low organic carbon presented in the soil with mineral fertilization and the high noise observed in its  $^{13}\text{C}$  NMR spectra, especially in that area (110-160 ppm). If we correlate the  $K_{\text{FOC}}$  with aromatic units, without using mineral fertilization the correlation improves tremendously, suggesting that higher aromatic compounds contents induce higher  $K_{\text{FOC}}$  values. As presented in chapter 4, where the soil organic matter of the soils used were characterized by several techniques such as  $^{13}\text{C}$  NMR and FT-IR spectroscopy, the farmyard manure presented several evidences of higher aromatic content. The more prevalent the aromatic content is, when compared to the hydrophilic (mostly polysaccharide), the greater the hydrophobicity of the organic matter. Thus, the obtained results could be an indication of

hydrophobic interactions as a key role in binding of atrazine to organic matter (Kulikova and Perminova, 2002).

A negative correlation was observed for alkyl and *O,N*-alkyl units. The soil supplied with mineral fertilizer and with compost presented higher alkyl units and lower carboxyl groups decreasing the possibility of hydrogen bonding that could explain the lower  $K_{\text{FOC}}$  observed. As indicated by the  $K_{\text{FOC}}$  values, the toxicity of atrazine applied to agricultural crops not only depends on the soil organic carbon content, but also on the nature as well, since the bonding mechanism and its intensity depend greatly on the units of organic matter available for binding. Thus, the same application rate of atrazine to the soil, containing the same organic matter content, is expected to result in a lower environmental impact on the soil fertilized with farmyard manure, containing higher aromatic content, comparatively to other soils with predominantly aliphatic structures. It is important to highlight that a compromise has to be reached between the content and nature of the organic matter applied to a specific soil.

The sorption isotherms for all soils in this study are non-linear ( $N < 1$ ), exhibiting values from 0.57, for soil fertilized with sewage sludge, to 0.79, for soil supplied with mineral fertilizer. Non-linear sorption isotherms (convex curvature) are related to a modification of the affinity between the pesticide molecule and soils when concentration increases (Boivin et al., 2005). With an increase in the initial concentration of pesticide, the percentage adsorbed by the soil decrease, probably by a decrease in accessibility of free sorption sites (Boivin et al., 2005).

#### *5.2.2.2. Desorption*

Desorption isotherms were obtained plotting the amount of the pesticide retained by the soil versus the pesticide concentration in the solution at equilibrium (Figure 5.2., 5.3., 5.4. and 5.5.). Desorption is a key process affecting pesticide behaviour in soils and controls the predisposition of a pesticide to be degraded and/or leached at different times (Boivin et al., 2005).

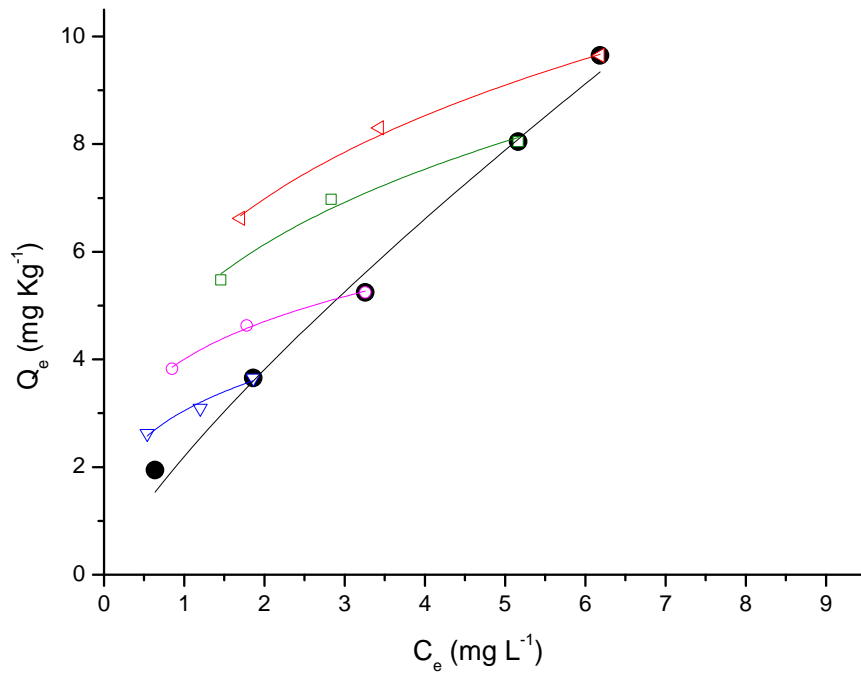


**Figure 5.2.** Freundlich sorption isotherms (filled symbol) and sequential desorption steps (open symbols) for atrazine onto soil subjected to compost fertilizations (COM).

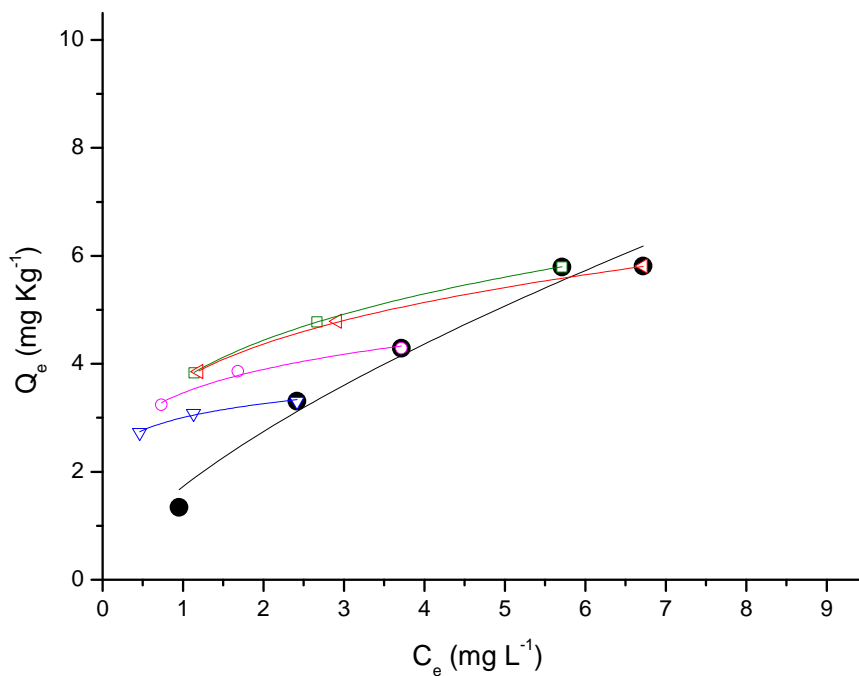


**Figure 5.3.** Freundlich sorption isotherms (filled symbol) and sequential desorption steps (open symbols) for atrazine onto soil subjected to farmyard manure (FYM).

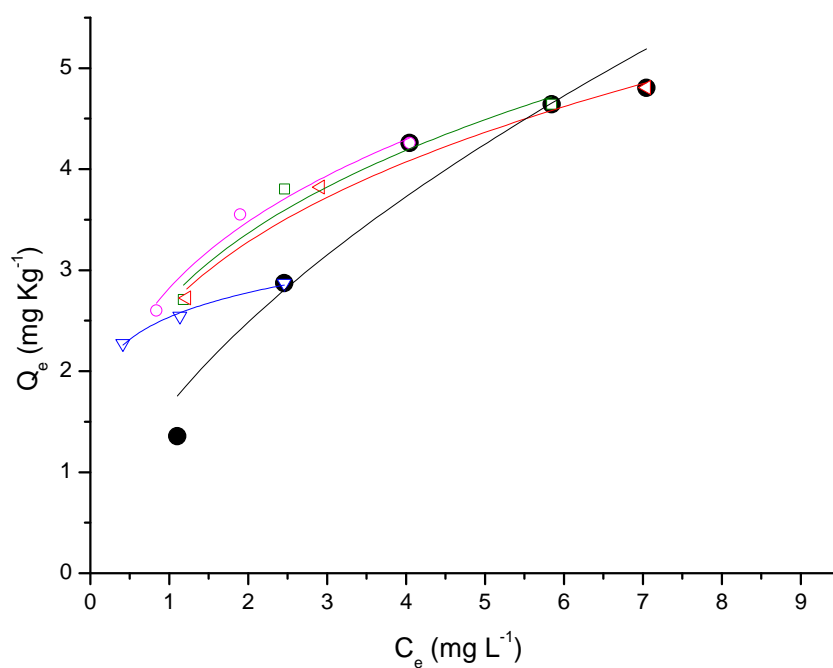


**Figure 5.4.** Freundlich sorption isotherms (filled symbol) and sequential desorption steps (open symbols) for atrazine onto soil subjected to sewage sludge fertilizer (SLU).

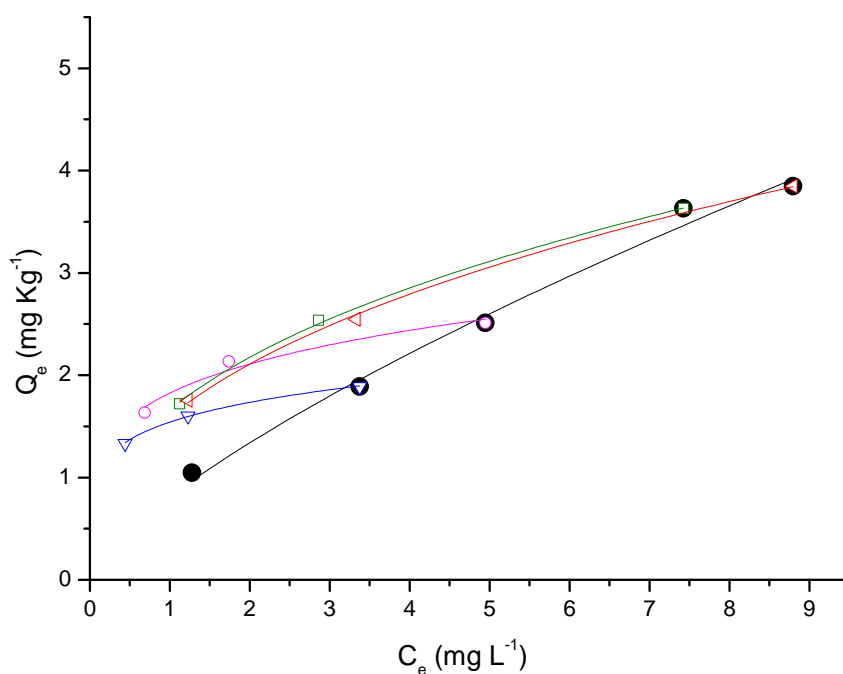


**Figure 5.5.** Freundlich sorption isotherms (filled symbol) and sequential desorption steps (open symbols) for atrazine onto soil subjected to mineral fertilizer (MIN).

The Freundlich equation has reasonably described desorption of atrazine on the four soil samples used, with correlation coefficient values ranging from 0.963 to 1.000. Comparing  $K_{Fdes}$  (Table 5.3.) obtained for the different soils it is possible to conclude that higher values are obtained for the soil fertilized with compost, followed by farmyard manure and sewage sludge amended soil. Soil supplied with mineral fertilizer presented  $K_{Fdes}$  values significantly lower than the rest of the soils. Higher  $K_{Fdes}$  values indicate a greater proportion of the chemical retained by the soil (Mersie and Seybold, 1996). It was possible to establish a relationship between the  $K_{Fdes}$  and the organic matter content: higher organic matter content induces higher  $K_{Fdes}$ , thus lower desorption capacity.

**Table 5.3.** Parameters of the Freundlich equation describing the desorption isotherms of atrazine to the four soil samples used (MIN – mineral fertilizer; SLU – sewage sludge fertilizer; FYM – farmyard manure; COM – compost fertilizer).

Soil	Initial concentration (mg L <sup>-1</sup> )	$K_{Fdes}^a$	$K_{FOCdes}^a$	$N_{des}^a$	$r$	AHI <sup>a</sup>
MIN	4	1.54 (0.01)	1.24 (0.01)	0.17 (0.01)	0.999	0.234 (0.02)
	6	1.83 (0.08)	1.48 (0.06)	0.21 (0.04)	0.985	0.288 (0.06)
	9	1.66 (0.03)	1.34 (0.02)	0.39 (0.01)	0.999	0.540 (0.06)
	10	1.59 (0.04)	1.28 (0.03)	0.41 (0.02)	0.999	0.559 (0.06)
SLU	4	2.54 (0.02)	1.28 (0.01)	0.13 (0.01)	0.995	0.229 (0.04)
	6	2.82 (0.12)	1.42 (0.06)	0.30 (0.04)	0.991	0.527 (0.12)
	9	2.71 (0.24)	1.37 (0.12)	0.31 (0.06)	0.981	0.546 (0.15)
	10	2.64 (0.15)	1.33 (0.07)	0.31 (0.06)	0.993	0.542 (0.12)
FYM	4	3.00 (0.02)	2.04 (0.01)	0.12 (0.01)	0.989	0.177 (0.03)
	6	3.46 (0.07)	2.35 (0.05)	0.17 (0.01)	0.992	0.255 (0.05)
	9	3.72 (0.01)	2.53 (0.01)	0.25 (0.01)	1.000	0.382 (0.05)
	10	3.71 (0.02)	2.52 (0.01)	0.23 (0.01)	1.000	0.351 (0.05)
COM	4	3.05 (0.08)	1.10 (0.03)	0.27 (0.05)	0.984	0.341 (0.07)
	6	4.00 (0.05)	1.44 (0.02)	0.23 (0.01)	0.998	0.292 (0.03)
	9	5.00 (0.23)	1.80 (0.08)	0.30 (0.04)	0.993	0.372 (0.06)
	10	5.72 (0.17)	2.06 (0.06)	0.29 (0.02)	0.997	0.363 (0.04)

<sup>a</sup>Standard deviation of the evaluated value is on parenthesis (n=5).

As presented in the adsorption study, the  $K_{Fdes}$  can also be normalized to the carbon level of the soil,  $K_{FOCdes}$ , allowing us to verify the existence, or not, of an influence in

desorption capacity due to the existence of differences on the organic matter properties, caused by differences in soil fertilizations. The higher  $K_{FOCdes}$  values were obtained for the soil fertilized with farmyard manure, suggesting a higher quantity of atrazine retained by this type of soil fertilization. A higher aromatic content is usually considered to be responsible for a high sorption of organic compounds, but also to contribute significantly to desorption hysteresis (Chefetz et al., 2004). Hysteresis is manifested by an increase in the difference between the adsorption and desorption isotherm slopes, which has been well documented (Mersie and Seybold, 1996; Prata et al., 2003; Spark and Swift, 2002; Yang et al., 2009). Such differences in isotherms may be caused by several factors including different types of binding involved in atrazine sorption by soil organic matter, such as hydrogen bonds, charge transfer, ionic bonds, cation bridges, hydrophobic interactions, and physical diffusion into the humic substances (Prata et al., 2003). Boivin et al. (2005) suggested the lack of similarity between adsorption and desorption to be probably a result of the binding to organic matter and mineral particles, particularly clay minerals (Fruhstorfer et al., 1993). Comparing the AHI values, it can be confirmed that the farmyard manure soil, with higher aromatic content and carboxyl units, is the one that presents lower AHI, thus higher desorption hysteresis. The aromatic content, responsible for the hydrophobicity of the organic matter, is involved in the hydrophobic interactions that are considered weak forces. However, the higher quantity of carboxyl units allows this type of organic matter to establish more hydrogen bonds than in the others soils' organic matter. Hydrogen bonds are stronger than hydrophobic interactions, thus more difficult to break, which can be an explanation for the lower desorption capacity observed in the soil fertilized with farmyard.

For all soils we can generally observe an increase in AHI, thus a decrease in hysteresis, with the amount of atrazine adsorbed. The trend of increasing desorption with the increasing of atrazine adsorbed can be explained by the existence of a limited number of sites available to establish stronger interactions. Therefore, most of these sites are occupied at low solute concentrations, whereas at high solute concentration more molecules are taken up by sites with the ability to establish weaker interactions and therefore can be readily desorbed (Drori et al., 2005).

## 5.3. EE2 sorption behaviour

---

### *5.3.1. Experimental procedure*

#### *5.3.1.1. Soil samples*

The soil samples used to evaluate EE2 sorption behaviour were described previously in section 1.2.1.

#### *5.3.1.2. Instrumentation and analysis conditions*

Experimental conditions were previously described on section 2.4.1.

#### *5.3.1.3. Adsorption studies*

Adsorption isotherm of EE2 was made using the batch equilibration technique (OECD 2000). Six hormone concentrations (0.4 to 4 mg L<sup>-1</sup>) were prepared in 0.01 mol L<sup>-1</sup> CaCl<sub>2</sub>. A 12.5 mL aliquot of each concentration was added to 250 mg of soil. Three adsorptions were made for each concentration. The tubes containing the mixtures were shaken head over head at 100 rpm for 15 h at 22±1°C. According to previous kinetic studies (section 2.4.2.3.), equilibrium was assumed to be reached within the 6 equilibration hours. Samples were then centrifuged at 4000 rpm for 20 min and the supernatant filtered. Ammonium hydroxide was added in order to obtain 0.1 mol L<sup>-1</sup> as final concentration and all of them were diluted 100 times prior to analysis. The procedure was repeated for each soil sample. The amount of hormone adsorbed by the soils was calculated from the difference between the initial and the equilibrium EE2 concentration in solution.

#### *5.3.1.4. Molecular modelling studies*

In order to further investigate the adsorption mechanism, the association between EE2 molecules (consistent with a co-operative adsorption model influenced by adsorbate-



adsorbate interactions) was evaluated by molecular modelling studies, kindly developed by Vânia Calisto (PhD) and Sérgio M. Santos (PhD).

Molecular modelling simulations were performed using GROMACS 4.5 (Hess et al., 2008; van der Spoel et al., 2005) with atomic parameters taken from the GAFF force field (Wang et al., 2004). The starting structure of the EE2 molecule was optimized at AM1 theory level. AM1BCC partial atomic charges were then assigned using Antechamber from Amber Tools 1.4 (Jakalian et al., 2000, 2002). The association of two EE2 molecules was first investigated by gas phase molecular dynamics at 300 K, during 2 ns using a time step of 1 fs. A total of 20000 co-conformations were collected and energy minimized by molecular mechanics. Subsequently, the lowest energy co-conformation was selected. To evaluate the stability of the selected structure in aqueous solution, the structure was solvated using the TIP3P water model (Jorgensen et al., 1983) in a cubic box with approximately  $40 \times 40 \times 40 \text{ \AA}^3$ , containing a total of 2148 water molecules. The system was then energy minimized to avoid undesired contacts and equilibrated at 300 K during 500 ps, under boundary periodic conditions, to bring the system's density to that of bulk water. Finally, a molecular dynamics collection step was run for 5 ns. The electrostatics interactions were described by the Particle Mesh Ewald Method, van der Waals interactions were subjected to a cut-off of  $10 \text{ \AA}$  and the LINCS algorithm was used to constrain bonds involving hydrogen atoms (Hess et al., 1997). Finally, 25000 structures were collected from the obtained trajectory and a simulation with implicit solvent (using the Generalized Born formalism) (van der Spoel et al., 2010) was performed, allowing the determination of the enthalpic contribution to the association free energy. The Still methodology was used to calculate the Born radii and the non-polar solvation energy was calculated by means of the Ace approximation. The surface tension was set to  $2.05 \text{ kJ nm}^{-2} \text{ mol}^{-1}$ . Molecular structures presented in Figure 5.8. were drawn using PyMOL (Delano, 2002).

### 5.3.2. Results and discussion

Kinetic results previously presented on section 2.4.2.3. demonstrated a typical experimental result, in which the pollutant, initially in the solution phase, undergoes initial rapid adsorption followed by a slow approach to equilibrium. These results can also be used to determine if particle diffusion is the rate limiting step for EE2 adsorption onto soils. Previous works (Banat et al., 2000; Calace et al., 2002) reported that if particle diffusion was involved in the adsorption process then a plot of adsorbate uptake versus the square root of the time needed to attain the equilibrium would present a linear relationship. Moreover, if such line passes through the origin, the particle diffusion can be considered the rate controlling step of the adsorption process. Figure 5.6. shows that a linear relationship can be obtained with a good correlation coefficient of 0.999.

Results show that particle diffusion is one of the mechanisms involved in adsorption process, but since the line does not pass through the origin it's not possible to affirm that is the only rate-limiting mechanism, indicating the presence of other mechanisms. These preliminary studies were only conducted using soil fertilized with farmyard manure.

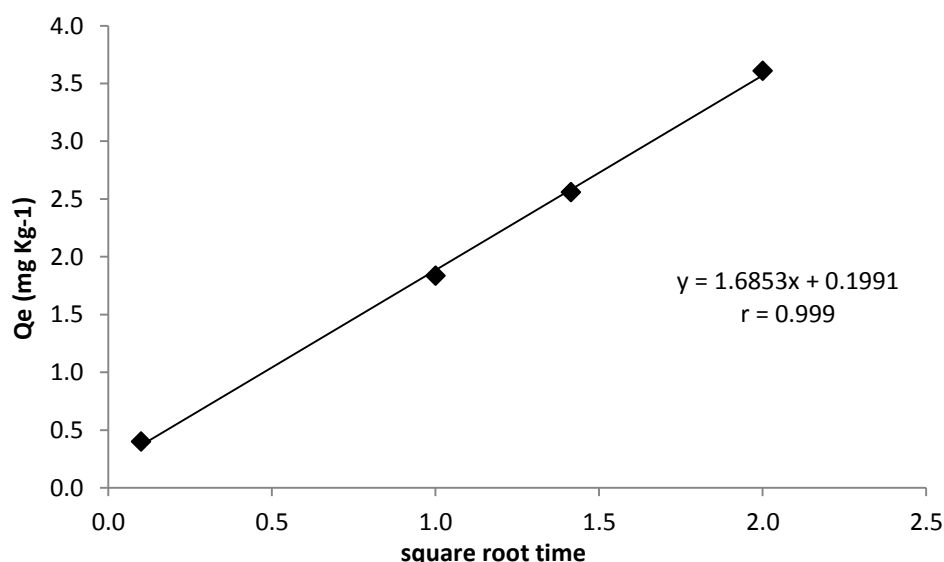


**Figure 5.6.** Linear relationship between sorbed amount of EE2 and the square root of time (hours) needed to attain sorption equilibrium. Initial EE2 concentration 2 mg L<sup>-1</sup>. Soil sample fertilized with farmyard manure.

As said before, transport models for assessing the mobility of chemicals require isotherm equations and determination of its parameters. Simple equations, such as Freundlich or Langmuir isotherms, are the most commonly used to describe adsorption data. Often, these equations do not accurately describe the data and more complicated expressions are needed. Lack of an accurate description of adsorption data may result in serious errors when applied to transport modelling (OECD, 2000). Therefore, it is essential that adsorption data are described adequately with an appropriate model equation.

As referred in chapter 2, generally, S isotherms have a concave shape at low concentrations, while both H and L isotherms have a convex shape. C isotherms are defined by a constant sorption affinity, expressed as a straight line in  $Q_e$  vs.  $C_e$  plots. As it can be seen in Figure 5.7., results present a sigmoidal-shaped (S) isotherm.

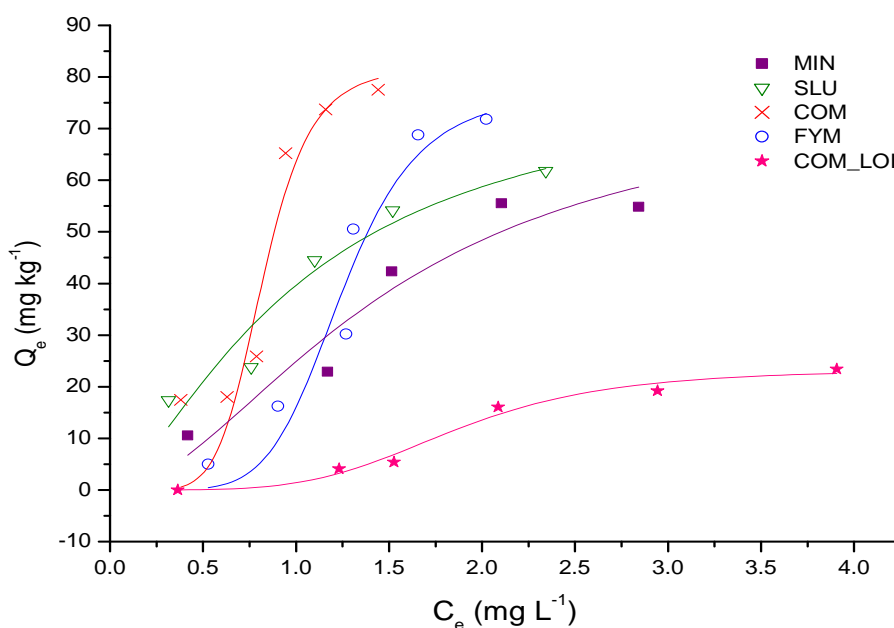


**Figure 5.7.** Adsorption isotherms with fitting using Hill Equation; SLU, sewage sludge fertilizer; MIN, mineral fertilizer; FYM, farmyard manure; COM, compost from organic household waste; COM\_LOI, composted soil submitted to loss on ignition.

Langmuir, Freundlich and Langmuir-Freundlich models are the most frequently applied to describe the behaviour of the adsorption isotherms' experimental data (Calace et al., 2002). For homogeneous surfaces, Langmuir equation is used. On the other hand,

Freundlich equation assumes that the surface is heterogeneous, thus the sorption energy depends on the binding sites and surface coverage, and that there are no limited levels of sorption. This model can represent the result of overlapping patterns of several Langmuir-type sorption phenomena occurring at different sites on complex sorbents. The Langmuir-Freundlich model presents the same behaviour of the Freundlich equation, but for high concentrations an adsorption maximum is achieved. This model assumes that surface is homogeneous but also that a cooperative process, due to sorbate-sorbate interactions, is present. For positive interactions  $b > 1$  the equation is known as Hill equation (Calace et al., 2002):

$$Q_e = Q_{max}(K_1 C_e)^b / (1 + (K_1 C_e)^b) \quad \text{Hill equation (} b > 1 \text{)}$$

where,  $Q_e$  is the amount adsorbed at equilibrium ( $\text{mg kg}^{-1}$ ),  $C_e$  is the equilibrium concentration of the sorbate ( $\text{mg L}^{-1}$ ) and  $Q_{max}$  ( $\text{mg kg}^{-1}$ ) is the maximum adsorption capacity,  $K_1$  is an affinity parameter and  $b$  is an empirical parameter which varies with the degree of heterogeneity (Calace et al., 2002).

The best results were obtained using the Langmuir-Freundlich and Hill equations; however, since the  $b$  value obtained was higher than 1, we used the Hill equation. Fitting parameters are presented in Table 5.4.

**Table 5.4.** Parameters obtained for the adsorption isotherm fitting with Hill equation.

Soil <sup>a</sup>	$K_1^b$	$Q_{max}^b$	$b^b$	$r$	$K_{10C}^b$
SLU	0.97 (0.08)	82 (13)	1.5 (0.2)	0.966	49 (4)
MIN	0.67 (0.10)	77 (15)	1.8 (1.0)	0.961	54 (8)
FYM	0.89 (0.07)	77 (13)	6.0 (3.0)	0.970	61 (5)
COM	1.22 (0.10)	82 (15)	6.4 (3.7)	0.942	44 (4)
COM_LOI	0.54 (0.04)	23 (2)	4.4 (1.2)	0.990	-----

<sup>a</sup>SLU, sewage sludge fertilizer; MIN, mineral fertilizer; FYM, farmyard manure; COM, compost from organic household waste; COM\_LOI, composted soil submitted to loss on ignition. <sup>b</sup>Standard deviation of the evaluated value is on parentheses.  $K_{10C}$ , affinity parameter ( $K_1$ ) normalized to total organic content.

The Hill equation reasonably described the adsorption of EE2 onto the soil samples used in this study, with correlation coefficients ranging from 0.942, for soil fertilized with compost, to 0.990 for soil fertilized with compost and submitted to LOI. Although in some cases the fitting using Hill equation may not be the most accurate, it is necessary to use the same fitting model to all soil samples in order to compare results and relate them to soils' organic matter characteristics.

As referred by Sarmah et al. (2008), although there have been a great number of studies that follow sorption of steroids hormones, such as EE2, on soils employing batch equilibration techniques, the experimental protocols in those studies differ considerably. This fact becomes a problem when we aim to compare our data with results already published. Freundlich is the commonly chosen model to describe the observed sorption behaviour and usually no saturation is observed with the increase of the concentration. In this study the soil/solution ratio is much lower and the EE2 concentration used is higher than the ones presented by Hildebrand et al. (2006). Therefore, the EE2 amount is higher and the sorbing sites lower than usually are. This can be an experimental difference that might explain the achievement of an adsorption maximum at high concentrations of sorbate, usually not achieved in other experiments.

The obtained S shaped curve indicates that "co-operative adsorption" might occur due to the association between the adsorbed EE2 molecules, which can pack in rows or clusters (Banat et al., 2000; Calace et al., 2002; Giles et al., 1974; Hinz, 2001). However, the obtained curve also shows that a plateau is achieved, indicating that the referred rows or clusters of EE2 molecules might not grow infinitely, reaching an equilibrium. To further investigate these hypotheses the association between two EE2 molecules was investigated by molecular modelling studies. The study of the interaction in gas phase revealed that the association between two EE2 molecules is favourable. The lowest energy co-conformation, presented in Figure 5.8.a, indicates that the molecules tend to be positioned parallel to each other, being stabilized by hydrophobic interactions between the methynic groups and face-to-face  $\pi$ - $\pi$  stacking interactions between the aromatic moieties of the two molecules. Also, the methylic groups tend to be orientated towards the exterior of the dimer. The stability of this association in aqueous solution

showed that the formation of the dimer is favourable (see adopted co-conformations during the simulation in water in Figure 5.8.b and c).

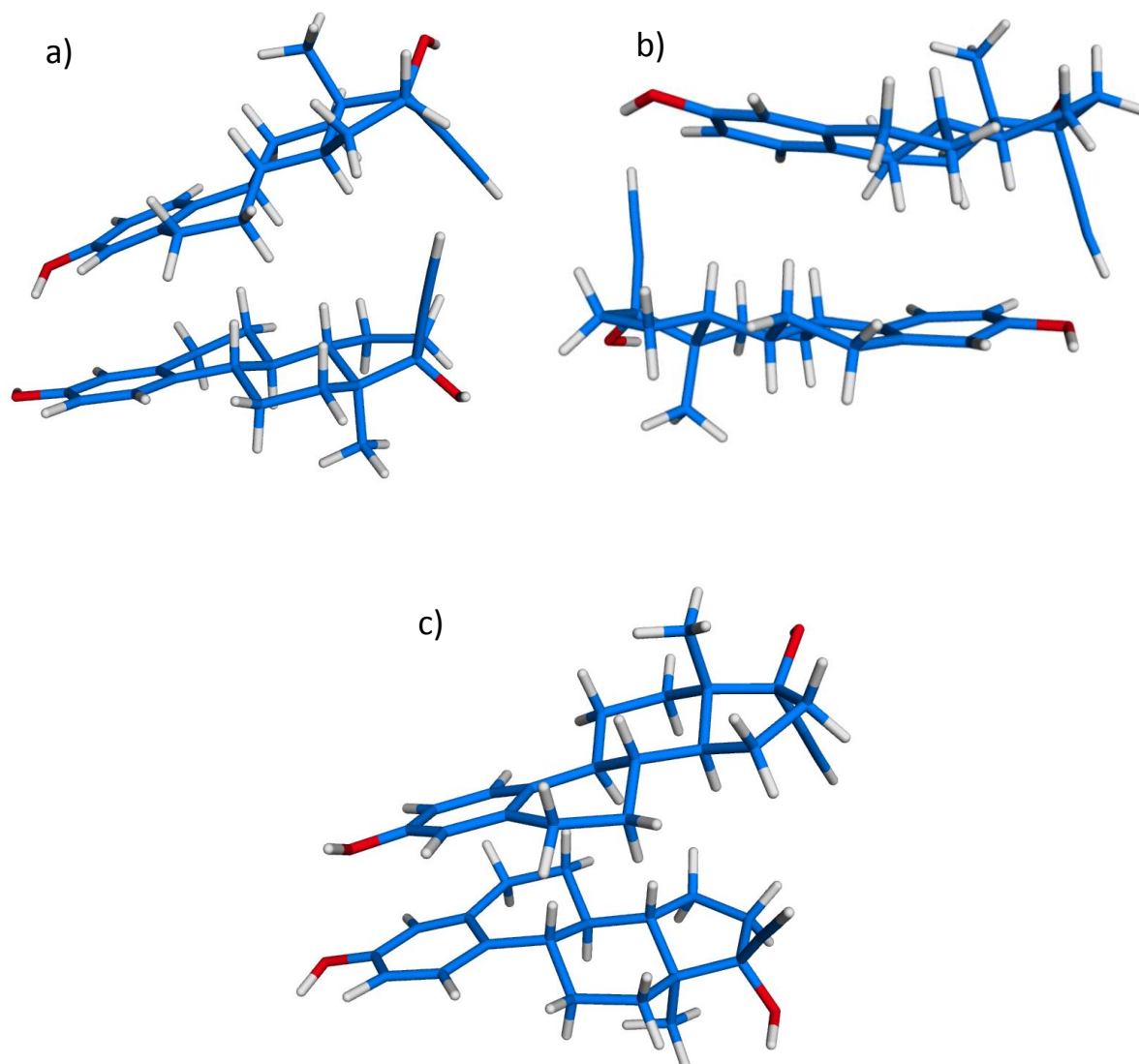


**Figure 5.8.** Association between two EE2 molecules: a) lowest energy co-conformation obtained in gas phase simulation; b) and c) co-conformations adopted during 5 ns of simulation in aqueous solution. Carbon, hydrogen and oxygen atoms are shown in blue, white and red, respectively.

The calculation of the enthalpy of association in aqueous solution shows that the solvation of two associated EE2 molecules (total energy of  $245.99 \text{ kcal mol}^{-1}$ ) in comparison with one solvated EE2 molecule (total energy of  $139.91 \text{ kcal mol}^{-1}$ ) results in

an energetic gain of  $-33.82 \text{ kcal mol}^{-1}$ , corroborating that the dimer naturally occurs. Again, the association is stabilized mainly by hydrophobic interactions that contribute with  $-7.48 \text{ kcal mol}^{-1}$  to the total energetic gain. Overall, the results clearly support the “co-operative adsorption” model, showing that after the adsorption of the first layer of EE2 molecules onto the soil, at least one more layer of EE2 is adsorbed, due to interactions established with the first adsorbed layer. Notwithstanding, taking into account that the association between two EE2 molecules occurs preferably by adopting the co-conformations illustrated in Figure 5.8. (with the methylic groups orientated towards the exterior of the dimer), packing a third row would imply interactions between two EE2 molecules that differ from the ones verified in the lowest energy structure (for instance, the methylic groups orientated towards the interior of the dimer). Thus, these data also explain the achieved plateau in the adsorption curve which indicates that, at a certain point, the amount of EE2 adsorbed does not depend on the increase of the EE2 concentration. In general, molecular modelling data seem to corroborate the EE2 adsorption isotherm results. Nevertheless, it is important to emphasize that, due to the impossibility of simulating the behaviour of EE2 molecules in the water/soil interface (instead of pure water), molecular modelling results should be faced as valuable complementary information and not as unquestionable results.

$Q_{max}$  ( $\text{mg kg}^{-1}$ ) is the maximum adsorption capacity and the soil fertilized with compost was the one that presented the higher value for this parameter. The soil fertilized with compost and submitted to loss on ignition was the one with lower value, while the same soil but not submitted to such procedure was the one presenting the higher value. Such results suggest a relation between the maximum adsorption capacity and soil organic matter content.  $K_1$  is an affinity parameter (sorption isotherm slope) for a given range of EE2 concentration. The higher  $K_1$  value obtained is usually associated to a greater affinity between the sorbate particle and the sorbent. The highest  $K_1$  value, among all soils presented in this study, was obtained for the soil fertilized with compost (1.22), which presents simultaneously the highest organic carbon (2.775%) and nitrogen (0.151%) contents. In contrast, mineral fertilized soil and soil fertilized with compost

submitted to loss on ignition were the ones with the lower values, 0.67 and 0.54, respectively. Soil fertilized with compost submitted to loss on ignition and thus with no organic content presented a low  $K_1$  value, but a sorbent-sorbate interaction still occurs. Such result shows that organic carbon is an important factor on sorption phenomenon, but not a prerequisite. Similar results were presented by Lai et al. (2000).

The correlation coefficient ( $r$ ) between  $K_1$  value and total organic carbon was calculated and is presented on Table 5.5.

**Table 5.5.** Correlation coefficients ( $r$ ) between parameter  $K_1$  or  $K_{1OC}$  and TOC or relative area distribution (percent of total spectrum area) of solid-state  $^{13}\text{C}$  CPMAS-NMR spectra.

	TOC	alkyl	<i>O,N</i> -alkyl	aromatic	carboxyl
Correlation Coefficient ( $r$ )	0.963 <sup>a</sup>	-0.906 <sup>b</sup>	-0.927 <sup>b</sup>	0.956 <sup>b</sup>	0.621 <sup>b</sup>

<sup>a</sup>Correlation coefficient using  $K_1$ . <sup>b</sup>Correlation using  $K_{1OC}$ .

A strong positive correlation between organic carbon content and soil sorption capacity is observed. Several studies refer soil organic content as the major influence property on estrogens sorption behaviour (Caron et al., 2010; Hildebrand et al., 2006). Due to this high correlation observed between total organic carbon content and  $K_1$ , and in order to evaluate the importance of different functional groups on sorption capacity of the soil,  $K_{1OC}$ , affinity parameter normalized to TOC, was determined. Previous works (Lima et al., 2010; Singh et al., 2010) tried to correlate different functional groups with  $K_{1OC}$  values obtained for sorption batch experiences using different soil samples. Since a strong positive correlation was observed between  $K_1$  and total organic carbon content, this fact could disguise the real influence of organic matter characteristics in sorption behaviour. The normalized  $K_{1OC}$  depends only on the soil specific organic matter characteristics, which can differ greatly in sorption capacity, due to differences promoted by diverse organic fertilizations. Hence, alkyl, *O,N*-alkyl, aromatic and carboxyl contents were correlated with  $K_{1OC}$  (Table 5.5.).



A strong positive correlation can be observed between aromatic units and  $K_{10C}$  values. Soil fertilized with farmyard manure presented higher relative area in the region usually attributed to aromatic moieties, probably due to lignin and lignin-like products, derived from cereal straws applied to soil in this organic fertilization (chapter 4). The more prevalent the aromatic content is, when compared to the hydrophilic (mostly polysaccharide), the greater the hydrophobicity of the organic matter. These results can indicate the hydrophobic interactions as a key role in the binding of EE2 onto soils organic matter (Yu et al., 2004; Lee et al., 2003). This positive correlation observed for aromatic units confirms the idea of a favoured association by the EE2 aromatic nuclei face to face with the surface and/or another EE2 molecule previously discussed in molecular modelling studies.

A positive correlation, although not very high, can be observed between carboxyl units and  $K_{10C}$  values.  $^{13}C$  NMR spectroscopy of soil supplied with farmyard manure and sewage sludge showed higher relative area in the region usually attributed to carboxyl, amide and ester functionalities. Specific sorbent-sorbate interactions due to hydrogen or covalent bonding are likely to occur due to the presence of phenolic function at C-3 and hydroxyl function at C-17 of the EE2 molecules that can react with carboxylic functional groups of soil organic matter.

A negative correlation was observed between  $K_{10C}$  values and alkyl and *O,N*-alkyl units. The soil fertilized with compost presented lower carboxyl and aromatic units, while mineral fertilized soil presented low carboxyl units. It is important to highlight the low organic carbon content of mineral fertilized soil and the high noise observed in its  $^{13}C$  NMR spectra, especially between 110-160 ppm (aromatic region), that could explain the high unexpected aromatic content observed (Lima et al., 2009). The lower carboxyl units observed for both soils and the aromatic content observed for soil fertilized with compost decrease the possibility of hydrogen bonding and hydrophobic interactions and thus, explain the low  $K_{10C}$ .

Results suggest that the fate of EE2 introduced into the environment depends not only on soil organic matter content, but also on its characteristics, since the bonding mechanisms depends greatly on the units of soil organic matter available for binding. Differences observed on soil samples used in this study are due to different organic fertilizations, applied on a long-term field experiment established almost 50 years ago. This causes changes on soils' organic matter functional groups and consequently on sorption behaviour of EE2 and its fate on the environment. Thus, agricultural crops can be used to minimize the residual toxicity of EE2. Farmyard manure or an organic fertilization that introduces aromatic and/or carboxyl units can combine its action as a detoxifying agent and as an organic fertilizer. It is also important to remind that a compromise has to be reached between the content and nature of the organic matter applied to the soil.

## 5.4. Conclusion

---

The toxicity of atrazine applied to agricultural crops will depend, not only on the content of organic carbon in the soil, but on its nature as well, since the bonding mechanism and its intensity depend greatly on the units of organic matter available for binding. The results of atrazine binding to organic matter pointed out that, carboxyl- and aromatics-rich organic matter are the most efficient binding agents for atrazine. The increase of aromatics-rich organic matter causes an increase in its hydrophobicity, thus increasing the hydrophobic interactions between atrazine and organic matter. The stronger interactions responsible for atrazine adsorption to organic matter are the hydrogen bonds due to the carboxyl units. Furthermore, the higher predominance of hydrogen bonds in adsorption of atrazine on soils will result in a decrease on desorption, since these are stronger binding forces than hydrophobic interactions, and thus reduce the leaching of atrazine into drinking water resources and reduce run-off to rivers and other surface waters.

It can also be concluded that EE2 strongly adsorb to soil organic matter and that sorption greatly depends on the total organic carbon present in soil, but is not a prerequisite, since adsorption still occurred on soil submitted to loss on ignition. Also EE2 molecules tend to be positioned parallel to each other, being stabilized by hydrophobic interactions between the methynic groups and face-to-face  $\pi$ - $\pi$  stacking interactions between the aromatic moieties, being stabilized mainly by hydrophobic interactions. Such interactions are the dominant mechanism of EE2 sorption onto soil organic matter. The positive correlation observed between aromatic units and  $K_{10C}$  values confirms the idea of a favoured association by the EE2 aromatic nuclei face to face with the surface and/or another EE2 molecule. Also a positive correlation can be observed between carboxyl units and  $K_{10C}$  values and specific sorbent-sorbate interactions due to hydrogen or covalent bonding are likely to occur due to the presence of phenolic function at C-3 and hydroxyl function at C-17 of the EE2 molecules that can react with carboxylic functional groups of soil organic matter.

Farmyard manure can be effectively used to minimize the residual toxicity of atrazine-treated or EE2 polluted agricultural fields. The advantage of this type of

traditional fertilization is its combined action as detoxifying agents and organic fertilizer. The same application rate of atrazine to the soil is expected to result in a lower environmental impact on the soil with farmyard manure, containing higher aromatic and carboxyl units, than in other soils with predominantly aliphatic structures. It is important to highlight that a compromise has to be reached between the content and nature of the organic matter applied to the soil.

## 5.5. References

---

- Banat, F.A., Al-Bashir, B., Al-Asheh, S., Hayajneh, O., **2000**. Adsorption of phenol by bentonite. *Environ. Pollut.* 107, 391-398.
- Boivin, A., Cherrier, R., Schiavon, M., **2005**. A comparison of five pesticides adsorption and desorption processes in thirteen contrasting field soils. *Chemosphere* 61, 668-676.
- Calace, N., Nardi, E., Petronio, B.M., Pietroletti, M., **2002**. Adsorption of phenols by papermill sludges. *Environ. Pollut.* 118, 315-319.
- Caron, A., Farenhorst, A., Zvomuya, F., Gaultier, J., Rank, N., Goddard, T., Sheedy, C., **2010**. Sorption of four estrogens by surface soils from 41 cultivated fields in Alberta, Canada. *Geoderma* 155, 19-30.
- Celano, G., Šmejkalová, D., Spaccini, R., Piccolo, A., **2008**. Interactions of three s-triazines with humic acids of different structure. *J. Agr. Food Chem.* 57, 7360-7366.
- Chefetz, B., Bilkis, Y.I., Polubesova, T., **2004**. Sorption-desorption behaviour of atrazine and phenylurea herbicides in Kishon river sediments. *Water Res.* 38, 4383-4394.
- Correia, F.V., Macrae, A., Guilherme, L.R.G., Langenbach, T., **2007**. Atrazine sorption and fate in a Ultisol from humid tropical Brazil. *Chemosphere* 67, 847-854.
- DeLano, W.L., **2002**. The PyMOL Molecular Graphics System DeLano Scientific, San Carlos, <http://www.pymol.org>.
- Drori, Y., Aizenshtat, Z., Chefetz, B., **2005**. Sorption-desorption behaviour of atrazine in soils irrigated with reclaimed wastewater. *Soil Sci. Soc. Am. J.* 69, 1703-1710.
- Emmerik, T.V., Angove, M.J., Johnson, B.B., Wells, J.D., Fernandes, M.B., **2003**. Sorption of 17 $\beta$ -estradiol onto selected soil minerals. *J. Colloid Interf. Sci.* 266, 33-39.
- Fruhstorfer, P., Schneider, R., Weil, L., Niessner, R., **1993**. Factors influencing the adsorption of atrazine on montmorillonitic and kaolinitic clays. *Sci. Total Environ.* 138, 317-328.
- Gao, J.P., Maguhn, J., Spitzauer, P., Kettrup, A., **1998**. Sorption of pesticides in the sediment of the Teufelsweiher pond (southern Germany) II: Competitive adsorption, desorption of aged residues and effect of dissolved organic carbon. *Water Res.* 32, 2089-2094.
- Giles, C.H., Smith, D., Huitson, A., **1974**. A general treatment and classification of the solute adsorption isotherm. I: Theoretical. *J. Colloid Interf. Sci.* 47, 755-765.
- Hess, B., Bekker, H., Berendsen, H.J.C., Fraaije, J.G.E.M., **1997**. LINC: A linear constraint solver for molecular simulations. *J. Comput. Chem.* 18, 1463-1472.

- Hess, B., Kutzner, C., van der Spoel, D., Lindahl, E., **2008**. GROMACS 4: Algorithms for highly efficient, load-balanced, and scalable molecular simulation. *J. Chem. Theory Comput.* 4, 435-447.
- Hildebrand, C., Londry, K.L., Farenhorst, A., **2006**. Sorption and desorption of three endocrine disruptors in soils. *J. Environ. Sci. Heal. B* 41, 907-921.
- Hinz, C., **2001**. Description of sorption data with isotherm equations. *Geoderma* 99, 225-243.
- Jakalian, A., Bush, B.L., Jack, D.B., Bayly, C.I., **2000**. Fast, efficient generation of high-quality atomic charges. AM1-BCC model: I. Method. *J. Comput. Chem.* 21, 132-146.
- Jakalian, A., Jack, D.B., Bayly, C.I., **2002**. Fast, efficient generation of high-quality atomic charges. AM1-BCC model: II. Parameterization and Validation. *J. Comput. Chem.* 23, 1623-1641.
- Jorgensen, W.L., Chandrasekhar, J., Madura, J.D., **1983**. Comparison of simple potential functions for simulating liquid water. *J. Chem. Phys.* 79, 926-935.
- Kah, M., Brown, C.D., **2007**. Changes in pesticide adsorption with time at high soil to solution ratios. *Chemosphere* 68, 1335-1343.
- Kovaios, I.D., Parakeva, C.A., Koutsoukos, P.G., Payatakes, A.C., **2006**. Adsorption of atrazine on soils: Model study. *J. Colloid Interf. Sci.* 299, 88-94.
- Kulikova, N.A., Perminova, I.V., **2002**. Binding of atrazine to humic substances from soil, peat, and coal related to their structure. *Environ. Sci. Technol.* 36, 3720-3724.
- Lai, K.M., Johnson, K.L., Scrimshaw, M.D., Lester, J.N., **2000**. Binding of waterborne steroid estrogens to solid phases in river and estuarine systems. *Environ. Sci. Technol.* 34, 3890-3894.
- Lee, L.S., Strock, T.J., Sarmah, A.K., Rao, P.S.C., **2003**. Sorption and dissipation of testosterone, estrogens, and their primary transformation products in soils and sediment. *Environ. Sci. Technol.* 37, 4098-4105.
- Lesan, H.M., Bhandari, A., **2003**. Atrazine sorption on surface soils: time-dependent phase distribution and apparent desorption hysteresis. *Water Res.* 37, 1644-1654.
- Lima, D.L.D., Santos, S.M., Scherer, H.W., Schneider, R.J., Duarte, A.C., Santos, E.B.H., Esteves, V.I., **2009**. Effects of organic and inorganic amendments on soil organic matter properties. *Geoderma* 150, 38-45.
- Lima, D.L.D., Schneider, R.J., Scherer, H.W., Duarte, A.C., Santos, E.B.H., Esteves, V.I., **2010**. Sorption-desorption behavior of atrazine on soils subjected to different organic long-term amendments. *J. Agric. Food Chem.* 58, 3101-3106.
- Loganathan, V.A., Feng, Y., Sheng, G.D., Clement, T.P., **2009**. Crop-residue-derived char influences sorption, desorption and bioavailability of atrazine in soils. *Soil Biol. Biochem.* 73, 967-974.

- Mersie, W., Seybold, C., **1996**. Adsorption and desorption of atrazine, deethylatrazine, deisopropylatrazine, and hydroxyatrazine on levy wetland soil. *J. Agr. Food Chem.* 44, 1925-1929.
- Nemeth-Konda, L., Füleky, G., Morovjan, G., Csokan, P., **2002**. Sorption behaviour of acetochlor, atrazine, carbendazim, diazinon, imidacloprid and isoproturon on Hungarian agricultural soil. *Chemosphere* 48, 545-552.
- OECD. Guideline TG 106, **2000**. OECD Guideline for the Testing of Chemicals. Adsorption – Desorption using a Batch Equilibrium Method. *Organization for Economic Co-operation and Development* (OECD), Paris.
- Prata, F., Lavorenti, A., Vanderborght, J., Burauel, P., Vereecken, H., **2003**. Miscible displacement, sorption and desorption of atrazine in a Brazilian oxisol. *Vadose Zone J.* 2, 728-738.
- Sarmah, A.K., Northcott, G.L., Scherr, F.F., **2008**. Retention of estrogenic steroid hormones by selected New Zealand soils. *Environ. Int.* 34, 749-755.
- Singh, N., Berns, A.E., Hennecke, D., Hoerner, J., Koedel, W., Schaeffer, A., **2010**. Effect of soil organic matter chemistry on sorption of trinitrotoluene and 2,4-dinitrotoluene. *J. Hazard. Mater.* 173, 343-348.
- Spark, K.M., Swift, R.S., **2002**. Effect of soil composition and dissolved organic matter on pesticide sorption. *Sci. Total Environ.* 298, 147-161.
- Stumpe, B., Marschner, B., **2007**. Long-term sewage sludge application and wastewater irrigation on the mineralization and sorption of 17 $\beta$ -estradiol and testosterone in soils. *Sci. Total Environ.* 374, 282-291.
- Stumpe, B., Marschner, B., **2009**. Factors controlling the biodegradation of 17 $\alpha$ -estradiol, estrone and 17 $\alpha$ -ethinylestradiol in different natural soils. *Chemosphere* 74, 556-562.
- Stumpe, B., Marschner, B., **2010**. Dissolved organic carbon from sewage sludge and manure can affect estrogen sorption and mineralization in soils. *Environ. Pollut.* 158, 148-154.
- van der Spoel, D., Lindahl, E., Hess, B., Groenhof, G., Mark, A.E., Berendsen, H.J.C., **2005**. GROMACS: Fast, flexible and free. *J. Comput. Chem.* 26, 1701-1718.
- van der Spoel, D., Lindahl, E., Hess, B., van Buuren, A.R., Apol, E., Meulenhoff, P.J., Tieleman, D.P., Sijbers, A.L.T.M., Feenstra, K.A., van Drunen, R., Berendsen, H.J.C., **2010**. Gromacs User Manual version 4.5, [www.gromacs.org](http://www.gromacs.org).
- Wang, J., Wolf, R.M., Caldwell, J.W., Kollman, P.A., Case, D.A., **2004**. Development and testing of a general amber force field. *J. Comput. Chem.* 25, 1157-1174.

Yang, W., Zhang, J., Zhang, C., Zhu, L., Chen, W., **2009**. Sorption and resistant desorption of atrazine in typical Chinese Soils. *J. Environ. Qual.* 38, 171-179.

Ying, G.-G., Kookana, R.S., Ru, Y.-J., **2002**. Occurrence and fate of hormone steroids in the environment. *Environ. Int.* 28, 545-551.

Yu, Z., Xiao, B., Huang, W., Peng, P., **2004**. Sorption of steroid estrogens to soils and sediments. *Environ. Toxicol. Chem.* 23, 531-539.



# CHAPTER 6

**DETERMINATION OF HOP IN WATER SAMPLES  
USING ELISA**

**CHAPTER 6****DETERMINATION OF HOP IN WATER SAMPLES USING ELISA**

6.1. Introduction .....	149
6.2. Experimental procedure .....	152
6.2.1. Water samples.....	152
6.2.2. Reagents and materials .....	155
6.2.3. ELISA procedure .....	156
6.2.4. Matrix effects .....	157
6.3. Results and discussion .....	157
6.3.1. Atrazine determination .....	157
6.3.1.1. Evaluation of matrix effects .....	157
6.3.1.2. Quantification of atrazine in ground, surface and wastewaters .....	165
6.3.2. EE2 determination.....	166
6.3.2.1. Optimization of antibody and tracer dilutions .....	166
6.3.2.2. Evaluation of assay performance.....	167
6.3.2.3. Cross-reactivity .....	169
6.3.2.4. Evaluation of matrix effects .....	170
6.3.2.5. Quantification of EE2 in ground, surface and wastewaters .....	176
6.4. Conclusions .....	178
6.5. References .....	179

## 6.1. Introduction

---

Hydrophobic organic pollutants, which include a long list of pesticides and pharmaceuticals, are introduced into the aquatic system through different pathways. Monitoring studies can provide important information on the occurrence and distribution of a great number of anthropogenic compounds in ground waters, lakes, rivers, estuaries, oceans and in waste waters. Sewage treatment plants effluents can contribute to the increase of pollutants in either surface or ground waters. Many pollutants are not significantly eliminated in STPs and thus are discharged into receiving waters (Gerecke et al., 2002).

Sewage treatment is an important public service in what concerns the safety of water resources and global environment. It includes physical, chemical, and biological processes to remove physical, chemical and biological contaminants. Its objective is to produce an environmentally safe fluid waste stream (or treated effluent) and a solid waste (or treated sludge) suitable for disposal or reuse (usually as farm fertilizer). Domestic and industrial effluents from Aveiro are collected in 10 different locations and are treated in two main sewage treatment plants (North and South of Aveiro) being discharged into the Atlantic Ocean, at a distance of 3.2 km from the coast, at approximately 17 m depth (SimRia, 2011). North STP is localized in Cacia, Aveiro and was projected to satisfy the effluent treatment needs of Águeda, Aveiro (part of), Albergaria-a-Velha, Estarreja, Murtosa, Oliveira do Bairro and Ovar. It is dimensioned to serve a population of 272 000 inhabitants and an average daily flow of 48 705 m<sup>3</sup> and performs the treatment of domestic and industrial effluents. South STP is localized in Gafanha da Encarnação, Ílhavo, and was projected to satisfy the effluent treatment needs of Aveiro (part of), Ílhavo, Mira and Vagos. It is dimensioned to serve a population of 159 700 inhabitants and an average daily flow of 39 278 m<sup>3</sup> and performs the treatment of domestic effluents only (SimRia, 2011). In these STPs there are four main stages: pre-treatment and primary decantation, which correspond to primary treatment, and biological treatment and secondary decantation, corresponding to secondary treatment (Figure 6.1.). Pre-treatment includes: screening (removal of large objects using bar screens or mesh screens of varying sizes); grit removal (a sand or grit channel or chamber where the velocity of the incoming

wastewater is adjusted to allow the settlement of sand, grit, stones, and broken glass); and a fat and grease removal (small tank where skimmers collect the fat floating on the surface). This primary treatment is important due to removal of materials that can damage pumps and other equipments of treatment plants and also fat and grease that has an adverse effect on secondary treatment.



**Figure 6.1.** Aerial photograph of North STP (adapted from SimRia, 2011); 1– Pre-treatment building; 2– Primary sedimentation; 3– Biological treatment; 4– Secondary sedimentation 5– Sludge thickening; 6– Primary digestion; 7– Sludge treatment building; 8 – Secondary digestion and gasometer; 9– Sludge silo; 10– Transformation point and workshop; 11– Offices.

In the primary sedimentation stage, residual waters, filtrated previously, undergo a physico-chemical decantation process, where suspended solid particles are separated from the sewage water. Biological treatment (Figure 6.2.A) occurs in reactors using aerobic biological processes. To be effective, the biota requires both oxygen and food to live, thus it consumes biodegradable soluble organic contaminants. Aerated basin systems are used to provide the needed oxygen to maintain aerobic microorganisms alive.

Biological treatment is followed by secondary sedimentation using several tanks, where suspended biological flocculate is settled and separated from the sewage water (Figure 6.2.B). The water obtained from the secondary sedimentation contains low levels of organic material and suspended matter and can be reused for washing or irrigation purposes. Accumulated sludge during the treatment process is subjected to an anaerobic

digestion, where fermentation occurs at 37°C and the biogas produced is used in generators for electricity production. Sludge is then thickened (dewatered) to reduce the volume and transported for agricultural usage. It is important to refer that, although the spread of sewage sludge on agricultural fields for fertilization purposes has been actively promoted as an economic way of recycling, sludge may contain toxic substances, which could be incorporated into agricultural products or contaminate ground waters (Ghanem et al., 2008).

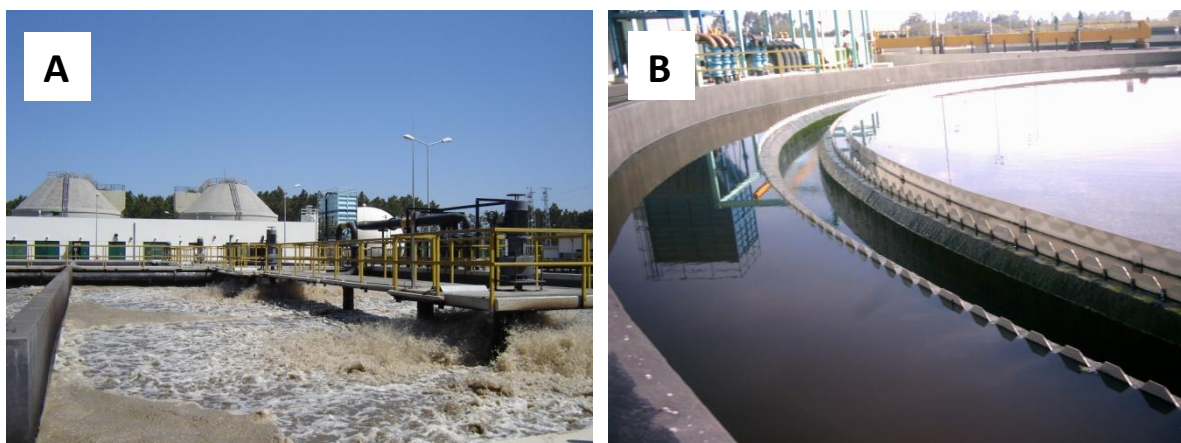


**Figure 6.2.** Photograph of North STP where A) biological treatment and B) secondary sedimentation occurs.

It is very important to control waste water pollutants, in order to improve the removal of such pollutants during the treatment. Also, a control in effluents that are discharged into surface waters should be performed. Moreover, effluents control can allow the evaluation of this source in surface water contamination. The purpose of this work is the development and application of an ELISA procedure to determine hydrophobic organic pollutants (atrazine and 17 $\alpha$ -ethinylestradiol) in ground, surface and also waste waters.

## 6.2. Experimental procedure

---

### 6.2.1. Water samples

Ria de Aveiro (Figure 6.3.) is a shallow lagoon (average depth of 1 m) situated in the Northwest Atlantic coast of Portugal (40°38'N, 8°45'W) with 45 km length and 10 km width (Figure 6.3.). The lagoon receives freshwater from two main rivers, the Antuã river with average flow of  $5 \text{ m}^3 \text{ s}^{-1}$  and the Vouga river with  $50 \text{ m}^3/\text{s}$ . Boco river, at the southern end of Ílhavo channel, and the Caster and Gonde rivers at the north end of São Jacinto channel, with average flow less than  $1 \text{ m}^3 \text{ s}^{-1}$ , are other small contributors of freshwater to the lagoon (Dias and Lopes, 2006a; Lopes et al., 2005).

The lagoon covers an area of  $83 \text{ km}^2$  at high tide and only  $66 \text{ km}^2$  at low tide. The hydrodynamic pattern of the lagoon is imposed by the tide and rivers have small contributions in terms of freshwater inputs, although they may have a long-term influence on the residues transport. Besides the mentioned rivers, Ria de Aveiro has a number of channels and among them are two more important, the São Jacinto and Espinheiro channels. These channels are directly connected to the lagoon mouth and have strong currents that reach values of about  $2 \text{ m s}^{-1}$  near the mouth, during spring tides and flooding periods. Studies show that tides are strongly deformed in their propagation from the mouth to the far end of each channel of the Ria de Aveiro, due to its geometry and bathymetry. Ria de Aveiro has witnessed growing anthropogenic activities near its margins, namely building and land occupation, agricultural and industrial activities, which result in a significant change of the lagoon morphology, in a constant input of anthropogenic nutrients and contaminants. Along with these changes a negative impact on the water circulation is observed, as well as on the water quality of the lagoon. The main anthropogenic sources of pollution are domestic and industrial discharge flows (Dias and Lopes, 2006a; Lopes et al., 2005).

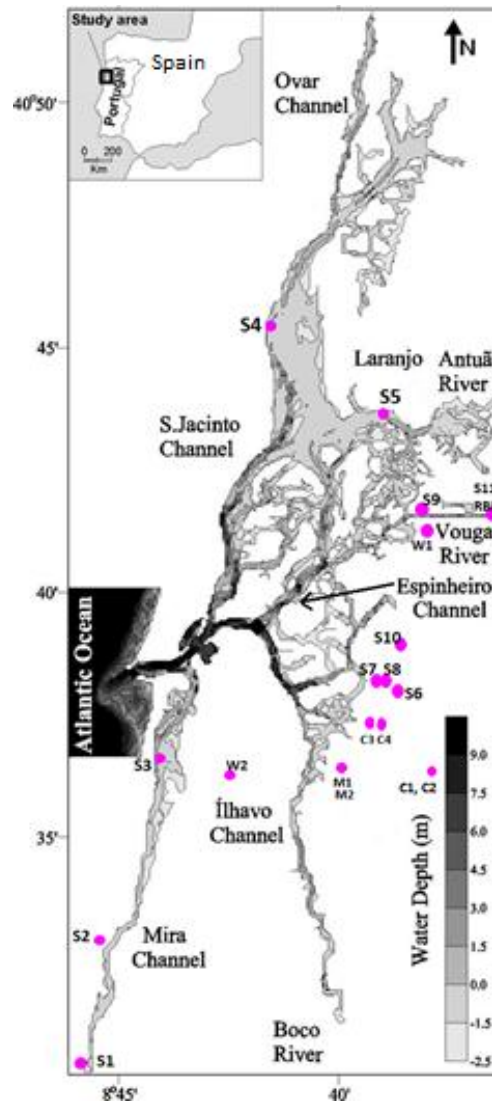


**Figure 6.3.** Map and the bathymetry of the Ria de Aveiro lagoon. Sampling sites: S1 Barrinha de Mira; S2 Poço da Cruz; S3 Costa Nova; S4 Torreira; S5 Cais do Bico; S6 Cais da Fonte Nova; S7 Rossio Channel; S8 S. Roque Channel; S9 Rio Novo Príncipe; S10 Mataduços; S11 Vouga River; M1 and M2: mines; C1-C4: water collecting wells; RBF: water from riverine bank filtration system in Vouga river; W1: North STP; W2: South STP (Image adapted from Dias and Lopes, 2006b).

Water samples included 7 groundwater locations currently used for Aveiro water supply (4 water collecting wells, 2 mines and 1 riverine bank filtration system on Vouga river). Pictures of different sampling sites are shown in Figure 6.4.



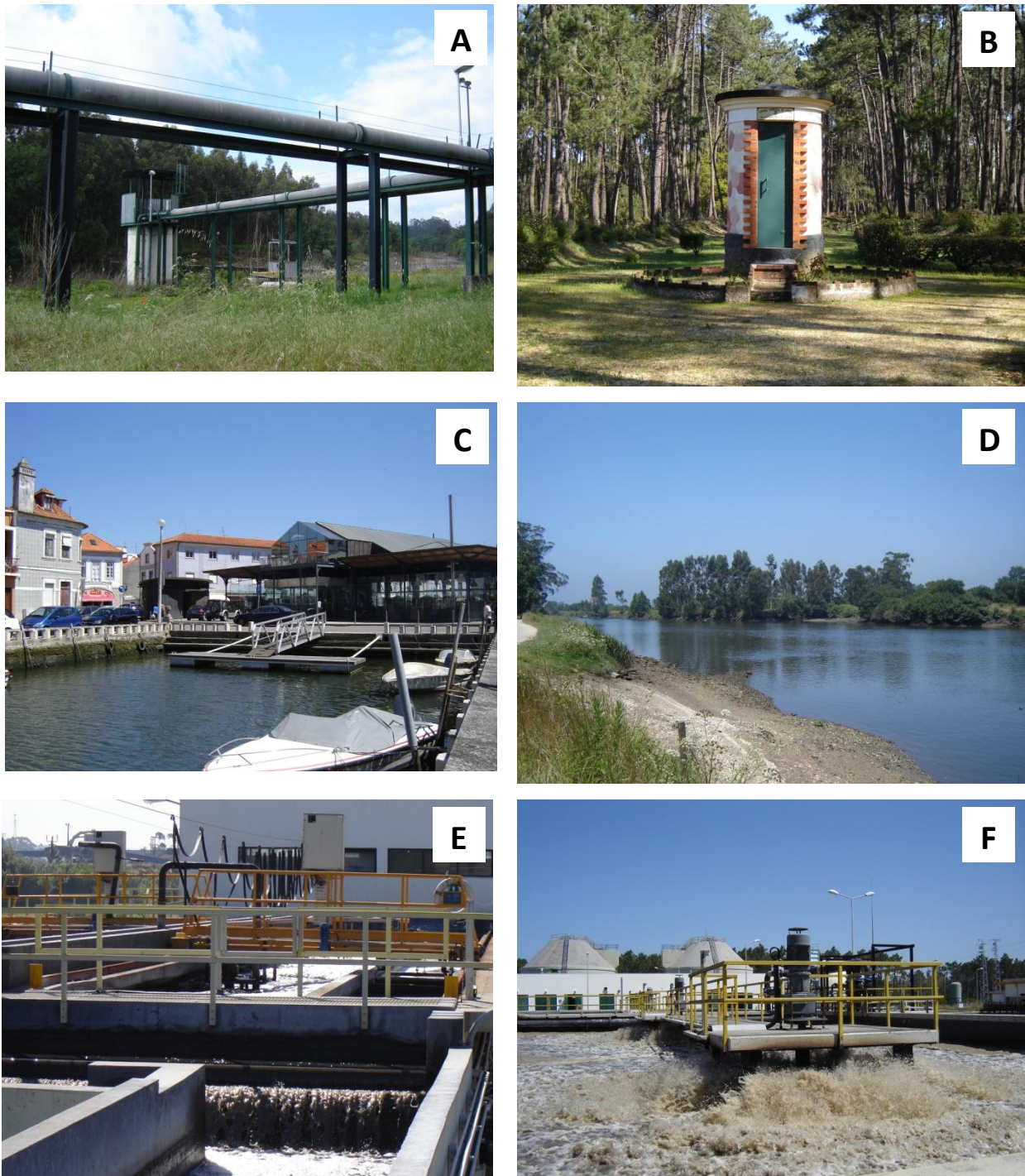


**Figure 6.4.** Pictures of sampling sites. A: RBF - water from riverine bank filtration system on Vouga river; B: mine; C: Rossio Channel; D: Rio Novo Príncipe; E: North STP after primary treatment; F: North STP after secondary treatment.

It must be highlighted that groundwaters and the Regional System of Carvoeiro supply the drinking water to the municipal system. Groundwater is applied in the drinking



water public supply through the exploitation of the aquifer Cretaceous system that exists in the area. Groundwater in this region is characterized by cation exchange processes, between calcium and sodium ions, as it approaches the coast (Melo et al., 1998). The regional system of Carvoeiro is a project constituted by water collection, treatment, transport and storage facilities, from its origin (in alluvial zones of Vouga river, near Carvoeiro village) to the associated partners (Águeda, Albergaria-a-Velha, Aveiro, Estarreja, Ilhavo e Murtosa) (AMC-V, 2011).

Also 11 surface water samples were collected from different locations of Ria de Aveiro pointed out in Figure 6.3. Both samples from Barrinha de Mira and Poço da Cruz belong to the Mira channel; the Torreira sample belongs to the S. Jacinto channel; Cais do Bico belongs to Laranjo's Bay; Cais da Fonte Nova, S. Roque and Rossio channel are located in the urban city center of Aveiro; Rio Novo Príncipe and Mataduços are located in the rural and agricultural area of Aveiro city. Another surface water sample was collected from the Vouga river.

Samples from two sewage treatment plants (North and south area of Aveiro city) were collected. Three sampling sites in the STPs were chosen: after primary treatment (decantation), after secondary biological treatment and after secondary decantation (final effluent).

All samples were collected in glass bottles, previously washed and, immediately after, they were filtered through 0.45  $\mu\text{m}$  nitrocellulose membrane filters (Millipore) and stored at 4°C until analysis.

### *6.2.2. Reagents and materials*

All reagents and buffers used were described in section 3.2.2.1. Besides buffers described previously, sample buffer with 1 mol L<sup>-1</sup> tris(hydroxymethyl)aminomethane (TRIS, p.a., from Sigma), 1.5 mol L<sup>-1</sup> sodium chloride (99.5%) (from Panreac), 107 mmol L<sup>-1</sup> ethylenediaminetetraacetic acid disodium salt dihydrate (p.a. from Panreac) and 1% bovine serum albumin (for electrophoresis, 98%, from Sigma) was used and adjusted to pH 7.60 with hydrochloric acid 37%. A stock commercial humic acid (HA) (technical, from

Sigma) solution of  $1 \text{ g L}^{-1}$  at pH 9 (using  $1 \text{ mol L}^{-1}$  ammonium hydroxide) was also prepared. Ultra-pure water, used in the preparation of all the solutions, was obtained using a Millipore water purification system (Milli-Q plus 185).

Atrazine quantification was made using the polyclonal antibody C193 and tracer t-Bu/Cl/C6, previously described in chapter 3. EE2 quantification was made using a polyclonal antibody and a tracer synthesized as described by Schneider et al. (2004) that were kindly provided by the BAM Federal Institute for Materials Research and Testing, Berlin.

### 6.2.3. ELISA procedure

A direct competitive ELISA was adapted for the analysis of atrazine or EE2 using microtiter plates coated with polyclonal antibody serum diluted 1:10000 (for atrazine) or 1:50000 (for EE2) in coating buffer using  $200 \mu\text{L}$  per well. Plates were covered with Parafilm™ to prevent evaporation. After overnight incubation at  $20^\circ\text{C}$  in the plate shaker at 750 rpm, the plates were washed three times with wash buffer concentrate diluted 60 times. After the three washing cycles standards/samples were added to the plate ( $100 \mu\text{L}$  per well) and the plate shaken at room temperature for 30 min. This was followed by addition of the respective enzyme conjugate in PBS (diluted 1:10000 for atrazine or 1:75000 for EE2,  $100 \mu\text{L}$  per well); the plate was shaken at room temperature for 30 min, followed by a second three-cycle washing step. Finally, the substrate solution was added ( $200 \mu\text{L}$  per well) and incubated for 30 min. The enzyme reaction was stopped by addition of sulphuric acid  $1 \text{ mol L}^{-1}$  ( $100 \mu\text{L}$  per well).

For the construction of calibration curves an analyte stock solution was prepared in methanol and then further diluted with ultra-pure water to obtain standard solutions with concentrations ranging from  $0.0001$  to  $1000 \mu\text{g L}^{-1}$ .

Absorbance was read at 450 nm and referenced to 620 nm. All determinations were at least made in triplicate. The mean values were fitted to a 4PL equation previously described (Dudley et al., 1985).

#### 6.2.4. Matrix effects

When determining the concentration of a given pollutant (atrazine or EE2) in a sample, matrix effects should be evaluated. Since surface water samples from Ria de Aveiro present high salinity levels, the influence of salinity was evaluated using sodium chloride with concentrations up to 30 g L<sup>-1</sup>. Also, wastewater samples were collected in order to quantify atrazine and EE2. Such samples present high levels of organic matter that are known to interfere in ELISA measurements. The influence of organic matter was evaluated using HA with concentrations up to 20 mg L<sup>-1</sup>. Calibration curves between 0.0001 and 1000 µg L<sup>-1</sup> were obtained containing 1, 10 and 20 mg L<sup>-1</sup> of HA. Also standards were spiked with different quantities of HA (0.5, 1, 2.5, 5, 10 and 20 mg L<sup>-1</sup>) and recovery rates were calculated. Similar recovery tests were performed in order to evaluate the influence of salinity, using different volumes of NaCl in order to obtain concentrations of 10, 20 and 30 g L<sup>-1</sup>. Organic matter and salinity tests were performed with and without the presence of sample buffer (described in section 6.2.2.). After selecting the optimal conditions of the assays, recovery tests were also carried out using real samples. Water samples were spiked with 0.01, 0.05 and 0.1 µg L<sup>-1</sup> of atrazine and 0.5, 1.0 and 1.5 µg L<sup>-1</sup> of EE2.

### 6.3. Results and discussion

---

#### 6.3.1. Atrazine determination

##### 6.3.1.1. Evaluation of matrix effects

The ELISA procedure for atrazine was already optimized to follow its sorption behaviour in Chapter 3. In order to determine atrazine in water samples there is a need to evaluate the matrix effects (salinity and organic matter). To follow sorption, prior to quantification, a dilution step was performed and no critical interference was observed thereafter. In this case and since the quantity of atrazine expected is so low and near the

quantification limit, no dilution could be performed to solve matrix effects. Thus, it was necessary to evaluate them and if necessary try to reduce them.

Four calibration curves were obtained, one in the absence of organic matter and another three with different concentrations of HA (Figure 6.5.). HA were used as model substances for the determination of matrix effects. The interference with HA lead to flattened calibration curves and the sigmoidal shapes tended to be lost with the increase of HA.

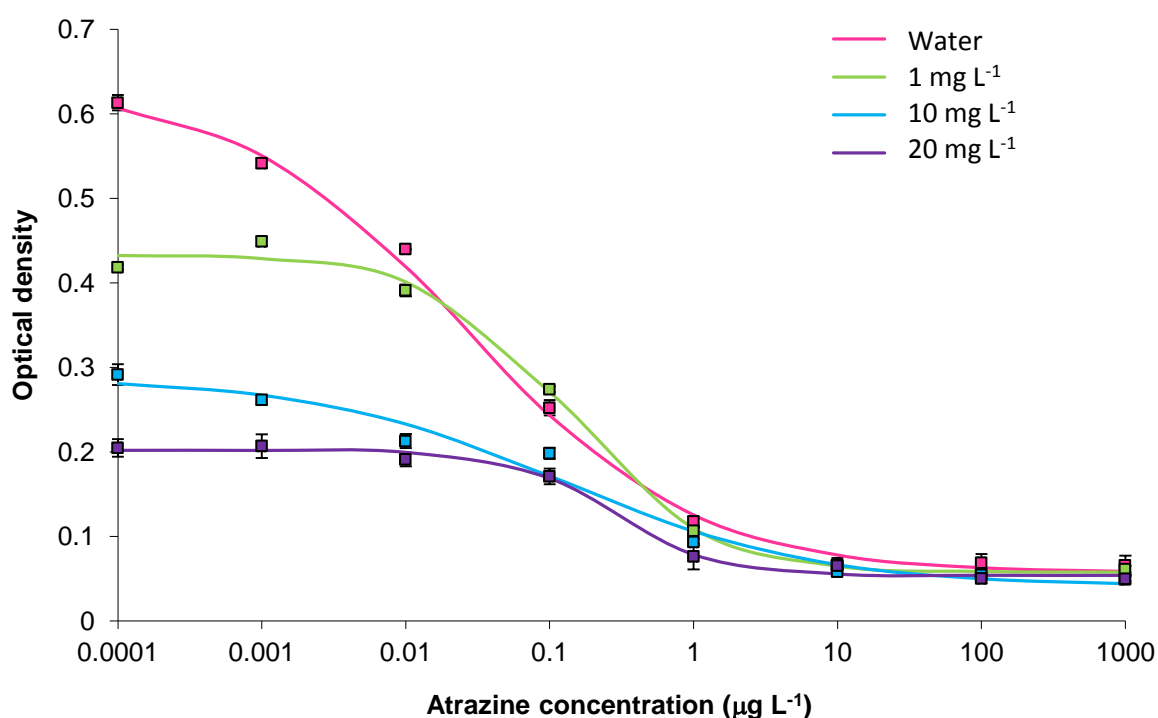


**Figure 6.5.** Evaluation of the organic matter effects on the ELISA calibration curves without sample buffer. Calibration curves obtained in the absence of organic matter and in the presence of 1, 10 and 20 mg L<sup>-1</sup> of HA.

Also, curves were slightly shifted to higher concentrations (increase of turning point values, presented in Table 6.1.) resulting in a loss of sensitivity. The intrinsic mechanism of this interference is unknown but maybe due to unspecific binding of HA to antibody, or due to tracer binding to HA, resulting in a decrease of optical density. This decrease in

optical density would result in an overestimation of atrazine in dependence of the HA concentration.

**Table 6.1.** Parameter values obtained for the four-parametric logistic equation (4PL) using atrazine standards prepared with and without HA.

Standard composition	A	B	C	D
Water	0.633	0.549	0.026	0.057
1 mg L <sup>-1</sup> HA	0.433	0.914	0.135	0.058
10 mg L <sup>-1</sup> HA	0.288	0.495	0.125	0.041
20 mg L <sup>-1</sup> HA	0.202	1.240	0.272	0.054

A = signal at zero dose, D = signal at excess dose, C = x-coordinate (concentration) of the turning point of the sigmoidal curve and B = slope parameter.

In order to solve these interferences a sample buffer was tested (composition described in section 6.2.2.). The sample buffer was added prior to the addition of the analyte. Moreover, the high concentration of salt had the purpose of masquerade the salt effect present in the sample, while BSA has a propensity to bind to organic matter, decreasing its effects on atrazine quantification. Using sample buffer, four calibration curves were obtained, as reported previously. The assay presented on Figure 6.6. exhibits a robust behaviour in the presence of HA. The sigmoidal shape of calibration curves is maintained even at high concentration of HA as 20 mg L<sup>-1</sup>. A slight decrease in the optical density at low atrazine concentrations with the increase of HA concentration was observed. This effect seems to be only critical at atrazine concentration below 0.01 µg L<sup>-1</sup>. However, further tests, such as recovery rates, should be done to evaluate the applicability of this optimized ELISA procedure for atrazine quantification in water samples.

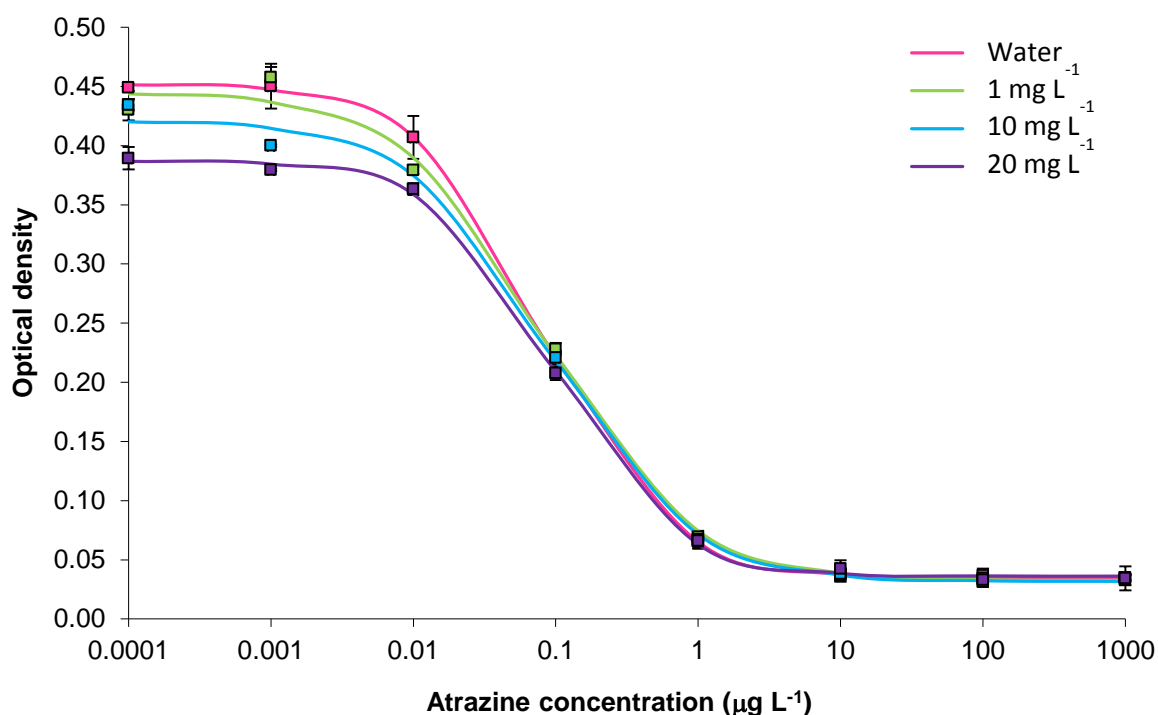


**Figure 6.6.** Evaluation of the organic matter effects on the ELISA calibration curves using sample buffer. Calibration curves obtained in the absence of organic matter and in the presence of 1, 10 and 20 mg L<sup>-1</sup> of HA.

Without sample buffer, the determined working range of this ELISA procedure was between 0.003 and 3  $\mu\text{g L}^{-1}$  (section 3.3.3). However the use of a sample buffer is known to decrease sensitivity, thus it was important to repeat the precision profile using the sample buffer. Sixteen standards (6 replicates per standard), with concentrations ranging from 0.0001 and 10  $\mu\text{g L}^{-1}$ , were used (Figure 6.7.).

Considering the maximum relative standard deviation of the concentration allowed of 30%, a working range between 0.006 and 1  $\mu\text{g L}^{-1}$  was obtained. Comparing with the one obtained without sample buffer (between 0.003 and 10  $\mu\text{g L}^{-1}$ ), it can be seen that a narrowing of the working range and a slight sensitivity decrease were observed using sample buffer.

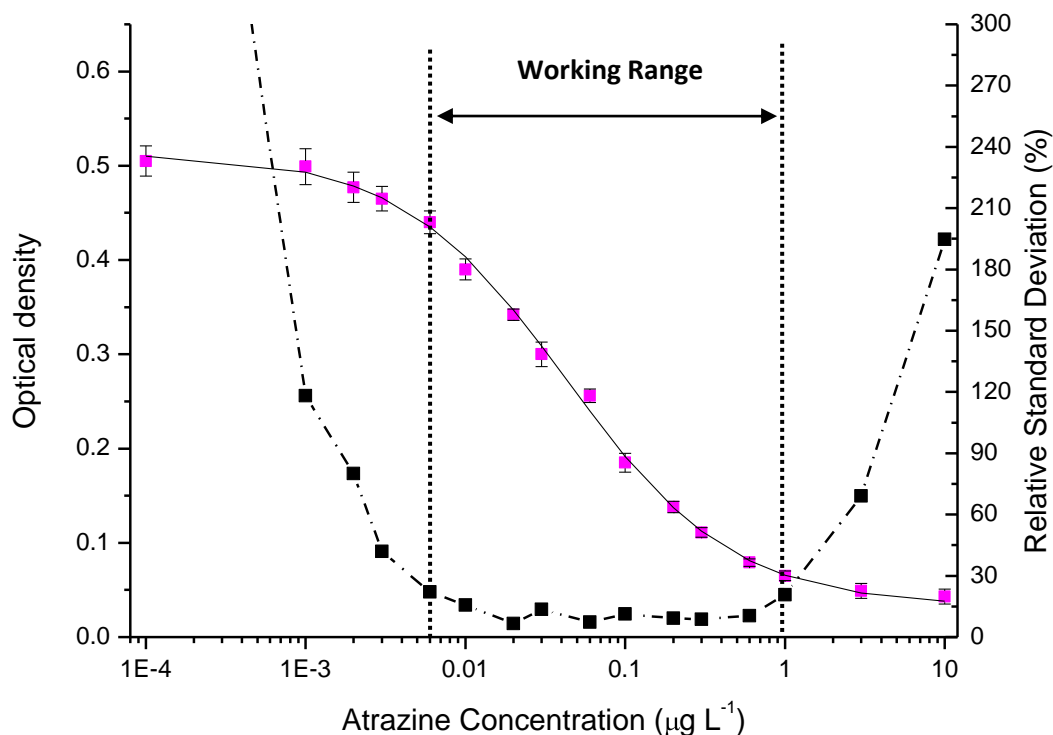


**Figure 6.7.** Calibration curve (pink squares) of ELISA ( $A = 0.513$ ;  $B = 0.835$ ;  $C = 0.043$ ;  $D = 0.033$ ;  $r = 0.998$ ) and precision profile (black squares). The precision profile and determination of the relative error of concentration were calculated in accordance with Ekins (1981).

Based on the established working range, recovery tests for a  $0.03 \mu\text{g L}^{-1}$  atrazine standard were made using different concentrations of HA. The atrazine standard was spiked with different volumes of an HA stock solution in order to obtain a final HA concentration of 0.5, 1, 2.5, 5, 10 and  $20 \text{ mg L}^{-1}$ . These tests were made with and without sample buffer.

Results (Figure 6.8.) show that without sample buffer, atrazine can be determined only in the presence of  $0.5 \text{ mg L}^{-1}$  of HA. With  $2.5 \text{ mg L}^{-1}$  of HA recovery rates reach almost 200%. On the other hand, using sample buffer, atrazine quantification can be accomplished with accuracy, in the presence of HA concentration up to  $20 \text{ mg L}^{-1}$ .

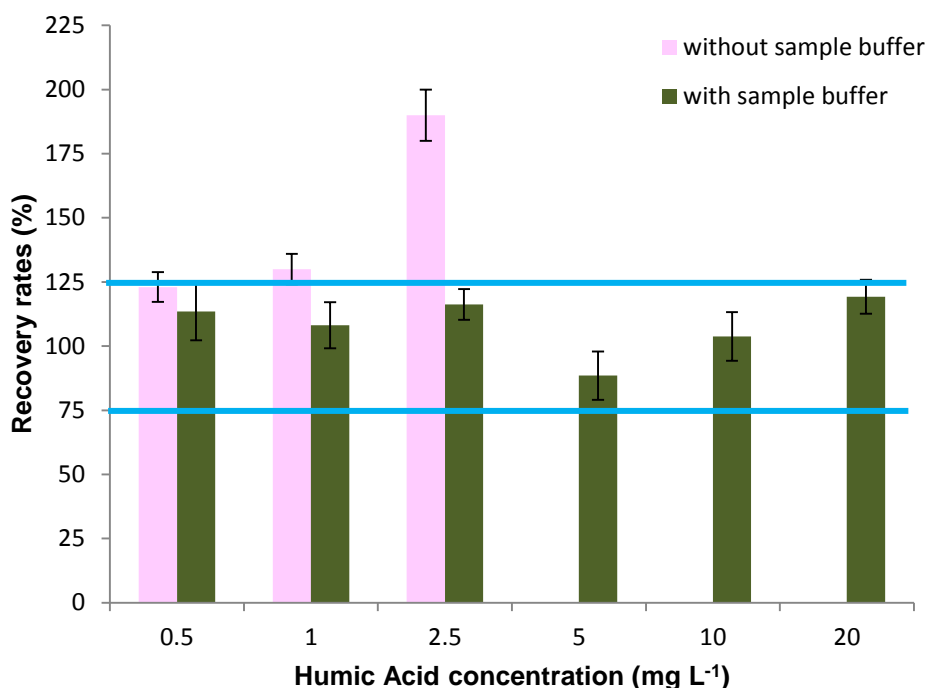


**Figure 6.8.** Recovery rates for a  $0.03 \mu\text{g L}^{-1}$  atrazine standard with different HA concentrations (between  $0.5$  and  $20 \text{ mg L}^{-1}$ ) ( $n=9$ ) with (green bars) and without (pink bars) the use of the sample buffer.

Also, recovery rates were calculated using sample buffer, for a  $0.3 \mu\text{g L}^{-1}$  atrazine standard with  $5$ ,  $10$  and  $20 \text{ mg L}^{-1}$  of HA. Results obtained ranged between  $88$  and  $100\%$ . Although, a shortening of the working range and a sensitivity decrease is observed, the reduction of matrix effects due to organic matter seems to be more than a good reason to use sample buffer in the assay.

Surface water samples, from Ria de Aveiro, can present high salt concentrations, so NaCl with concentrations ranging up to  $30 \text{ g L}^{-1}$  were used to simulate salty waters, in order to evaluate its interference in atrazine quantification. Atrazine standards with concentrations  $0.03$  and  $0.3 \mu\text{g L}^{-1}$  were spiked with a NaCl solution in order to obtain final concentrations of  $10$ ,  $20$  and  $30 \text{ g L}^{-1}$ .

For  $0.03 \mu\text{g L}^{-1}$  atrazine standard (Figure 6.9.), recovery rates obtained for all NaCl concentrations tested were within the defined range ( $75$  and  $125\%$ ). It appears that the salinity does not influence the accuracy of atrazine determination.



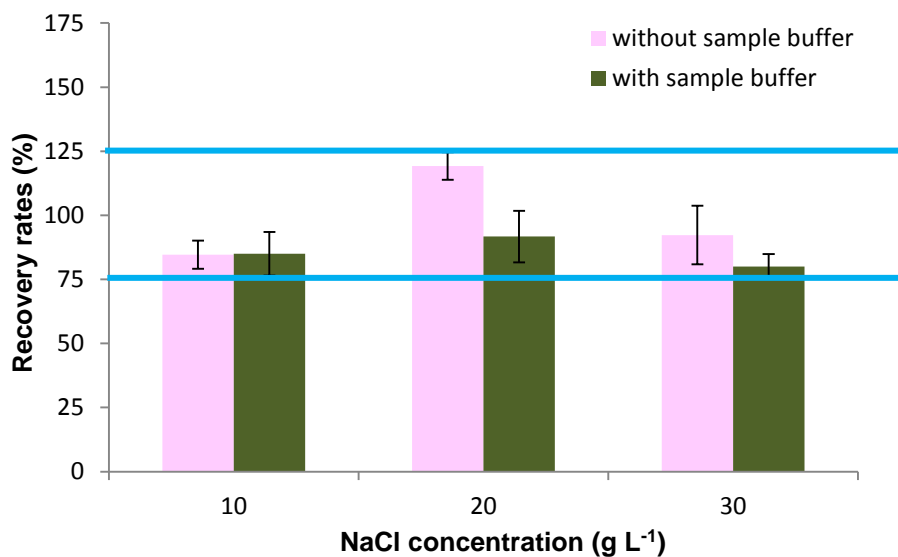


**Figure 6.9.** Recovery rates for a 0.03 µg L<sup>-1</sup> atrazine standard with different NaCl concentrations (between 10 and 30 g L<sup>-1</sup>) (n=9) with (green bars) and without (pink bars) the use of the sample buffer.

The same behaviour can be observed for a 0.3 µg L<sup>-1</sup> atrazine standard (Figure 6.10.).

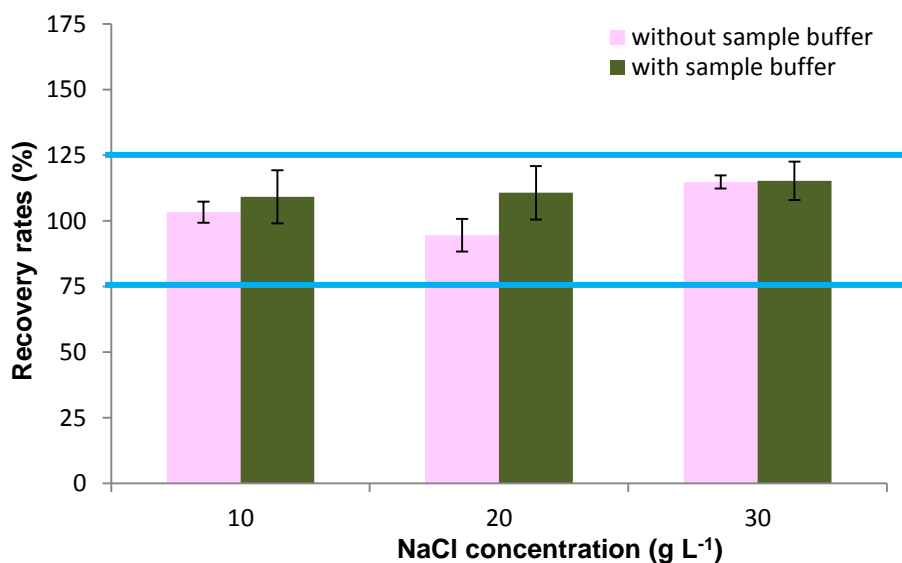


**Figure 6.10.** Recovery rates for a 0.3 µg L<sup>-1</sup> atrazine standard with different NaCl concentrations (between 10 and 30 g L<sup>-1</sup>) (n=9) with (green bars) and without (pink bars) the use of the sample buffer.

These results demonstrate that salinity does not affect the atrazine quantification by ELISA and no sample buffer needs to be used. Since in the water samples collected,

besides salinity, organic matter is also present, there is the need to use the sample buffer in order to eliminate the interference caused by such organic matter.

Recovery tests were also performed using real water samples, which present different organic matter compositions than the HA solution previously used. Three samples from North STP (after primary treatment, after biological treatment and final effluent) and two surface waters, Rossio channel and Barrinha de Mira, were spiked with 0.01, 0.05 and 0.1  $\mu\text{g L}^{-1}$  of atrazine. Concentration results obtained were plotted against spiked levels and linear regression parameters are presented on Table 6.2.

**Table 6.2.** Parameters of linear regression for determination of atrazine recovery rates in surface and waste water

Sample	Intercept ( $\mu\text{g L}^{-1}$ )	Slope (x100%)	<i>r</i>
Rossio Channel	0.001 $\pm$ 0.002	98 $\pm$ 3	0.999
Barrinha de Mira	0.003 $\pm$ 0.008	80 $\pm$ 1	0.974
North STP1	0.013 $\pm$ 0.003	102 $\pm$ 6	0.997
North STP2	0.036 $\pm$ 0.001	107 $\pm$ 2	0.999
North STP3	0.059 $\pm$ 0.004	120 $\pm$ 6	0.997

North STP1 – North sewage treatment plant after primary treatment; North STP2 – North sewage treatment plant after biological treatment; North STP3 – North sewage treatment plant final effluent;

Recovery rates were calculated as the slope of each regression line multiplied by 100 (Hintemann et al., 2006). Surface waters, with high organic matter (Rossio Channel) and high salinity level (Barrinha de Mira), presented good recoveries of 98 $\pm$ 3% and 80 $\pm$ 1%, respectively. Recoveries obtained for STP samples ranged between 102 $\pm$ 6 and 120 $\pm$ 6%. Such recoveries demonstrated that the optimized method can be used to accurately quantify atrazine in water samples with matrix as complex as the one in STP samples. Also correlation coefficients (*r*) ranged between 0.974 and 0.999, which indicates a linear behaviour and that no major interferences are caused by organic matter and/or salinity presence in water samples.

### 6.3.1.2. Quantification of atrazine in ground, surface and wastewaters

In the ground and surface water samples analysed, no atrazine was detected. The fact that atrazine has been banned from the market since 2007 can be the explanation for such results. Results of water samples from sewage treatment plant analysis, using the optimized ELISA procedure, are presented on Table 6.3.

**Table 6.3.** Atrazine concentrations ( $\pm$  standard deviation)

Sample	Atrazine concentration ( $\mu\text{g L}^{-1}$ )
North STP1	$0.014 \pm 0.001$
North STP2	$0.035 \pm 0.003$
North STP3	$0.052 \pm 0.003$

North STP1 – North sewage treatment plant after primary treatment; North STP2 – North sewage treatment plant after biological treatment; North STP3 – North sewage treatment plant final effluent;

Samples from South STP did not present atrazine in a quantifiable concentration. Although atrazine has not been sold since 2007 that does not mean that farmers could not use it. Gerecke et al. (2002) revealed that the main source of atrazine in STPs can be explained with improper operations of farmers applying atrazine onto corn fields, such as filling of sprayers, washing of measuring utilities, disposing of packing material, cleaning of spraying equipment, among others. Atrazine was only detected in the STP located at North of Aveiro city, the main STP of the area that receives almost 9 million  $\text{m}^3$  of domestic and industrial effluent of 272 000 inhabitant-equivalents, compared with the 7 million  $\text{m}^3$  of domestic effluent from 159 700 inhabitant-equivalents of the STP located at South of Aveiro (SIMRIA, 2011). Since the maximum legal limit allowed in drinking water is  $0.1 \mu\text{g L}^{-1}$ , the values between  $0.014$  and  $0.052 \mu\text{g L}^{-1}$  detected in STPs are even below this legal limit. It is also relevant to highlight that more studies should be done in order to verify the existence or not of terbuthylazine, since it presents 4% of cross-reactivity in the optimized ELISA procedure. Also, sampling should be repeated and should comprise a large number of samples that could be considered a representative sample.

### 6.3.2. EE2 determination

#### 6.3.2.1. Optimization of antibody and tracer dilutions

EE2 antibody and tracer were produced at BAM Federal Institute for Materials Research and Testing, thus only the optimization of antibody and tracer dilutions was needed. In accordance with previous information, four combinations were tested using Ab diluted 1:50000 and 1:75000 and tracer diluted 1:50000 and 1:75000 (Figure 6.11.).

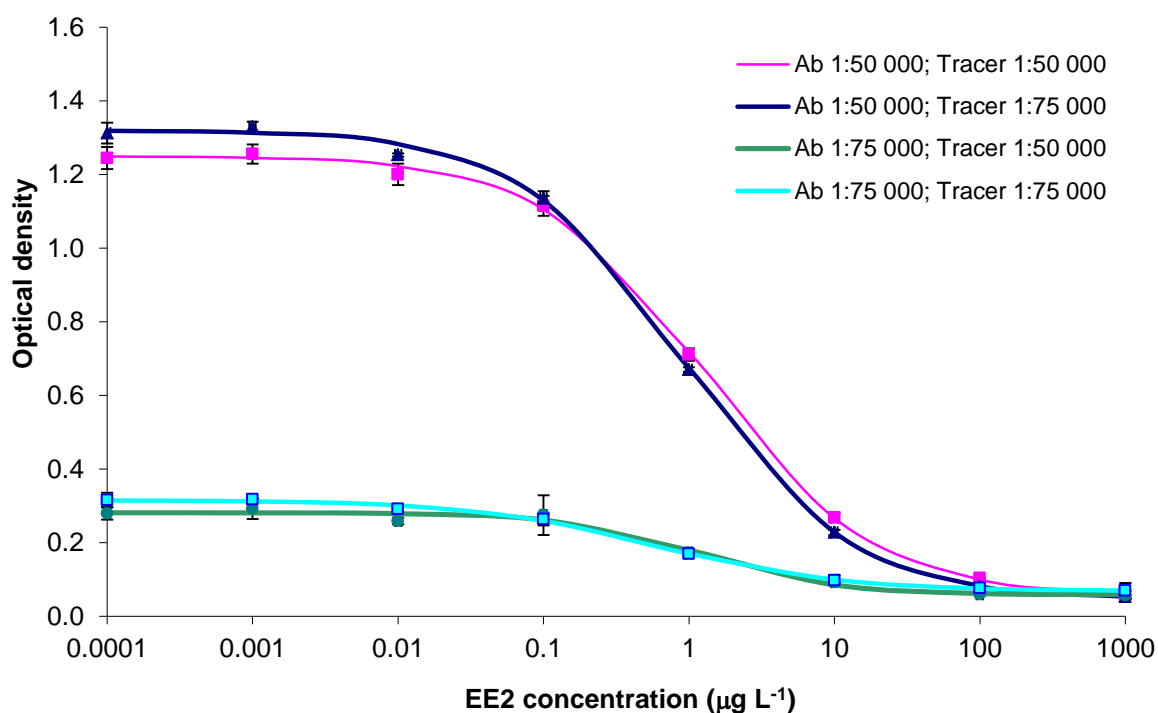


**Figure 6.11.** Calibration curves obtained using different antibody and tracer dilutions for direct ELISA for EE2 measurements.

The parameters obtained for the 4PL equation curve fitting using the different combinations of antibody and tracer dilution, are presented in Table 6.4.

**Table 6.4.** Parameter values obtained for the 4PL equation using different dilutions of polyclonal antibody and tracer for EE2.

Dilutions	A	B	C	D
Ab 1:50000; Tracer 1:50000	1.250	0.767	1.320	0.058
Ab 1:50000; Tracer 1:75000	1.320	0.767	0.963	0.047
Ab 1:75000; Tracer 1:50000	0.281	0.937	1.200	0.058
Ab 1:75000; Tracer 1:75000	0.315	0.686	0.599	0.068

A = signal at zero dose, D = signal at excess dose, C = x-coordinate (concentration) of the turning point of the sigmoidal curve and B = slope parameter.

The combination of tracer and antibody dilution chosen was antibody diluted 1:50000 and tracer 1:75000. Although this combination does not present the lowest C parameter (associated to sensitivity) it is the one that presents a low value for C parameter and a higher difference between the OD value of the lower and higher standard (higher difference between A and D parameters).

### 6.3.2.2. Evaluation of assay performance

After choosing the antibody and tracer dilution it is important to evaluate the performance of the developed assay. This evaluation includes the precision profile where we can define the working range. The accuracy and precision of the method was also evaluated.

In what concerns precision profile, in Figure 6.12. the calibration curve and the respective precision profile are presented. The precision profile was obtained using 16 standards with concentrations ranging from 0.0001 to 100  $\mu\text{g L}^{-1}$  (6 replicates per standard).

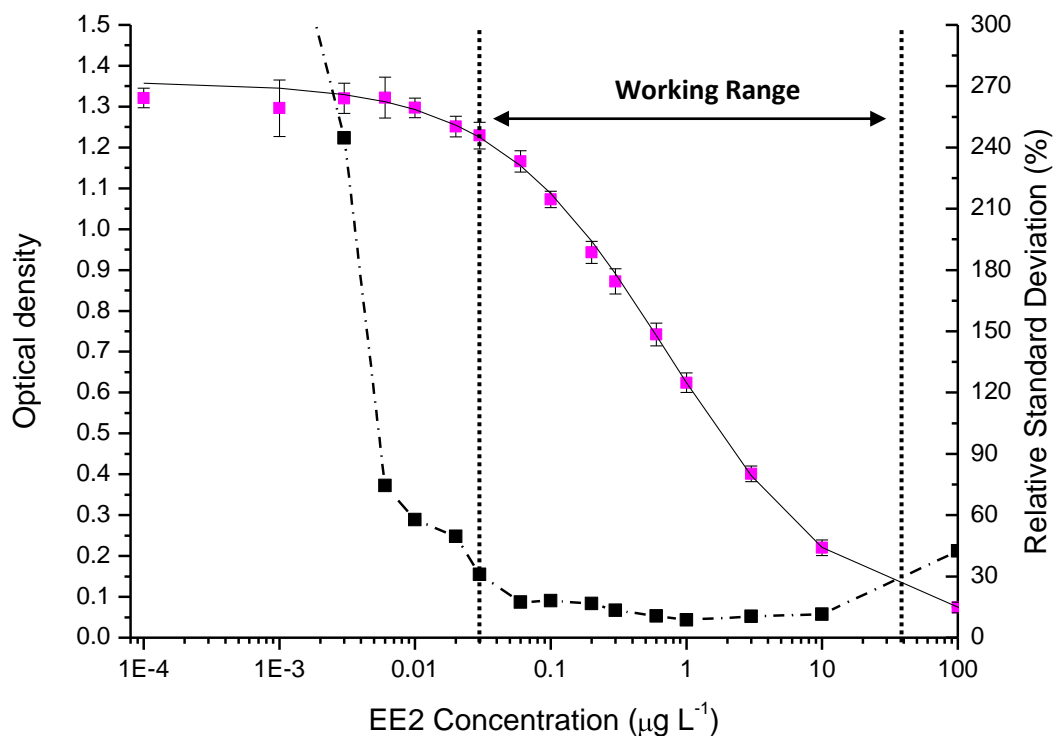


**Figure 6.12.** Calibration curve (pink squares) of ELISA ( $A = 1.360$ ;  $B = 0.683$ ;  $C = 0.729$ ;  $D = 0.030$ ;  $r = 0.999$ ) and precision profile (black squares). The precision profile and determination of the relative error of concentration were calculated in accordance with Ekins (1981).

The quantification range obtained using the maximum RSD of 30% was between 0.03 and 40  $\mu\text{g L}^{-1}$ . This assay can be used over three orders of magnitude in analyte concentration.

In order to evaluate the accuracy of the method, a 1  $\mu\text{g L}^{-1}$  EE2 standard was determined (32 replicates) and a plot of the concentration obtained for each well, upper and lower limit allowed, considering a 25% deviation from the real standard concentration, is presented in Figure 6.13.

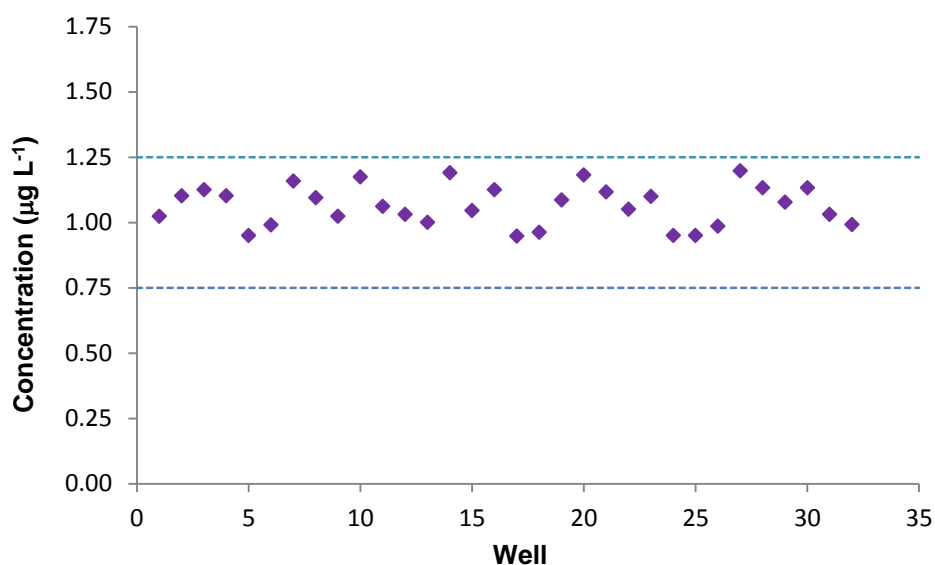


**Figure 6.13.** Plot of concentration obtained for each well for 1 µg L<sup>-1</sup> EE2 standard and respective upper and lower limit for a 25% deviation.

Results demonstrate that all the concentrations obtained are within the pre-established limit, indicating that the method can be considered accurate. The mean obtained for the 32 replicates was 1.07 µg L<sup>-1</sup>, with a relative standard deviation of 7.2%, thus, besides accurate, the method can also be considered precise.

#### 6.3.2.3. Cross-reactivity

The relative sensitivity of ELISA towards other steroid hormones was determined. Cross-reactivity was calculated as the ratio of molar concentration at the inflection points (midpoints, C parameter) of the corresponding calibration curves, expressed in percentage relative to the midpoint of EE2. Molar cross-reactivities obtained for E1, E2 and E3 are presented on Table 6.5.

**Table 6.5.** Cross-reactivities (CR, %) of some selected hormones at the center points of their calibration curves.

Hormone	CR (%)
EE2	100
E1	0.21
E2	0.62
E3	0.19

Cross-reactivities obtained for the studied hormones are very low (< 1%) indicating that the method presents high sensitivity for EE2, and that not any interference of these hormones is expected, when present in the same sample as EE2.

#### 6.3.2.4. Evaluation of matrix effects

Matrix effects can cause an influence on the determination of EE2, so it is important to evaluate them. Since water samples collected can contain organic matter, HA were used as model substance to simulate water's organic matter. Four calibration curves (Figure 6.14.) were obtained with standards prepared in the absence and in the presence of HA (from 1 to 20 mg L<sup>-1</sup>).

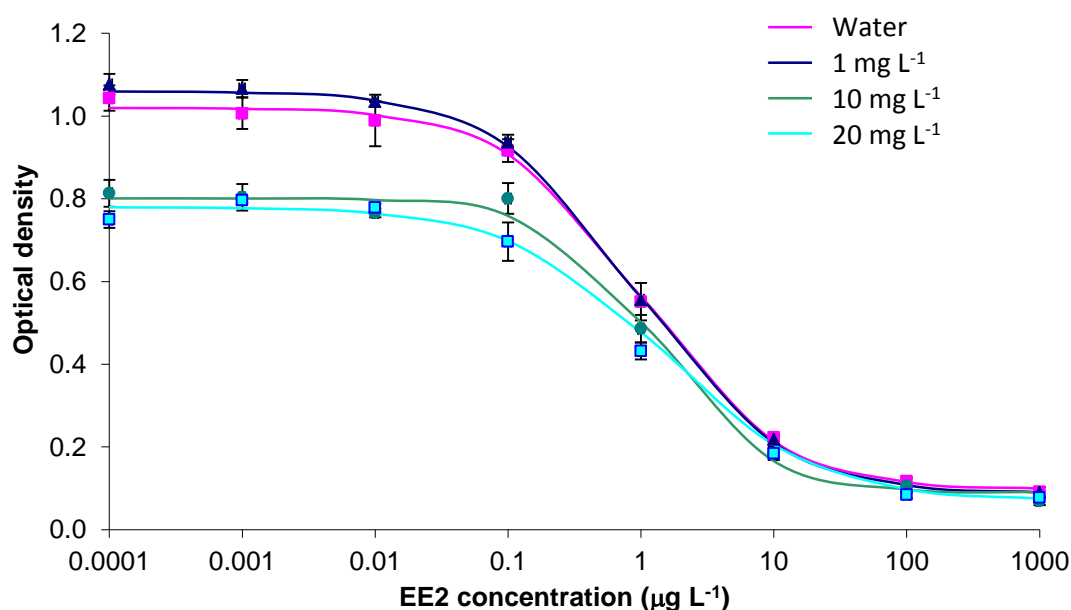


**Figure 6.14.** Evaluation of the organic matter effect on the ELISA calibration curve.



As it could be seen in section 6.3.1.1. for atrazine, a flattening of the calibration curve with the increase of HA concentration is observed. The increase of the turning point presented in Table 6.6. demonstrates the deviation of the curve to higher concentrations, resulting in the loss of sensitivity. It is also important to highlight that small concentrations of HA (such as  $1 \text{ mg L}^{-1}$ ) do not interfere in EE2 quantification, the HA only becomes a problem when its concentration reaches values such as  $10 \text{ mg L}^{-1}$ .

**Table 6.6.** Parameter values obtained for the 4PL equation using EE2 standards prepared with and without HA.

Standard composition	A	B	C	D
Water	1.020	0.847	1.030	0.097
$1 \text{ mg L}^{-1}$ HA	1.060	0.819	0.941	0.087
$10 \text{ mg L}^{-1}$ HA	0.801	1.060	1.350	0.090
$20 \text{ mg L}^{-1}$ HA	0.780	0.756	1.480	0.070

A = signal at zero dose, D = signal at excess dose, C = x-coordinate (concentration) of the turning point of the sigmoidal curve and B = slope parameter.

The decrease in the OD with the increase of HA concentration will give an overestimation of the EE2 concentration; for this reason, it is necessary to evaluate the influence of the organic matter, present in the samples, in the EE2 quantification. The mechanism of this interference, as mentioned before, is not well understood, but it may be due to unspecific binding of HA to the antibody or to the tracer, resulting in a decrease of optical density.

To overcome this interference observed for high concentration of HA, the same sample buffer tested for atrazine was used. Four calibration curves were obtained, in the absence and presence of HA, but adding sample buffer prior to the addition of the analyte. BSA present in sample buffer has a propensity of binding to organic matter, decreasing its effects on EE2 quantification. Calibration curves obtained are presented in Figure 6.15. The assay exhibits a robust behaviour in the presence of HA.

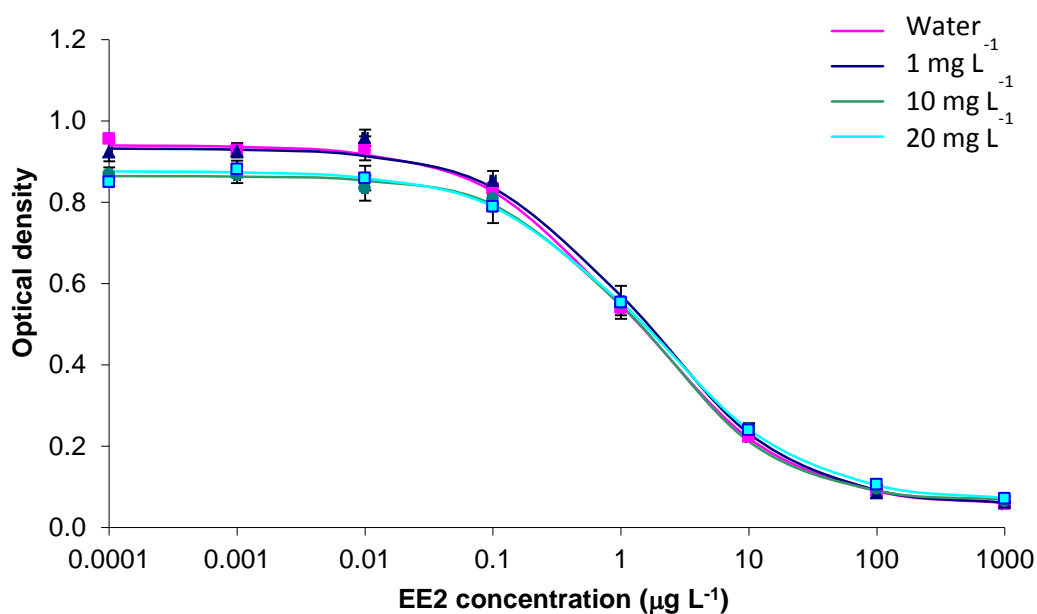


**Figure 6.15.** Evaluation of the organic matter effect on the ELISA calibration curve in the presence of sample buffer.

The use of sample buffer seems to solve the organic matter interferences, since the sigmoidal shape is maintained, even at such high concentration of HA as 20 mg L<sup>-1</sup>. A slight decrease in optical density for the lower standards is observed in the presence of more than 10 mg L<sup>-1</sup> of HA. This seems to be a problem for concentrations lower than 0.1 µg L<sup>-1</sup>. Recovery tests were also performed to evaluate the HA interference for lower EE2 concentrations and high levels of HA.

A precision profile should be determined using sample buffer in order to obtain the working range and sensitivity in these new conditions. Sixteen standards with concentrations ranging between 0.0001 and 100 µg L<sup>-1</sup> were used (six replicates per standard) and 30% was the maximum relative standard deviation allowed for the determination of the working range (Figure 6.16.). Using sample buffer, the obtained working range was between 0.1 and 20 µg L<sup>-1</sup>, much narrower than the one obtained without sample buffer (0.03 and 40 µg L<sup>-1</sup>). The lower value of the range increased considerably with the sample buffer, meaning that interferences due to organic matter can be overcome, but the loss of sensitivity can be critical, since low EE2 concentrations

are expected in water samples. This loss of sensitivity is also observed with the C parameter of the curve that increased from 0.729 to 1.61, using sample buffer.

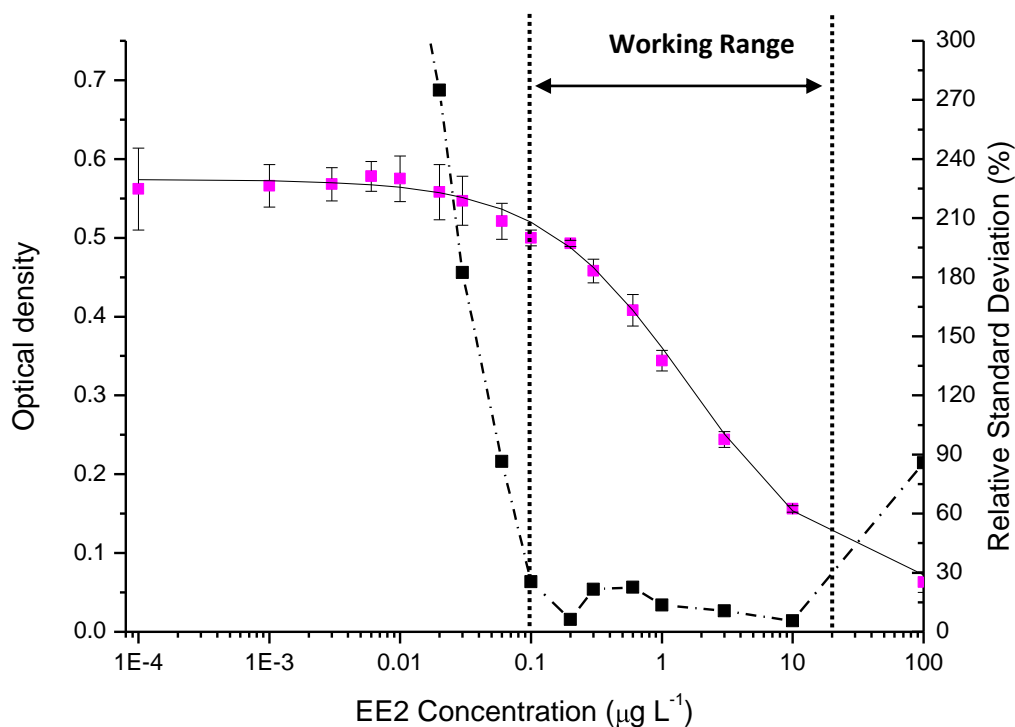


**Figure 6.16.** Calibration curve (pink squares) of ELISA ( $A = 0.574$ ;  $B = 0.776$ ;  $C = 1.610$ ;  $D = 0.052$ ;  $r = 0.998$ ) and precision profile (black squares). The precision profile and determination of the relative error of concentration were calculated in accordance with Ekins (1981).

Based on the working ranges and turning points obtained, with and without sample buffer, recovery rates were determined for a  $1.0 \mu\text{g L}^{-1}$  EE2 standard in the presence of different concentrations of HA. The standard was spiked with different volumes of an HA stock solution in order to obtain a final concentration of 0.5, 1, 2.5, 10 and  $20 \text{ mg L}^{-1}$ . These tests were performed with and without the presence of sample buffer and results obtained are presented in Figure 6.17.

Results demonstrate that EE2 quantification can be performed using sample buffer even when HA are present in concentration as high as  $20 \text{ mg L}^{-1}$ . Avoiding the sample buffer use, due to the loss of sensitivity that it causes, caution should be taken when HA

concentrations present in samples are higher than  $10 \text{ mg L}^{-1}$ . For  $20 \text{ mg L}^{-1}$  of HA in water samples, recovery rates rise up to 156%.

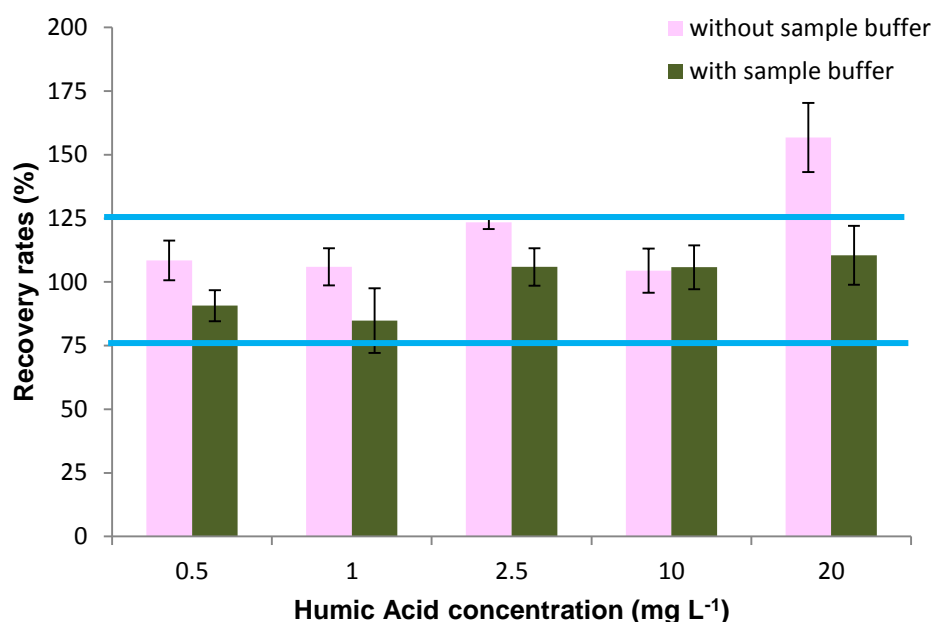


**Figure 6.17.** Recovery rates for a  $1 \mu\text{g L}^{-1}$  EE2 standard with different HA concentrations (between  $0.5$  and  $20 \text{ mg L}^{-1}$ ) ( $n=9$ ) with (green bars) and without (pink bars) the use of sample buffer.

An evaluation of each case has to be done in order to weight the advantages and disadvantages of sample buffer use. In cases that influence of organic matter is not expected, the sample buffer should be avoid.

Another important factor that can introduce errors in EE2 quantification is the presence of high salt concentrations. NaCl was used to simulate salty waters in order to evaluate its interference in quantification. EE2 standards, with  $1.0 \mu\text{g L}^{-1}$  concentration, were spiked with NaCl in order to obtain concentrations ranging from  $10$  to  $30 \text{ g L}^{-1}$ . Recovery rates obtained in presence or absence of sample buffer, did not differ considerably (Figure 6.18.). Values ranged between  $79$  and  $96\%$  for both cases.

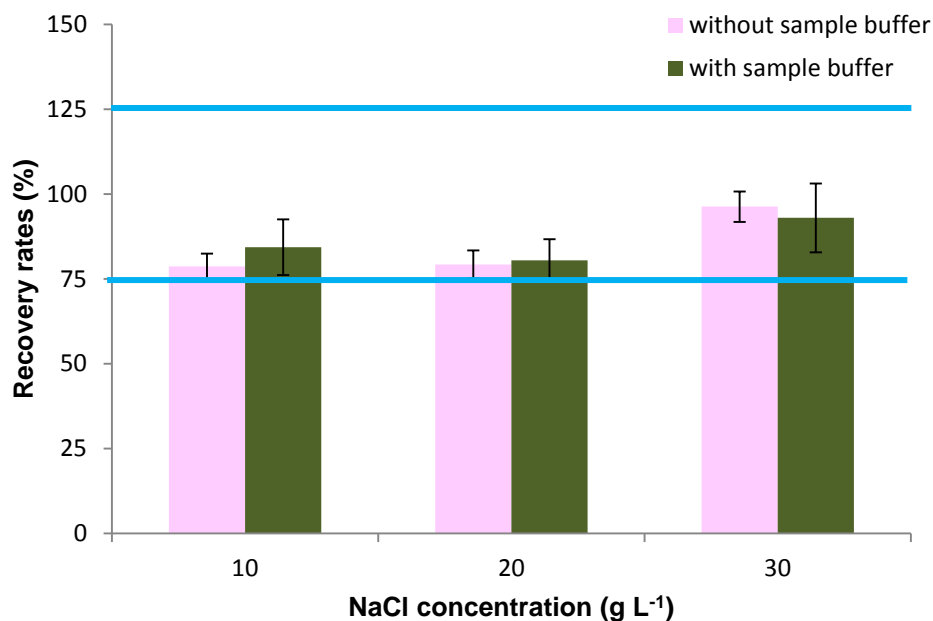


**Figure 6.18.** Recovery rates for a  $1 \mu\text{g L}^{-1}$  EE2 standard with different NaCl concentrations (between 10 and  $30 \text{ g L}^{-1}$ ) ( $n=9$ ) with (green bars) and without (pink bars) the use of the sample buffer.

These results demonstrate that salinity does not seem to interfere with EE2 quantification and that organic matter is the most problematic issue in what concerns to matrix effects.

Real water samples were also subjected to recovery tests, spiking known volumes of EE2 standards into those samples. One STP sample, after primary treatment, and one surface water sample (Rossio channel) were spiked with  $0.5$ ,  $1.0$  and  $1.5 \mu\text{g L}^{-1}$  of EE2 and determined, using the previously optimized ELISA procedure without sample buffer. Concentration results obtained were plotted against spiked levels and linear regression parameters were obtained and presented on Figure 6.19. Recovery rates for each sample can be calculated multiplying the slope by 100% (Hintemann et al., 2006). In STP sample, with high levels of organic matter, the obtained recovery rate was  $106 \pm 3\%$ , while Rossio channel sample, that can present high salinity levels and organic matter effects, presented  $84 \pm 3\%$  of recovery rate. Also, the obtained correlation coefficients were close to 1, which indicates a linear behaviour and that no major interferences due to matrix occur.

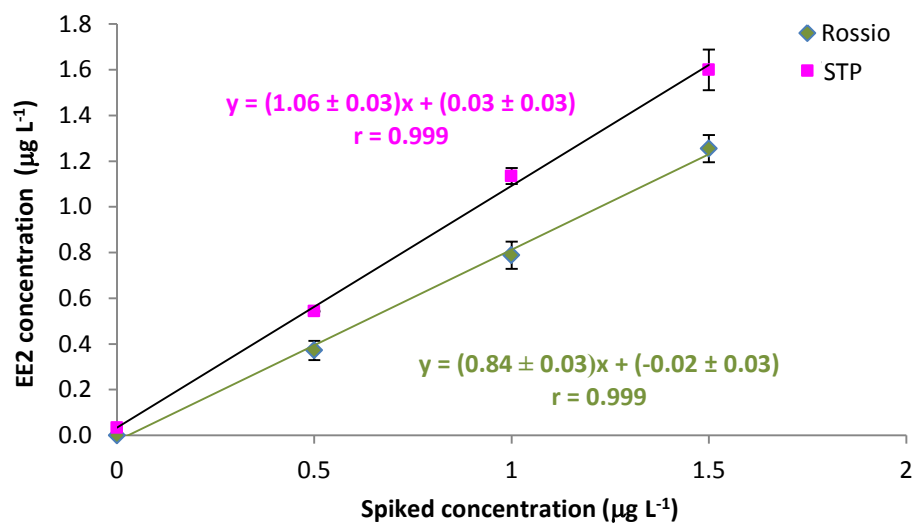


**Figure 6.19.** Plot of EE2 concentrations determined by ELISA without sample buffer after spiking a STP sample (pink squares) and a surface water sample (green diamonds) with three EE2 concentrations.

Results obtained for recovery rates in real samples demonstrated that EE2 can be quantified correctly without the interference of organic matter or salinity using the optimized ELISA.

#### 6.3.2.5. Quantification of EE2 in ground, surface and wastewaters

Ground and surface water samples did not present EE2 on a quantifiable level. Previous works reported EE2 concentration in surface water of 1 ng L<sup>-1</sup> (Hintemann et al., 2006), up to 5.1 ng L<sup>-1</sup> (Ying et al., 2002), up to 2.9 ng L<sup>-1</sup> (Cargouët et al., 2004) and from 0.23 to 1.76 ng L<sup>-1</sup> (Ra et al., 2011). Also Duong et al. (2010) reported levels from 2.3 to 10.2 ng L<sup>-1</sup> of EE2 in surface waters. Since quantification range without the use of sample buffer was between 0.03 and 40 µg L<sup>-1</sup> it is natural that EE2 was not detected. These results demonstrate the need, in the future, of sample pre-concentration in order to be able of quantify EE2 in this type of water samples.

In what concerns north and south sewage treatment plants samples, EE2 was detected only after primary treatment (Table 6.7.).

**Table 6.7.** EE2 concentrations ( $\pm$  standard deviation) detected in STP

Sample	EE2 concentration ( $\mu\text{g L}^{-1}$ )
North STP1	$0.091 \pm 0.008$
South STP1	$0.033 \pm 0.003$

North STP1 – North sewage treatment plant after primary treatment; South STP1 – South sewage treatment plant after primary treatment.

The higher value obtained for north STP was expected since this treatment plant covers 272 000 inhabitants, compared to the 159 700 of south treatment plant. However, both results are much higher than expected. Previous values reported for EE2 concentration detected on STPs were  $1.7 \text{ ng L}^{-1}$  in Italy (Baronti et al., 2000),  $15 \text{ ng L}^{-1}$  in Germany and  $42 \text{ ng L}^{-1}$  in Canada (Ternes et al., 1999). Recently, Zhou et al. (2010) detected EE2 in a STP in Beijing, China, at a concentration of  $187.9 \text{ ng L}^{-1}$ . Authors explain this high value with the government birth control policy. Also values of  $70 \text{ ng L}^{-1}$  were reported for a STP in Europe, Austria (Clara et al., 2005). It is important to highlight that in a STP the estrogen source is the human population, therefore, estrogen levels in raw sewage are a function of population characteristics (size, sex, age distribution, contraception practices) (Combalbert and Hernandez-Raquet, 2010).

The impact of sewage treatments on hormones' concentration was already referred. As it can be seen, EE2 was only detected after primary treatment. During the secondary treatment the removal by sorption to organic material (e.g., colloids and biomass flocs or biofilms), as well as biological degradation and/or transformation, can be responsible for the decrease of EE2 concentration (Combalbert and Hernandez-Raquet, 2010).

## 6.4. Conclusions

---

In this chapter enzyme-linked immunosorbent assays were developed in order to quantify hydrophobic organic pollutants, such as atrazine and 17 $\alpha$ -ethinylestradiol, in water samples. For both pollutants, HA interference causes a flattening of the calibration curve and the increase of the calibration curve turning point to higher concentrations, resulting in a loss of sensitivity and also to an overestimation of the concentration. The use of a sample buffer has proven to reduce matrix interference, although a reduction in the quantification range, especially for the EE2 assay was observed. Salinity does not seem to affect quantification of either atrazine or EE2. Recovery tests performed in real water samples revealed that the method seems to be suitable for the quantification of these pollutants in real water samples.

A total of 24 water samples (including ground, surface and waste water samples) collected in Aveiro were analyzed. Atrazine was detected in the three water samples from north sewage treatment plant, while EE2 was detected in both sewage treatment plants, but only after primary treatment. Detected values were a little higher than the ones generally presented in most European studies, but already reported in Austria STP.

This study is preliminary, therefore it needs to be improved since more STP samples should be collected during 24 hours and in different days, in order to obtain a composite sample that could be representative of the pollutants' behavior in STPs. Also methods for sample pre-concentration should be developed, in order to decrease the limit of detection to values lower than 1 ng L<sup>-1</sup>.



## 6.5. References

---

- AMC-V - Associação de Municípios do Carveiro – Vouga (<http://www.amcv.pt/www.amcv.pt/>), **2011**.
- Baronti, C., Curini, R., D'Ascenzo, G., Di Corcia, A., Gentili, A., Samperi, R., **2000**. Monitoring natural and synthetic estrogens at activated treatment plants and in receiving river water. *Environ. Sci. Technol.* 34, 5059-5066.
- Cargouët, M., Perdiz, D., Mouatassim-Souali, A., Tamisier-Karolak, S., Levi, Y., **2004**. Assessment of river contamination by estrogenic compounds in Paris area (France). *Sci. Total Environ.* 324, 55-66.
- Clara, M., Kreuzinger, N., Strenn, B., Gans, O., Kroiss, H., **2005**. The solids retention time: a suitable design parameter to evaluate the capacity of wastewater treatment plants to remove micropollutants. *Water Res.* 39, 97–106.
- Combalbert, S., Hernandez-Raquet, G., **2010**. Occurrence, fate, and biodegradation of estrogens in sewage and manure. *Appl. Microbiol. Biotechnol.* 86, 1671–1692.
- Dias, J.M., Lopes, J.F., **2006a**. Implementation and assessment of hydrodynamic, salt and heat transport models: The case of Ria de Aveiro Lagoon (Portugal). *Environ. Modell. Softw.* 21, 1-15.
- Dias, J.M., Lopes, J.F., **2006b**. Calibration and validation of hydrodynamic, salt and heat transport models for Ria de Aveiro Lagoon (Portugal). *J. Coastal Res. SI* 39, 1680-1684.
- Dudley, R.A., Edwards, P., Ekins, R.P., Finney, D.J., McKenzie, I.G., Raab, G.M., Rodbard, D., Rodgers, R.P., **1985**. Guidelines for immunoassay data processing. *Clin. Chem.* 31, 1264-1271.
- Duong, C.N., Ra, J.S., Cho, J., Kim, S.D., Choi, H.K., Park, J.-H., Kim, K.W., Inam, E., Kim, S.D., **2010**. Estrogenic chemicals and estrogenicity in river waters of South Korea and seven Asian countries. *Chemosphere* 78, 286-293.
- Ekins, R.P., **1981**. The "Precision Profile": Its use in RIA assessment and design. *The Ligand Quarterly* 4, 33-44.
- Gerecke, A.C., Schärer, M., Singer, H.P., Müller, S.R., Schwarzenbach, R.P., Sägesser, M., Ochsenbein, U., Popow, G., **2002**. Sources of pesticides in surface waters in Switzerland: pesticide load through waste water treatment plants – current situation and reduction potential. *Chemosphere* 48, 307-315.

- Ghanem, A., Bados, P., Perreau, F., Benabdallah, R., Plagellat, C., Alencastro, L.F., Einhorn, J., **2008**. Multiresidue analysis of atrazine, diuron and their degradation products in sewage sludge by liquid chromatography tandem mass spectrometry. *Anal. Bioanal. Chem.* 391, 345–352.
- Hintemann, T., Schneider, C., Schöler, H.F., Schneider, R.J., **2006**. Field study using two immunoassays for the determination of estradiol and ethinylestradiol in the aquatic environment. *Water Res.* 40, 2287-2294.
- Lopes, J.F., Dias, J.M., Cardoso, A.C., Silva, C.I.V., **2005**. The water quality of the Ria de Aveiro lagoon, Portugal: From the observations to the implementation of a numerical model. *Mar. Environ. Res.* 60, 594-628.
- Melo, M.T.C., Silva, M.A.M., Edmunds, W.M., Evolução Hidrogeoquímica do sistema Multiaquífero Cretácico do Baixo Vouga – Aveiro, Portugal, in “4<sup>o</sup> Congresso da Água” Conference Proceedings, Lisbon, March **1998**.
- Ra, J.-S., Lee, S.-H., Lee, J., Kim, H.Y., Lim, B.J., Kim, S.H., Kim, S.D., **2011**. Occurrence of estrogenic chemicals in South Korean surface waters and municipal wastewaters. *J. Environ. Monit.* 13, 101-109.
- Schneider, C., Schöler, H.F., Schneider, R.J., **2004**. A novel enzyme-linked immunosorbent assay for ethinylestradiol using a long-chain biotinylated EE2 derivative. *Steroids* 69, 245-253.
- SimRia - Sistema Multimunicipal de Saneamento da Ria de Aveiro ([www.simria.pt](http://www.simria.pt)), May **2011**.
- Ternes, T.A., Stumpf, M., Mueller, J., Haberer, K., Wilken, R.D., Servos, M., **1999**. Behaviour and occurrence of estrogens in municipal sewage treatment plants – I. Investigations in Germany, Canada and Brazil. *Sci. Total Environ.* 225, 81-90.
- Ying, G.-G., Kookana, R.S., Ru, Y.-J., **2002**. Occurrence and fate of hormone steroids in the environment. *Environ. Int.* 28, 545-551.
- Zhou, H., Huang, X., Wang, X., Zhi, X., Yang, C., Wen, X., Wang, Q., Tsuno, H., Tanaka, H., **2010**. Behaviour of selected endocrine-disrupting chemicals in three sewage treatment plants of Beijing, China. *Environ. Monit. Assess.* 161, 107–121.

# PART IV

## CONCLUSIONS AND FUTURE WORK

# CONCLUSIONS

In the first part of this work, several methodologies were developed with the intention of obtain a simple, fast and precise method, to follow sorption behaviour of organic pollutants onto soil samples, using batch equilibrium experiments. Micellar electrokinetic chromatography has proven to be a valid alternative to HPLC or liquid scintillation. Several advantages can be pointed out to MEKC, like equipment simplicity and operation price, less time-consuming, less sample manipulation and less waste generation, since there is no need for sample cleaning, thus time of analysis is lower than 15 min and there is no need to use organic solvents. From the application of batch equilibrium technique will result several samples that have to be measured at least three times. The number of analysis needed to obtain an isotherm, that represents the sorption of one pollutant to one soil sample, is considerable. Hence, a UV spectral deconvolution was tested to follow sorption of atrazine to soil samples. Results obtained were compared with the ones obtained, previously using MEKC, and did not present statistical differences at 95% confidence level. UVSD, when compared to MEKC, is a faster technique (less than 1 min for each replicate), much simple (only a dilution is needed) and the only equipment needed is a UV-Vis spectrophotometer, the most common equipment in chemical laboratories. Another alternative tested to follow atrazine sorption behaviour was ELISA. This methodology is particularly interesting when the sample volume available is very low (ELISA needs 100  $\mu\text{L}$  for each replicate) or when the concentration in aqueous phase is very low ( $\text{ng L}^{-1}$  levels). Obtained results were also compared with the ones obtained previously using MEKC. Applying student *t*-test, no statistical difference at 95% confidence level was observed. The work developed provide several options in terms of methodology to follow sorption of atrazine onto soils; however, the choice depends on the laboratory conditions and/or on the analyst preferences. The advantages and disadvantages of each methodology should be evaluated first.

EE2 sorption onto soil samples was also a purpose of this work. Therefore, a methodology able to quantify EE2 present in a soil aqueous extract was optimized. Since EE2 presents low UV light absorbance, UVSD preliminary results were not suitable. On the other hand, EE2 and similar aromatic compounds are known for its fluorescence capacity, thus the same UVSD principle was applied using fluorescence emission spectra.

Preliminary studies showed random residuals, low detection limit ( $1.58 \mu\text{g L}^{-1}$ ), high correlation coefficients, and good recovery results (between 87.4 and 112.2%). Results obtained for soil organic carbon sorption coefficient were similar to the ones reported by other authors, suggesting that the developed method is suitable to follow EE2 adsorption onto soil organic matter.

The second part of this work consisted in the study of sorption behaviour of two different hydrophobic organic pollutants (EE2 and atrazine). As mentioned, the transport and fate of hydrophobic organic pollutants in the environment involve complex phenomena, being sorption to soil components one of the most important. In order to understand the binding mechanism responsible for this interaction, it is necessary to have soil organic matter characterization. It was possible to conclude that both EE2 and atrazine adsorption depends greatly on the total organic carbon. The results of atrazine binding to organic matter pointed out that carboxyl units and aromatic-rich organic matter are the most efficient binding agents for atrazine. Aromatic compounds are responsible for hydrophobic interactions, while carboxyl units are responsible for hydrogen bonds between soil and organic matter, stronger binding forces, that will reduce desorption, and thus decrease the leaching and runoff into water resources. EE2 adsorbs strongly to soil organic matter and is mainly stabilized by hydrophobic interactions through aromatic nuclei face to face with the surface and/or another EE2 molecule association. Moreover, specific sorbent-sorbate interactions, due to hydrogen or covalent bonding, are likely to occur due to the presence of phenolic function at C-3 and hydroxyl function at C-17 of the EE2 molecule.

Soil fertilized with farmyard manure contains higher aromatic and carboxyl units, indicating that this type of manure can be effectively used to minimize the residual toxicity of EE2 and atrazine present in soils, increasing the sorption and reducing leaching onto water resources.

Since the final destination of organic pollutants can be ground, surface or waste waters, a preliminary screening of these pollutants in some water samples was performed. ELISA was the analytical technique chosen for this screening and several tests to determine matrix interferences were performed. For both pollutants, humic acid

interference cause a flattening of the calibration curve and the increase of turning point to higher concentrations, resulting in a loss of sensitivity and an overestimation of the concentration. The use of a sample buffer overcomes this problem, although it was observed a decrease of the working range, especially for EE2. A total of 24 samples, collected from different locations around Aveiro city, including ground, surface and waste water samples, were analyzed. Atrazine was detected only in samples from north sewage treatment plant (all samples collected along the treatment), while EE2 was only detected in waste water samples from sewage treatment plants collected after the primary treatment. The obtained values were a little higher than expected and generally detected in Europe. Since this is a preliminary study, further research should be done to increase detection limit and to analyze more representative samples.

# **FUTURE WORK**



As mentioned before, monitoring studies can provide important information on the occurrence and distribution of a great number of anthropogenic compounds in ground waters, lakes, rivers, estuaries, oceans and waste waters. A wide range of anthropogenic compounds has been found in waters, and it has been shown that some are potentially harmful even at trace concentrations. Its quantification in environment constitutes a challenge, due to low concentrations, from  $\mu\text{g L}^{-1}$  to less than  $\text{ng L}^{-1}$ , and to the complexity of matrices. Primary techniques for PPCPs analysis are GC or liquid chromatography (LC) coupled to a mass spectrometer (MS) detector. GC-MS is less used due to the common need of derivatization, which bears time consumption, non-reproducible derivatization at trace levels and, sometimes, formation of unwanted by-products. In the last decades, LC-MS and LC-MS-MS have experienced an impressive progress and have been indicated as techniques of choice for environmental analysis because of sensitiveness and selectivity. However, they are also expensive, costly to maintain and require specifically trained analysts to be implemented in routine quality control laboratories. Due to low concentration and matrices complexity, analyte enrichment is normally required when more affordable techniques, such as HPLC and CE, are used. SPE importance has grown considerably in the last decade. However, high pre-concentration difficulty, some interfering compounds co-elution and relative expensiveness of SPE sorbent, create the need of a new low cost alternative. Sorbents such as molecularly imprinted polymers (MIPs), considered a "tailor-made material", can be synthesized to improve selectivity of SPE for a given analyte. MIPs have been applied on determination of pharmaceuticals in water samples. Also, unconventional sorbents using agricultural, industrial and municipal waste, already used for water treatment, could be tested as low cost materials to substitute normal SPE columns packing sorbents. An alternative to SPE is hollow-fiber liquid phase microextraction (HF-LPME), based on the use of single, low-cost, disposable, porous hollow fibers made of polypropylene. By HF-LPME, analytes of interest are extracted from aqueous samples through a thin layer of organic solvent, immobilized within the pores of the fiber, into an acceptor solution (aqueous or organic). This extraction technique has been used in environmental applications using HPLC, GC and CE.

Due to the small volume of extracting solvent, no further concentration prior to analysis is required, decreasing analysis time and solvent consumption.

Nowadays, considering laboratories financial restrictions, it is crucial to create new and low cost methodologies able to concentrate and determine, at environmental levels, these emerging contaminants that have raised great concern in the last years. Therefore, the main purpose of the work will be the development of low cost methodologies for the analysis of PPCPs in environmental samples, developing strategies in the field of sample preparation and on lowering the limit of detection.